

POLAR AND IONIC LIQUID CRYSTALS BASED ON THE $[CLOSO-1-CB_9H_{10}]^-$
AND $[CLOSO-1-CB_{11}H_{12}]^-$ BORON CLUSTERS

By

JACEK GRZEGORZ PECYNA

Dissertation

Submitted to the Faculty of the
Graduate School of Vanderbilt University
in partial fulfillment of the requirements

for the degree of

DOCTOR OF PHILOSOPHY

in

Chemistry

May, 2015

Nashville, Tennessee

Approved:

Professor Piotr Kaszynski

Professor Timothy Hanusa

Professor Jeffrey Johnston

Professor Kane Jennings

Table of contents

Acknowledgements	vi
List of figures	viii
List of tables	xv
Part I. Introduction	1
Chapter 1. Scope of the work	1
Chapter 2. Fundamentals of boron clusters and liquid crystals	15
2.1 Boron clusters	15
2.2 Liquid crystals.....	17
2.3 Boron clusters as core elements of liquid crystals	24
2.4 The [<i>closo</i> -1-CB ₁₁ H ₁₂] ⁻ cluster - chemistry and properties	36
2.4.1 General information	36
2.4.2 The [<i>closo</i> -1-CB ₁₁ H ₁₂] ⁻ anion.....	36
2.4.3 Functionalization of the [<i>closo</i> -1-CB ₁₁ H ₁₂] ⁻ cluster	40
2.4.4 Carbon substitution	42
2.4.5 Boron substitution.....	54
2.4.6 Summary	68
2.4.7 References.....	68
Part II. Polar liquid crystalline materials derived from the [<i>closo</i>-1-CB₉H₁₀]⁻ and [<i>closo</i>-1-CB₁₁H₁₂]⁻ anions	76
Chapter 3. Methods and key intermediates to polar liquid crystals	81
3.1 Introduction.....	81
3.2 The preparation of [<i>closo</i> -1-CB ₉ H ₈ -1-COOH-10-(4-C ₃ H ₇ C ₅ H ₉ S)] as intermediate to polar liquid crystals.....	81
3.2.1 Description and contributions	81
3.2.2 Manuscript	82
3.2.2.1 Introduction.....	82
3.2.2.2 Results and discussion	85
3.2.2.3 Conclusions.....	97

3.2.2.4 Experimental.....	98
3.2.2.5 Acknowledgements.....	110
3.2.2.6 References.....	110
3.3 Synthesis and characterization of 12-pyridinium derivatives of the [<i>closo</i> -1-CB ₁₁ H ₁₂] ⁻ anion.	112
3.3.1 Description and contributions.....	112
3.3.2 Manuscript.....	113
3.3.2.1 Introduction.....	113
3.3.2.2 Results and discussion.....	116
3.3.2.3 Summary and conclusions.....	135
3.3.2.4 Computational details.....	136
3.3.2.5 Experimental section.....	137
3.3.2.6 Acknowledgements.....	147
3.3.2.7 References.....	147
Chapter 4. High $\Delta\epsilon$ materials – synthesis and characterization.....	150
4.1 Introduction.....	150
4.2 Investigation of high $\Delta\epsilon$ derivatives of the [<i>closo</i> -1-CB ₉ H ₁₀] ⁻ anion for liquid crystal display applications.....	151
4.2.1 Description and contributions.....	151
4.2.2 Manuscript.....	152
4.2.2.1 Introduction.....	152
4.2.2.2 Results.....	153
4.2.2.3 Discussion.....	171
4.2.2.4 Conclusions.....	172
4.2.2.5 Computational details.....	173
4.2.2.6 Experimental Part.....	173
4.2.2.7 Acknowledgements.....	208
4.2.2.8 References.....	208
4.3 Zwitterionic pyridinium derivatives of [<i>closo</i> -1-CB ₉ H ₁₀] ⁻ and [<i>closo</i> -1-CB ₁₁ H ₁₂] ⁻ clusters as polar liquid crystals for LCD applications.	211
4.3.1 Description and contributions.....	211

4.3.2 Manuscript	211
4.3.2.1 Introduction.....	212
4.3.3.2 Results and discussion	212
4.3.2.3 Conclusions.....	222
4.3.2.4 Computational details	223
4.3.2.5 Experimental part.....	223
4.3.2.6 Acknowledgements.....	230
4.3.2.7 References.....	230
Chapter 5. Isostructural polar/non-polar liquid crystals for probing polarity effect in liquid crystals.....	233
5.1 Introduction.....	233
5.2 The effect of molecular polarity on nematic stability in 12-vertex carboranes....	234
5.2.1 Description and contributions	234
5.2.2 Manuscript	235
5.2.2.1 Introduction.....	235
5.2.2.2 Results.....	237
5.2.2.3 Discussion and conclusions	246
5.2.2.4 Computational details	248
5.2.2.5 Experimental.....	249
5.2.2.6 Acknowledgements.....	258
5.2.2.7 References.....	259
Part III. Ionic liquid crystals based in the [<i>closo-1-CB₉H₁₀</i>] ⁻ cluster	263
6.1 Introduction.....	265
6.2 Anion driven ionic liquid crystals: The effect of the connecting group in [<i>closo-1-CB₉H₁₀</i>] ⁻ derivatives on mesogenic properties.....	265
6.2.1 Description and contributions	265
6.2.2 Manuscript	266
6.2.2.1 Introduction.....	266
6.2.2.2 Results and discussion	268
6.2.2.3 Conclusions.....	277
6.2.2.4 Experimental.....	277

6.2.2.5 Acknowledgements.....	280
6.2.2.6 References.....	280
Part IV. Other projects involving the [closo-1-CB₉H₁₀]⁻ and [closo-1-CB₁₁H₁₂]⁻ cages	282
7.1 Introduction.....	282
7.2 Transmission of electronic effects through the {closo-1-CB ₉ } and {closo-1-CB ₁₁ } cages: Dissociation constants for a series of [closo-1-CB ₉ H ₈ -1-COOH-10-X] and [closo-1-CB ₁₁ H ₁₀ -1-COOH-12-X] acids.	282
7.2.1 Description and contributions	282
7.2.2 Manuscript	283
7.2.2.1 Introduction.....	284
7.2.2.2 Results and discussion	287
7.2.2.3 Conclusions.....	297
7.2.2.4 Computational details	298
7.2.2.5 Experimental section.....	298
7.2.2.6 Acknowledgements.....	309
7.2.2.7 References.....	309
Part V. Summary and outlook.....	312

Acknowledgements

I would like to express my gratitude to my advisor Dr. Piotr Kaszynski for giving me this great opportunity to perform research in his laboratory. I would have not been able to go through this journey without his guidance, advice and patience. Thank you so much for your support, encouragement and giving me the opportunity to be a part of the exciting research.

I am truly grateful to the members of my PhD committee, Dr. Jeffrey Johnston, Dr. Timothy Hanusa and Dr. Kane Jennings, for their valuable advice, guidance and trust as well as for the knowledge I gained during their classes and seminars.

I cannot forget about all the members of the Kaszynski lab that I have met and worked with during my graduate career, undergraduate students Rich Denicola, Ajan Sivaramamoorthy, Harrison Gray, visiting professor Min-yan Zheng and graduate student Jason Gerding. In particular, I would like to thank Dr. Aleksandra Jankowiak. Ola is not only a great scientist, but also a wonderful friend and mentor, who patiently helped me become more familiar with the world of organic chemistry. In this place, I also would like to thank Dr. Agnieszka Bodzioch, a great friend, but also a great advisor in organic synthesis. I am extremely thankful Dr. Bryan Ringstrand for his guidance and patience while introducing me into the exciting area of boron clusters chemistry. My special thanks go to my best friend, Dr. Marta Szulik. We have been best friends for over twelve years. Thank you so much Marta for inspiring me and encouraging me to take this opportunity to pursue my graduate career. Thank you so much for all your support and always being there for me.

I would not have been here without the love and support of my family. I am extremely grateful to my mom, my dad and my sister for always being there for me, for their encouragement and inspiration. Thank you for your understanding and patience. I could not do it all without you. I also would like to thank other members of my family and my friends, who have been very supportive and loving. I would like to acknowledge Sandra Ford for all her help related not only to graduate school life.

This work would have not been possible without the support of the National Science Foundation and the Department of Chemistry at Vanderbilt University. I would like to thank the Vanderbilt Graduate School for providing travel grants thanks to which I was able to attend scientific conferences.

List of figures

Chapter 1

Figure 1. General structure of ionic liquid crystals based on $[closo-1-CB_{11}H_{12}]^-$ (1) and $[closo-1-CB_9H_{10}]^-$ (2) anions.	3
Figure 2. Dinitrogen (3 , 4 , 7 and 8) and iodo derivatives (5 and 9) of 1 and 2	3
Figure 3. Preparation of pyridinium zwitterions of type 1C and 2C through the dinitrogen intermediate 3 and 6	5
Figure 4. Formation of the pyridinium zwitterions (type 1C and 2C) directly from 1-amino derivatives 14 and 15	5
Figure 5. Synthesis of pyridinium zwitterions of type 1F	6
Figure 6. Preparation of pyridinium zwitterions of type 1F	7
Figure 7. Preparation of sulfonium esters of type 23 from iodo acid 21	8
Figure 8. Pyridinium 13 and 11 and sulfonium 23 zwitterions.	8
Figure 9. Polar (24) and non-polar (25) esters based on the $[closo-1-CB_{11}H_{12}]^-$ (1) and $[closo-C_2B_{10}H_{12}]$ clusters.	9
Figure 10. General scheme of investigated ionic liquid crystals.	10
Figure 11. Carboxylic acid based on the $[closo-1-CB_{11}H_{12}]^-$ and $[closo-1-CB_9H_{10}]^-$ anions.	10

Chapter 2

Figure 1. Skeletal representation of the 12- and 10-vertex boron clusters. Each vertex represents a BH fragment. The sphere is a CH fragment.	16
Figure 2. General scheme of a calamitic liquid crystal molecule. <i>L</i> stands for a linking group.	19
Figure 3. Building blocks of rigid cores of calamitic liquid crystal molecules.	19
Figure 4. Typical linking groups in used in rod-like mesogens.	20
Figure 6. Schematic representation of the Fréedericksz transition.	24
Figure 7. Cylindrical shapes of the 12- (1) and 10-vertex (2) monocarba- <i>closo</i> -borates.	25
Figure 8. Polar (QP and DP), ionic (IO) and nonpolar (NP) derivatives of boron clusters.	26

Figure 9. Skeletal representations of the [<i>closo</i> -1-CB ₁₁ H ₁₂] ⁻ (1) cluster. Each vertex represents a B-H fragment and the dark sphere a carbon atom.....	37
Figure 10. Examples of zwitterionic (2 [10] b , 1c) ^{14,15} and ionic (2f) ¹⁶ liquid crystals derived from 1	38
Figure 11. Synthesis of 1 by Knoth et al. ^{17,18}	39
Figure 12. Synthesis of 1 by Kennedy. ²⁰	39
Figure 13. Electrophilic substitution in the [<i>closo</i> -1-CB ₁₁ H ₁₂] ⁻ (1) and [<i>closo</i> -1-CB ₉ H ₁₀] ⁻ clusters.	41
Figure 14. Substitution at the carbon vertex in 1	42
Figure 15. Synthesis of C-phenyl derivatives of 1 by Breloch's protocol.....	43
Figure 16. Synthesis of C-substituted aryl derivatives of 1 by insertion of arylhalocarbenes into [<i>nido</i> -B ₁₁ H ₁₃] ²⁻ 12	43
Figure 17. Cross-coupling reaction between C-metalated carborane anion 14 and aryl halides.	44
Figure 18. Synthesis of carboxylic acids 16 and 17	44
Figure 19. Synthesis of functionalized monocarbadodecaborate alcohols 18 based on 1	45
Figure 20. Synthesis of 1-cyano derivative 19 of the [<i>closo</i> -1-CB ₁₁ H ₁₂] ⁻ cluster 1	45
Figure 21. Conversion of carboxylic acid 22 into nitrile 24	46
Figure 22. Synthesis of [<i>closo</i> -1-CB ₁₁ H ₁₁ -1-NH ₃] amine (25).....	46
Figure 23. Synthesis of iodo amine 26 by direct iodination of amine 25 and by conversion of the carboxylic acid group in 16 into amine group.	47
Figure 24. Diazotization of amine 32 to afford pyridinium zwitterion 31	48
Figure 25. Synthesis of pyridinium zwitterions 31 from functionalized amines 33 and pyrylium salts.....	48
Figure 26. Synthesis of 1-(4-pentylquinuclidin-1-yl)-1-carba- <i>closo</i> -dodecaborane 34 . ..	49
Figure 27. Conversion of 1-amine 35 into 1-isonitrile 37	49
Figure 28. Synthesis of 1-thiol 38	50
Figure 29. Formation of sulfonium zwitterion 42 from amine 33	50
Figure 30. Preparation of 1-halo derivatives of the [<i>closo</i> -1-CB ₁₁ H ₁₂] ⁻ anion.....	51
Figure 31. Preparation of phosphorus derivatives 45	52
Figure 32. Preparation of 1-hydroxy-carba- <i>closo</i> -dodecaborane 46	52

Figure 33. Transformation of 12-pentyl-1-amine 47 into 1-hydroxy derivative 48	52
Figure 34. Preparation of TIPS-substituted derivative 49	53
Figure 35. Synthesis of boronic acid 50	53
Figure 36. Preparation of boronic acid ester 51	54
Figure 37. Preparation of iodo 15 and 52 and iodonium 53 and 54 derivatives of 1	55
Figure 38. Synthesis of 12-fluoro derivative 55	55
Figure 39. Preparation of 12-chloro derivative 56	56
Figure 40. Bromination of 1 at the B(12) vertex.	56
Figure 41. Preparation of 15	57
Figure 42. Polyiodination of 1	57
Figure 43. Transformations of B-iodo derivatives.	58
Figure 44. Synthesis of iodo acid 17	59
Figure 45. Kumada cross-coupling of iodo derivative 15	60
Figure 46. Microwave-assisted Kumada cross-coupling of 12-iodo derivatives of 1	60
Figure 47. Negishi cross-coupling of 25	61
Figure 48. Preparation of 12-hexyl-1-carboxylic acid 61	61
Figure 49. Alkylation of 62 with hexyl zinc chloride.	61
Figure 50. Transformation of 15 and 53 into cyano derivative 64 and its subsequent hydrolysis to carboxylic acid 65	62
Figure 51. Preparation of amino acid 66	62
Figure 52. Preparation of amines 67 and 68	63
Figure 53. Diazotization of amino acid 66	63
Figure 54. Diazotization of 1-substituted 12-amines 69 , 70 and 71	64
Figure 55. Transformation of 4-methoxypyridinium compound 74 into higher alkoxy pyridinium derivatives 72 via pyridone intermediate 73	64
Figure 56. Transformation of iodonium zwitterion 53 into pyridinium derivative 71	65
Figure 57. Preparation of zwitterions 75 and 76	65
Figure 58. Preparation of protected mercaptane 77	66
Figure 59. Formation of 12-hydroxy carba- <i>closo</i> -dodecaborate 78	66
Figure 60. Synthesis of 12-oxonium zwitterion 79	67
Figure 61. Preparation of 80	67

Figure 62. Preparation of inner triphenylphosphonium derivative 81	68
Chapter 3	
Figure 1. Schematic representation of the Fréedericksz transition.	76
Figure 2. Sulfonium 3 and quinuclidinium 4 derivatives of the [<i>closo</i> -1-CB ₉ H ₁₀] ⁻ anion (2).....	77
Figure 3. Multi-step synthesis of sulfonium 5 and pyridinium 8 acids from decaborane, B ₁₀ H ₁₄	78
Figure 1. Acid 1 as a precursor to 1,10-difunctionalized derivatives of the { <i>closo</i> -1-CB ₉ } cluster, which include polar (I) and ionic (II) liquid crystals. Q ⁺ is pyridinium, ammonium or sulfonium, R, R ¹ ,R ² = alkyl, ester. For X and Y see text.	83
Figure 2. Structures for acid 2[5] and ester 3[5]a	84
Figure 3. Interconversion of the <i>trans</i> and <i>cis</i> isomers of esters of ester 3[3] . Two major conformers are shown.	97
Figure 1. The structures of the [<i>closo</i> -1-CB ₉ H ₁₀] ⁻ and [<i>closo</i> -1-CB ₁₁ H ₁₂] ⁻ anions (A and B), and their zwitterionic 1,10– (IA , IIA) and 1,12–disubstituted (IB , IIB) derivatives. Q ⁺ represents an onium fragment such as quinuclidinium, sulfonium or pyridinium. Each vertex represents a BH fragment and the sphere is a carbon atom.	114
Figure 2. The structures of pyridinium zwitterions.	116
Figure 3. A DSC trace of 1c . Cr - crystal; SmA - smectic A; I - isotropic. The heating and cooling rates are 5 K min ⁻¹	121
Figure 4. Optical texture of a SmA phase observed for 1c at 130 °C on cooling from the isotropic phase.	121
Figure 5. A comparison of thermal properties for two isomers 1c and 13 . Data for 13 was taken from ref ⁵	121
Figure 6. Electronic absorption spectra for 2b and 3b (CH ₃ CN).	124
Figure 7. B3LYP/6-31G(d,p)-derived contours and energies of molecular orbitals relevant to low energy excitations in 2b and 3b in vacuum.	124
Figure 8. Thermal ellipsoid diagram of (a) 12-(4-methoxypyridinium)-1-carbadodecaborate (2b) and (b) 1-(4-methoxypyridinium)-1-carbadodecaborate (3b). Hydrogen atoms are omitted for clarity. Pertinent molecular dimensions are listed in Table 3.	127

Figure 9. Proposed mechanism for the formation of **2**. 130

Figure 10. A sequence of ^{11}B NMR spectra showing the transformation of amine **4c[NMe₄]** (black line) to CD₃CN adduct **16c**. The asterisks indicate trace impurities in the amine. The sample was taken at $-40\text{ }^\circ\text{C}$, dissolved in CD₃CN at $-40\text{ }^\circ\text{C}$, and placed in the spectrometer at ambient temperature before immediate recording of the spectra. ... 132

Chapter 4

Figure 1. The structure of the [*closo*-1-CB₉H₁₀]⁻ cluster (**A**) and its polar derivatives **IA** and **IIA**. Each vertex represents a BH fragment, the sphere is a carbon atom, and Q⁺ stands for an onium group such as an ammonium, sulfonium or pyridinium..... 153

Figure 2. Plot of peak temperatures of the N-I transition vrs concentration in **CI Ester**. 162

Figure 3. Dielectric parameters of binary mixtures of **4[3]e** (black) and **4[3]c** (red) in **CI Ester** as a function of concentration. 163

Figure 4. Interconversion of the *trans* and *cis* isomers of ester **4[n]**. 166

Figure 1. The structures of the [*closo*-1-CB₉H₁₀]⁻ and [*closo*-1-CB₁₁H₁₂]⁻ anions (**A** and **B**), and their zwitterionic 1,10- (**IA**, **IIA**) and 1,12-disubstituted (**IB**, **IIB**) derivatives. Q⁺ represents an onium fragment such as ammonium, sulfonium or pyridinium. Each vertex represents a BH fragment and the sphere is a carbon atom. 213

Figure 2. Electronic absorption spectra of **1[6]c** and **2[6]c** in MeCN. 215

Figure 3. B3LYP/6-31G(d,p) derived contours and energies of FMOs involved in low energy excitations in **1[6]b** (left) and **2[6]b** (right). 216

Figure 4. Left: DSC trace of **2[10]b**. The heating and cooling rates are 5 K min⁻¹. Right: The optical texture of **2[10]b** obtained at 190 °C on cooling from the isotropic phase.. 217

Figure 5. XRD pattern for **2[10]b** at 195 °C. 218

Figure 6. Dielectric parameters as a function of concentration of **2[10]b** in **CI Ester**.... 220

Chapter 5

Figure 1. Structures of nematics derived from 10-vertex (**[10]**) and 12-vertex (**[12]**) clusters. Each vertex represents a BH fragment and the sphere is a carbon atom. 236

Figure 2. A plot of the ΔT_{NI} for series **[10]** (black) and for series **[12]** (red). ΔT_{NI} represents the difference between T_{NI} of polar (**2**) and T_{NI} of non-polar (**1**) mesogen in each series. 240

Figure 3. A plot of ΔT_{NI} for the [10] series versus the ΔT_{NI} of the [12] analogues; slope = 0.55, $r^2 = 0.96$.	241
Figure 4. A plot of T_{NI} of the [10] series <i>vs</i> the T_{NI} of the [12] analogues for the non-polar (circles) and polar (diamonds) derivatives. Best fit functions: $T_{\text{NI}}[\mathbf{12}] = 1.03 \times T_{\text{NI}}[\mathbf{10}] - 11.2$, $r^2 = 0.998$ for series 1 (excluding 1b); $T_{\text{NI}}[\mathbf{12}] = 0.87 \times T_{\text{NI}}[\mathbf{10}] + 36.3$, $r^2 = 0.999$ for series 2 .	242
Figure 5. Optimized geometry of two molecules of 2[12]d obtained at the M06-2x/3-21G* level of theory in gas phase.	245
Figure 6. N–I transition temperature (T_{NI}) as a function of the diameter of ring A in 1e .	247

Chapter 6

Figure 1. The structures of the [<i>closo</i> -1-CB ₉ H ₁₀] [−] (A) and [<i>closo</i> -1-CB ₁₁ H ₁₂] [−] (B) clusters and ion pairs of their 1,10- (IA) and 1,12-disubstituted (IB) derivatives with the counterion Q ⁺ (metal or an onium ion). Each vertex represents a BH fragment and the sphere is a carbon atom.	267
Figure 2. The structures of compounds 1–3 .	267
Figure 3. A plot of N–I (dots) and SmA–N (diamonds) transition temperatures for binary mixtures of 1a[Pyr] (black solid) and 1b[Pyr] (gray dotted) in 2a[Pyr] as a function of mole fraction.	274
Figure 4. Natural charges for key molecular fragments and extended Newman projection along the long molecular axes of acid 5a and 5b showing conformational minima. The bars represent the substituents, and the filled circle is the connecting atom.	274
Figure 5. A plot of N–I (dots) and SmA–N (diamonds) transition temperatures for binary mixtures of 1a[Pyr] (black solid) and 1b[Pyr] (gray dotted) in 3a as a function of mole fraction of the ion pair.	276

Chapter 7

Figure 1. The structures of benzene (A), bicyclo[2.2.2]octane (BCO, B), 1,10-dicarba- <i>closo</i> -decaborane (10-vertex <i>p</i> -carborane, C), 1,12-dicarba- <i>closo</i> -dodecaborane (12-vertex <i>p</i> -carborane, D), 1-carba- <i>closo</i> -decaborate (E), 1-carba- <i>closo</i> -dodecaborate (F). In C–F each vertex corresponds to a BH fragment and the sphere represents a carbon atom.	285
--	-----

Figure 2. The Hammett plot of $\Delta pK_a'$ values for derivatives of [closo-1-CB ₉ H ₈ -1-COOH-10-X] ⁻ 1 (black dots, $\rho = 0.87 \pm 0.04$, $r^2 = 0.99$) and [closo-1-CB ₁₁ H ₁₀ -1-COOH-12-X] ⁻ 2 (red squares, $\rho = 1.00 \pm 0.09$, $r^2 = 0.97$) in 50% EtOH (v/v) at 24 °C. The blue diamond represents the datapoint for 1c	294
Figure 3. The plot of ΔG_{298} for isodesmic reaction in Scheme 3 for series 1 (black dots, $m = 0.63 \pm 0.02$, $r^2 = 0.99$) and 2 (red squares, $m = 0.53 \pm 0.02$, $r^2 = 0.99$) versus ΔG_{298} values for benzoic acid derivatives. Datapoints for l and m are excluded.....	296
Figure 1. Polar materials based on sulfonium acids 4	312
Figure 2. Selected polar esters based on sulfonium acids.....	313
Figure 3. Selected mesogenic pyridinium zwitterions based on 1 (left) and 2 (right)....	313
Figure 4. Pyridinium zwitterions of type 1F	314
Figure 5. Polar / non-polar materials based on [closo-1-CB ₁₁ H ₁₂] ⁻ and [closo-1,2-C ₂ B ₁₀ H ₁₂] clusters.	314

List of tables

Chapter 1

Table 1. Polar liquid crystals based on the [<i>closo</i> -1-CB ₁₁ H ₁₂] ⁻ (1) and [<i>closo</i> -1-CB ₉ H ₁₀] ⁻ (2) anions.	1
---	---

Chapter 3

Table 1. Optimization of preparation of [<i>arachno</i> -6-CB ₉ H ₁₃ -6-COOH] ⁻ NEt ₄ ⁺ (5). ^a	87
Table 2. Optimization of formation of [<i>closo</i> -2-CB ₉ H ₉ -2-COOH] ⁻ NEt ₄ ⁺ (4). ^a	90
Table 3. Transition temperatures (°C) and enthalpies (kJ) for 3[n]a . ^a	96
Table 1. Selected electronic parameters for 2b and 3b	123
Table 2. Crystallographic data for 2b and 3b . ^a	125
Table 3. Selected interatomic distances and angles for 2b and 3b . ^a	128
Table 4. Thermodynamic parameters (kcal mol ⁻¹) for transformation of 14 to 2 . ^a	130
Table 5. Bonding properties of selected dinitrogen derivatives. ^a	134

Chapter 4

Table 1. Transition temperatures (°C) and enthalpies (kJ/mol, in italics) for 3[n] . ^a	157
Table 2. Transition temperatures (°C) and enthalpies (kJ/mol, in italics) for 4[3] . ^a	158
Table 4. Extrapolated experimental (upper) and predicted (lower in italics) dielectric data and results of Maier-Meier analysis for selected compounds. ^a	164
Table 5. Calculated molecular parameters for selected compounds. ^a	167
Table S1. Solubility data for 3[n]b . ^a	194
Table S2. Solubility data for selected esters 4[3] . ^a	195
Table S3. Transition temperatures (°C) and enthalpies (kJ/mol, in italics) for 4[n] . ^a	196
Table S4. <i>T</i> _{NI} for solutions of 4[3]b in CinnCN	197
Table S5. <i>T</i> _{NI} for solutions of 4[3]d in ClEster	197
Table S6. <i>T</i> _{NI} for solutions of 4[3]d in CinnCN	198
Table S7. <i>T</i> _{NI} for solutions of 4[3]e in ClEster	198
Table S8. <i>T</i> _{NI} for solutions of 4[3]e in CinnCN	199
Table S9. <i>T</i> _{NI} for solutions of 4[3]h in ClEster	199
Table S10. <i>T</i> _{NI} for solutions of 4[3]l in ClEster	200
Table S11. Dielectric parameters for 3[5]b in ClEster at 25 °C.	201

Table S12. Dielectric parameters for 4[3]c in ClEster at 25 °C.....	201
Table S13. Dielectric parameters for 4[3]d in ClEster at 25 °C.	202
Table S14. Dielectric parameters for 4[3]e in ClEster at 25 °C.....	202
Table S15. Dielectric parameters for 4[3]h in ClEster at 25 °C.	202
Table S16. Dielectric parameters for 4[3]j in ClEster at 25 °C.	203
Table S17. Dielectric parameters for 4[3]k in ClEster at 25 °C.	203
Table S18. Dielectric parameters for 4[7]j in ClEster at 25 °C.	204
Table 1. Transition temperatures (°C) and enthalpies (kJ/mol, in italics) for 1[n] and 2[n] ^a	217
Table 2. Extrapolated dielectric data for selected compounds. ^a	221
Table 3. Calculated molecular parameters for selected compounds. ^a	222
Chapter 5	
Table 1. Transition temperatures for [12]b–[12]f and [10]f . ^a	239
Table 2. Calculated molecular parameters for [12]b–[12]f . ^a	243
Table 3. Selected structural parameters for [12]b–[12]f . ^a	245
Chapter 6	
Table 1. Transition temperatures (°C) and enthalpies (kJ/mol) for selected compounds. ^a	271
Table 2. Virtual transition temperatures (°C) for ionic liquid crystals. ^a	273
Chapter 7	
Table 1. Apparent ionization constants pK_a' for selected derivatives of [<i>closo</i> -1-CB ₉ H ₈ -1-COOH-10-X] (1) and [<i>closo</i> -1-CB ₁₁ H ₁₀ -1-COOH-12-X] (2) in 50% EtOH (v/v) at 24 °C	293
Table S1. ¹¹ B NMR chemical shift for the B(10) atom in acids 1 and B(12) atom in acids 2 as acid extracts and upon deprotonation in CD ₃ CN.....	306
Table S2. Free energy change in isodesmic reaction involving the parent and substituted carboxylic acids	308

Part I. Introduction

Chapter 1. Scope of the work

The main objective of my dissertation is the development of the fundamental chemistry of the $[closo-1-CB_{11}H_{12}]^-$ (**1**) and, to some extent, the $[closo-1-CB_9H_{10}]^-$ (**2**) anions as well as design and investigation of properties of molecular materials incorporating these clusters as core elements. Such materials can be divided into two groups: polar and ionic liquid crystals.

Polar liquid crystals derived from **1** and **2** are molecules in which a positively charged organic fragment (quinuclidinium, sulfonium or pyridinium) is attached to the negatively charged cluster at the carbon or boron vertex (Table 1).

Table 1. Polar liquid crystals based on the $[closo-1-CB_{11}H_{12}]^-$ (**1**) and $[closo-1-CB_9H_{10}]^-$ (**2**) anions.

$L \backslash Q^+$						
	✓	✓	✓	✗	✓	✓
	A	B	C	D	E	F
	✓	✓	✓	✗	✓	✓
	A	B	C	D	E	F

✓ - investigated; ✗ - not investigated.

This unique combination of an inorganic anion and organic cation gives access to a new class of highly polar materials, whose properties depend on the type of the cluster,

type of the substituent and the position of the substituent on the cluster. Highly polar liquid crystals are of interest as materials for electrooptical applications. For nearly 15 years, such materials have been investigated in our group. The developed synthetic methodologies allow for access to each type of zwitterions shown in Table 1. The real breakthrough in access to polar materials based on the [*closo*-1-CB₉H₁₀]⁻ anion (**2**) was the development of functionalization methods of **2** and synthesis of iodo acid [*closo*-1-CB₉H₈-1-COOH-10-I]⁻.¹ Further transformation of iodo acid [*closo*-1-CB₉H₈-1-COOH-10-I]⁻ opened access to other functionalities such as amine,² diazo,² and alkyl.³ The initial studies began with the polar materials of type **1A** and **2A** (Table 1).^{4,5} These zwitterions did not exhibit liquid crystalline properties and were high-melting solids of low solubility in nematic hosts. However, quinuclidinium derivatives **2A** increased the dielectric anisotropy $\Delta\epsilon$ of nematic medium. Analogous to **1A** and **2A**, isomeric quinuclidinium zwitterions **1D** and **2D** are expected to also exhibit low solubility (as a result of being high-melting solids) and, for this reason, they have not been investigated. Other investigations showed that materials based on the sulfonium (**2E**) and pyridinium (**2F**) zwitterions exhibited mesogenic behavior, and had better solubility in nematic hosts.⁶ Based on these results, other materials incorporating the sulfonium and pyridinium fragments were anticipated to be also compatible with nematic hosts and to exhibit liquid crystalline properties. Further investigation of molecular materials based on the sulfonium (type **2B** and **2E**),⁷ and pyridinium (type **1C**, **2C**, and **1F**)⁸⁻¹⁰ zwitterions have confirmed the expectations. My work included materials based mainly on structures **1C**, **1F**, **2C** and **2E**.

The second group of investigated materials involves ionic liquid crystals, which typically are a combination of an inorganic anion and an organic cation, whose proper geometry ensures mesogenic properties. Boron clusters offer a new type of combination of the anion and cation: it is now the anion that is the source of mesogenic properties (Figure 1).^{3,11,12}

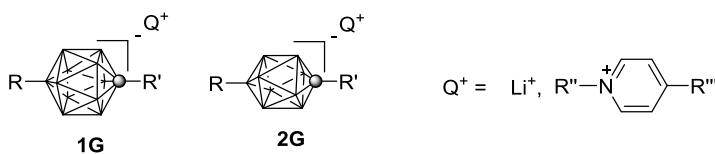


Figure 1. General structure of ionic liquid crystals based on $[closo-1-CB_{11}H_{12}]^-$ (**1**) and $[closo-1-CB_9H_{10}]^-$ (**2**) anions.

Ionic liquid crystals are of interest as ion-conductive materials, which could be used in lithium batteries or dye-sensitized solar cells.

Access to polar and ionic liquid crystals based on **1** and **2** required efficient methods of functionalization of the clusters. Until recent discoveries, functionalization of both clusters was either through dinitrogen (compounds **3**, **4**, **7** and **8**) or iodo (compounds **5** and **9**) derivatives shown in Figure 2.

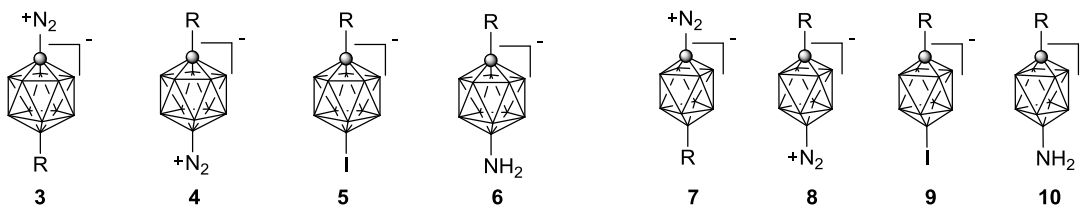


Figure 2. Dinitrogen (**3**, **4**, **7** and **8**) and iodo derivatives (**5** and **9**) of **1** and **2**.

The use of iodo derivatives **5** and **9** was limited to introduction of only alkyl or aryl substituents onto the boron vertex by means of Pd-catalyzed cross-coupling reactions. Additionally, iodo compounds **5** and **9** could be conveniently converted to the corresponding amines **6** and **10**,^{2,13} which upon diazotization lead to dinitrogen derivatives **4** and **8**.^{2,9} Dinitrogen compounds **3** and **7** were also prepared from corresponding amines in a similar manner.^{4,14}

Dinitrogen derivative **8** was found to be a convenient intermediate to a class of polar materials of type **2E** and **2F** (Table 1) due to its high stability.⁶ Derivatives **3**, **4** and **7** were expected to exhibit similar behavior. However, as demonstrated by experimental results and quantum mechanical calculations,^{9,14} these three dinitrogen intermediates were either unstable (**3** and **4**) or their synthetic use was limited by mechanistic issues (**7**), which are discussed below. Therefore, it became necessary to search for more practical and efficient methods to materials based on structures **1C**, **2C**, and **1F** (Table 1).

Pyridinium zwitterions **11** (type **2C**) can be obtained as minor products by thermolysis of the dinitrogen derivative **7** in neat pyridine (Figure 3), accompanied by byproducts **12**, which are postulated to originate from a radical anion mechanism.¹⁴ The dinitrogen derivative of **3** is highly unstable and the pyridinium products **13** (type **1C**) are obtained in very low yields (3-5%), (Figure 3).⁴

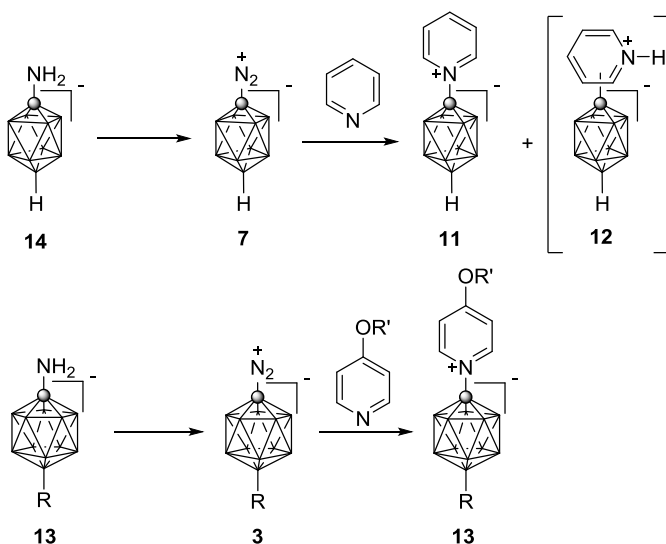


Figure 3. Preparation of pyridinium zwitterions of type **1C** and **2C** through the dinitrogen intermediate **3** and **6**.

Therefore, I began to search for alternative methods for formation of pyridinium compounds and discovered that pyridinium zwitterions of type **1C** and **2C** can be conveniently synthesized directly from amines **14** and **15** and pyrylium salts (Figure 4).⁸

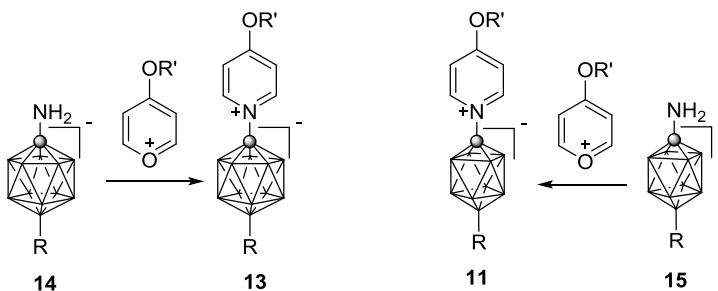


Figure 4. Formation of the pyridinium zwitterions (type **1C** and **2C**) directly from 1-amino derivatives **14** and **15**.

The new method allows for preparation of such pyridinium derivatives **1C** and **2C** based on the [*closo*-1-CB₁₁H₁₂]⁻ (**1**) and [*closo*-1-CB₉H₁₀]⁻ (**2**) anions in much higher

yields, higher purity and extends the scope of substituents to higher functionalized pyridines.

Synthetic access to 12-pyridinium derivatives of the $[closo-1-CB_{11}H_{12}]^-$ cluster (**1**), (type **1F**), was also very inefficient. The yield of the products, obtained by diazotization of an appropriate 12-amine derivatives **16** is strongly dependent on the length of the alkyl chain in the 4-alkoxypyridine used as the solvent and the presence of other functional groups on the cluster.¹⁰ Due to high basicity of the 12-amino derivatives of the $[closo-1-CB_{11}H_{12}]^-$ anion (**1**), reaction between the amines **17** and pyrylium salts did not yield the desired products (Figure 5).

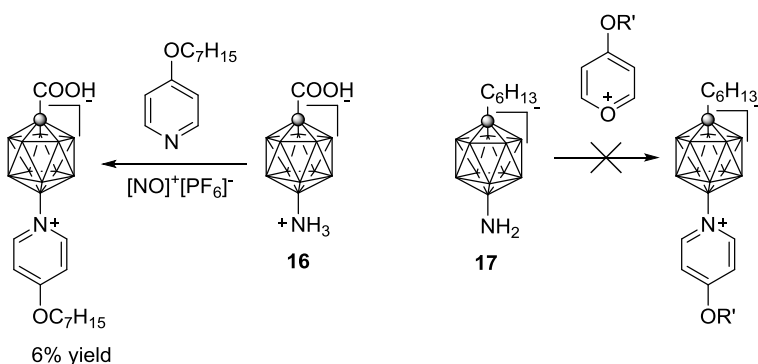


Figure 5. Synthesis of pyridinium zwitterions of type **1F**.

In search of more practical and higher-yielding methods for synthesis of 12-pyridinium zwitterions of type **1F**, I analyzed the *O*-alkylation of γ -pyrones with alkyl triflates used in the process of synthesis of pyrylium salts.⁸ By analogy to that route, I decided to examine the *O*-alkylation of 12-(4-pyridones) **18** derived from 12-(4-methoxypyridinium) derivatives **19** (Figure 6). I discovered that the formation of the 12-(4-pyridone) **18** by demethylation of 12-(4-methoxypyridinium) derivatives **19** and their subsequent *O*-alkylation with alkyl triflates to form **20** proceed nearly quantitatively

(Figure 6). Moreover, derivatives **19** are obtained from amines **6** in about 50% yield making this route to polar liquid crystals practical.⁹

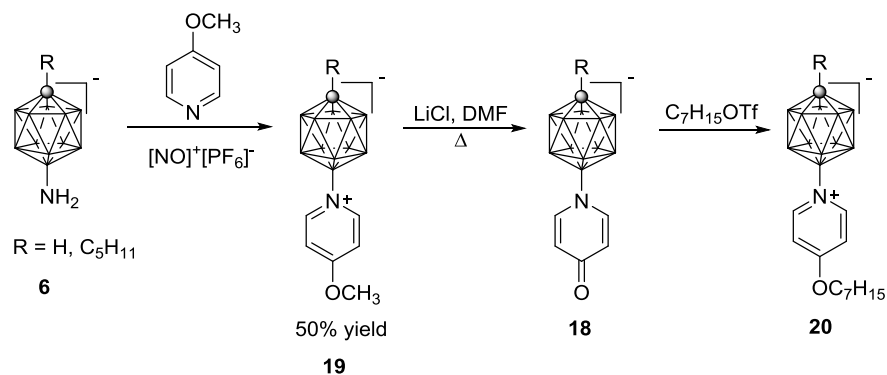


Figure 6. Preparation of pyridinium zwitterions of type **1F**.

Thus, the overall yield of converting **6** to **20** was improved by an order of magnitude when compared to previous methods in Figure 5. The new protocol allows for introduction of more complex alkyl chains and the work contributed to the fundamental knowledge about the stability of 12-dinitrogen derivatives **4**.⁹

Another part of research focused on development of more efficient and more practical method of the preparation of iodo acid [*closo*-1-CB₉H₈-1-COOH-10-I]⁻ (**21**), an important intermediate in synthesis of sulfonium acids [*closo*-1-CB₉H₈-1-COOH-10-(4-C_nH_{2n+1}C₅H₉S)] (**22**), (Figure 7). These acids are important precursors to polar liquid crystals of type **2E** (Table 1). The existing methods of preparation of the iodo acid **21** were impractical as they required large volumes of solvents and large excess of reagents. My work involved optimization of the process of preparation of the iodo acid **21**.¹⁵ As a result of my research, reactions leading to **21** became efficient, required smaller volumes of solvents and had better temperature control. The new procedure was shown to be scalable up to 40 g of B₁₀H₁₄ and could be performed conveniently in a 3-L vessel.

Synthesis of the sulfonium acid **22** was also improved by using cesium carbonate as the base.

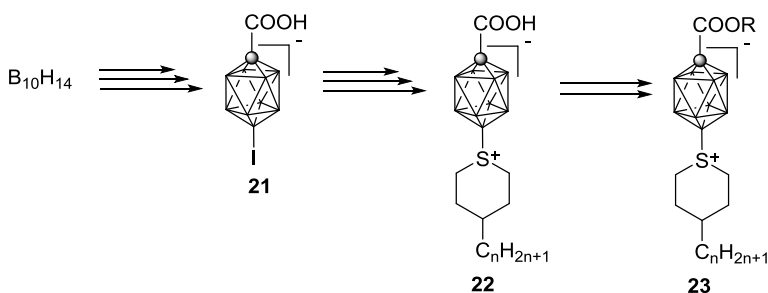


Figure 7. Preparation of sulfonium esters of type **23** from iodo acid **21**.

In the next phase of my PhD project, I synthesized and investigated properties of zwitterionic liquid crystals of general structures **2B** and **2E**. Having a relatively efficient protocol for the preparation of sulfonium acids [*closo*-1-CB₉H₈-1-COOH-10-(4-C_nH_{2n+1}C₅H₉S)],¹⁵ I synthesized and investigated a series of their esters **23** as high $\Delta\epsilon$ additives to nematic hosts.⁷ In a similar manner, I examined 1-pyridinium derivatives (type **1C** and **2C**) of the [*closo*-1-CB₁₁H₁₂]⁻ (**1**) and [*closo*-1-CB₉H₁₀]⁻ (**2**) anions (Figure 8).⁸ I analyzed their optical, thermal and electro-optical properties and assessed their suitability as high $\Delta\epsilon$ materials for LCD applications.

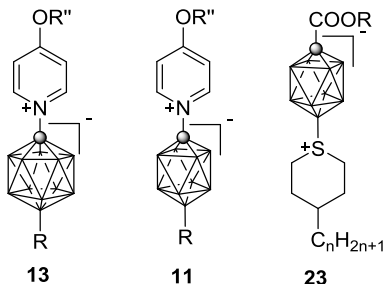


Figure 8. Pyridinium **13** and **11** and sulfonium **23** zwitterions.

Many liquid crystal technologies rely on polar molecules. It is essential to understand how molecular dipole moment affects the stability of a mesophase. However, the lack of proper molecular models was the key reason why experimental investigation of the influence of the dipole moment as the only variable on mesophase stability was hindered. It was demonstrated, however, that upon replacement of a C–C bond with an isosteric and isoelectronic N⁺–B[−] fragment, the only molecular property that was changed, was the molecular dipole moment, while the molecular geometry remained practically unaffected.¹⁶ That allowed for the assessment of how the molecular dipole moment affects stability of the liquid crystalline materials based on the isosteric [*closo*-1-CB₉H₁₀][−] and [*closo*-1,10-C₂B₈H₁₀] clusters. Following this path, I prepared and characterized a series of polar esters **24** and their non-polar isosteric analogues **25** based on the [*closo*-1-CB₁₁H₁₂][−] (**1**) and [*closo*-1,12-C₂B₁₀H₁₂] clusters, respectively (Figure 9).¹⁰

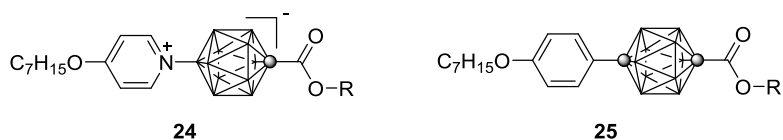


Figure 9. Polar (**24**) and non-polar (**25**) esters based on the [*closo*-1-CB₁₁H₁₂][−] (**1**) and [*closo*-1,12-C₂B₁₀H₁₂] clusters.

Ionic liquid crystals (ILC), which combine properties of liquid crystals and ionic liquids, have been gaining more and more attention. The source of mesogenicity in many common ILCs is the anisometric organic cation. It was shown, recently, in our group that upon proper substitution of **1** and **2**, it can be the carbaborate anion that induces mesogenic properties in ionic liquid crystals.^{3,11} In continuation of the search for new

ILCs based on clusters **1** and **2**, I investigated the effect of the change of alkyl chain on the phase transition by replacing the $-\text{CH}_2-$ group with oxygen and sulfur atom (Figure 10).¹²

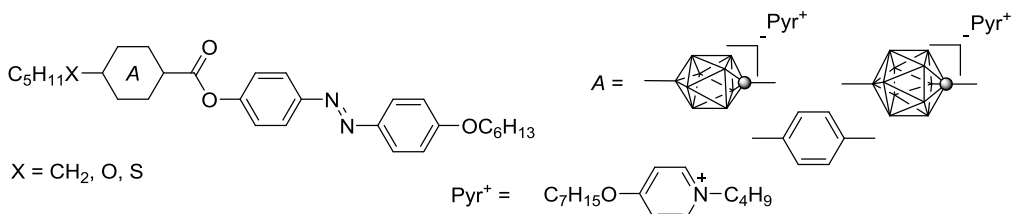


Figure 10. General scheme of investigated ionic liquid crystals.

Having access to some intermediates to functionalized materials based on [*closo*-1- $\text{CB}_{11}\text{H}_{12}$][−] (**1**) and [*closo*-1- CB_9H_{10}][−] (**2**) anions in hand, I had an opportunity to investigate more fundamental properties of these anions. Thus, I investigated the transmission of electronic effects through the [*closo*-1- $\text{CB}_{11}\text{H}_{12}$][−] (**1**) and [*closo*-1- CB_9H_{10}][−] (**2**) clusters. I synthesized a series of carboxylic acids based on anions **1** and **2**, substituted at the B(12) and B(10) positions, respectively (Figure 11). By analysis of the determined dissociation constants pK_a in correlation with Hammett's constants, I was able to comment on the electronic properties of each cluster.¹³ While this work was an additional project, it was of great significance for extending the fundamental knowledge about the [*closo*-1- $\text{CB}_{11}\text{H}_{12}$][−] and [*closo*-1- CB_9H_{10}][−] anions.

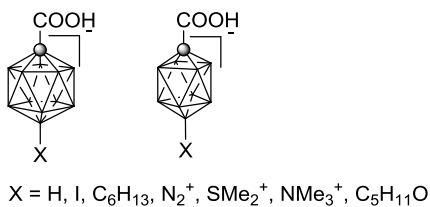


Figure 11. Carboxylic acid based on the [*closo*-1- $\text{CB}_{11}\text{H}_{12}$][−] and [*closo*-1- CB_9H_{10}][−] anions.

The newly developed methods as well as the recent discovery by Kaszynski and Ringstrand¹⁷ greatly improve the possibilities of functionalization of the monocarba-*closo*-borate anions **1** and **2**. The new methods extend functionalization to other types of boron hydride clusters.

In summary, my work covers a diverse area of fundamental chemistry of the [*closo*-1-CB₁₁H₁₂]⁻ (**1**) and [*closo*-1-CB₉H₁₀]⁻ (**2**) anions and their applications in design of molecular materials with unique properties. My research involves synthesis and characterization of new materials using classical and advanced physicochemical methods, and greatly contributes to the general knowledge on polar and ionic materials.

My dissertation consists of five parts. Each part is divided into chapters. The chapters are further divided into sections. Each chapter and section contains their own compound numbering system and reference list. Each chapter begins with a short introduction and each section begins with description of the projects goals, accomplishments and responsibilities of each author. The numbering system in each section is consistent with the one in the original manuscript. Part I is an introduction to boron clusters and liquid crystals, in which chemistry and properties of the [*closo*-1-CB₁₁H₁₂]⁻ anion are also reviewed. Part II and III cover the main scope of my PhD work: the former is dedicated to polar liquid crystalline materials based on the [*closo*-1-CB₉H₁₀]⁻ (**2**) and [*closo*-1-CB₁₁H₁₂]⁻ (**1**) anions, while Part III provides details about my published work in the area of ionic liquid crystals. Part IV describes an additional project involving the [*closo*-1-CB₁₁H₁₂]⁻ (**1**) and [*closo*-1-CB₉H₁₀]⁻ (**2**) clusters. Part V is a summary and outlook of my research.

References

- (1) Ringstrand, B.; Balinski, A.; Franken, A.; Kaszynski, P., A practical synthesis of isomerically pure 1,10-difunctionalized derivatives of the [*closo*-1-CB₉H₁₀]⁻ anion. *Inorg. Chem.* **2005**, *44*, 9561-9566.
- (2) Ringstrand, B.; Kaszynski, P.; Young, V. G. Jr.; Janoušek, Z., The anionic amino acid [*closo*-1-CB₉H₈-1-COOH-10-NH₃] and dinitrogen acid [*closo*-1-CB₉H₈-1-COOH-10-N₂] as key precursors to advanced materials: synthesis and reactivity. *Inorg. Chem.* **2010**, *49*, 1166-1179.
- (3) Ringstrand, B.; Kaszynski, P.; Monobe, H., Anion-driven mesogenicity: ionic liquid crystals based on the [*closo*-1-CB₉H₁₀]⁻ cluster. *J. Mater. Chem.* **2009**, *19*, 4805-4812.
- (4) Pecyna, J.; Ringstrand, B.; Pakhomov, S.; Piecek, W.; Kaszynski, P., Zwitterionic derivatives of the [*closo*-1-CB₁₁H₁₂]⁻ as high $\Delta\epsilon$ additives to nematic liquid crystals. *unpublished results*.
- (5) Ringstrand, B.; Kaszynski, P.; Januszko, A.; Young, V. G. Jr., Polar derivatives of the [*closo*-1-CB₉H₁₀]⁻ cluster as positive $\Delta\epsilon$ additives to nematic hosts. *J. Mater. Chem.* **2009**, *19*, 9204-9212.
- (6) Ringstrand, B.; Kaszynski, P., High $\Delta\epsilon$ nematic liquid crystals: fluxional zwitterions of the [*closo*-1-CB₉H₁₀]⁻ cluster. *J. Mater. Chem.* **2011**, *21*, 90-95.
- (7) Pecyna, J.; Kaszynski, P.; Ringstrand, B.; Bremer, M., Investigation of high $\Delta\epsilon$ derivatives of the [*closo*-1-CB₉H₁₀]⁻ anion for liquid crystal applications. *J. Mater. Chem. C* **2014**, *2*, 2956-2964.

(8) Pecyna, J.; Pocięcha, D.; Kaszynski, P., Zwitterionic pyridinium derivatives of [*closo*-1-CB₉H₁₀]⁻ and [*closo*-1-CB₁₁H₁₂]⁻ as high Δε additives to a nematic host. *J. Mater. Chem. C* **2014**, *2*, 1585-1591.

(9) Pecyna, J.; Ringstrand, B.; Domagala, S.; Kaszynski, P.; Wozniak, K., Synthesis of 12-pyridinium derivatives of the [*closo*-1-CB₁₁H₁₂]⁻ anion. *Inorg. Chem.* **2014**, *53*, 12617-12626.

(10) Pecyna, J.; Denicola, R. P.; Gray, H. M.; Ringstrand, B.; Kaszynski, P., The effect of molecular polarity on nematic phase stability in 12-vertex carboranes. *Liq. Cryst.* **2014**, *41*, 1188-1198.

(11) Ringstrand, B.; Jankowiak, A.; Johnson, L. E.; Pocięcha, D.; Kaszynski, P.; Gorecka, E., Anion-driven mesogenicity: a comparative study of ionic liquid crystals based on the [*closo*-1-CB₉H₁₀]⁻ and [*closo*-1-CB₁₁H₁₂]⁻ clusters. *J. Mater. Chem.* **2012**, *22*, 4874-4880.

(12) Pecyna, J.; Sivaramamoorthy, A.; Jankowiak, A.; Kaszynski, P., Anion-driven ionic liquid crystals: the effect of the connecting group in [*closo*-1-CB₉H₁₀]⁻ derivatives on mesogenic properties. *Liq. Cryst.* **2012**, *39*, 965-971.

(13) Pecyna, J.; Ringstrand, B.; Kaszynski, P., Transmission of electronic effects through the {*closo*-1-CB₉} and {*closo*-1-CB₁₁} cages: apparent dissociation constants for a series of [*closo*-1-CB₉H₈-1-COOH-10-X] and [*closo*-1-CB₁₁H₁₀-1-COOH-12-X] acids. *Inorg. Chem.* **2012**, *51*, 5353-5359.

(14) Ringstrand, B.; Kaszynski, P.; Franken, A., Synthesis and reactivity of [*closo*-1-CB₉H₉-1-N₂]: functional group interconversion at the carbon vertex of the {*closo*-1-CB₉} cluster. *Inorg. Chem.* **2009**, *48*, 7313-7329.

(15) Pecyna, J.; Denicola, R. P.; Ringstrand, B.; Jankowiak, A.; Kaszynski, P., The preparation of [*closo*-1-CB₉H₈-1-COOH-10-(4-C₃H₇C₅H₉S)] as intermediate to polar liquid crystals. *Polyhedron* **2011**, *30*, 2505-2513.

(16) Ringstrand, B.; Kaszynski, P., How much can an electric dipole moment stabilize a nematic phase? Polar and non-polar isosteric derivatives of [*closo*-1-CB₉H₁₀]⁻ and [*closo*-C₂B₈H₁₀]. *J. Mater. Chem.* **2010**, *20*, 9613-9615.

(17) Kaszynski, P.; Ringstrand, B., Functionalization of *closo*-borates through iodonium zwitterions. *Angew. Chem. Int. Ed.* **2015**, accepted.

Chapter 2. Fundamentals of boron clusters and liquid crystals

2.1 Boron clusters

Boron, the 5th element in the periodic table, was discovered by Joseph-Louis Gay-Lussac and Louis-Jaques Thenard, and independently by Humphry Davy in 1808.¹ It is a metalloid, which means it bears properties between metals and non-metals. Boron has only three valence electrons and for this reason many boron compounds are electron acceptors. Low number of electrons causes that boron has a preference for three-centered two-electron bonds to satisfy the octet rule.² That leads to the formation of trigonal boron faces and hypercoordination resulting in cluster structures.³ Such structures were envisioned by William Lipscomb⁴ and Ronald Hoffmann, and experimentally confirmed by Alfred Stock. The prototypical structure for many boron hydride clusters is the [*closo*-B₁₂H₁₂]²⁻ dianion. It possesses the ideal icosahedral symmetry (I_h), and was isolated by Pitochelli and Hawthorne in 1960 as a by-product of a reaction between 2-iododecaborane and trimethylamine.⁵ The discovery of polyhedral boron hydrides led to further investigations and synthesis of first icosahedral carboranes, isoelectronic with the [*closo*-B₁₂H₁₂]²⁻ dianion, in which one of the BH vertices was replaced with a CH⁺ fragment giving the [*closo*-1-CB₁₁H₁₂]⁻ anion. Further substitution leads to the neutral [*closo*-C₂B₁₀H₁₂] cluster, which exists as three isomers: *ortho*, *meta* and *para*. The analogous 10-vertex clusters also exist and are derived from the prototypical [*closo*-B₁₀H₁₀]²⁻ dianion (Figure 1).

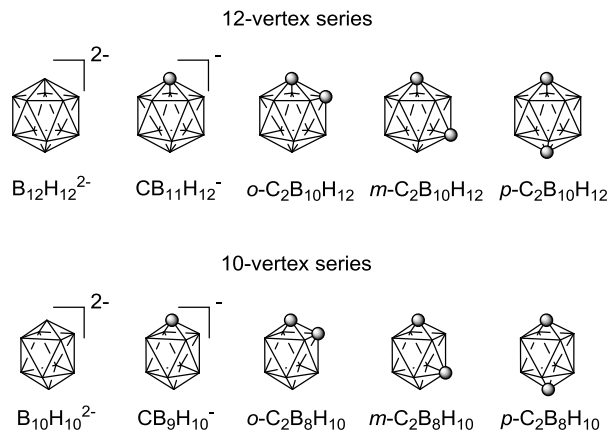


Figure 1. Skeletal representation of the 12- and 10-vertex boron clusters. Each vertex represents a BH fragment. The sphere is a CH fragment.

Carbon is not the only element that can be incorporated into the cluster. Other main-group elements include: phosphorus,^{6,7} sulphur,^{8,9} nitrogen,¹⁰ aluminium,⁷ selenium,¹¹ germanium,¹² and tin.^{13,14}

Closo-borate [*closo*-B₁₂H₁₂]²⁻, and other *closo*-boranes are thermally, electrochemically and chemically stable. The [*closo*-B₁₂H₁₂]²⁻ 2[Cs]⁺ is stable up to 810 °C and is inert to many reagents.¹⁵ This high stability is related to the electron delocalization in the boron cluster framework. Carboranes are frequently called σ -aromatic three-dimensional analogues of benzene. However, bonding in boron clusters cannot be described using the classical two-centered two-electron bonding concept. It is rather a network of two-electron three-centered bonds. Consequently, the lines connecting vertices as shown in Figure 1, are there just to visualize the geometry.¹⁶ They do not represent the actual bonding.

High thermal and chemical stability and inertness of the clusters in many environments make them suitable for applications in medicine, among others. Due to

their lipophilic and strongly hydrophobic character, and, especially, low toxicity they are attractive for biomedical applications, especially boron neutron capture therapy (BNCT).^{17,18} In this technique, the nuclei of the ^{10}B isotope are bombarded with neutrons. The reaction produces an α -particle ($^4\text{He}^{2+}$), and $^7\text{Li}^{3+}$ ion of 2.4 MeV kinetic energy and a 480 keV photon. These high-energy ions cause ionization in biological tissue in a range of about 5-9 μm , ensuring precise cell-killing. The key to success in BNCT requires developing of methods for selective delivery of boron compounds to the tumor tissue in relatively high concentrations, but low enough in the surrounding cells, however, to prevent healthy cell damage. Common compounds used in BNCT include aminoacids, nucleotides and nucleosides, porphyrins, cholesterol derivatives or polymers.¹⁸

Well-developed functionalization methods and significant pharmacological activity of carborane and metallacarborane derivatives are used in other areas of medicine like boron neutron capture synovectomy, molecular imaging and radiotherapy. Boron clusters derivatives also serve as pharmacophores, X-ray contrast agents and anti-tumor agents.³

The ease of functionalization, robustness and high stability made carboranes attractive in other area like organocatalysis,^{19,20} polymers,^{21,22} molecular machines design,^{23,24} carborane-based ceramics,²⁵ non-linear optics materials,^{26,27} and liquid crystals studied exclusively in our research group.²⁸⁻³¹

2.2 Liquid crystals

A liquid crystalline phase, often called a mesophase, is a state of matter intermediate between that of a crystalline solid and that of an ordinary liquid. It was discovered by an Austrian botanist F. Reinitzer in 1888 while he was investigating

cholesteryl benzoate. He observed that the ester had two melting points. Upon heating to 145 °C, the solid turned into a cloudy liquid, which upon further heating, became clear at 179 °C.³² This discovery is often considered as the beginning of the liquid crystal era. Liquid crystals, frequently referred to as the fourth state of matter, possess some characteristics of a liquid such as high fluidity, formation of droplets, etc. On the other hand, they exhibit some properties of crystalline solids such as partial positional and orientational order as evidenced by X-ray.^{33,34} Today, applications of liquid crystals mostly in LCD technology is a multi-billion industry. Other uses of liquid crystal include nonlinear optics, optical communication and image processing.³⁵

Liquid crystalline materials can be classified into two large categories: thermotropic and lyotropic liquid crystals. Thermotropic liquid crystals refer to molecules which form LC phases in a certain range of temperature. Lyotropic liquid crystals are formed in solution and the phase induction can be controlled by temperature and concentration change.³⁶

Thermotropic liquid crystals usually comprise anisometric organic molecules. It is essential that such a molecule has some element of rigidity in its central part to maintain its liquid crystalline properties. The rigidity ensures the existence of intermolecular interactions that favor the proper alignment of the molecules. Mesogenic molecules can be rod-like (calamitics), disc-like (discotics) or banana-like (bent-core) in shape.³³ There are two main building elements of calamitics: central rigid core unit and flexible tails (Figure 2).

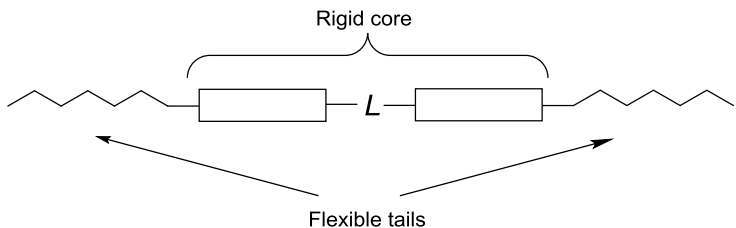


Figure 2. General scheme of a calamitic liquid crystal molecule. *L* stands for a linking group.

The rigid core unit may be built of more than one block and the blocks can be connected with a linking group (*L*). The most common rigid core units are formed by 1,4-disubstituted benzene, *trans*-cyclohexane or bicyclo[2.2.2]octane. Less common building blocks include 2,5-disubstituted pyrimidine, 2,6-disubstituted naphthalene or 2,5-disubstituted *trans*-dioxane (Figure 3).^{37,38}

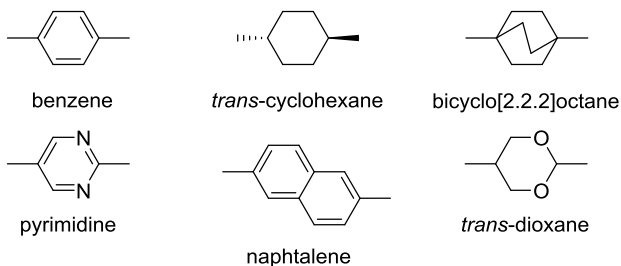


Figure 3. Building blocks of rigid cores of calamitic liquid crystal molecules.

The common flexible tails are alkyl or alkoxy groups. The rigid core elements are connected directly or through a linking group such as: ester, azo, ethylene, acetylene, imine or dimethylene, azoxy, nitron, thioester, azine (Figure 4).^{34,37,38} Proper choice between the flexible tails group and the rigid core elements allows to tune the properties of liquid crystals.

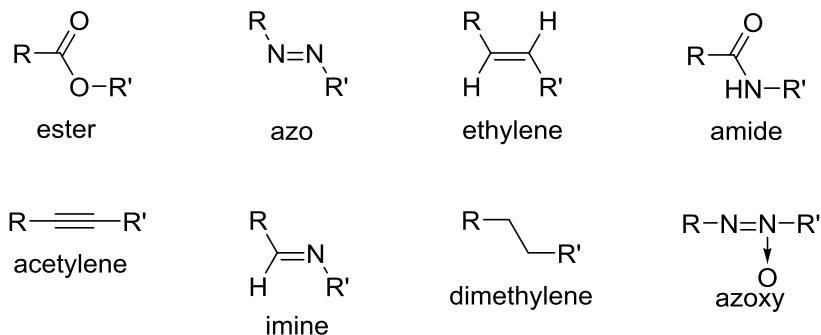


Figure 4. Typical linking groups in used in rod-like mesogens.

Depending on the amount of order in the material, thermotropic liquid crystals form many liquid crystalline phases, called mesophases.^{36,39} As the temperature increases, the ordering of the molecules in the phase decreases and *vice versa*. Transition temperatures can be measured by means of differential scanning calorimetry (DSC), which also is used to establish transition enthalpy. The enthalpy values can also be used for preliminary phase identification. Transition from a crystalline solid to a liquid crystalline phase or the isotropic liquid is usually associated with a considerable structural change of the supramolecular assembly. Typical values of enthalpy for such a transition are in the range of 30-50 kJ/mol. Transitions from a liquid crystalline phase to another liquid crystalline phase or to the isotropic liquid involve much smaller enthalpies of 4-6 kJ/mol. The smallest enthalpies, 1-2 kJ/mol, are related to nematic to isotropic phase transition.³⁸

In an ordinary liquid, referred to as the isotropic phase (I), the molecules are randomly oriented in all directions and they do not have positional order (Figure 5). In the nematic phase (N), the least ordered and the simplest liquid crystalline phase, the molecules exhibit only long-range orientational order. On average, the molecules are oriented along their molecular axes. The direction of their orientation is called the

director and is denoted by \mathbf{n} . The order parameter S gives the average alignment of the long axes of the molecules with respect to the director, and is defined as:

$$S = \frac{1}{2} \langle 3 \cos^2 \theta - 1 \rangle \quad (\text{Equation 1})$$

where θ is the average angle between the molecular axis and the director \mathbf{n} . For an isotropic liquid, $S = 0$. For a perfectly aligned sample, $S = 1$. The order parameter S is in the range of 0.3 - 0.8 for a typical liquid crystalline substance.

As the ordering of the molecules increases, a smectic phase is formed. Smectics possess orientational order, but also partial positional order, forming layers with a well-defined interlayer spacing. The molecules are restricted to flow between the layers, but they can flow freely within the layers in two dimensions and can rotate around their long axis. The molecules are oriented along the director in the smectic A (SmA) phase (the least ordered smectic phase), while in the smectic C (SmC) phase, the molecules are tilted by angle θ , called the tilt angle, with the respect to the layer normal (Figure 5). The interlayer interactions are weaker than the intermolecular interactions, and the layers can slide over each other relatively easily. This leads to higher viscosities in smectics compared to nematics. There exists a few more smectic phases such as hexagonal SmB phase, or pseudo-hexagonal SmF, SmG, SmJ phases.³⁶ An element of chirality in a molecule may induce chiral modification of the liquid crystalline phase. Essentially, all LC phases have their chiral analogues characterized by supramolecular chiralities.

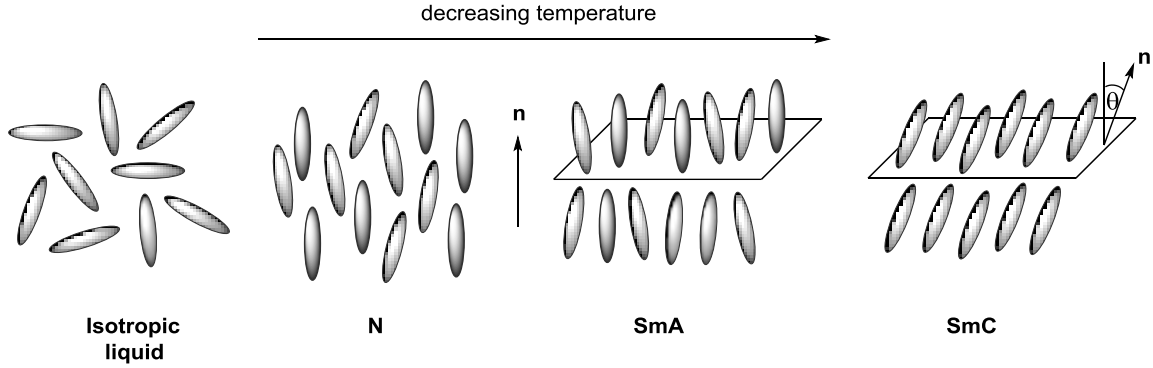


Figure 5. Schematic representations of typical liquid crystal phases: nematic (N), smectic A (SmA), and smectic C (SmC); the arrow represents the director \mathbf{n} and θ is the tilt angle.

Thermotropic liquid crystalline molecules are anisotropic in nature, which means that their properties differ depending on the direction of measurement. The anisometric shape of the molecules is manifested not only in the orientational ordering, but also in anisotropy of their optical, dielectric, magnetic and mechanical properties. Light passing through a layer of liquid crystal undergoes a double refraction. The refractive indices (i.e. velocity) of light propagating perpendicular (ordinary) and parallel (extraordinary) are different. Double refraction, that is birefringence (Δn), is defined as the difference of both the extraordinary (n_e) and ordinary (n_o) refractive indices:⁴⁰

$$\Delta n = n_e - n_o \text{ or } \Delta n = n_{\parallel} - n_{\perp} \quad (\text{Equation 2})$$

When light passes through a polarizer and then through a layer of liquid crystal, the direction of polarization of light may change and the light can pass through the analyzer, which is perpendicular to the polarizer. With no liquid crystal between the polarizer and analyzer, light would not be able to pass through the analyzer. Varying the thickness of a LC layer results in darker and lighter areas. Colors of the textures observed under polarized microscope are a consequence of existence of domains with directors of

different orientations. The observed colors consist of all the wavelengths which were not blocked by the analyzer. The dark regions are areas where the orientation of the director is completely parallel or perpendicular to the polarizer or analyzer. Polarizing optical microscopy is a key tool for studying liquid crystals and phase identification. Many liquid crystal phases can be identified by their distinctive textures that appear in sandwich cells with planar or homeotropic alignment.³³ Both differential scanning calorimetry (DSC) and polarizing optical microscopy (POM), are complementary tools used to identify liquid crystalline phases. When phase identification by POM and DSC is uncertain or impossible, powder X-ray analysis has proven to be a powerful tool in phase structure analysis.

Similar to optical properties, the response of liquid crystals to an external electric field has anisotropic character as well. Dielectric anisotropy, $\Delta\epsilon$, can be defined as the difference between the parallel (ϵ_{\parallel}) and perpendicular (ϵ_{\perp}) dielectric permittivities:

$$\Delta\epsilon = \epsilon_{\parallel} - \epsilon_{\perp} \quad (\text{Equation 3})$$

As a consequence, molecules of materials with $\Delta\epsilon > 0$ reorient parallel to the applied electric field; molecules of materials with $\Delta\epsilon < 0$ reorient perpendicular to the applied electric field.⁴¹

In a classical display based on a twisted nematic cell, a layer of aligned liquid crystal is placed between two electrodes and two polarizers (parallel and perpendicular). In the absence of electric field, the orientation of LC molecules is defined by the alignment at the surface of the electrodes; they are coated with a special polymer, which ensures that the molecules arrange themselves in a twisted structure. In this configuration, direction of linearly polarized light passing through the twisted layer of liquid crystal

undergoes a 90 ° rotation, and the light can pass through the second polarizer. When voltage is applied to the electrodes, the molecules reorient in a way that the molecular dipole moments align with the direction of the electric field, the twist is destroyed and the light cannot pass through the analyzer resulting in dark areas. Reorientation of the molecules by an external electric field requires certain threshold voltage V_{th} (Equation 4) and is called the Fréedericksz transition (Figure 6).⁴²

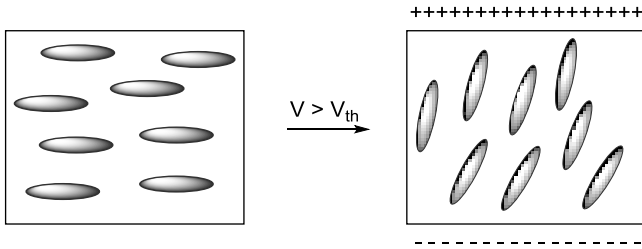


Figure 6. Schematic representation of the Fréedericksz transition.

$$V_{th} = \pi \sqrt{\frac{K}{\Delta\epsilon \cdot \epsilon_0}} \quad \Delta\epsilon \sim \mu^2 (1 - \cos^2 \beta) \quad V_{th} \sim \frac{1}{\mu} \quad (\text{Equation 4})$$

Dielectric anisotropy, $\Delta\epsilon$, is proportional to the molecular dipole moment μ and its orientation. The threshold voltage V_{th} is inversely proportional to dielectric anisotropy $\Delta\epsilon$. Molecules with high dipole moment μ reorient faster and require lower V_{th} . Therefore, molecules with high $\Delta\epsilon$ are attractive for LCD technology.

2.3 Boron clusters as core elements of liquid crystals

Boron clusters possess a number of properties that make them attractive as structural elements of liquid crystals. Many theories of liquid crystals use cylinders to represent liquid crystal molecules. In regard to that, one of the most important features of the boron clusters is their unique three dimensional cylindrical shape (Figure 7).

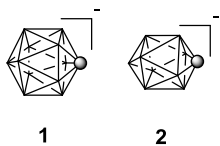


Figure 7. Cylindrical shapes of the 12- (**1**) and 10-vertex (**2**) monocarba-*closo*-borates.

The clusters exhibit σ -aromaticity. They are UV transparent above 200 nm, display large electronic polarizability, while their three-dimensional symmetry guarantees low birefringence (all have average refractive indices).⁴³ High thermal, chemical and electrochemical stability of the clusters often translates into the properties of LC molecules derived from the polyhedral boron hydrides. Moreover, the charge in the anionic clusters is highly delocalized, which makes them one of the nucleophilic anions.⁴⁴ The extent of interaction between the clusters and π substituents may be weaker or stronger, and depends on the type of the clusters and the substituent.⁴⁵ The molecular size of the clusters is larger than those of benzene, bicyclo[2.2.2]octane and cubane.⁴³ Molecular symmetry and size, which define conformational minima, have a significant effect on mesophase stability and are probably the reason why the boron clusters derivatives have been shown to form nematic phase preferentially over other liquid crystalline phases.^{43,46} Functionalization of clusters **1** and **2** at the antipodal positions proceeds smoothly and the current synthetic methods allow for introduction of a variety of substituents.^{47,48}

Carbaborates, which are the subject of this work, are derived from the prototypical [*closo*-B₁₀H₁₀]²⁻ and [*closo*-B₁₂H₁₂]²⁻ dianions. Charge compensation achieved by replacement of one BH vertex with CH fragment leads to monocarba-*closo*-borates, [*closo*-1-CB₉H₁₀]⁻ (**2**) and [*closo*-1-CB₁₁H₁₂]⁻ (**1**). Replacement of another BH

vertex with one more CH fragment gives neutral [*closo*-C₂B₈H₁₀] and [*closo*-1-C₂B₁₀H₁₂] species. Combination of these three types of clusters, dianions, monoanions and neutral species with appropriate substituents gives access to different types of liquid crystals: polar (**QP** – quadrupolar, **DP** - dipolar), ionic (**IO**) and nonpolar (**NP**) (Figure 8).

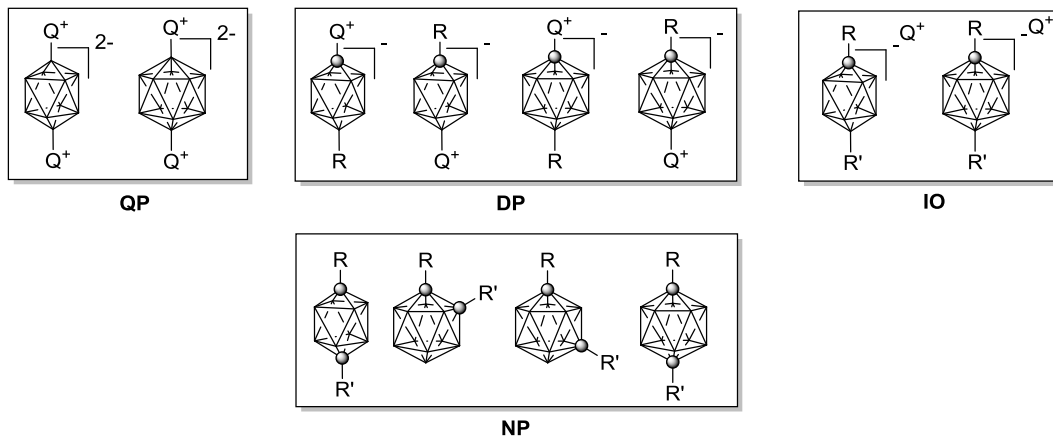


Figure 8. Polar (**QP** and **DP**), ionic (**IO**) and nonpolar (**NP**) derivatives of boron clusters.

Charge compensation in polar materials of type **QP** and **DP** is achieved by attaching a positively charged substituent (Q⁺) such as pyridinium (**1C**, see Table 1),⁴⁹ sulfonium (**2E**)³¹ or quinuclidinium (**2A**).²⁸ Ionic liquid crystals (type **IO**) require an organic or inorganic cation.^{30,50}

The resulting quadrupolar and dipolar molecules (type **QP** and **DP**) possess high dipole moments.^{28,31} Advantageously, the molecular dipole moment in these derivatives is oriented along the molecule's long axis. High dipole moment is critical for electro-optical applications as the resulting high dielectric anisotropy ensures fast response of the material to the applied electric field (see Equation 4).

A great number of liquid crystalline materials containing the 10- and 12-vertex boron clusters as structural elements have been prepared and investigated up to date. The first group of liquid crystalline materials that were investigated were those derived from the neutral *p*-carboranes (**NP**, Figure 8). The results clearly indicated that the boron clusters are nematogenic, that is, they promote formation of a nematic phase.^{51,52} Only in few cases *p*-carboranes derivatives display smectic phase.⁵³ It was also found that the thermal stability of mesophase was lower than that of benzene and bicyclo[2.2.2]octane. Due to the nonpolar character of the *p*-carboranes, this type of liquid crystals is not of special interest and has little importance in the search for materials for technological applications.

Much more promising for LCD applications are polar materials based on the [*closo*-1-CB₉H₁₀]⁻ (**2**) and [*closo*-1-CB₁₁H₁₂]⁻ (**1**) anions (**DP**, Figure 8). Upon proper substitution with a pyridinium, sulfonium or quinuclidinium fragment (See Chapter 1, Figure 1), one can obtain compounds characterized by high dipole moment. Initially, there was a limited use of the 10-vertex monocarba-*closo*-borate anion due to the lack of method of functionalization of the cluster. The discovery of the Brelloch's reaction{Brellochs, 2004 #124} opened access to functionalized 1,10-disubstituted derivatives of the [*closo*-1-CB₉H₁₀]⁻ (**2**) anion.⁵⁴ These derivatives gave the opportunity to design highly polar materials for electrooptical applications. The 10-iodo derivatives became key intermediates to sulfonium, pyridinium and quinuclidinium derivatives (See Chapter 1, Figure 1). 1-Quinuclidinium (**2A**) and 1-sulfonium (**2B**) derivatives of the [*closo*-1-CB₉H₁₀]⁻ anion (**2**) did not exhibit liquid crystalline properties, but they greatly enhanced the dielectric anisotropy $\Delta\epsilon$ of a nematic host.²⁸ Sulfonium and pyridinium

zwitterions of the [*closo*-1-CB₉H₁₀]⁻ (**2**) cluster (**2E** and **2F**, respectively) substituted at the B(10) position exhibited nematic phase, were more compatible with a nematic host, showed greater miscibility, and significantly increased the $\Delta\epsilon$ of the host.^{31,55} One of the esters had extrapolated value of $\Delta\epsilon$ of 113.⁵⁵ Newly developed and improved synthetic methods opened access to polar 1-pyridinium derivatives of the [*closo*-1-CB₉H₁₀]⁻ (**2**) and [*closo*-1-CB₁₁H₁₂]⁻ (**1**) anions (**2C** and **1C**, respectively).²⁹ These derivatives were found to have good properties as for highly polar materials suitable for electrooptical applications. Few of the materials exhibited smectic A phase driven by dipolar interactions. 12-Pyridinium derivatives (type **1F**) were also found to exhibit nematic behavior.^{49,56} Polar derivatives are the most promising group of derivatives of both 10- and 12-vertex monocarba-*closo*-borates for technological applications.

A relatively new group of liquid crystalline materials derived from carboranes are ionic liquid crystals (type **1G** and **2G**, see Table 1). They represent a new concept in design of ILCs. It was found that it was the carborane-derived anion, not the organic cation, that is the source of mesogenicity.⁵⁰ Some of the derivatives exhibited smectic A and nematic phases.³⁰ Ionic liquid crystals are of potential interest as electrolytes in batteries and dye-sensitized solar cells.

References

- (1) Adams, R. M. *Boron, metallo-boron compounds and boranes*; Interscience Publishers: New York, 1964.
- (2) Muetterties, E. L. *The chemistry of boron and its compounds*; John Wiley & Sons, Inc.: New York, 1967.

- (3) Sivaev, I. B.; Bregadze, V. V. *Polyhedral boron hydrides in use: current status and perspectives*; Nova Science Publishers, Inc: New York, NY, 2009.
- (4) Dickerson, R. E.; Lipscomb, W. N., Semitopological approach to boron - hydride structures. *J. Chem. Phys.* **1957**, *27*, 212-217.
- (5) Pitochelli, A. R.; Hawthorne, F. M., The isolation of the icosahedral $B_{12}H_{12}^{-2}$ ion. *J. Am. Chem. Soc.* **1960**, *82*, 3228-3229.
- (6) Little, J. L.; Moran, J. T.; Todd, L. J., Phosphaboranes and carbaphosphaboranes. *J. Am. Chem. Soc.* **1967**, *89*, 5495-5496.
- (7) Getman, T. D.; Deng, H. B.; Hsu, L. Y.; Shore, S. G., Synthesis of *closo*-1-methylphosphadodecaborane(12), $B_{11}H_{11}PCH_3$ and *nido*-7-methylphosphaundecaborane(13), $B_{10}H_{12}PCH_3$, from the $[B_{11}H_{13}]^{2-}$ anion and their molecular structures. *Inorg. Chem.* **1989**, *28*, 3612-3616.
- (8) Pretzer, W. R.; Rudolph, R. W., New heteroborane, 1-thia-*closo*-decaborane(9) B_9H_9S . *J. Am. Chem. Soc.* **1973**, *95*, 931-932.
- (9) Hnyk, D.; Vajda, E.; Buehl, M.; von Rague Schleyer, P., Molecular structure of 1-thia-*closo*-dodecaborane(II) studied by electron diffraction complemented by ab initio calculations. *Inorg. Chem.* **1992**, *31*, 2464-2467.
- (10) Najafian, K.; von Rague Schleyer, P.; Tidwell, T. T., Stability and three-dimensional aromaticity of *closo*- $NB_{n-1}H_n$ azaboranes, $n = 5-12$. *Inorg. Chem.* **2003**, *42*, 4190-4203.
- (11) Little, J. L.; Friesen, G. D.; Todd, L. J., Preparation and properties of selenaboranes and telluraboranes. *Inorg. Chem.* **1977**, *16*, 869-872.

- (12) Chapman, R. W.; Kester, J. G.; Folting, K.; Streib, W. E.; Todd, L. J., Synthesis and chemistry of $B_{11}H_{11}Sn^{2-}$ and its germanium and lead analogs. Crystal structure of $[B_{11}H_{11}SnCH_3]PPh_3CH_3 \cdot CH_2Cl_2$. *Inorg. Chem.* **1992**, *31*, 979-983.
- (13) Molinos, E.; Player, T. P. H.; Kociok-Köhn, G.; Ruggerio, G. D.; Weller, A. S., $[1-Me-1-closo-SnB_{11}H_{11}]^-$ as a potential weakly coordinating anion: Synthesis of $Rh(PPh_3)_2(1-Me-closo-SnB_{11}H_{11})$ and comparisons with $Rh(PR_3)_2(1-H-closo-CB_{11}H_{11})$. *Heteroat. Chem.* **2006**, *17*, 174-180.
- (14) Hagen, S.; Pantenburg, I.; Weigend, F.; Wickleder, C.; Wesemann, L., Gold-Gold interaction-stannaborate $[SnB_{11}H_{11}]^{2-}$ coordination chemistry. *Angew. Chem. Int. Ed.* **2003**, *42*, 1501-1505.
- (15) Sivaev, I. B.; Bregadze, V. V.; Sjöberg, S., Chemistry of *closo*-dodecaborate anion $[B_{12}H_{12}]^{2-}$: A review. *Collect. Czech. Chem. Commun.* **2002**, *67*, 679-727.
- (16) Lipscomb, W. N. *Boron hydrides*; W. A. Benjamin, Inc.: New York, 1963.
- (17) Sivaev, I. B.; Bregadze, V. V.; Kuznetsov, N. T., Derivatives of the *closo*-dodecaborate anion and their application in medicine. *Russ. Chem. Bull., Intl. Ed.* **2002**, *51*, 1362-1374.
- (18) Sivaev, I. B.; Bregadze, V. V., Polyhedral boranes for medical applications: current status and perspectives. *Eur. J. Inorg. Chem.* **2009**, 1433-1450.
- (19) Gu, W.; Haneline, M. R.; Douvris, C.; Ozerov, O. V., Carbon-carbon coupling of $C(sp^3)-F$ bonds using alumenium catalysis. *J. Am. Chem. Soc.* **2009**, *131*, 11203-11212.

- (20) Douvris, C.; Ozerov, O. V., Hydrodefluorination of perfluoroalkyl groups using silylium-carborane catalysts. *Science* **2008**, *321*, 1188-1190.
- (21) Gratton, S. E. A.; Parrott, M. C.; Adronov, A., Preparation of carborane-containing polymers by atom transfer radical polymerization. *J. Inorg. Organomet. Polym. Mater.* **2005**, *15*, 469-475.
- (22) Parrott, M. C.; Marchington, E. B.; Valliant, F.; Adronov, A., Synthesis and properties of carborane-functionalized aliphatic polyester dendrimers. *J. Am. Chem. Soc.* **2005**, *127*, 12081-12089.
- (23) Morin, J.-F.; Sasaki, T.; Shirai, T.; Guerrero, J. M.; Tour, J. M., Synthetic routes toward carborane-wheeled nanocars. *J. Org. Chem.* **2007**, *72*, 9481-9490.
- (24) Prokop, A.; Vacek, J.; Michl, J., Friction in carborane-based molecular rotors driven by gas flow or electric field: classical molecular dynamics. *ACS Nano* **2012**, *6*, 1901-1914.
- (25) Brown, D. A.; Colquhoun, H. M.; Daniels, J. A.; MacBride, J. A. H.; Stephenson, I. R.; Wade, K., Polymers and ceramics based on icosahedral carboranes. Model studies of the formation and hydrolytic stability of aryl ether, ketone, amide and borane linkages between carborane units. *J. Mater. Chem.* **1992**, *2*, 793-804.
- (26) Tsuboya, N.; Lamrani, M.; Hamasaki, R.; Ito, M.; Mitsuishi, M.; Miyashita, T.; Yamamoto, Y., Nonlinear optical properties of novel carborane-ferrocene conjugated dyads. Electron-withdrawing characteristics of carboranes *J. Mater. Chem.* **2002**, *12*, 2701-2705.
- (27) Abe, J.; Nemoto, N.; Nagase, Y.; Shirai, Y.; Iyoda, T., A new class of carborane compounds for second-order nonlinear optics: ab initio molecular orbital study

of hyperpolarizabilities for 1-(1',X'-Dicarba-*closo*-dodecaborane-1'-yl)-*closo*-dodecaborate dianion (X = 2, 7, 12). *Inorg. Chem.* **1998**, *37*, 172-173.

(28) Ringstrand, B.; Kaszynski, P.; Januszko, A.; Young, V. G. Jr., Polar derivatives of the [*closo*-1-CB₉H₁₀]⁻ cluster as positive Δε additives to nematic hosts. *J. Mater. Chem.* **2009**, *19*, 9204-9212.

(29) Pecyna, J.; Pocięcha, D.; Kaszynski, P., Zwitterionic pyridinium derivatives of [*closo*-1-CB₉H₁₀]⁻ and [*closo*-1-CB₁₁H₁₂]⁻ as high Δε additives to a nematic host. *J. Mater. Chem. C* **2014**, *2*, 1585-1591.

(30) Ringstrand, B.; Jankowiak, A.; Johnson, L. E.; Pocięcha, D.; Kaszynski, P.; Gorecka, E., Anion-driven mesogenicity: a comparative study of ionic liquid crystals based on the [*closo*-1-CB₉H₁₀]⁻ and [*closo*-1-CB₁₁H₁₂]⁻ clusters. *J. Mater. Chem.* **2012**, *22*, 4874-4880.

(31) Pecyna, J.; Kaszynski, P.; Ringstrand, B.; Bremer, M., Investigation of high Δε derivatives of the [*closo*-1-CB₉H₁₀]⁻ anion for liquid crystal applications. *J. Mater. Chem. C* **2014**, *2*, 2956-2964.

(32) Reinizter, F., Beiträge zur Kenntniss des Cholesterins. *Monatsch. Chem.* **1888**, *9*, 421-441.

(33) Demus, D.; Goodby, J. W.; Gray, G. W.; Spiess, H.-W.; Vill, V. *Handbook of liquid crystals*; Wiley-VCH: New York, 1998; Vol. 1.

(34) Khoo, I.-C. *Liquid crystals, Second edition*; Wiley & Sons, Inc.: Hoboken, NJ, 2007.

(35) Vicari, L. *Optical application of liquid crystals*; IOP Publishing Ltd.: Philadelphia, PA, 2003.

- (36) Singh, S. *Liquid crystals: fundamentals*; World Scientific Publishing C. Pte. Ltd.: River Edge, NJ, 2002.
- (37) Kumar, S. *Liquid crystals. Experimental study of physical properties and phase transitions*; Cambridge University Press: Cambridge, UK, 2001.
- (38) Collings, P. J.; Hird, M. *Introduction to liquid crystals: chemistry and physics*; CRC Press: Bristol, PA, 1997.
- (39) Blinov, L. M. *Structure and properties of liquid crystals*; Springer: New York, NY, 2011.
- (40) Chen, R. H. *Liquid crystals displays. Fundamental physics and technology*; Wiley & Sons, Inc.: Hoboken, NJ, 2011.
- (41) Yang, D.-K.; Wu, S.-T. *Fundamentals of liquid crystal devices*; John Wiley & Sons, 2006.
- (42) Fréedericksz, V.; Zolina, V., Forces causing the orientation of an anisotropic liquid. *Trans. Faraday Soc.* **1933**, 29, 919-930.
- (43) Kaszynski, P.; Douglass, A. G., Organic derivatives of *closo*-boranes: a new class of liquid crystal materials. *J. Organomet. Chem.* **1999**, 581, 28-38.
- (44) Reed, C. A., Carboranes: a new class of weakly coordinating anions for strong electrophiles, oxidants, and super acids. *Acc. Chem. Res.* **1998**, 31, 133-139.
- (45) Kaszynski, P.; Pakhomov, S.; Young, V. G. J., Investigations of electronic interactions between *closo*-boranes and triple-bonded substituents. *Collect. Czech. Chem. Commun.* **2002**, 67, 1061-1083.

- (46) Piecek, W.; Kaufman, J. M.; Kaszynski, P., A comparison of mesogenic properties for one- and two-ring dipentyl derivatives of *p*-carboranes, bicyclo[2.2.2]octane, and benzene. *Liq. Cryst.* **2003**, *30*, 39-48.
- (47) Ringstrand, B.; Kaszynski, P., Functionalization of the [*closo*-1-CB₉H₁₀]⁻ anion for the construction of new classes of liquid crystals. *Acc. Chem. Res.* **2013**, *46*, 214-225.
- (48) Körbe, S.; Sowers, D. B.; Franken, A.; Michl, J., Preparation of 1-*p*-halophenyl and 1-*p*-biphenyl substituted monocarbadodecaborate anions [*closo*-1-Ar-CB₁₁H₁₁]⁻ by insertion of arylhalocarbenes into [*nido*-B₁₁H₁₄]⁻. *Inorg. Chem.* **2004**, *43*, 8158-8161.
- (49) Pecyna, J.; Ringstrand, B.; Domagala, S.; Kaszynski, P.; Wozniak, K., Synthesis of 12-pyridinium derivatives of the [*closo*-1-CB₁₁H₁₂]⁻ anion. *Inorg. Chem.* **2014**, *53*, 12617-12626.
- (50) Ringstrand, B.; Kaszynski, P.; Monobe, H., Anion-driven mesogenicity: ionic liquid crystals based on the [*closo*-1-CB₉H₁₀]⁻ cluster. *J. Mater. Chem.* **2009**, *19*, 4805-4812.
- (51) Czuprynski, K. L.; Kaszynski, P., Homostructural two-ring mesogens: a comparison of *p*-carboranes, bicyclo[2.2.2]octane and benzene as structural elements. *Liq. Cryst.* **1999**, *26*, 775-778.
- (52) Czuprynski, K. L.; Douglass, A. G.; Kaszynski, P.; Drzewinski, W., Carborane-containing liquid crystals: a comparison of 4-octyloxy-4'-(12-pentyl-1,12-dicarbadodecaboran-1-yl) with its hydrocarbon analogs. *Liq. Cryst.* **1999**, *26*, 261-269.

- (53) Douglass, A. G.; Czuprynski, K.; Mierzwa, M.; Kaszynski, P., Effects of carborane-containing liquid crystals on the stability of smectic phases. *Chem. Mater.* **1998**, *10*, 2399-2402.
- (54) Ringstrand, B.; Balinski, A.; Franken, A.; Kaszynski, P., A practical synthesis of isomerically pure 1,10-difunctionalized derivatives of the [*closo*-1-CB₉H₁₀]⁻ anion. *Inorg. Chem.* **2005**, *44*, 9561-9566.
- (55) Ringstrand, B.; Kaszynski, P., High $\Delta\epsilon$ nematic liquid crystals: fluxional zwitterions of the [*closo*-1-CB₉H₁₀]⁻ cluster. *J. Mater. Chem.* **2011**, *21*, 90-95.
- (56) Pecyna, J.; Denicola, R. P.; Gray, H. M.; Ringstrand, B.; Kaszynski, P., The effect of molecular polarity on nematic phase stability in 12-vertex carboranes. *Liq. Cryst.* **2014**, *41*, 1188-1198.

2.4 The [*closo*-1-CB₁₁H₁₂]⁻ cluster - chemistry and properties

2.4.1 General information

The [*closo*-1-CB₁₁H₁₂]⁻ anion has been the subject of several reviews, which focus on different aspects of the cluster. The most recent paper by Michl et al.¹ is concentrated mostly on the properties and chemistry of the monocarba-*closo*-dodecaborate anion [*closo*-1-CB₁₁H₁₂]⁻ anion and its derivatives. This comprehensive review covers the published work since the previous review by Štibr in 1992.² The cluster and its derivatives have been extensively studied as one of the most weakly-coordinating anions, and the previous reports concentrated mainly on this aspect. The most notable reviews include those by Reed^{3,4} and Strauss.⁵ Similar work was published by Raabe⁶ and Seppelt.⁷ A chapter dedicated to the [*closo*-1-CB₁₁H₁₂]⁻ cluster is also included in a comprehensive book by Grimes.⁸

The following chapter is a review of functionalization methods of the [*closo*-1-CB₁₁H₁₂]⁻ anion in positions 1 and 2 (antipodal positions) suitable for the design of elongated liquid crystal molecules. The review starts with a brief introduction to *closo*-boranes, which is followed by the methods of synthesis of the [*closo*-1-CB₁₁H₁₂]⁻ anion. Next, methods of functionalization of the carbon vertex are reviewed, followed by similar review of methods for introduction of substituents on the B(12) boron vertex. The review ends with a short summary.

2.4.2 The [*closo*-1-CB₁₁H₁₂]⁻ anion

The monocarba-*closo*-dodecaborate anion [*closo*-1-CB₁₁H₁₂]⁻ (**1**) (Figure 9), belongs to a broad group of polyhedral borane and carborane clusters characterized by delocalized electron-deficient 3-center-2-electron bonding.

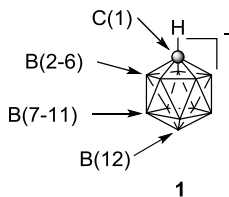


Figure 9. Skeletal representations of the $[\textit{closo}\text{-}1\text{-CB}_{11}\text{H}_{12}]^{-}$ (**1**) cluster. Each vertex represents a B–H fragment and the dark sphere a carbon atom.

Electron-deficiency is compensated by the formation of trigonal faces and hypercoordination.⁹ The unusual delocalized bonding results in high chemical, thermal and electrochemical stability of the cluster. The chemical inertness, even towards the most aggressive reagents, is often reflected in the properties of the molecules containing the clusters. The $[\textit{closo}\text{-}1\text{-CB}_{11}\text{H}_{12}]^{-}$ and its polyhalo and polyalkyl derivatives are among the least coordinating anions, while their conjugate acids are the strongest Brønsted acids known.¹⁰ The low-toxicity of the *closo*-boranes made them suitable for boron neutron capture therapy.¹¹⁻¹³ The $[\textit{closo}\text{-}1\text{-CB}_{11}\text{H}_{12}]^{-}$ (**1**) anion aside with its 10-vertex analogue, $[\textit{closo}\text{-}1\text{-CB}_9\text{H}_{10}]^{-}$ cluster, possess certain properties that make them very attractive as building elements of many compounds, including liquid crystals. Both clusters have unique geometry and highly delocalized negative charge, which allows for the formation of polar and ionic liquid crystals molecules. Examples are shown in Figure 10.

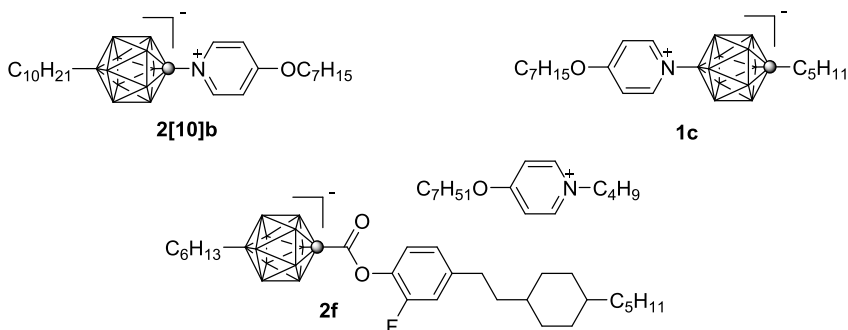


Figure 10. Examples of zwitterionic (**2[10]b**, **1c**)^{14,15} and ionic (**2f**)¹⁶ liquid crystals derived from **1**.

Moreover, functionalization of the clusters at the antipodal positions, which is essential from the point of view of synthesis of elongated liquid crystal molecules, proceeds relatively smoothly.

The [*closo*-1-CB₁₁H₁₂]⁻ (**1**) anion can be considered as a derivative of the prototypical [*closo*-B₁₂H₁₂]²⁻ dianion, in which one of the boron vertices has been replaced with a carbon atom leading to the monoanion **1**.

The [*closo*-1-CB₁₁H₁₂]⁻ cluster was first prepared by Knoth in 1967 in five steps from commercially available decaborane B₁₀H₁₄ (**2**) and sodium cyanide (Figure 11).^{17,18} Thus, treatment of decaborane (**2**) with NaOH/NaCN mixture gives 10-vertex [*arachno*-6-(CN)B₁₀H₁₃]²⁻ cluster (**3**). Subsequent addition of HCl leads to incorporation of the carbon into the polyhedral structure to give 11-vertex species [*nido*-7-H₃N-7-CB₁₀H₁₂]⁻ (**4**). The amino group is then methylated with dimethyl sulfate to give [*nido*-7-Me₃N-7-CB₁₀H₁₂]⁻ (**5**) intermediate, which is reduced with Na in liquid ammonia to yield [*nido*-CB₁₀H₁₃]⁻ (**6**). The last step involves heating the deaminated *nido* product **6** in neat BH₃·NEt₃ to give pure [*closo*-1-CB₁₁H₁₂]⁻ anion (**1**). The reaction, however, poses some

safety issues since gaseous HCN is produced in one of the steps. Moreover, it includes reduction with sodium in liquid ammonia, and boron insertion stage requires heating up to 200 °C (Figure 11).

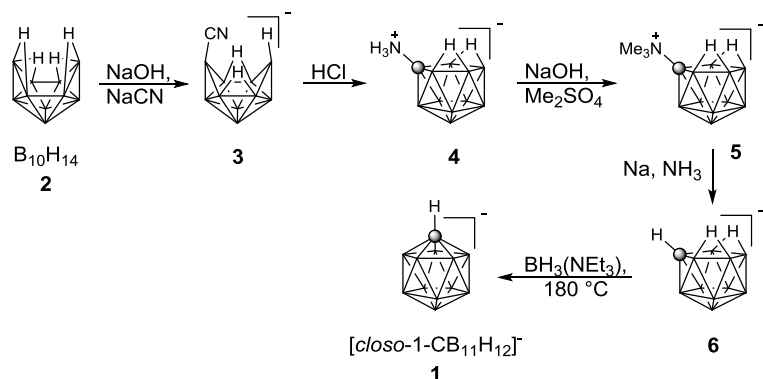


Figure 11. Synthesis of **1** by Knoth et al.^{17,18}

Soon, a modification of Knoth's method was developed by Heřmánek, but it was still a multi-step process, which required high temperatures and the use of cyanides.¹⁹ More conveniently, the cluster can be prepared in just two steps using the Breilochs protocol in which decaborane, $\text{B}_{10}\text{H}_{14}$ (**2**), is reacted with formaldehyde in the presence of a base for several hours at rt. The resulting intermediate, $[\text{nido-6-CB}_9\text{H}_{12}]^-$ (**7**), undergoes a double BH vertex insertion giving the anion **1** in about 65% overall yield (Figure 12).²⁰

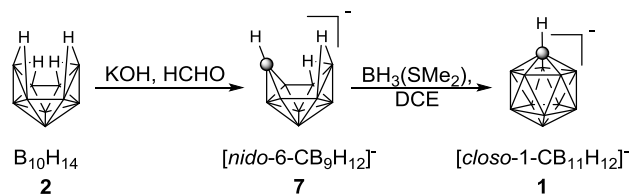


Figure 12. Synthesis of **1** by Kennedy.²⁰

This 2-step process is in contrast to the multi-step synthesis of derivatives of the $[\text{closo-CB}_9\text{H}_{10}]^-$ cluster. As far as many methods of functionalization of the $[\text{closo-}$

$\text{CB}_{11}\text{H}_{12}]^-$ (**1**) were developed soon after its discovery, synthesis of functionalized derivatives of the $[\textit{closo}\text{-}1\text{-CB}_9\text{H}_{10}]^-$ anion were practically unknown until the discovery of the Brellocks reaction and synthesis of the isomerically pure 1,10-difunctionalized derivatives of the $[\textit{closo}\text{-}1\text{-CB}_9\text{H}_{10}]^-$ anion,²¹ which makes the synthesis and use of the $[\textit{closo}\text{-}1\text{-CB}_{11}\text{H}_{12}]^-$ (**1**) more practical.

2.4.3 Functionalization of the $[\textit{closo}\text{-}1\text{-CB}_{11}\text{H}_{12}]^-$ cluster

There are four distinct sites for functionalization of the $[\textit{closo}\text{-}1\text{-CB}_{11}\text{H}_{12}]^-$ (**1**) cluster, the carbon vertex and the boron vertices: C(1), B(2-6), B(7-11) and B(12) (Figure 9).

The difference in reactivity pattern results from the fact that the C–H bond is relatively acidic, and the B–H bonds have hydridic character.³ Additionally, the cluster can undergo a redox process of removal of a delocalized electron, or a process of addition of an electron to the cage. Furthermore, the substituents on the cluster can be transformed into other groups. And lastly, a cage atom extrusion from the cluster has been demonstrated.⁹

Since the carbon vertex in **1** is weakly acidic, it can be deprotonated using strong bases such as alkyllithiums. The resulting 1-lithio derivatives can then react with different electrophiles. As shown by experimental data, the pK_a of the Li^+ salt of **1** in DMSO is about 21.7.⁹ However, the acidity of the carbon vertex strongly depends on the cluster substitution. Some substituents may increase, while other may decrease the C–H bond acidity. For instance, deprotonation of polyhalogenated derivatives of **1** runs smoothly, while the same deprotonation of polymethylated clusters is virtually impossible.²²

On the other hand, the B–H bonds have hydridic character and are prone to electrophilic attack with the B(12) vertex being the most reactive. The B(7-11) vertices are only slightly less susceptible towards electrophiles. The B(2-6) vertices are the weakest nucleophiles. Alike the C–H bond acidity, the reactivity of the B–H bond is strongly dependent on the cluster substitution. For instance, an exhaustive methylation of 1-halo derivatives of **1** with methyl triflate in sulfolane at room temperature runs in only 6 hours if the halide is fluorine. The process takes 6 days if chlorine is the C(1)-substituent. When bromine or iodine are the substituents, the reaction is complete in 25 and 46 days, respectively.²²

Electrophilic substitution at the boron vertices plays an important role in synthesis of key intermediates incorporating the boron clusters. An important advantage of using $[closo-1-CB_{11}H_{12}]^-$ over $[closo-1-CB_9H_{10}]^-$ anion is the fact that in the $[closo-1-CB_{11}H_{12}]^-$ anion, electrophilic attack occurs preferentially at the B(12) position, antipodal to C(1), which is in contrast to the $[closo-1-CB_9H_{10}]^-$ cage, where the electrophile attacks mainly the B(6) vertex (Figure 13).

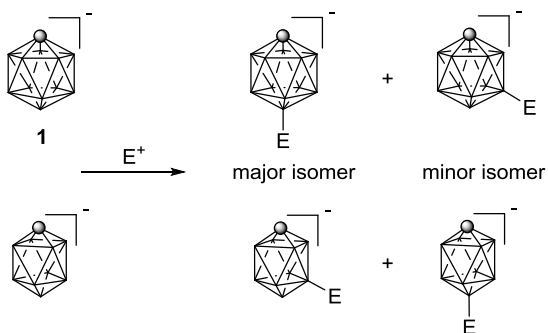


Figure 13. Electrophilic substitution in the $[closo-1-CB_{11}H_{12}]^-$ (**1**) and $[closo-1-CB_9H_{10}]^-$ clusters.

Functionalization of **1** has become more and more diverse. The current synthetic methods allow for introduction of a wide variety of functional groups on the cluster. The following paragraphs will highlight some of the methods of functionalization of the antipodal positions (C(1) and B(12) vertices), which are important for synthesis of functional molecules, with special emphasis on liquid crystals.

2.4.4 Carbon substitution

Carbon-carbon bonds

Due to acidic character of the C–H bond, deprotonation of the carbon vertex proceeds easily using strong bases such as *n*-butyllithium. High nucleophilicity of the anions derived from **1** and its derivatives makes them reactive towards a wide range of carbon electrophiles, which constitutes a convenient method for the formation of C(1)–C bond. For instance, treatment of a solution of **1** in THF with *n*-BuLi leads to the formation of a C(1)–lithio derivative, which undergoes alkylation with primary alkyl,^{23,24} allyl,²⁵ and benzyl²⁴ bromides and iodides (Figure 14).

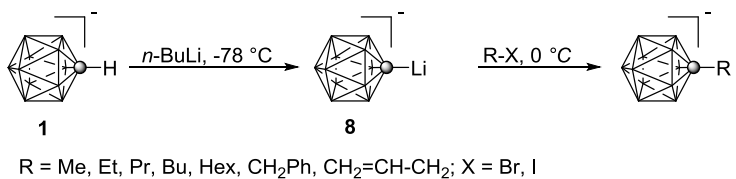


Figure 14. Substitution at the carbon vertex in **1**.

Introduction of aryl substituents, however, requires different conditions. Typical routes to C(1)-aryl substituted derivatives of **1** follow the Brelochs' protocol. For example, decaborane, B₁₀H₁₄ (**2**), is treated with PhCHO in KOH to give [6-Ph-*nido*-6-CB₉H₁₁][−] (**9**), which then undergoes a double boron insertion to yield [*closo*-1-Ph-1-

$CB_{11}H_{11}]^-$ (**10**).²⁶ This path, however, leads to a 2:1 mixture (75% combined yield) of $[closo-1-Ph-1-CB_{11}H_{11}]^-$ (**10**) and $[closo-1-Ph-1-CB_9H_9]^-$ (**11**) clusters, respectively (Figure 15).

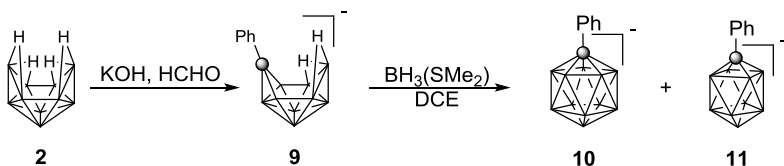


Figure 15. Synthesis of C-phenyl derivatives of **1** by Breloch's protocol.

An alternative method follows insertion of arylhalocarbenes into $[nido-B_{11}H_{13}]^{2-}$ species (**12**), but gives the products, *p*-halophenyl and *p*-biphenyl substituted monocarbadodecaborate anions (**13**), in low to moderate yield (12-41%) (Figure 16).²⁷

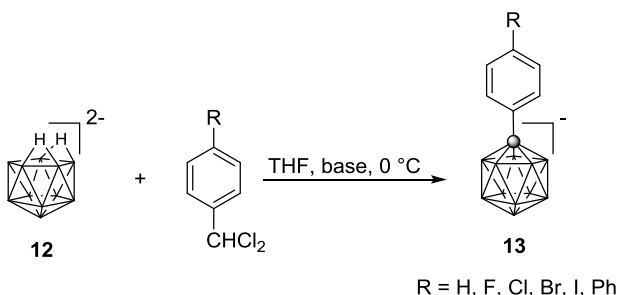


Figure 16. Synthesis of C-substituted aryl derivatives of **1** by insertion of arylhalocarbenes into $[nido-B_{11}H_{13}]^{2-}$ **12**.

Recently, a more efficient method for $C_{cage}-C_{aryl}$ bond formation was developed, which utilizes the Wade's arylation protocol. The new protocol not only gives the C(1)-substituted aryl derivatives in higher yields and higher purity, but also extends the scope of substituents to alkenyls, alkynyls and heteroaryls. The method includes conversion of **1** into its C(1)-lithio derivative, followed by formation of copper(I) carborate

intermediate **14**, which, subsequently, is reacted with appropriate iodide or bromide in the presence of palladium catalyst at room temperature (Figure 17).²⁸

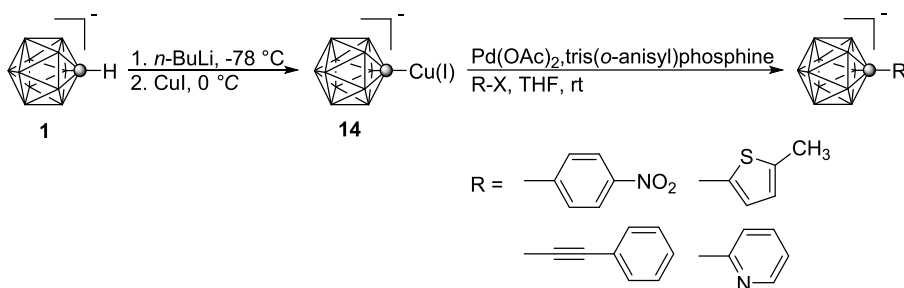


Figure 17. Cross-coupling reaction between C-metalated carborane anion **14** and aryl halides.

The reaction proceeds smoothly in just several hours at room temperature and uses commonly available Pd catalyst and copper(I) iodide.

Other carbon electrophiles that can easily react with the monocarboranyl carbanions include carbon dioxide, giving the corresponding carboxylic acids. For example, lithiation of **1** or 12-iodo derivative **15** in THF in the presence of TMEDA, and treatment of the resulting carbanions with CO_2 give the [*closo*-1- $\text{CB}_{11}\text{H}_{11}$ -1-COOH]⁻ (**16**),²⁹ and [*closo*-1- $\text{CB}_{11}\text{H}_{10}$ -1-COOH-12-I]⁻ (**17**) acids,²³ respectively (Figure 18).

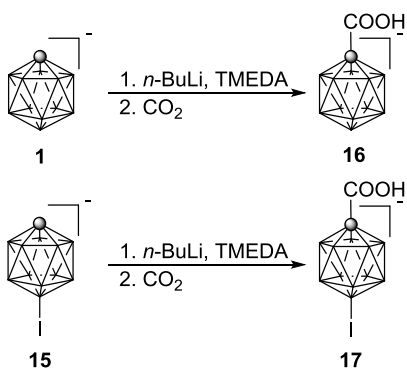


Figure 18. Synthesis of carboxylic acids **16** and **17**.

Other carbonyl compounds are also susceptible to nucleophilic attack by the monocarbaborate carbanions. Thus, a reaction between the 1-lithio derivative **8** and aldehydes or propylene oxide affords monocarbododecaborate alcohols **18** in high yields (Figure 19).³⁰ Such alcohols can be used in synthesis of other derivatives incorporating the cluster.

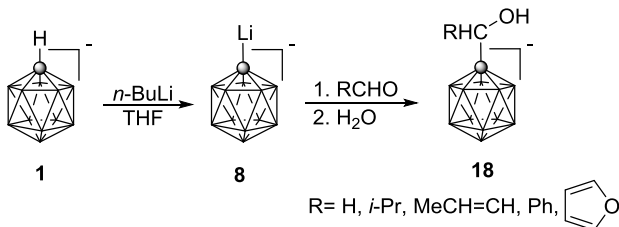


Figure 19. Synthesis of functionalized monocarbododecaborate alcohols **18** based on **1**.

Currently, there are two ways of introduction of the cyano group onto the carbon vertex. The first approach is a two-step process that involves lithiation of the C–H bond in **1** and subsequent treatment of the resulting lithium intermediate **8** with phenyl cyanate.³¹ The products are obtained in high to excellent yields (Figure 20). The resulting [*closo*-1-CB₁₁X₁₁-1-CN]⁻ salts (X = H, F, Cl, Br, I) are stable against aqueous solutions of acids and bases except for the perfluoro derivative.

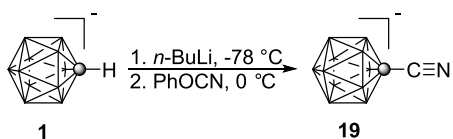


Figure 20. Synthesis of 1-cyano derivative **19** of the [*closo*-1-CB₁₁H₁₂]⁻ cluster **1**.

The second path to cyano derivatives requires conversion of derivative **20** to carboxylic acid **21**, which then is treated with DCC, DMAP, and NH₃ is added at -78 °C to yield an amide **23** in 76% yield. The amide **23** is then dehydrated with oxalyl chloride

and trimethylamine in DMF at $-196\text{ }^{\circ}\text{C}$ to afford the desired nitrile **24** in 87% yield (Figure 21).³²

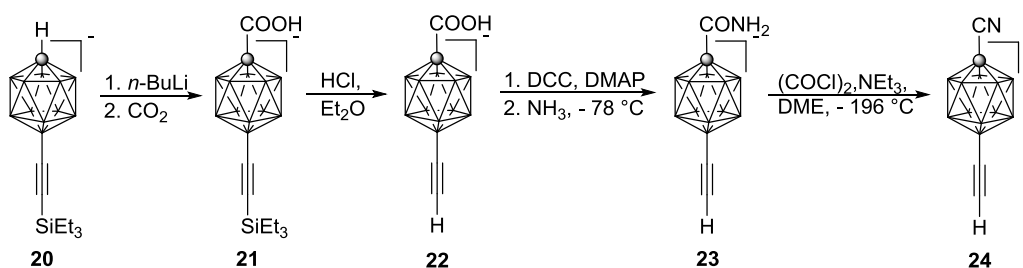


Figure 21. Conversion of carboxylic acid **22** into nitrile **24**.

The overall yields for $[\textit{closo}\text{-}1\text{-CB}_{11}\text{H}_{11}\text{-}1\text{-CN}]^{-}$ (**19**) by both methods are similar and are 84% and 76% for cyanate and amide routes, respectively.

Carbon-nitrogen bonds

The number of compounds containing C(1)–N bond is smaller than the number of species with the C(1)–C bond. One of the first examples includes the synthesis of the parent amine $[\textit{closo}\text{-}1\text{-CB}_{11}\text{H}_{11}\text{-}1\text{-NH}_3]$ amine (**25**). The preparation of **25** involves conversion of decaborane, $\text{B}_{10}\text{H}_{14}$ (**2**), into $[\textit{nido}\text{-}7\text{-H}_3\text{N}\text{-}7\text{-CB}_{10}\text{H}_{12}]$ (**4**) intermediate, which is then heated up to $220\text{ }^{\circ}\text{C}$ in the presence of $\text{NEt}_3\cdot\text{BH}_3$ giving $[\textit{closo}\text{-}1\text{-CB}_{11}\text{H}_{11}\text{-}1\text{-NH}_3]$ (**25**) as shown in Figure 22.^{19,29} The amine is a relatively strong acid and its measured pK_a is about 6.03.

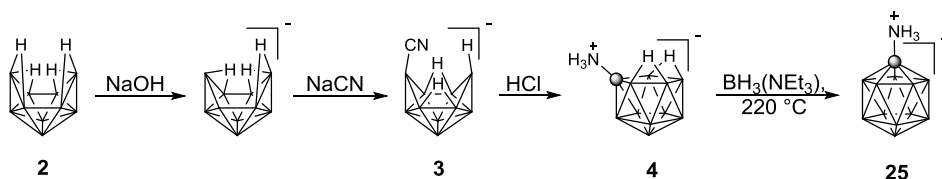


Figure 22. Synthesis of $[\textit{closo}\text{-}1\text{-CB}_{11}\text{H}_{11}\text{-}1\text{-NH}_3]$ amine (**25**).

The amine **25** is a key intermediate in synthesis of other important derivatives, such as the iodo amine [*closo*-1-CB₁₁H₁₀-1-NH₂-12-I]⁻ (**26**).¹⁴ The iodo amine **26** can be prepared by two methods. One includes direct iodination of the parent amine **25** with ICl in AcOH at 80 °C³³ or with ICl in CH₃CN at 60 °C.³⁴ The major product formed in this reaction, the 12-iodo amine **26**, is contaminated with up to 20% of the B(7) isomer. The alternative route involves transformation of the carboxylic group in the iodo acid [*closo*-1-CB₁₁H₁₀-1-COOH-12-I]⁻ (**16**) into acid chloride **27** using oxalyl chloride (Figure 23). Subsequent treatment of **27** with trimethylsilyl azide in the presence of ZnCl₂ at 0 °C affords acyl azide **28**, which upon heating in CH₃CN undergoes Curtius rearrangement to give isocyanate **29**. Refluxing the isocyanate **29** in a mixture of *t*-BuOH and CH₃CN yields Boc-protected amine **30**. Acidic hydrolysis of the protected amine **30** in MeOH in the presence of HCl leads to the desired iodo amine **26** (Figure 23).¹⁴

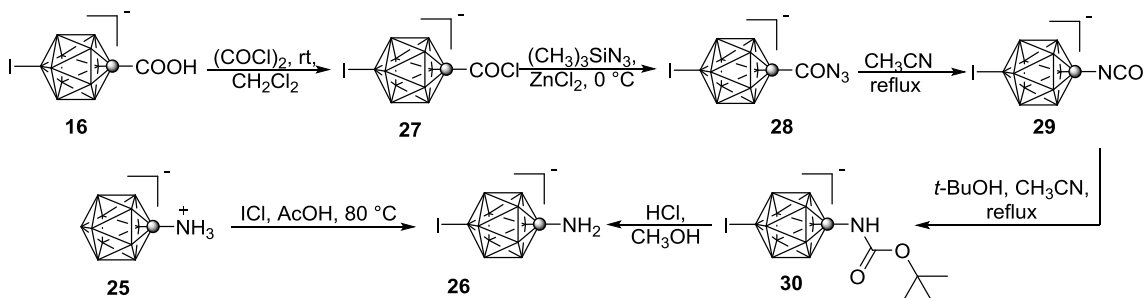


Figure 23. Synthesis of iodo amine **26** by direct iodination of amine **25** and by conversion of the carboxylic acid group in **16** into amine group.

The amine **25** and iodo amine **26** are key precursors to other derivatives of the [*closo*-1-CB₁₁H₁₂]⁻ cluster like pyridinium compounds **31**.³³ Access to such compounds was limited for a long time. The previous method involved diazotization of the 1-amine **32** with [NO]⁺[BF₄]⁻, formation of an unstable dinitrogen intermediate, [*closo*-1-

$\text{CB}_{11}\text{H}_{11}\text{-1-N}_2\text{]}^-$, its thermolysis and subsequent trapping of the resulting carbon ylide with a pyridine nucleophile (Figure 24).³³

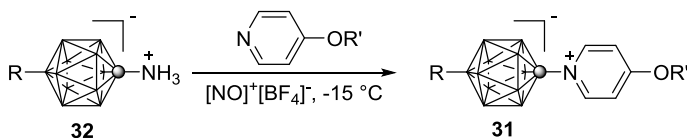


Figure 24. Diazotization of amine **32** to afford pyridinium zwitterion **31**.

However, due to mechanistic issues, this route was low-yielding (3-5%) and impractical. A new, more efficient method was developed.¹⁴ It follows reacting the appropriate amine **33** with pyrylium salts to give **31** in 31-65% yield (Figure 25).

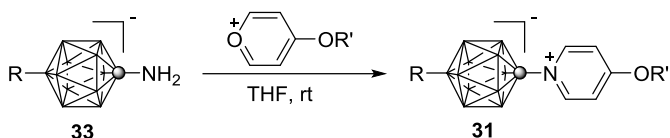


Figure 25. Synthesis of pyridinium zwitterions **31** from functionalized amines **33** and pyrylium salts.

This method allows for introduction of long and branched alkyl chain 4-alkoxypyridines in much higher yields than the previous method and proceeds smoothly at room temperature.¹⁴

The amine group can also undergo transformation into other groups such as quinuclidinyl moiety. This transformation was achieved by refluxing the amine **25** with tribromide in CH_3CN under hydrolytic conditions using potassium carbonate as the base (Figure 26). The product **34** is obtained in 29% yield.³⁵

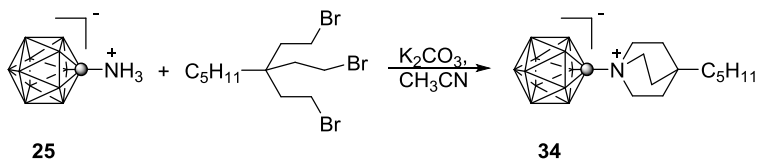


Figure 26. Synthesis of 1-(4-pentylquinuclidin-1-yl)-1-carba-*closo*-dodecaborane **34**.

Recently, conversion of C(1)-NH₂ derivative to the corresponding isonitrile was demonstrated. Thus, amine **35** was formylated with acetic formic anhydride in DME at 0 °C to give product **36** in 60% yield. In the next step, the formamide **36** was treated with (COCl)₂ and NEt₃ at -196 °C in DME to form the desired isonitrile **37** in 85% yield (Figure 27).³²

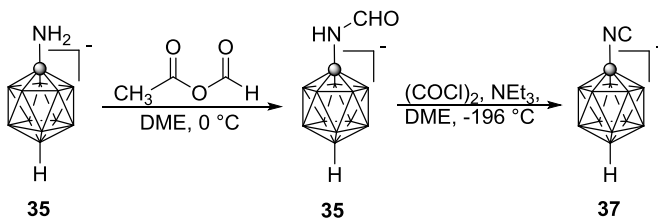


Figure 27. Conversion of 1-amine **35** into 1-isonitrile **37**.

Carbon-sulfur bonds

Only a limited number of compounds containing the C(1)–S bond is known. The original procedure for making the [*closo*-1-CB₁₁H₁₁-1-SH]⁻ involves reacting the 1-lithio derivative **8** with elemental sulfur. Acidic work-up and deprotonation of the sulphur atom reportedly leads to 1-mercapto derivative, [*closo*-1-CB₁₁H₁₁-1-SH]⁻[NMe₄]⁺ **38**.²⁹ This method, however, seemed irreproducible. Later studies demonstrated that the initial product of the reaction of **8** with S₈ leads to disulfide **39**, rather than directly to **38**. Thus, in the improved version of this method, the initially formed disulfide **39** was reduced

with zinc in AcOH to form mercaptane **38**, isolated as its $[\text{NMe}_4]^+$ salt, in 97% yield (Figure 28).

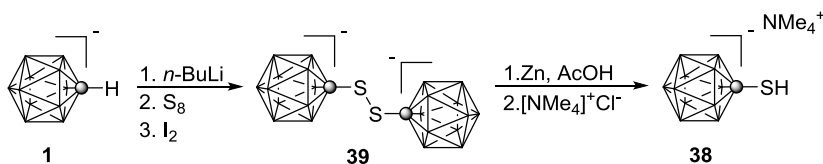


Figure 28. Synthesis of 1-thiol **38**.

Alternatively, sulfur derivatives can be obtained starting from 12-alkyl-1-amine intermediates. This route follows diazotization of the amine **33** with NaNO_2 in AcOH, formation of the transient dinitrogen intermediate **40** and trapping of the resulting carbonium ylide with 1,1,3,3-tetramethylthiourea to give 1-(bis-*N,N*-dimethylaminomethyl)thio derivative, [*closo*-1- $\text{CB}_{11}\text{H}_{10}$ -1- $\text{SC}(\text{NMe}_2)_2$ -12-alkyl] **41**, in 10-25% yield.³³ The resulting protected mercaptane **41** was then reacted with appropriate dibromide under hydrolytic conditions using $[\text{NMe}_4]^+[\text{OH}]^- \cdot 5\text{H}_2\text{O}$ as the base to form the desired sulfonium derivatives **42** (Figure 29).

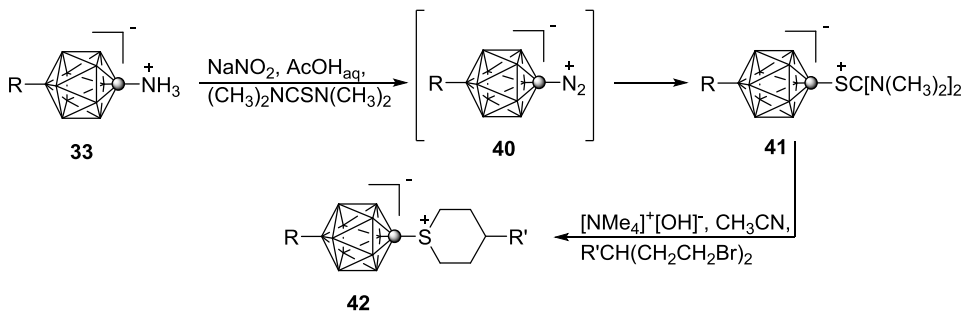


Figure 29. Formation of sulfonium zwitterion **42** from amine **33**.

Carbon-halide bonds

The first C(1)-halogen derivatives were prepared as potential intermediates for the synthesis of 1-aryl substituted carborane anions by Pd-catalyzed coupling reactions.³⁷

The general path to C(1)-halogen compounds involved formation of the C(1)-lithio

derivative **8**, which, in the next step, was transmetallated to C(1)-copper intermediate **14**, followed by addition of the appropriate *N*-halo succinimide. This route allowed for synthesis of C(1)-chloro, C(1)-bromo and C(1)-iodo derivatives **43** (Figure 30).³⁷ Unlike the other halides, formation of C(1)-bromo compound proceeded in the absence of CuCl. If copper(I) chloride was used, a 1:1 mixture of C(1)- and B(12)-substituted bromides, [*closo*-1-CB₁₁H₁₁-1-X]⁻ (**42**, X = Br) and [*closo*-1-CB₁₁H₁₁-12-Br]⁻, respectively, is formed. The synthesis of C(1)-fluoro derivative **43** does not require CuCl and is accomplished by addition of *N*-fluorobis(benzenesulfonyl)amine to the solution of carboranyl lithium reagent **8**.

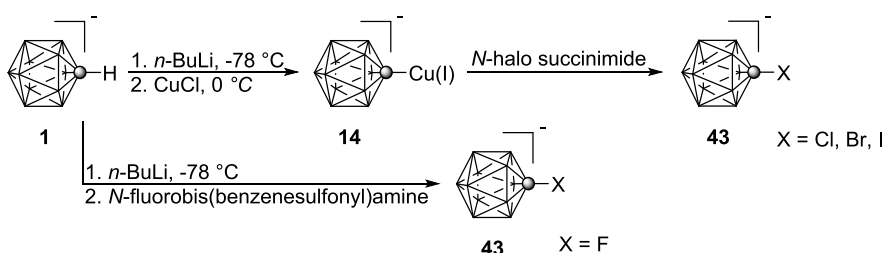


Figure 30. Preparation of 1-halo derivatives of the [*closo*-1-CB₁₁H₁₂]⁻ anion.

Attempted Suzuki, Stille and Negishi cross-couplings using these C-halogenated derivatives were not successful, however.³⁷

Carbon-phosphorus bonds

Derivatives containing C(1)-P bonds are very rare. Additionally, their use may be limited due to sensitivity to oxygen, and facile formation of corresponding phosphine oxides **44**.³⁸ The general method for synthesis of such derivatives requires lithiation of the carbon vertex and subsequent treatment of the resulting intermediate **8** with dialkyl^{38,39} or diaryl²⁴ chlorophosphine to give the desired product of substitution **45** (Figure 31).

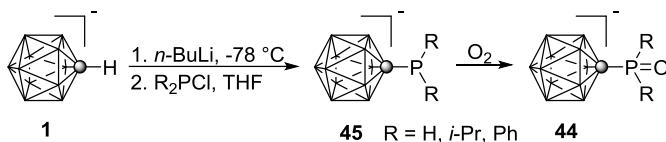


Figure 31. Preparation of phosphorus derivatives **45**.

Carbon-oxygen bonds

C(1)-Hydroxy derivatives could potentially serve as intermediates to oxy derivatives and oxonium zwitterions. The simplest C(1)-hydroxy derivative **46** was obtained in 36% yield by diazotization of the parent 1-amine **25** in the presence of HNO_2 and conc. HCl at 0°C and subsequent heating of the mixture with zinc dust for 3 hr (Figure 32).²⁹ Compound **46** is expected to be a relatively strong acid due to low electron density on the C(1) carbon.

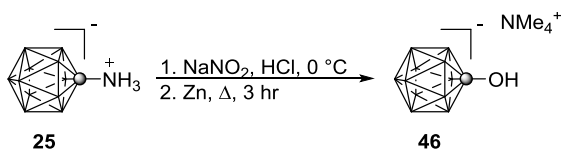


Figure 32. Preparation of 1-hydroxy-carba-*closo*-dodecaborane **46**.

Alternatively, 12-pentyl-1-amine **47** was diazotized with nitrosylsulfuric acid in aqueous solution of acetic acid.³³ After stirring for 2 days at rt, the product, [*closo*-1-CB₁₁H₁₀-1-OH-12-C₅H₁₁]⁻ **48** is isolated as its [NMe₄]⁺ salt in about 40% yield (Figure 33).

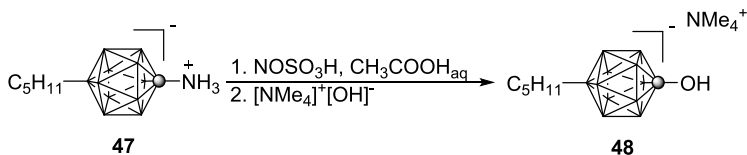


Figure 33. Transformation of 12-pentyl-1-amine **47** into 1-hydroxy derivative **48**.

Carbon-silicon bonds

Silicon functional groups can be introduced on the C(1) vertex in a reaction between carbanion, such as **8**, and appropriate silyl chloride.^{25,40} For instance, TIPS-substituted derivative **49** was obtained in 40% yield by reacting **8** with triisopropylsilyl chloride in THF (Figure 34).²⁴

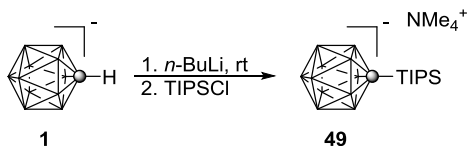


Figure 34. Preparation of TIPS-substituted derivative **49**.

Carbon-boron bonds

A few examples of such derivatives exist. Thus, boronic acid **50** was prepared in 62% yield by treatment of the lithium intermediate **8** with trimethylborate at -78 °C (Figure 35).²³

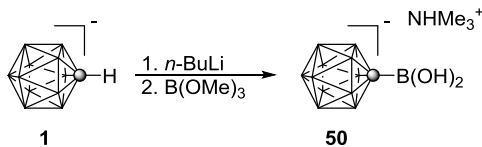


Figure 35. Synthesis of boronic acid **50**.

Carboranylboronic acid pinacol ester **51** was obtained in a similar manner by reacting C(1)-lithio derivative **8** with 2-isopropoxy-4,4,5,5-tetramethyl-1,3,2-dioxaborolane to give the product in 75% yield (Figure 36).⁴¹

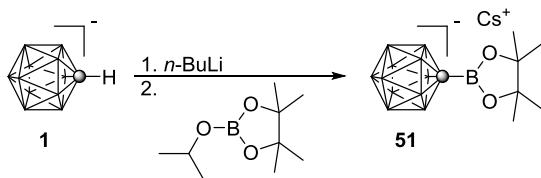


Figure 36. Preparation of boronic acid ester **51**.

2.4.5 Boron substitution

Boron substitution is a more complex process than carbon substitution due to the fact that there are three different types of boron atoms present in the cluster: the upper belt, the lower belt and the antipodal position (Figure 9).

Boron-halide bonds

Halogen-substituted derivatives play an important role in boron cluster chemistry and are a starting point for introduction of other elements on the boron vertices. They can be divided into two groups depending on the halide valency. The first group includes compounds containing monovalent iodine atom. Such compounds have been known for several decades and constitute an important group of intermediates in functional synthesis. The second group, recently discovered by Kaszynski et al.,⁴² incorporates a trivalent iodine, and has been gaining importance in synthesis of new functional molecules, to which access was hindered before by the lack of synthetic methodologies or mechanistic issues. Synthesis of the new class of iodonium compounds is usually easier and less time-consuming, and more selective when compared to the traditional way of introducing iodine atom onto the boron vertex (Figure 37).⁴² Also, their reactivity is different compared to the monovalent iodine derivatives.

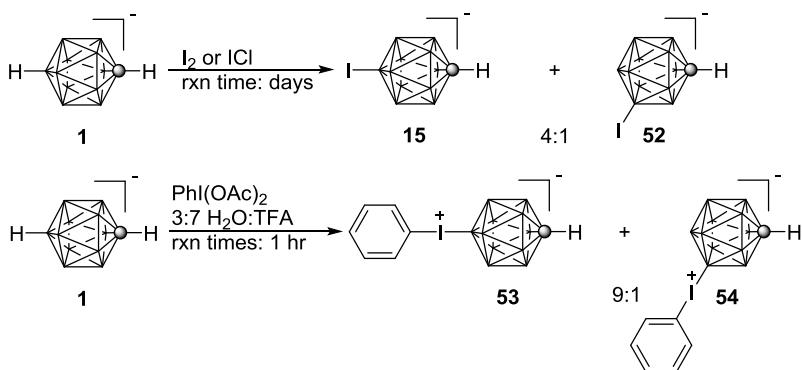


Figure 37. Preparation of iodo **15** and **52** and iodonium **53** and **54** derivatives of **1**.

The first boron-substituted halides were synthesized nearly 30 years ago by Štibr et al.²⁹ and included chloro-, bromo- and iodo-substituted compounds at the B(12) position. Analogous fluoro-substituted derivative was obtained 10 years later in the context of preparation of new weakly coordinating anions. The product, [*closo*-1-CB₁₁H₁₁-12-F]⁻ **55**, was obtained in 96% yield by stirring the parent [*closo*-1-CB₁₁H₁₂]⁻ anion with liquid anhydrous HF (LAHF) for 20 hr at rt (Figure 38).⁴³ Alternative method includes treatment of the parent anion **1** with 1-chloromethyl-4-fluoro-1,4-diazoniabicyclo[2.2.2]octane bis(tetrafluoroborate) (F-TEDA) in CH₃CN to give a mixture of fluorinated products, whose composition is temperature-dependent (Figure 39).⁴⁴

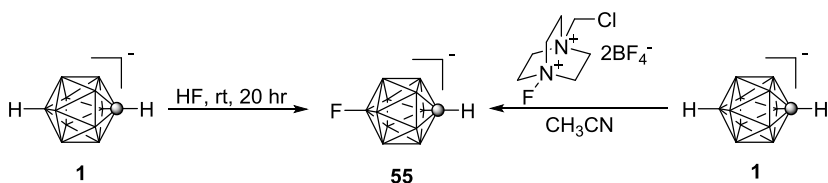


Figure 38. Synthesis of 12-fluoro derivative **55**.

Monochlorination at the B(12) position was achieved by reacting **1** with *N*-chlorosuccinimide in DMF (Figure 39), and the product, **56**, was obtained in 60% yield.²⁴

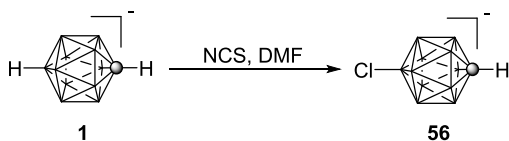


Figure 39. Preparation of 12-chloro derivative **56**.

Bromo derivative **57** can be prepared in two ways (Figure 40). The first route employs *N*-bromosuccinimide as the brominating reagent (62% yield), while the second uses elemental bromine in the presence of K_2CO_3 (71% yield).²⁴

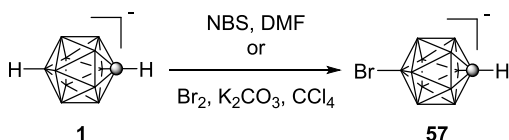


Figure 40. Bromination of **1** at the B(12) vertex.

From synthetic point of view, the most important group of halo derivatives of **1** are B(12)-iodo compounds. They are key intermediates in a number of cross-coupling and substitution reactions. The simplest route to introduce iodine at the B(12) position is to react the parent cluster **1** with elemental I_2 in AcOH at slightly elevated temperatures (40 °C) for few days (Figure 41). At higher temperatures, iodination at the B(7) position is more pronounced.²⁹ This approach works for both the parent and C(1)-alkyl-substituted anions. For example, iodination of C(1)-pentyl derivative gave the product, C(1)-pentyl-B(12)-iodo cluster in about 77% yield.¹⁵

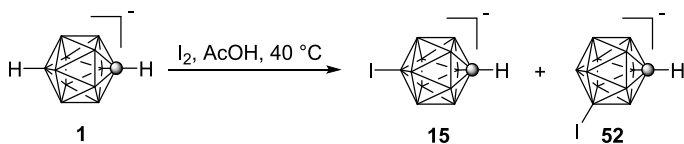


Figure 41. Preparation of **15**.

Certain derivatives of the parent cluster such as C(1)-amino **25** or C(1)-quinuclidinyl **34** require stronger iodinating conditions which involve ICl in AcOH and elevated temperatures.^{33,34,35} Iodination of the parent cluster under these conditions (65 °C) leads to hexaiodinated product (substitution at B(7)–B(12) vertices).⁴⁵ At higher temperature (200 °C) undeca-iodinated derivative is formed as the major product (Figure 42).⁴⁶

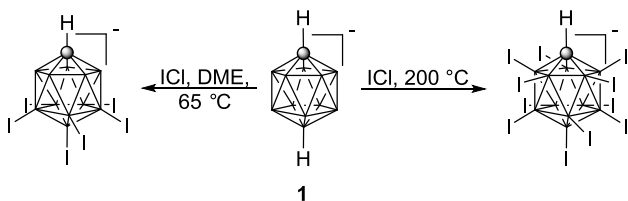


Figure 42. Polyiodination of **1**.

The B-iodo derivatives can undergo many types of transition metal-catalyzed cross-coupling reactions, allowing for formation of different bonds between boron and other atoms such as carbon, nitrogen, phosphorus, and silicon (Figure 43).

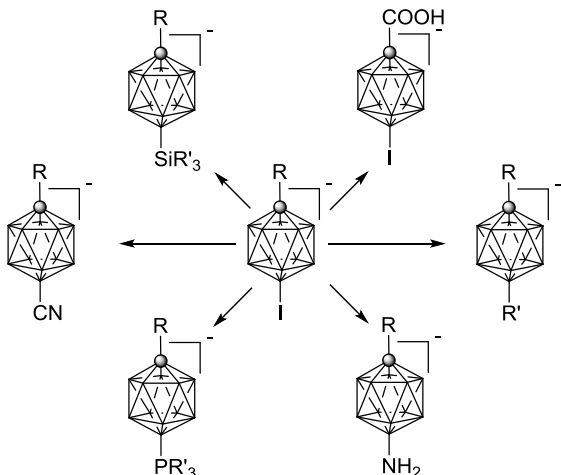


Figure 43. Transformations of B-iodo derivatives.

Alternatively, formation of some bonds accessible through metal-catalyzed reactions, can be achieved through iodonium zwitterions, often in higher yields and shorter reaction times. Moreover, iodonium compounds allowed for introduction of certain functional groups not available by previous methods such as protected thiol or hydroxyl groups.

Of many iodo derivatives of the $[closo-1-CB_{11}H_{12}]^-$ anion (**1**), one of the most important compounds in the synthesis of functional molecules is the iodo acid, $[closo-1-CB_{11}H_{10}-1-COOH-12-I]^-$ (**17**). The acid can be obtained in high yields in just two steps starting with iodination of the parent anion **1** with I_2 in AcOH at 60 °C for 3 days. Pure B(12)-iodo isomer, obtained by recrystallization from hot H_2O , is lithiated and then carboxylated to give the desired iodo acid **17** (Figure 44). Alternatively, iodo acid **17** can be synthesized by iodination of carboxylic acid $[closo-1-CB_{11}H_{11}-1-COOH]^-$ (**16**) (Figure 44). Recrystallization of the mixture of **17** and **58** from aqueous EtOH gives isomerically pure iodo acid **17**.

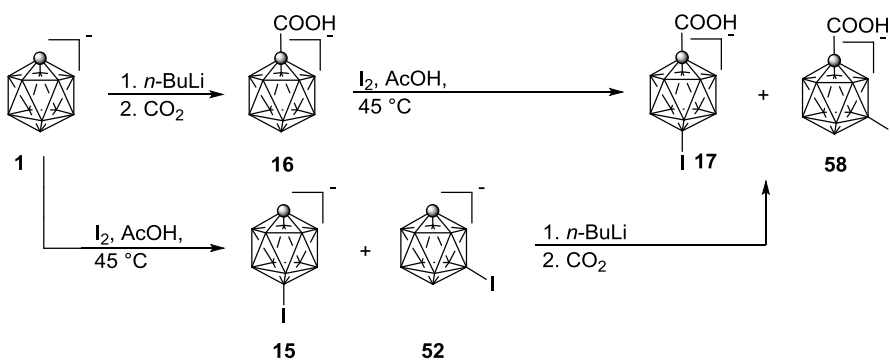


Figure 44. Synthesis of iodo acid **17**.

The iodo acid **17** is important from the point of view of synthesis of liquid crystal molecules. For example, isomerically pure iodo acid [*closo*-1-CB₉H₈-1-COOH-12-I]⁻ is obtained in a multi-step process in about 10% overall yield,²¹ while [*closo*-1-CB₁₁H₁₀-1-COOH-12-I]⁻ (**17**) can be synthesized in about 25-30% overall yield in only 4 steps from commercial B₁₀H₁₄.¹⁶ Iodination of the parent [*closo*-1-CB₁₁H₁₂]⁻ cluster (**1**) as well as the parent carboxylic acid [*closo*-1-CB₁₁H₁₁-1-COOH]⁻ (**15**) occurs mainly at the B(12) vertex. This is in contrast to iodination of the [*closo*-1-CB₉H₁₀]⁻ anion, in which electrophilic attack occurs nearly exclusively at the B(6) vertex.

The iodo acid [*closo*-1-CB₁₁H₁₀-1-COOH-12-I]⁻ (**17**) undergoes a series of functional group transformations leading to key intermediates in the synthesis of liquid crystal molecules. Both iodine and carboxylic groups can be transformed into other moieties.

Boron-carbon bonds

Pd-catalyzed formation of the boron-carbon bonds allows for introduction of alkyl, aryl, alkenyl and even alkynyl groups onto the boron vertex. Early examples include synthesis of B(12)-methyl, ethyl, butyl, hexyl and phenyl derivatives by Kumada

coupling of B(12)-iodo compound **15** and appropriate Grignard reagents in the presence of Pd(PPh₃)₂Cl₂ in THF (Figure 45). The products were obtained in 49-63% as their NMe₄⁺ or Cs⁺ salts.⁴⁷

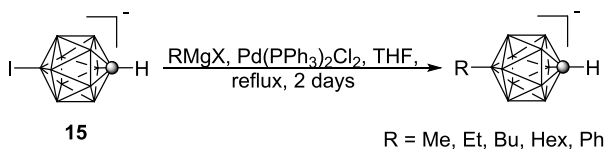


Figure 45. Kumada cross-coupling of B(12)-iodo derivative **15**.

Alkynyl groups were introduced in a similar manner.⁴⁸ Substituted B(12)-phenyl derivatives were also obtained by means of microwave-assisted Pd-catalyzed Kumada cross-coupling of **59** in higher yields, shorter times, and required smaller Grignard reagent excess and lower catalyst load (Figure 46). The same method was used to introduce alkenyl and alkynyl substituents on the boron vertex.^{34,49}

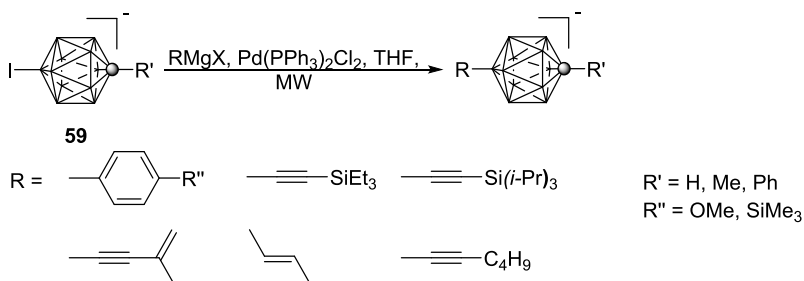


Figure 46. Microwave-assisted Kumada cross-coupling of B(12)-iodo derivatives of **1**.

Beside Kumada cross-coupling, there are other cross-coupling methods used for formation of boron-carbon bonds. For example, the B(12)-hexyl-C(1)-amine derivative **60** was successfully obtained by Negishi coupling of the B(12)-iodo-C(1)-amine **26** with appropriate hexyl zinc chloride in the presence of Pd₂dba₃ and [HPCy₃]⁺[BF₄]⁻ in a THF/NMP mixture (Figure 47).¹⁴ Other B(12)-alkyl-C(1)-amines (alkyl = pentyl, hexyl,

decyl) were synthesized in a similar manner using Pd(PPh₃)₂Cl₂ as the catalyst (Figure 47).³³

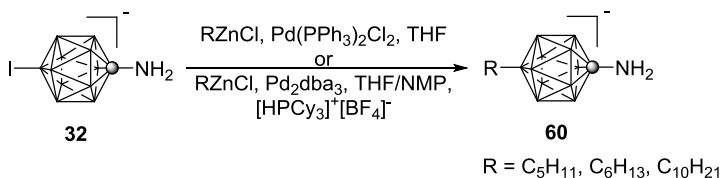


Figure 47. Negishi cross-coupling of **25**.

Similar conditions, Pd₂dba₃ and [HPCy₃]⁺[BF₄]⁻ in a mixture of THF/NMP, were used to transform the iodo acid, [*closo*-1-CB₁₁H₁₀-1-COOH-12-I]⁻ **17**, and convert it into its B(12)-hexyl derivative **61** (Figure 48) to obtain the product as its NEt₄⁺ salt in 61% yield.¹⁶

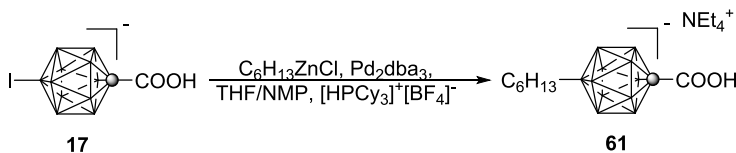


Figure 48. Preparation of 12-hexyl-1-carboxylic acid **61**.

Alkylation B(12)-iodo-C(1)-(4-pentylquinuclidin-1-yl) derivative **62** with hexylzinc chloride was carried out with two different catalytic systems, Pd(PPh₃)₄ or Pd₂dba₃/[HPCy₃]⁺[BF₄]⁻, and the product **63** was obtained in comparable yields (Figure 49).³³

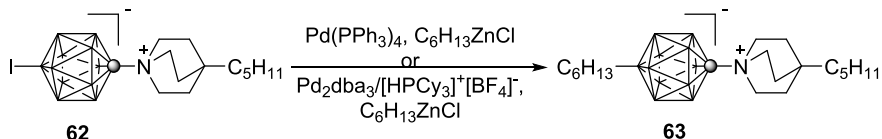


Figure 49. Alkylation of **62** with hexylzinc chloride.

The cyano group was conveniently introduced on boron vertex by reacting the iodo cluster **15** with CuCN in the presence of catalytic amount of Pd(OAc)₂ under microwave radiation (Figure 50). The product **64** was formed in 80% yield in just 15 min. Subsequent hydrolysis of the cyano derivative in a mixture of HCl and acetic acid yields carboxylic acid **65**.⁵⁰ Alternatively, nitrile **64** was obtained from phenyliodonium derivative **53** upon treatment with [NEt₄]⁺[CN]⁻ (Figure 50).⁴²

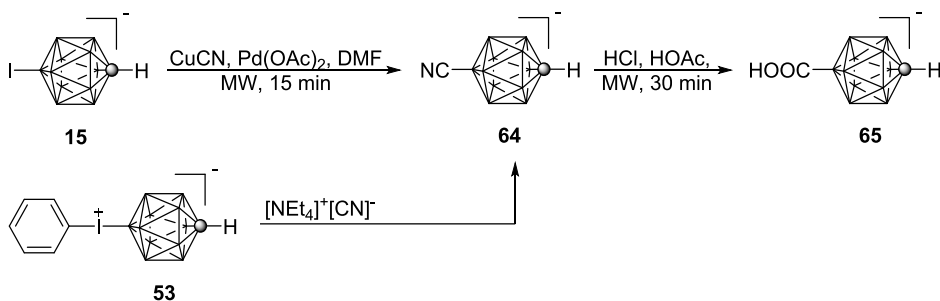


Figure 50. Transformation of **15** and **53** into cyano derivative **64** and its subsequent hydrolysis to carboxylic acid **65**.

Boron-nitrogen bonds

Derivatives of the [*closo*-1-CB₁₁H₁₂]⁻ anion containing the B–N of bond were unknown until the discovery of Pd-catalyzed amination of the [*closo*-1-CB₉H₈-1-COOH-10-I]⁻ acid.⁵¹ The same methodology was successfully applied to the synthesis of amino acid **66**. Thus, the iodo acid [*closo*-1-CB₁₁H₁₀-1-COOH-12-I]⁻ (**17**) was converted into amino acid **66** in the presence of Pd₂dba₃ and 2-(dicyclohexylphosphino)biphenyl using LiHMDS as ammonia equivalent to afford the product in 40% yield (Figure 51).⁵²

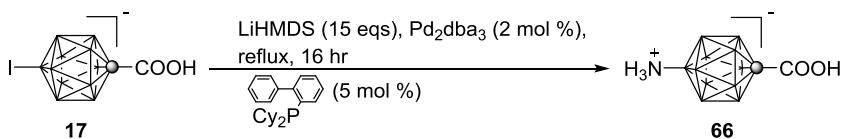


Figure 51. Preparation of amino acid **66**.

The same conditions were used to prepare B(12)-amino **67** (R = H) and C(1)-pentyl-B(12)-amine **68** (R = C₅H₁₁) derivatives in 40% and 97% yield, respectively (Figure 52).¹⁵

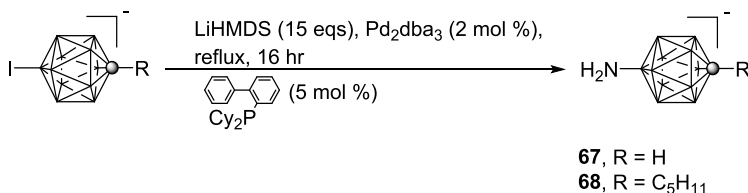


Figure 52. Preparation of amines **67** and **68**.

Recently, an improved microwave-assisted synthesis of the B(12) amine **67** was published, in which the product was obtained in shorter time (2 hr) and higher yield (70%).⁵³

The amino acid **66** is a key precursor in the synthesis of another important intermediate to liquid crystals, 4-heptyloxypyridinium acid **69**. The synthetic path to the pyridinium acid **69** includes diazotization of the amino acid **66** and subsequent trapping of the *in situ* formed boronium ylide with 4-heptyloxypyridine, which also plays the role of the solvent for the reaction (Figure 53). The product is obtained in 6% yield.⁵²

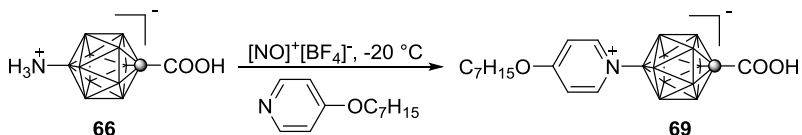


Figure 53. Diazotization of amino acid **66**.

Other B(12)-substituted pyridinium derivatives can be obtained in a similar manner. However, the yield of the diazotization is strongly dependent on the length of the alkoxy chain on the pyridine ring and the substituent on the carbon vertex. For example,

diazotization of the parent B(12)-amine in 4-heptyloxypyridine gives the product **70** in only 15% yield. If 4-methoxypyridine is used as the solvent, the pyridinium zwitterion **71** is obtained in about 50% yield (Figure 54).¹⁵

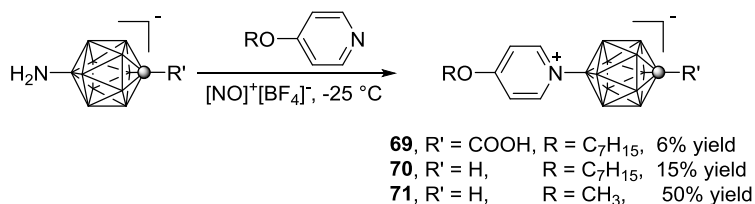


Figure 54. Diazotization of 1-substituted 12-amines **69**, **70** and **71**.

Alternative path to higher alkoxy pyridinium derivatives **72** follows *O*-alkylation of B(12)-pyridone compounds **73** (Figure 55). Aside from amines and pyridinium zwitterions, B(12)-pyridones constitute another group of compounds containing the boron-nitrogen bond. Pyridones can be obtained by LiCl-promoted demethylation of the B(12)-(4-methoxypyridinium) derivatives **74** in DMF.¹⁵

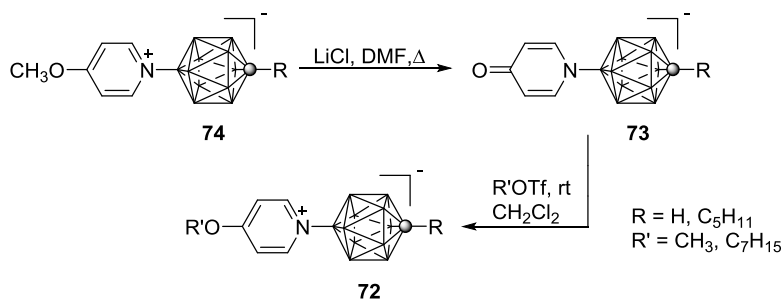


Figure 55. Transformation of 4-methoxypyridinium compound **74** into higher alkoxy pyridinium derivatives **72** via pyridone intermediate **73**.

The overall yield gets greatly improved as the process of dealkylation and *O*-alkylation proceed almost quantitatively. Thus, B(12)-(4-heptyloxypyridinium) compound (**70**, R' = C₇H₁₅, R = H) is obtained in 15% yield when diazotization is

performed using 4-heptyloxy pyridine, while it's 40% overall yield when following the dealkylation–*O*-alkylation path.¹⁵

Alternatively, 12-(4-methoxypyridinium) **71** can be conveniently accessed by heating 12-phenyliodonium derivative **53** in neat 4-methoxypyridine, giving the product in 87% yield (Figure 56).⁴²

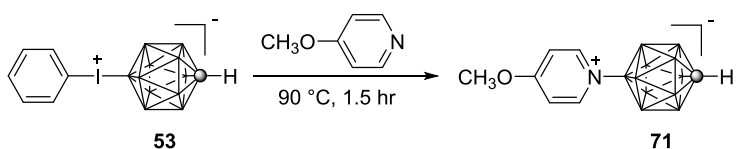


Figure 56. Transformation of iodonium zwitterion **53** into pyridinium derivative **71**.

Boron-sulphur bonds

For a long time, the only examples of zwitterionic sulfur-substituted derivatives of the [closo-1-CB₁₁H₁₂]⁻ at the B(12) vertex were clusters with dimethylsulfide and 2,4-dithiapentane groups (Figure 57).²⁹ They were prepared by reacting **1** with dimethyl sulfoxide and sulfuric acid in acetic anhydride at 90 °C for 4 hr. The zwitterions **75** and **76** were separated by chromatography and obtained in 44% and 23% yield, respectively.²⁹

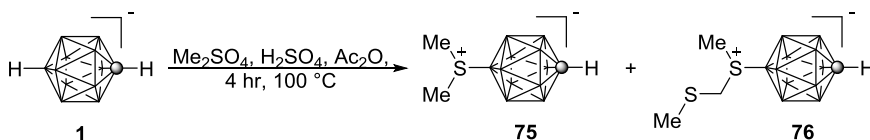


Figure 57. Preparation of zwitterions **75** and **76**.

The route to 10-sulfonium derivatives of [closo-1-CB₉H₁₀]⁻ anion includes formation of the protected mercaptane obtained by reacting the stable dinitrogen

derivative with *N,N*-dimethylthioformamide. The protected mercaptane is then reacted with appropriate dibromide under hydrolytic conditions.⁵⁴ However, similar route to the analogous derivatives of the [*closo*-1-CB₁₁H₁₂]⁻ cluster was hindered due to the lack of proper synthetic tools. The situation changed with the discovery of the B(12)-iodonium derivatives of **1**. It was demonstrated that the protected mercaptane **77** can be obtained by heating the 12-phenyliodonium derivative **53** in neat *N,N*-dimethylthioformamide (Figure 58).⁴²

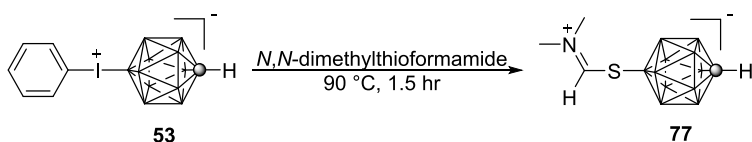


Figure 58. Preparation of protected mercaptane **77**.

In the next step, the protected mercaptane is treated with appropriate dibromide to yield the cyclic sulfonium compound.

Boron-oxygen bonds

Compounds with this type of bond are very rare. The first example of monosubstituted derivative containing a boron-oxygen bond was [*closo*-1-CB₁₁H₁₁-12-OH]⁻ **78** obtained in 83% yield by heating the parent cluster **1** with 80% H₂SO₄ at 175 °C for 5 hr (Figure 59).⁵⁵

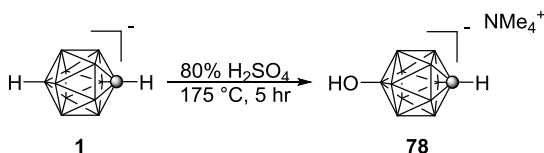


Figure 59. Formation of 12-hydroxy carba-*closo*-dodecaborate **78**.

Heating the parent anion **1** with dioxane as the solvent at 175 °C in the presence of dimethyl sulfate led to a zwitterionic oxonium derivative **79** containing a dioxane ring at the B(12) vertex isolated in 27% yield as colorless crystalline solid (Figure 60).⁵⁵ Such derivative could be useful as an intermediate for introduction of other functional groups due to cleavage of the ring by nucleophiles.⁵⁵

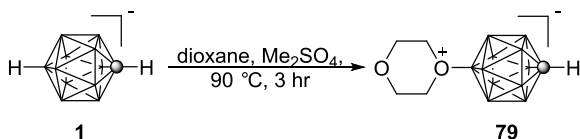


Figure 60. Synthesis of 12-oxonium zwitterion **79**.

Access to potentially broader group of cyclic oxonium compounds may be possible through the protected hydroxyl derivative **80**. It was shown it can be prepared by reacting 12-phenyliodonium derivative **53** with neat *N,N*-dimethylacetamide (Figure 61).⁴²

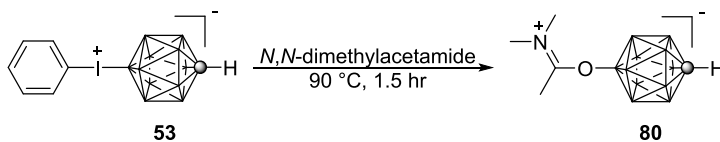


Figure 61. Preparation of **80**.

Boron-phosphorus bonds

Triphenylphosphonium derivative **81** (Figure 62) is a by-product formed in a microwave-assisted Kumada cross-coupling of B(12)-iodo compounds with Grignard reagents. This inner salt can be prepared selectively in 88% yield by reacting B(12)-iodo derivative **14** with PPh_3 in the presence of a catalytic amount of $\text{Pd}(\text{PPh}_3)_4$.⁴⁹

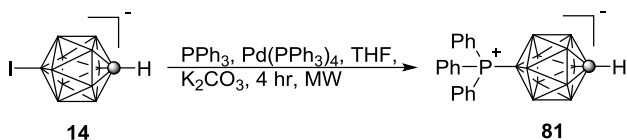


Figure 62. Preparation of triphenylphosphonium derivative **81**.

2.4.6 Summary

This review highlighted the methods of functionalization of the [closo-1-CB₁₁H₁₂][−] anion in antipodal positions. Introduction of substituents at the C(1) and B(12) vertices is important from the point of view of synthesis of molecular materials including liquid crystals. Synthesis of the cluster is achieved in only two steps. Functionalization of the carbon vertex follows nucleophilic substitution mechanism. The B(12) vertex is attacked by different electrophiles, preferentially over other vertices. Current functionalization methods allow for introduction of a wide range of functional groups. Further transformations of these substituents open access to a broader group of derivatives based on the [closo-1-CB₁₁H₁₂][−] cluster and new functional materials and pharmacophores.

2.4.7 References

- (1) Douvris, C.; Michl, J., Update 1 of: Chemistry of the carba-closo-dodecaborate(−) anion, CB₁₁H₁₂[−]. *Chem. Rev.* **2013**, *113*, 179-233.
- (2) Štibr, B., Carboranes other than C₂B₁₀H₁₂. *Chem. Rev.* **1992**, *92*, 225-250.
- (3) Reed, C. A., Carboranes: a new class of weakly coordinating anions for strong electrophiles, oxidants, and super acids. *Acc. Chem. Res.* **1998**, *31*, 133-139.
- (4) Reed, C. A., H⁺, CH₃⁺, and R₃Si⁺ carborane reagents: When triflates fail. *Acc. Chem. Res.* **2010**, *43*, 121-128.

- (5) Strauss, S. H., The search for larger and more weakly coordinating anions. *Chem. Rev.* **1993**, *93*, 927-942.
- (6) Krossing, I.; Raabe, I., Noncoordinating anions—fact or fiction? A survey of likely candidates. *Angew. Chem. Int. Ed.* **2004**, *43*, 2066-2090.
- (7) Seppelt, K., "Noncoordinating" Anions, II. *Angew. Chem. Int. Ed.* **1993**, *32*, 1025-1027.
- (8) Grimes, R. N. *Carboranes, Second Edition*; Academic Press: Burlington, MA, 2011.
- (9) Körbe, S.; Schreiber, P. J.; Michl, J., Chemistry of the carba-*closo*-dodecaborate(-) anion, $\text{CB}_{11}\text{H}_{12}^-$. *Chem. Rev.* **2006**, *106*, 5208-5249.
- (10) Juhasz, M.; Hoffmann, S.; Stoyanov, E.; Kim, K.-C.; Reed, C. A., The strongest isolable acid. *Angew. Chem. Int. Ed.* **2004**, *43*, 5352-5355.
- (11) Soloway, A. H.; Tjarks, W.; Barnum, B. A.; Rong, F.-G.; Barth, R. F.; Codogni, I. M.; Wilson, J. G., The chemistry of neutron capture therapy. *Chem. Rev.* **1998**, *98*, 1515-1562.
- (12) Sivaev, I. B.; Bregadze, V. V., Polyhedral boranes for medical applications: current status and perspectives. *Eur. J. Inorg. Chem.* **2009**, 1433-1450.
- (13) Sivaev, I. B.; Bregadze, V. V.; Kuznetsov, N. T., Derivatives of the *closo*-dodecaborate anion and their application in medicine. *Russ. Chem. Bull., Intl. Ed.* **2002**, *51*, 1362-1374.
- (14) Pecyna, J.; Pocięcha, D.; Kaszynski, P., Zwitterionic pyridinium derivatives of $[\textit{closo}\text{-}1\text{-CB}_9\text{H}_{10}]^-$ and $[\textit{closo}\text{-}1\text{-CB}_{11}\text{H}_{12}]^-$ as high $\Delta\epsilon$ additives to a nematic host. *J. Mater. Chem. C* **2014**, *2*, 1585-1591.

- (15) Pecyna, J.; Ringstrand, B.; Domagala, S.; Kaszynski, P.; Wozniak, K., Synthesis of 12-pyridinium derivatives of the [*closo*-1-CB₁₁H₁₂]⁻ anion. *Inorg. Chem.* **2014**, *53*, 12617-12626.
- (16) Ringstrand, B.; Jankowiak, A.; Johnson, L. E.; Pocięcha, D.; Kaszynski, P.; Gorecka, E., Anion-driven mesogenicity: a comparative study of ionic liquid crystals based on the [*closo*-1-CB₉H₁₀]⁻ and [*closo*-1-CB₁₁H₁₂]⁻ clusters. *J. Mater. Chem.* **2012**, *22*, 4874-4880.
- (17) Knoth, W. H., 1-B₉H₉CH⁻ and B₁₁H₁₁CH⁻. *J. Am. Chem. Soc.* **1967**, *89*, 1274-1275.
- (18) Knoth, W. H., B₁₀H₁₂CNH₃, B₉H₉CH⁻, B₁₁H₁₁CH⁻, and metallomonocarboranes. *Inorg. Chem.* **1971**, *10*, 598-605.
- (19) Plešek, J.; Jelínek, T.; Drdáková, E.; Heřmánek, S.; Štíbr, B., A convenient preparation of 1-CB₁₁H₁₂⁻ and its C-amino derivatives. *Collect. Czech. Chem. Commun.* **1984**, *49*, 1559-1562.
- (20) Franken, A. B., N. J.; Jelínek, T.; Thornton-Pett, M.; Teat, S. J.; Clegg, W.; Kennedy, J. D.; Hardie, M. J., Structural chemistry of halogenated monocarbaboranes: the extended structures of Cs[1-HCB₉H₄Br₅], Cs[1-HCB₁₁H₅Cl₆] and Cs[1-HCB₁₁H₅Br₆]. *New. J. Chem.* **2004**, *28*, 1499-1505.
- (21) Ringstrand, B.; Balinski, A.; Franken, A.; Kaszynski, P., A practical synthesis of isomerically pure 1,10-difunctionalized derivatives of the [*closo*-1-CB₉H₁₀]⁻ anion. *Inorg. Chem.* **2005**, *44*, 9561-9566.

- (22) Vyakaranam, K.; Janoušek, Z.; Eriksson, L.; Michl, J., Preparation of undecamethylated and hexamethylated 1-halocarba-*closo*-dodecaborate anions. *Heteroat. Chem.* **2006**, *17*, 217-223.
- (23) Valášek, M.; Štursa, J.; Pohl, R.; Michl, J., Microwave-assisted alkylation of $[\text{CB}_{11}\text{H}_{12}]^-$ and related anions. *Inorg. Chem.* **2010**, *49*, 10247-10254.
- (24) Jelínek, T.; Baldwin, P.; Schedit, W. R.; Reed, C. A., New weakly coordinating anions. 2. Derivatization of the carborane anion $\text{CB}_{11}\text{H}_{12}^-$. *Inorg. Chem.* **1993**, *32*, 1982-1990.
- (25) Nava, M. J.; Reed, C. A., High yield C-derivatization of weakly coordinating carborane anions. *Inorg. Chem.* **2010**, *49*, 4726-4728.
- (26) Jelínek, T.; Kilner, C. A.; Thornton-Pett, M.; Kennedy, J. D., Monocarborane anion chemistry. The elusive C-arylated $[\text{PhCB}_{11}\text{H}_{11}]^-$, $[\text{PhCB}_9\text{H}_9]^-$ and $[\text{PhCB}_8\text{H}_8]^-$ anions. *Chem. Commun.* **2001**, 1790-1791.
- (27) Körbe, S.; Sowers, D. B.; Franken, A.; Michl, J., Preparation of 1-*p*-halophenyl and 1-*p*-biphenyl substituted monocarbadodecaborate anions [*closo*-1-Ar- $\text{CB}_{11}\text{H}_{11}]^-$ by insertion of arylhalocarbenes into $[\text{nido-B}_{11}\text{H}_{14}]^-$. *Inorg. Chem.* **2004**, *43*, 8158-8161.
- (28) Kanazawa, J.; Takita, R.; Jankowiak, A.; Fujii, S.; Kagechika, H.; Hashizume, D.; Shudo, K.; Kaszynski, P.; Uchiyama, M., Copper-mediated C–C cross-coupling reaction of monocarba-*closo*-dodecaborate anion for the synthesis of functional molecules. *Angew. Chem. Int. Ed.* **2013**, *52*, 8017-8021.

- (29) Jelínek, T.; Plešek, J.; Heřmánek, S.; Štíbr, B., Chemistry of compounds with the 1-carba-*closo*-dodecaborane(12) framework. *Collect. Czech. Chem. Commun.* **1986**, *51*, 819-829.
- (30) Zakharkin, L. I.; Ol'shevskaya, V. A.; Petrovskii, P. V.; Morris, J. H., Simple synthesis of anions of *closo*-monocarbon carborane-substituted alcohols. *Mendeleev Commun.* **2000**, *10*, 71-72.
- (31) Finze, M.; Sprenger, J. A. P.; Schaack, B. B., Salt of the 1-cyanocarba-*closo*-dodecaborate anions [1-NC-*closo*-1-CB₁₁X₁₁]⁻ (X = H, F, Cl, Br, I). *Dalton Trans.* **2010**, *39*, 2708-2716.
- (32) Hailmann, M.; Konieczka, S. Z.; Himmelspach, A.; Löblein, J.; Reiss, G. J.; Finze, M., Carba-*closo*-dodecaborate anions with two functional groups: [1-R-12-HC≡C-*closo*-1-CB₁₁H₁₀]⁻ (R = CN, NC, CO₂H, C(O)NH₂, NHC(O)H). *Inorg. Chem.* **2014**, *53*, 9385-9399.
- (33) Pecyna, J.; Ringstrand, B.; Pakhomov, S.; Piecek, W.; Kaszynski, P.; Young, V. G. Jr., Zwitterionic derivatives of the [*closo*-1-CB₁₁H₁₂]⁻ as high Δε additives to nematic liquid crystals. *unpublished results*.
- (34) Hailmann, M.; Herkert, L.; Himmelspach, A.; Finze, M., Difunctionalized {*closo*-1-CB₁₁} clusters: 1- and 2-amino-12-ethynylcarba-*closo*-dodecaborates. *Chem. Eur. J.* **2013**, *19*, 15745-15758.
- (35) Douglass, A. G.; Janoušek, Z.; Kaszynski, P.; Young, V. G. Jr., Synthesis and molecular structure of 12-iodo-1-(4-pentylquinuclidin-1-yl)-1-carba-*closo*-dodecaborane. *Inorg. Chem.* **1998**, *37*, 6361-6365.

- (36) Kennedy, J. D.; Stern, C. L.; Mirkin, C. A., Zwitterionic weak-link approach complexes based on anionic icosahedral monocarbaboranes. *Inorg. Chem.* **2013**, *52*, 14064-14071.
- (37) Janoušek, Z.; Hilton, C. L.; Schreiber, P. J.; Michl, J., C-halogenation of the *closo*-[CB₁₁H₁₂]⁻ anion. *Collect. Czech. Chem. Commun.* **2002**, *67*, 1025-1034.
- (38) Drisch, M.; Sprenger, J. A. P.; Finze, M., Carba-*closo*-dodecaborate anions with cluster carbon-phosphorus bonds. *Z. Anorg. Allg. Chem.* **2013**, *639*, 1134-1139.
- (39) El-Hellani, A.; Kefalidis, C. E.; Tham, F. S.; Maron, L.; Lavallo, V., Structure and bonding of a zwitterionic iridium complex supported by a phosphine with the parent carba-*closo*-dodecaborate CB₁₁H₁₁⁻ ligand substituent. *Organometallics* **2013**, *32*, 6887-6890.
- (40) King, B. T.; Körbe, S.; Schreiber, P. J.; Clayton, J.; Němcová, A.; Havlas, Z.; Vyakaranam, K.; Fete, M. G.; Zharov, I.; Ceremuga, J.; Michl, J., The sixteen CB₁₁H_nMe_{12-n}⁻ anions with fivefold substitution symmetry: anodic oxidation and electronic structure. *J. Am. Chem. Soc.* **2007**, *129*, 12960-12980.
- (41) Janoušek, Z.; Lehmann, U.; Častulík, J.; Císařová, I.; Michl, J., Li⁺-induced σ -bond metathesis: aryl for methyl exchange on boron in a methylated monocarbododecaborate anion. *J. Am. Chem. Soc.* **2004**, *126*, 4060-4061.
- (42) Kaszynski, P.; Ringstrand, B., Functionalization of *closo*-borates through iodonium zwitterions. *Angew. Chem. Int. Ed.* **2015**, accepted.

(43) Ivanon, S. V.; Lupinetti, A. J.; Miller, S. M.; Anderson, O. P.; Solntsev, K. A.; Strauss, S. H., Regioselective fluorination of $\text{CB}_{11}\text{H}_{12}^-$. New weakly coordinating anions. *Inorg. Chem.* **1995**, *34*, 6419-6420.

(44) Ivanon, S. V.; Lupinetti, A. J.; Solntsev, K. A.; Strauss, S. H., Fluorination of deltahedral *closo*-borane and -carbaborane anions with *N*-fluoro reagents. *J. Fluorine Chem.* **1998**, *89*, 65-72.

(45) Xie, Z.; Manning, J.; Reed, R. W.; Mathur, R.; Boyd, P. D. W.; Benesi, A.; Reed, C. A., Approaching the silylium (R_3Si^+) ino: trends with hexalo (Cl, Br, I) carboranes as counterions. *J. Am. Chem. Soc.* **1996**, *118*, 2922-2928.

(46) Xie, Z.; Tsang, C.-W.; Sze, E. T.-P.; Yang, Q.; Chan, D. T. W.; Mak, T. C. W., Highly chlorinated, brominated, and iodinated icosahedral carborane anions: 1-H- $\text{CB}_{11}\text{X}_{11}^-$, 1- $\text{CH}_3\text{-CB}_{11}\text{X}_{11}^-$ (X = Cl, Br, I); 1-Br- $\text{CB}_{11}\text{Br}_{11}^-$. *Inorg. Chem.* **1998**, *37*, 6444-6451.

(47) Grüner, B.; Janoušek, Z.; King, B. T.; Woodford, J. N.; Wang, C. H.; Vřetečka, V.; Michl, J., Synthesis of 12-Substituted 1-Carba-*closo*-dodecaborate Anions and First Hyperpolarizability of the 12- $\text{C}_7\text{H}_6^+\text{-CB}_{11}\text{H}_{11}^-$ Ylide. *J. Am. Chem. Soc.* **1999**, *121*, 3122-3126.

(48) Finze, M., Carba-*closo*-dodecaborates with one or two alkynyl substituents bonded to boron. *Inorg. Chem.* **2008**, *47*, 11857-11867.

(49) Himmelpach, A.; Reiss, G. J.; Finze, M., Microwave-assisted Kumada-type cross-coupling reactions of iodinated carba-*closo*-dodecaborate anions. *Inorg. Chem.* **2012**, *51*, 2679-2688.

(50) Rosenbaum, A. J.; Juers, D. H.; Juhasz, M. A., Copper-promoted cyanation of a boron cluster: synthesis, x-ray structure, and reactivity of 12-CN-*closo*-CHB₁₁H₁₀⁻. *Inorg. Chem.* **2013**, *52*, 10717-10719.

(51) Ringstrand, B.; Kaszynski, P.; Young, V. G. Jr.; Janoušek, Z., The anionic amino acid [*closo*-1-CB₉H₈-1-COOH-10-NH₃] and dinitrogen acid [*closo*-1-CB₉H₈-1-COOH-10-N₂] as key precursors to advanced materials: synthesis and reactivity. *Inorg. Chem.* **2010**, *49*, 1166-1179.

(52) Pecyna, J.; Denicola, R. P.; Gray, H. M.; Ringstrand, B.; Kaszynski, P., The effect of molecular polarity on nematic phase stability in 12-vertex carboranes. *Liq. Cryst.* **2014**, *41*, 1188-1198.

(53) Konieczka, S. Z.; Himmelpach, A.; Hailmann, M.; Finze, M., Synthesis, characterization, and selected properties of 7- and 12-ammoniocarba-*closo*-dodecaboranes. *Eur. J. Inorg. Chem.* **2013**, 134-146.

(54) Pecyna, J.; Denicola, R. P.; Ringstrand, B.; Jankowiak, A.; Kaszynski, P., The preparation of [*closo*-1-CB₉H₈-1-COOH-10-(4-C₃H₇C₅H₉S)] as intermediate to polar liquid crystals. *Polyhedron* **2011**, *30*, 2505-2513.

(55) Grüner, B.; Císařová, I.; Čáslavský, J.; Bonnetot, B.; Cornu, D., Synthesis of 12-hydroxy and 12-dioxane derivatives of the *closo*-1-carbadodecaborate(1-) ion. Variations on the Plešek's bis(dicarbollide) pattern. *Collect. Czech. Chem. Commun.* **2002**, *67*, 953-964.

*Part II. Polar liquid crystalline materials derived from the [closo-1-CB₉H₁₀]⁻ and
[closo-1-CB₁₁H₁₂]⁻ anions*

The Fréedericksz transition,¹ in which polar molecules reorient in an external electric field, is the working principle of almost all liquid crystal display devices. The value that plays the critical role here is the threshold voltage V_{th} , which is the minimum voltage required for the molecules to begin changing their orientation. This voltage is inversely proportional to the square root of dielectric anisotropy, $\Delta\epsilon$, which, in turn, depends on the magnitude of the dipole moment (Figure 1). The larger, the dipole moment, the larger the dielectric anisotropy. High values of the dipole moment, μ , result in high values of dielectric anisotropy, $\Delta\epsilon$, which in turn leads to low values of threshold voltage and V_{th} . For this reason, molecules possessing high dipole moment are sought as materials for liquid crystal display applications.

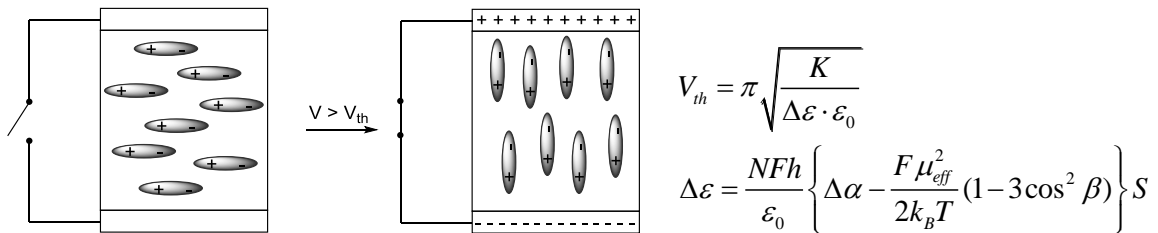


Figure 1. Schematic representation of the Fréedericksz transition.

Introduction of polar substituents such as CN, SCN or F to the liquid crystal molecules usually results in induction of only moderate dipole moments. Significantly larger values of dipole moments are offered by zwitterionic molecules. However, common zwitterions are often not suitable as polar materials for LCD applications due to geometries being not compatible with the requirements for nematic materials. Consequently, only several examples of liquid crystalline zwitterions are known. On the

other hand, zwitterions derived from *closo*-carbaborates appear to be suitable for the formation of calamitic liquid crystals upon proper substitution at the antipodal positions. Results for derivatives of *p*-carboranes showed that their derivatives form nematic phase preferentially over other mesophases.^{2,3} Two of the clusters have been found to be especially attractive building blocks of highly polar materials for LCD applications: the [*closo*-1-CB₁₁H₁₂]⁻ (**1**) and [*closo*-1-CB₉H₁₀]⁻ (**2**) anions. They possess highly delocalized charge, and introduction of an onium fragment, such as sulfonium, pirydinium or quinuclidinium, results in substantial longitudinal dipole moment (See Chapter 1, Table 1).

As previously demonstrated by our research group,⁴ 1-sulfonium **3** (type **2B**, see Table 1) and 1-quinuclidinium **4** (type **2A**) derivatives of the [*closo*-1-CB₉H₁₀]⁻ anion (**2**) were found to be effective high $\Delta\epsilon$ additives to nematic hosts (Figure 2).

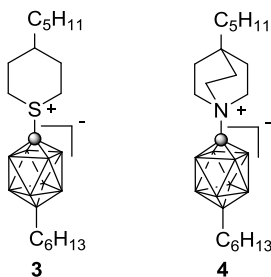


Figure 2. Sulfonium **3** and quinuclidinium **4** derivatives of the [*closo*-1-CB₉H₁₀]⁻ anion (**2**).

Analogous to **3** sulfonium derivatives of type **2E** (see Chapter 1, Table 1) seemed to be more promising and were expected to be also compatible with nematic hosts. However, the overall yield of preparation of key intermediates such as sulfonium acid **5** was low ($\approx 1.5\%$ from B₁₀H₁₄) and the multi-step process required large-scale preparation

of the precursors (Figure 3). Especially, the synthesis of iodo acid **6** required large volumes of aqueous solutions and large excess of reagents.

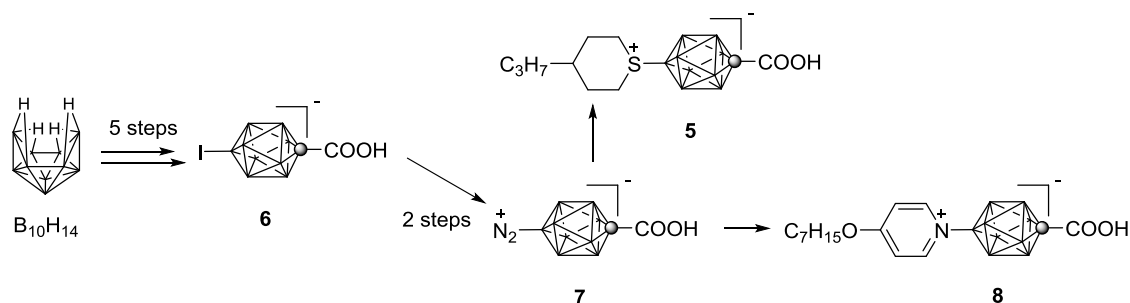


Figure 3. Multi-step synthesis of sulfonium **5** and pyridinium **8** acids from decaborane, $B_{10}H_{14}$.

Pyridinium derivatives of the [*closo*-1- CB_9H_{10}] $^-$ anions (type **2F**, see Chapter 1, Table 1)⁵ were also shown to be attractive materials for electro-optical applications. However, access to analogous 12-pyridinium zwitterions based on the [*closo*-1- $CB_{11}H_{12}$] $^-$ cluster (type **1F**) was hindered due to instability of the dinitrogen derivative of the [*closo*-1- $CB_{11}H_{12}$] $^-$ analogous to **7**, and side reactions, which resulted in low-yielding synthesis of the pyridinium acid [*closo*-1- $CB_{11}H_{10}$ -1-COOH-12-(4- $C_7H_{15}OC_5H_4N$)].⁶ Similar synthetic issues hampered access to 1-pyridinium derivatives of the [*closo*-1- $CB_{11}H_{12}$] $^-$ cluster (type **1C**). When thermolyzed, the stable dinitrogen derivative [*closo*-1- CB_9H_9 -1- N_2] reacts with pyridine by two parallel mechanisms: SET followed by radical homolysis of the carbon–nitrogen bond, and heterolysis of the carbon-nitrogen bond, which also hinders access to 1-pyridinium derivatives of the [*closo*-1- CB_9H_{10}] $^-$ anion (type **2C**).⁷ These issues were addressed in my research and results are described in this chapter.

Thus, Chapter 3 consists of two sections, which provide details on the synthesis of key precursors to sulfonium (type **2E**) and pyridinium (type **1F**) zwitterionic derivatives

of the [*closo*-1-CB₉H₁₀][−] and [*closo*-1-CB₁₁H₁₂][−] anions, respectively. Synthetic details and investigation of the properties of polar materials derived from the sulfonium acid **1** (type **2E**) and materials based on 1-pyridinium zwitterionic derivatives (type **1C** and **2C**) of both clusters are discussed in two sections of Chapter 4. Chapter 5 describes investigation of the fundamental phenomenon, the role of the molecular dipole moment in mesophase stabilization, using compounds prepared from the developed intermediates and methods.

References

- (1) Fréedericksz, V.; Zolina, V., Forces causing the orientation of an anisotropic liquid. *Trans. Faraday Soc.* **1933**, *29*, 919-930.
- (2) Czuprynski, K. L.; Douglass, A. G.; Kaszynski, P.; Drzewinski, W., Carborane-Containing Liquid Crystals: A Comparison of 4-Octyloxy-4'-(12-Pentyl-1,12-dicarbododecaboran-1-yl) with Its Hydrocarbon Analogs. *Liq. Cryst.* **1999**, *26*, 261-269.
- (3) Czuprynski, K. L.; Kaszynski, P., Homostructural two-ring mesogens: a comparison of *p*-Carboranes, bicyclo[2.2.2]octane and benzene as structural elements. *Liq. Cryst.* **1999**, *26*, 775-778.
- (4) Ringstrand, B.; Kaszynski, P.; Januszko, A.; Young, V. G. J., Polar Derivatives of the [*closo*-1-CB₉H₁₀][−] Cluster as Positive Δε Additives to Nematic Hosts. *J. Mater. Chem.* **2009**, *19*, 9204-9212.
- (5) Ringstrand, B.; Kaszynski, P., High Δε nematic liquid crystals: fluxional zwitterions of the [*closo*-1-CB₉H₁₀][−] cluster. *J. Mater. Chem.* **2011**, *21*, 90-95.

(6) Pecyna, J.; Denicola, R. P.; Gray, H. M.; Ringstrand, B.; Kaszynski, P., The effect of molecular polarity on nematic phase stability in 12-vertex carboranes. *Liq. Cryst.* **2014**, *41*, 1188-1198.

(7) Ringstrand, B.; Kaszynski, P.; Franken, A., Synthesis and reactivity of [*closo*-1-CB₉H₉-1-N₂]: functional group interconversion at the carbon vertex of the {*closo*-1-CB₉} cluster. *Inorg. Chem.* **2009**, *48*, 7313-7329.

Chapter 3. Methods and key intermediates to polar liquid crystals

3.1 Introduction

The first section describes the process of scaling up and optimization of preparation of sulfonium acids [*closo*-1-CB₉H₈-1-COOH-10-(4-C_nH_{2n+1}C₅H₉S)], synthesis of their esters, and investigation of the properties of resulting liquid crystalline materials (type **2E**). The second section provides details of development of synthetic access to 12-pyridinium derivatives (type **1F**) based on the [*closo*-1-CB₁₁H₁₂]⁻ anion (**1**).

3.2 The preparation of [*closo*-1-CB₉H₈-1-COOH-10-(4-C₃H₇C₅H₉S)] as intermediate to polar liquid crystals.

3.2.1 Description and contributions

This work was performed when I joined Prof. P. Kaszynski's group in June 2010. The goal of the project was to develop a practical synthesis of iodo acid [*closo*-1-CB₉H₈-1-COOH-10-I]⁻ (**1**), a key precursor to sulfonium acids [*closo*-1-CB₉H₈-1-COOH-10-(4-C_nH_{2n+1}C₅H₉S)] from decaborane B₁₀H₁₄. This multistep process was developed for 40 g of decaborane, B₁₀H₁₄. The preparation of the [*arachno*-6-CB₉H₁₃-6-COOH]⁻ (**5**), the critical step in the process, now uses four times smaller volumes of the aqueous phase. Oxidation process of **5** to [*closo*-2-CB₉H₉-2-COOH]⁻ (**4**) requires fewer equivalents of iodine, can be run conveniently in 10-fold smaller volumes of solvents and shorter times. The iodo acid **1** was prepared in 8-10% overall yield starting from decaborane, B₁₀H₁₄. The sulfonium acid **2[3]** was obtained from iodo acid **1** through a subsequent amination of **1** followed by diazotization of the amino acid [*closo*-1-CB₉H₈-1-COOH-10-NH₃] (**8**) and thermolysis of the dinitrogen derivative [*closo*-1-CB₉H₈-1-COOH-10-N₂] (**10**) in thiane **17[3]** in 13% overall yield. Improvement of amination of iodo acid **1** using

different ligands was attempted, but was not successful. Lastly, liquid crystalline properties of ester **3[3]a** prepared from sulfonium acid **2[3]** and 4-butoxyphenol were investigated.

I was involved in all aspects of this research, which includes synthesis, characterization of compounds and optimization of the procedures for the iodo acid **1** and its intermediates. I was responsible for investigation of the amination process of iodo acid [*closo*-1-CB₉H₈-1-COOH-10-I]⁻ (**1**) using Pd(0) catalysts. I also searched for alternative methods for preparation of the sulfonium acid **2[3]**. My work also included synthesis and investigation of liquid crystalline properties of ester **3[3]a** prepared from sulfonium acid **2[3]** and 4-butoxyphenol. Dr. Bryan Ringstrand and Dr. Aleksandra Jankowiak contributed to the process of preparation of the iodo acid **1**. Rich Denicola, an undergraduate student, assisted with preparation of some intermediates.

In the following chapter the entire text of the manuscript is included for consistency of the narrative, however, the experimental section contains only experiments performed by me.

3.2.2 The manuscript

Reproduced with permission from Elsevier
Pecyna, J.; Denicola, R. P.; Ringstrand, B.; Jankowiak, A.; Kaszynski, P. *Polyhedron* **2011**, *30*, 2505-2513.
Copyright 2011 Elsevier. Available online:

<http://www.sciencedirect.com/science/article/pii/S0277538711003974>

3.2.2.1 Introduction

The Brellocks' synthesis [1,2] of the {CB₉} cluster from B₁₀H₁₄ followed by Kennedy's halogenation and rearrangement [3] of the {*closo*-2-CB₉} opened up possibilities for preparing 1,10-difunctional derivatives of the [*closo*-1-CB₉H₁₀]⁻ anion. Subsequently, we reported [4] the first practical synthesis of isomerically pure iodo acid

[*closo*-1-CB₉H₈-1-COOH-10-I]⁻ (**1**), which has been the key intermediate in the synthesis of new classes of polar [5-7] and ionic [8] liquid crystals **I** and **II**, respectively (Figure 1). In this context, the carboxyl group in **1** has been converted into X = ester [6-9], amino [4,8], dinitrogen [8], azo [8], and sulfonium [5,9] groups, while the iodine to Y = alkyl [5,8], amino [9], dinitrogen [9], pyridinium [6,7,9], and sulfonium [6,9] derivatives. Among the 10-sulfonium derivatives are esters of acid **2**[5], such as **3**[5], which exhibit nematic behavior [6] (Figure 2). Due in part to their fluxional behavior and facile epimerization at the sulfur center, esters **3**[5] such as the 4-butoxyphenyl ester **3**[5]**a**, are sufficiently soluble in liquid crystalline hosts and are of interest for display applications. However, further exploration of these unusual molecular materials and their practical applications require significant quantities of the iodo acid **1** and is limited by access to [*closo*-2-CB₉H₉-2-COOH]⁻ (**4**).

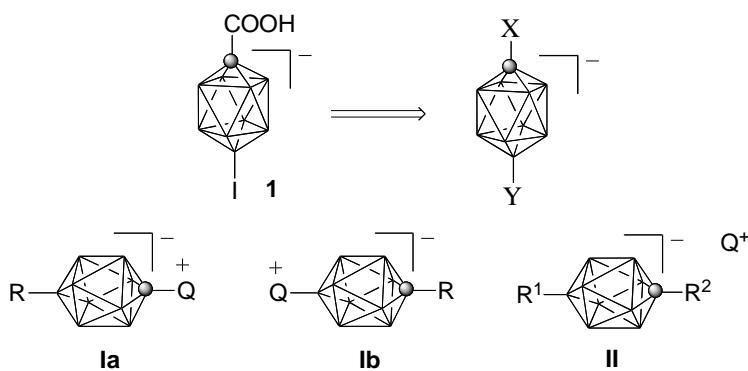


Figure 1. Acid **1** as a precursor to 1,10-difunctionalized derivatives of the {*closo*-1-CB₉} cluster, which include polar (**I**) and ionic (**II**) liquid crystals. Q⁺ is pyridinium, ammonium or sulfonium, R, R¹, R² = alkyl, ester. For X and Y see text.

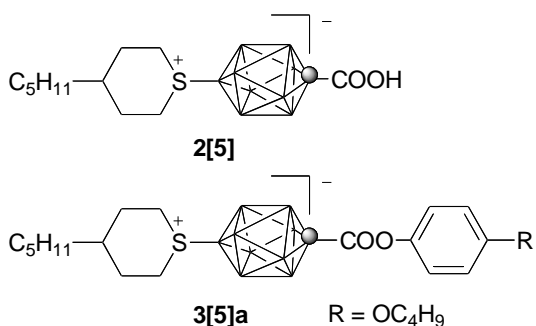
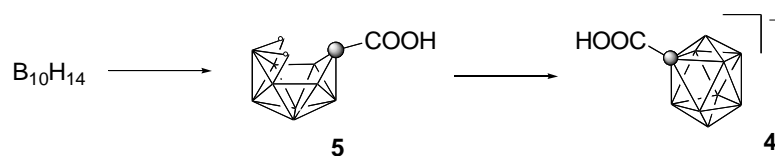


Figure 2. Structures for acid **2[5]** and ester **3[5]a**.

The preparation of *closo* acid **4** (Scheme 1) described by Kennedy involves large volumes of solvents and large excess of reagents [10]. For instance, the total volume of solution in the Brelloch's reaction is 100 mL/g of B₁₀H₁₄. The second step, an oxidation, uses an even larger volume of solvents at 150 mL/g of *arachno* acid **5**. Thus, the first two reactions used in the preparation of *closo* acid **4** are impractical to scale up in their present form.



Scheme 1. Preparation of *arachno* acid **5** and subsequent oxidation to *closo* acid **4** starting from B₁₀H₁₄.

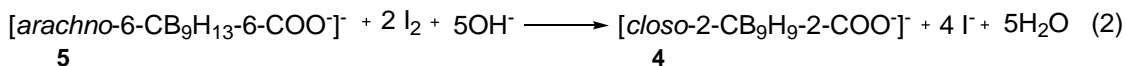
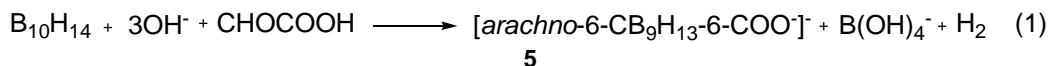
Here we describe optimization of the synthesis of acid **4** and a convenient procedure for its preparation that uses up to 40 g of B₁₀H₁₄ at a time, large-scale preparation of iodo acid **1**, and its conversion to sulfonium acid **2[3]**. Finally, we demonstrate liquid crystalline ester **3[3]a** derived from acid **2[3]** and compare its properties those of the higher homologue **3[5]a**.

3.2.2.2 Results and discussion

Optimization of synthesis of [closo-2-CB₉H₉-2-COOH]⁻ (4)

Initially, we reproduced the original procedure [10,11] for the Brellocks' reaction of B₁₀H₁₄ with glyoxylic acid (run 1, Table 1). This reaction conducted at 1 g and 4 g scale of B₁₀H₁₄ gave consistent results of the arachno acid 5 in about 60% yield [12] and 85% to 90% purity, which is comparable to 53% originally reported [10,11]. The ¹¹B NMR spectrum was nearly identical to that reported for the arachno acid 5 with the main impurity associated with the signals at -12.1 and -0.5 ppm in addition to boric acid at 20.2 ppm in the NMR spectrum.

Since the original procedure uses several-fold excess of glyoxylic acid and base relative to that required by stoichiometry (equation 1), our attempts were directed at reducing amounts of the reagents and the volume of the solution. Optimization reactions were conducted on 1 g of B₁₀H₁₄.



Reducing the amount of glyoxylic acid by half gave lower yield of the product with comparable purity in a range of 85%-95% (run 2). When the amount of base was also reduced by half and less water used (run 3), the product was obtained in higher yield and similar purity. Further reduction of the amount of glyoxylic acid led to unstable product that decomposed upon isolation (run 4). Other experiments showed that the volume of water could be reduced further without affecting the yield or purity (run 5, 6, and 7). In all reactions in which the amount of glyoxylic acid was reduced (run 3, 4, 8,

9), the precipitation procedure was complicated by excessive foaming during quenching with HCl, and frequent formation of the product as a clumpy, sticky goo rather than a microcrystalline solid. Even though the amount of base can be reduced, excess base helps with fast dissolution of B₁₀H₁₄.

Considering the difficulties with isolation of the *arachno* acid **5** with smaller amounts of the reagents, we decided to pursue the concentrated version of the original procedure. Thus, decreasing the volume of water by 4 times gave the *arachno* acid **5** in yield and purity comparable to the original procedure (run 10a vs. run 1). Additional reduction of volume of the reaction was accomplished by increasing the concentration of HCl from 5% in the original procedure to 18%. Overall, this procedure reduces the volume of water from 100 mL/g of B₁₀H₁₄ to 25 mL/g of B₁₀H₁₄ and is considered a significant improvement. This procedure (run 10a) was successfully scaled from 1 g to 10 g (run 10b) and then to 20 g (run 10c) of B₁₀H₁₄. The 10-g scaled reaction was reproducible over several runs giving average yields of 60 % with purities of about 90%.

The 20 g scale reaction posed new challenges related to heat dissipation during acid-base reactions (addition of glyoxylic acid and quenching with HCl) and consequently exotherm control. The reaction was conducted conveniently in a 2-L vessel in an ice-bath with efficient mechanical stirring and an internal thermometer. The reaction was closely reproducible as long as the internal temperature of the mixture was maintained around 5 °C, and gave an average yield of 70% with purities of about 90% over several runs. The total volume of the aqueous solution after quenching with HCl is approximately 500 mL. Insufficient acidification and failure to adjust the pH to about 3 lead to the formation of pyrophoric products, as it was observed in one instance: product

of a reaction on a 50 g scale of B₁₀H₁₄ spontaneously ignited after overnight drying. ¹¹B NMR spectrum of the pyrophoric material revealed a possibly different chemical structure than that routinely obtained at 20 g with fully adjusted pH [13].

The preparation of *arachno* acid **5** was successfully scaled to 30 g of B₁₀H₁₄ by adding crushed ice to the basic solution and using less concentrated HCl (12% *vs* 18%) during work-up for better control of the exotherm (run 10d). Finally, the reaction was scaled to 40 g of B₁₀H₁₄ and run reproducibly several times in a 3-L vessel (run 10e). The exotherm of neutralization processes is controlled by using crushed ice (200 g) and freezer-chilled 20% solutions of HCl.

Table 1. Optimization of preparation of [*arachno*-6-CB₉H₁₃-6-COOH]⁻ NEt₄⁺ (**5**).^a

Run	B ₁₀ H ₁₄	KOH	HOOCCHO	H ₂ O	Yield ^b
	mmol	mmol	mmol	mL	%
1	8.2	112.5	55	50	62
2	8.2	112.5	28.2	50	47 ^c
3	8.2	70	28.2	35	79 ^c
4	8.2	60	12.4	15	^d
5	8.2	60	28.2	10	62 ^c
6	8.2	53.3	20.5	10	72 ^c
7	8.2	112.5	55	20	78
8	8.2	70	28.2	15	81 ^c
9	8.2	85.7	28.2	10	56 ^c

10a	8.2	112.5	55	10	49
	Scale up				
10b	82	1120	543	100	67 avr
10c	164	2240	1080	200	70 avr
10d	246	3360	1620	300	61 ^e
10e	327	4480	2160	500	66-71

^a All reactions are run at ice bath temperature; reaction time 2 hrs.

^b Product precipitated from the reaction mixture. See footnote [12].

^c The precipitate often is a tacky goo instead of crystalline solid.

^d Expected product **5** was not formed; excessive decomposition during workup.

^e Crushed ice was added to the basic solution. See experimental procedure.

Overall, results indicate that good yields and purity of *arachno* acid **5** can be obtained using fewer equivalents of base and glyoxylic acid in the Brellocks' reaction. However, the workup procedure is complicated by excessive foaming during quenching with HCl, and the sticky, difficult to work with form of the product. This is avoided by using larger amounts of reagents as described in the original procedure. The desired reduction of the volume of the reaction is achieved by using ~ 6 times more concentrated solution of base and 4 times more concentrated HCl. These reactions also require finely ground B₁₀H₁₄ for quick dissolution at < 5 °C and slow addition of glyoxylic acid and HCl to allow for efficient heat dissipation.

The oxidation of the *arachno* acid **5** to *closo* acid **4** was originally conducted using hypiodite under basic solutions [10,11]. The stoichiometry of the oxidation of the

arachno acid **4** requires 2 moles of I₂ [14] (equation 2), while the original procedure used 2.75 moles of I₂ with a total volume of aqueous solution of 150 mL/g of *arachno* acid **5**. Since excess I₂ is small, our focus was mainly on reducing the volume of solvents used in the process and exploring alternative oxidants.

As we reported earlier [4], a briefly optimized oxidation required up to 90% excess of I₂ at ambient temperature, which was the recommended temperature in the original procedure [10,11]. The same reaction run at ice bath temperature was completed with stoichiometric (2 moles) amounts of I₂ (run 1, Table 2), less base, and in shorter time (1.5 hr vs. 6 hr). The volume of water was reduced by a factor of 12 from 150 mL/g of *arachno* acid **5** to 12 mL/g. The need for only stoichiometric amounts of I₂ and hence its more efficient use at 0 °C may be explained by the higher stability of hypoiodite at low temperature. The progress of the oxidation was monitored by ¹¹B NMR of a small aliquot of the basic solution in D₂O. The analysis demonstrated that the reaction is completed in less than 2 hr instead 6 hr as originally reported. To assure complete oxidation of **5**, a 15% excess I₂ was used for large-scale preparations of acid **4**, which was typically obtained in 43%-58% yield (run 2, Table 2).

We also tested hypobromite as the oxidant for the *arachno* acid **5**, but the results were significantly less satisfactory (runs 3–6, Table 2). The solutions of the hypobromite had to be prepared separately, required relatively large volumes of the aqueous phase, and the yield was low although with comparable purity.

Table 2. Optimization of formation of [*closo*-2-CB₉H₉-2-COOH]⁻ NET₄⁺ (**4**).^a

Run	5	KOH	Oxidant		H ₂ O	Time	Yield
	mmol		mmol				
1	5	40	I ₂	10	15	0.5	54
2	217	1742	I ₂	500	645	2	43- 58
3	5	40	Br ₂	15	15	0.5	35
4	24.3	192	Br ₂	97.2	72.3	0.75	23
5	62	496	Br ₂	248	92	0.75	34 ^b
6	20.8	166	Br ₂	83.2	62.4	0.75	^c

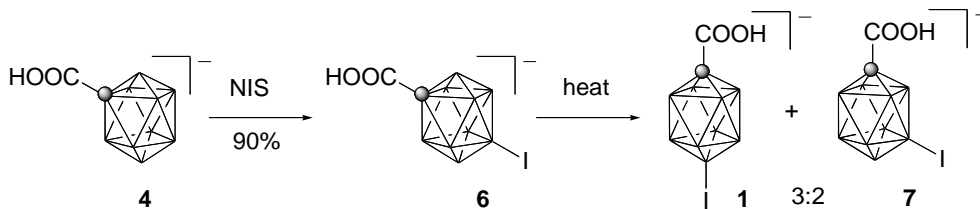
^a All reactions are run at ice bath temperature

^b Solution turned black upon addition of HCl

^c Resubmission of product from reaction 5 led to decomposition.

Optimization of synthesis of [*closo*-1-CB₉H₈-1-COOH-10-I]⁻ (**1**)

The previously reported iodination [4] of *closo* acid **4** with 50% excess NIS to form iodo acid **6** (Scheme 2) was used without modification on a scale of up to 30 g of *closo* acid **4**. The impurities in the *arachno* acid **5** were largely removed during the oxidation step and nearly completely during work-up after iodination. The iodination step now has higher yield of about 90% than the originally reported [4] (67% yield) due to higher purity of acids **5** and **4**.



Scheme 2. Transformation of *closo* acid **4** to iodo acid **1**.

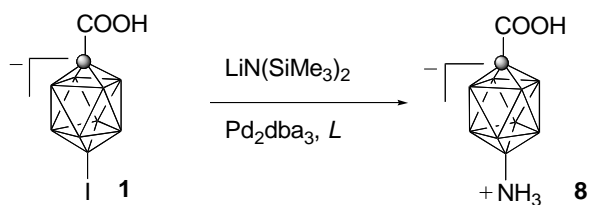
In addition, two other iodinating reagents, ICl and I₂, were investigated for the preparation of iodo acid **6**. Reactions of *closo* acid **4** with NIS, I₂, and ICl were conducted at the 100 mg scale for 72 hrs at -10 °C. Reaction with NIS reproduced the results previously obtained on a large scale, I₂ gave only recovered starting material **4**, and ICl gave iodo acid **6** with only 20% conversion.

The final two steps, rearrangement of the iodo acid **6** to a mixture of iodo acids **1** and **7** (Scheme 2) followed by separation of isomers, remain straightforward, and scaling up was simple. Starting from a 38 g batch of iodo acid **6**, thermal rearrangement gave an expected [4] 3:2 mixture of iodo acids **1** and **7** (68-86%), which after two recrystallizations from aqueous EtOH gave about 11 grams of 99 % pure isomer **1**. Attempts to harvest more iodo acid **1** from the remaining mixture of the isomeric iodo acids were unsuccessful.

Optimization of synthesis of [closo-1-CB₉H₈-1-COOH-10-NH₃] (8)

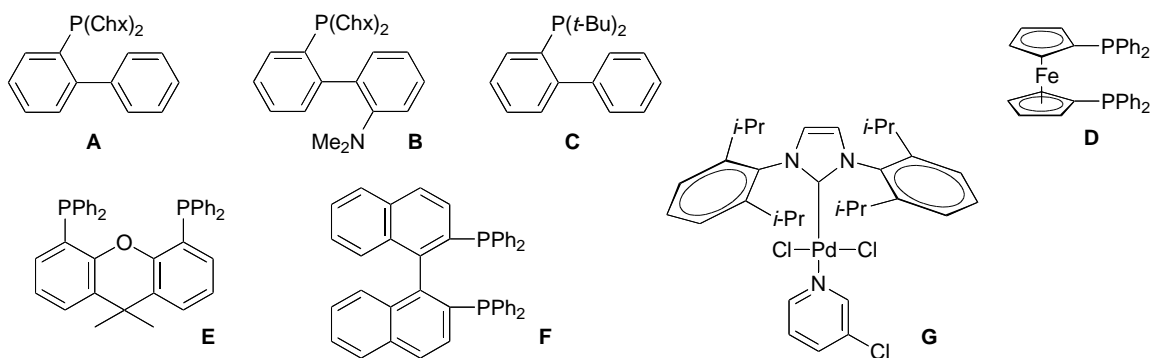
The originally reported [9] amination of the iodo acid **1** to amino acid **8** (Scheme 3) was accomplished using 2-(dicyclohexylphosphino)biphenyl (**A**) as a ligand for the Pd(0) catalyst. The reaction requires a large excess (> 10 eq) of LiHMDS and gives significant amounts, up to 20%, of the deiodinated product [closo-1-CB₉H₉-1-COOH]

(9). In an effort to improve this process, we investigated six other ligands *L* (CHART I), which have been used for amination of aromatic halides [15].



Scheme 3. The preparation of amino acid **8**.

CHART I

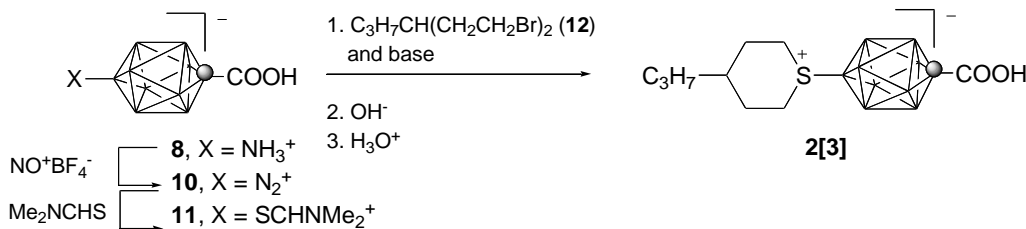


Test reactions were run on a 50 mg scale of iodo acid **1** using conditions reported previously [9] and a phosphine ligand *L* selected from the list in CHART I. After 24 hr of reflux and full workup, the reaction mixtures were analyzed as ethereal extracts from aqueous acid. ^{11}B NMR results demonstrated that for ligand **B** the iodo acid **1** was practically consumed and the amino acid **8** was contaminated with about 20% of diiodinated product **9** and the same amounts of 10-phosponium byproducts. The same reaction run on a 1 g scale gave the amino acid **8** isolated in 44% yield. Conversion of **1** was only 50% when ligand **C** was used, and the reaction mixture contained additional by-products presumably decarboxylation products. No conversion of iodo acid **1** was observed for other ligands, DPPF (**D**), XANTPHOS (**E**), BINAP (**F**), and PEPPSI-IR (**G**).

Overall, the amination reaction was conveniently run on a 15 gram scale of iodo acid **1** using phosphine **A** as the ligand giving the amino acid **8** in 43%–56% yield. It appears that ligands based on the 2-(dicyclohexylphosphino)biphenyl core, such as **A** and **B**, are particularly effective for *B*-amination [9] and *B*-amidation [16] of *closo*-boranes.

Synthesis of [closo-1-CB₉H₈-1-COOH-10-(4-C₃H₇C₅H₉S)] (2[3])

Amino acid **8** was converted to the dinitrogen acid **10** with a typical yield of 55%–65% by diazotization with NO⁺BF₄⁻ in pyridine solutions as described before [9] (Scheme 4). Subsequent thermolysis of **10** in Me₂NCHS gave protected mercaptan **11**, which was cycloalkylated with dibromide [17] **12** under hydrolytic conditions to form the sulfonium acid **2[3]**.

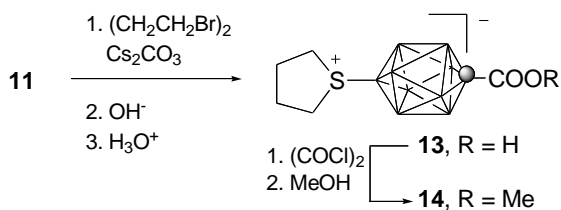


Scheme 4. Preparation of acid **2[3]**.

The alkylation reaction run under conditions described previously [6] for **2[5]**, Me₄N⁺OH⁻•5H₂O in MeCN, gave the acid **2[3]** in a modest yield of about 36% after recrystallization, which is comparable to that obtained [6] for **2[5]**. ¹H NMR spectra revealed formation of olefins and esters as by-products. The latter were converted to the acid by hydrolysis with alcoholic NaOH. However, the formation of the olefin complicated the purification of the acid. In effort to improve the yield and simplify the

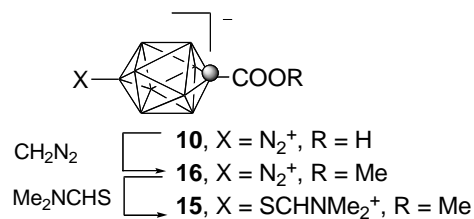
procedure, we investigated several other conditions and methods for the formation of acid **2**.

Changing the base from $\text{Me}_4\text{N}^+\text{OH}^- \cdot 5\text{H}_2\text{O}$ to Cs_2CO_3 resulted in improvement of the yield of **2[3]** to 45%-47% based on crude protected mercaptane **11** or 42%-44% based on dinitrogen acid **10**. Although the carboxyl group was still esterified under these conditions, the olefin formation was not observed. In both methods the crude acid can be purified additionally by converting to methyl ester **3[3]b**, chromatography, and basic hydrolysis back to acid **2[3]**. Using this method we also prepared tetramethylenesulfonium acid **13**, which was isolated as its methyl ester **14** (Scheme 5).

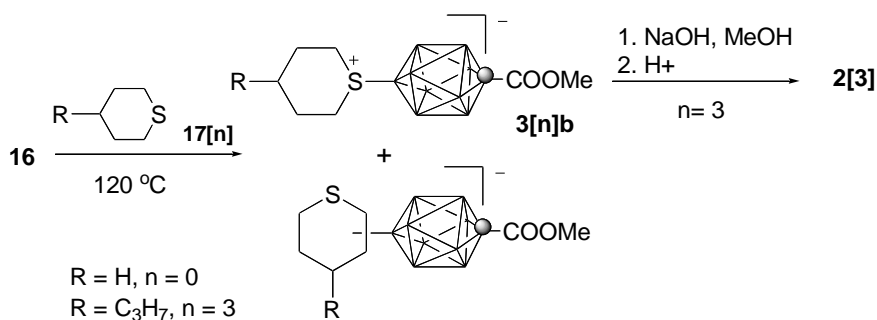


Scheme 5. Preparation of methyl ester **14**.

To avoid complications of formation of esters with dibromide **12**, we focused on methyl ester **15** prepared from the reported [9] dinitrogen ester **16** (Scheme 6). Cycloalkylation of **15** with dibromide **12** in the presence of Cs_2CO_3 and catalytic amounts of $\text{Bu}_4\text{N}^+\text{Br}^-$ in MeCN at 60 °C gave acid **2[3]** in 45% yield after hydrolysis of the intermediate methyl ester **3[3]b**. It was apparent that the reaction of the ester was slower than for the acid, and required higher temperatures presumably due to electron withdrawing effect of the COOMe group, when compared to the COO^- , and consequently lower reactivity of the sulfur atom.



Scheme 6. Preparation of methyl ester **15**.

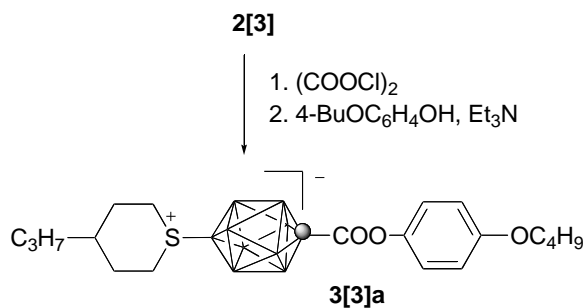


Scheme 7. Preparation of methyl esters **3[n]b** and acid **2[3]**.

Finally, we explored the formation of sulfonium acids **2[n]** directly from dinitrogen derivative **10** and appropriate thiane **17[n]**. Since the dinitrogen acid **10** was insoluble in thiane, we focused on its methyl ester **16** [9]. Thermolysis of the ester in solutions of the parent thiane (**17[0]**) gave the expected sulfonium ester **3[0]b** in 64% yield as the first less polar fraction. The second fraction contained a very polar by-product, presumably product of C-H insertion (Scheme 7), which was identified by the downfield shift of the B(10) nucleus ($\delta = +48$ ppm), characteristic for B(10)-alkyl derivatives [8], and MS spectrometry. A similar reaction of **16** with 4-propylthiane (**17[3]**) gave the ester **3[3]b** in 49% yield. Considering the yield of preparation of ester **16** and the hydrolysis step, the overall efficiency of this method is comparable to that involving cycloalkylation of **11** with dibromide **12** (Scheme 4).

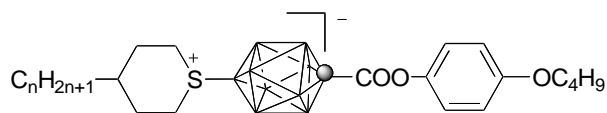
Liquid crystalline properties of esters

Ester **3[3]a** was prepared by estrification of sulfonium acid **2[3]** with 4-butoxyphenol (Scheme 8). Thermal analysis of **3[3]a** revealed a monotropic nematic phase with the clearing temperature of 96 °C (Table 3). Surprisingly, this temperature for the N-I transition is nearly the same as observed [6] for its higher homologue **3[5]a**. However, the melting temperature is lower by 10 K for **3[3]a** than for **3[5]a**.



Scheme 8. Preparation of ester **3[3]a**.

Table 3. Transition temperatures (°C) and enthalpies (kJ) for **3[n]a**.^a



<i>n</i>	
3	Cr 111 (N 96) I 29.3 1.1
5	Cr 101 (N 97) I ^b 28.6 0.6

^a Cr-crystal, N-nematic, I-isotropic. Monotropic transitions in parentheses. Transition enthalpies are given below in italics. ^b Ref [6].

Ester **3[3]a** and also methyl ester **3[3]b** and acid **2[3]** exist in solutions as mixtures of interconverting *trans* and *cis* isomers due to low epimerization barrier at the sulfur center [6] (Figure 3). This is evident from NMR spectra that show two sets of signals in about 4:1 ratio. The lower intensity signals are attributed to the *cis* isomer in which the B(10) nucleus is upfield by 2 ppm. In the *cis* isomer of **3[3]a** the hydrogen atoms of the two methylene groups adjacent to the sulfonium center are moved from their positions at 3.43 ppm (br t) and 3.71 (br doublet) in the *trans* isomer to form a multiplet centered at about 3.55 ppm. The carboxyl group substituent is also affected by epimerization at the sulfur atom. Thus, the methyl group in ester **3[3]b** is deshielded by 0.004 ppm in the *cis* isomer.

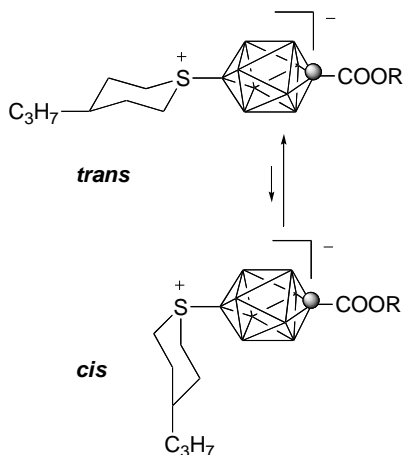


Figure 3. Interconversion of the *trans* and *cis* isomers of esters of ester **3[3]**. Two major conformers are shown.

3.2.2.3 Conclusions

We have developed a practical, large-scale preparation of acid [*closo*-2-CB₉H₉-2-COOH]⁻ (**4**) primarily by reducing the volume of the aqueous phase and better control of reaction temperature. The new procedure was demonstrated on a 40 g scale of B₁₀H₁₄,

which can be run conveniently in a 3-L vessel. The overall yield of the iodo acid **1** typically is about 10 g –12 g or 8%–10% from 40 g of $B_{10}H_{14}$, which is essentially the same as previously reported for 4 g of $B_{10}H_{14}$.

Our search for a more efficient Pd catalyst was unsuccessful, and the amination procedure for iodo acid **1** that gives about 50% of amino acid **8** could not be improved. The cycloalkylation reaction and formation of the sulfonium acid **2[n]** was improved by using Cs_2CO_3 as the base, nevertheless the yield remains under 50%. The overall yield of the sulfonium acid **2[3]** from the iodo acid **1** was about 13%. Thus, 1.3 g of **2[3]** can be obtained from 40 g of $B_{10}H_{14}$. Further increase of the overall yield can be achieved by improving the amination and cycloalkylation steps, and complete separation of the isomeric iodo acids.

3.2.2.4 Experimental

Reagents, excluding decaborane, and solvents were obtained commercially and used as supplied. KOH and HCl solutions were pre-chilled in the freezer (-10 to -20 °C) before use. Reactions and subsequent manipulations were conducted in air. NMR spectra were obtained at 400.1 MHz (1H) or 128.4 MHz (^{11}B) in CD_3CN , unless specified otherwise. 1H NMR spectra were referenced to the solvent signals, while ^{11}B NMR chemical shifts were referenced to an external boric acid sample in CH_3OH that was set to 18.1 ppm.

Purification of decaborane ($B_{10}H_{14}$)

Technical grade decaborane (200 g, 1.64 mol) was suspended in CH_2Cl_2 /hexane (1:9, 300 mL) and passed through a silica gel plug (6 in x 6 in), which was continuously washed with CH_2Cl_2 /hexane (1:9) until mass recovery was constant (176 g, 88%). The decaborane was further purified by vacuum sublimation (100–110 °C, 0.5 mm Hg) onto a

cold finger. A light yellow residue was left over in some cases. Mass recovery was greater than 95% for sublimation.

Preparation of [closo-1-CB₉H₈-1-COOH-10-I]⁻[NMe₄]⁺ (1) and [closo-1-CB₉H₈-1-(COOH)-6-I]⁻[NMe₄]⁺ (7) [4].

A solution of [closo-2-CB₉H₈-2-COOH-7-I]⁻[NEt₄]⁺ (**6**, 38.48 g, 0.091 mol) in CH₃CN (150 mL) was refluxed for 22 hrs. Solvent was removed *in vacuo*, 10 % HCl (275 mL) was added, and the mixture was extracted with Et₂O (4 x 100 mL). Water (350 mL) was added to the combined Et₂O extracts, and the solvent was completely removed *in vacuo*. The resulting suspension was filtered, [NMe₄]⁺Cl⁻ (11.05 g, 0.101 mol) was added, and the white precipitate was filtered off, washed with H₂O (3 x 100 mL), press dried, and further dried overnight in air giving 22.5 g – 28.5 g (68%–86% yield) of a 3:2 mixture of iodo acids **1** and **7** based on ¹¹B NMR, which was consistent with that reported in the literature [4].

Isolation of [closo-1-CB₉H₈-1-COOH-10-I]⁻[NMe₄]⁺ (1) [4].

A 3:2 mixture of iodo acids **1** and **7** (25.74 g, 0.071 mol) was suspended in near boiling H₂O (250 mL). EtOH (120 mL) was added slowly until the solution became homogeneous. The solution was further heated until solid material began to develop, and then a minimal amount of EtOH (~10 mL) was added to completely redissolve the material. The solution was removed from heat, and left to cool to ambient temperature at which white needles began to grow. The needles were filtered, washed with a small amount of water (50 mL), and dried in air. The needles were recrystallized a second time giving 10.8 g – 14.7 g of 99% pure isomer (42%–57% yield). ¹¹B NMR was consistent

with that reported in the literature [4]. The combined filtrates from the two recrystallizations contained a 2:3 ratio of iodo acids **1** and **7** by ^{11}B NMR.

Preparation of [closo-1-CB₉H₈-1-COOH-10-(4-C₃H₇C₅H₉S)] (2[3])

Method A. A crude protected mercaptan [closo-1-CB₉H₈-1-COOH-10-SCHNMe₂] (**11**, 2.00 g, 7.90 mmol) was added to a solution of Cs₂CO₃ (10.29 g, 31.6 mmol) and [NBu₄]⁺Br⁻ (0.255 g, 0.79 mmol) in CH₃CN (200 mL), which resulted in the formation of a white precipitate. 1,5-Dibromo-3-propylpentane (**12**, 2.22 mL, 11.84 mmol) [17] was added and the reaction mixture was stirred for 24 hrs at 85 °C. The reaction mixture was evaporated to dryness, the residue dissolved in a MeOH solution (50 mL) containing NaOH (0.304 g, 7.59 mmol) and the mixture was stirred at 55 °C for 4 hrs, to hydrolyze the ester by-product. Water was added (20 mL), the solvent was removed nearly to dryness, and 10% HCl (300 mL) was added. The suspension was stirred vigorously with Et₂O (50 mL) until the aqueous layer became homogeneous. The Et₂O layer was separated, and the aqueous layer was further extracted with Et₂O (4 x 50 mL). The Et₂O layers were combined, washed with water, dried (Na₂SO₄), and evaporated leaving crude sulfonium acid **2[3]** as an orange solid. The material was passed through a short silica gel plug (CH₃OH/CH₂Cl₂, 1:19, R_f = 0.4), solvent evaporated, and the residue washed with hot hexane giving 1.67 g–2.08 g of an off-white solid. The solid was recrystallized from EtOH or MeOH to give 1.09 g – 1.13 g (45%–47% yield) of pure acid **2[3]** as colorless needles. Crystallization from toluene gave colorless blades of acid **2[3]** as a solvate with toluene (1:1) from which the solvent was removed by heating at 100 °C in vacuum for 2 hrs: mp 252-254 °C; ^1H NMR major signals: δ 0.6-2.6 (br m, 8H), 0.93 (t, $J = 7.1$ Hz, 3H), 1.31-1.45 (m, 4H), 1.64-1.75 (m, 2H), 2.05-2.15 (m, 1H), 2.33

(dm, $J = 11.8$ Hz, 2H), 3.39 (t, $J = 12.4$ Hz, 2H), 3.74 (dm, $J = 12.0$ Hz, 2H), 9.7 (brs, 1H); minor signals: δ 2.29-2.33 (m), 3.47-3.56 (m); ^{11}B NMR δ major signals: -20.3 (d, $J = 141$ Hz, 4B), -14.8 (d, $J = 158$ Hz, 4B), 32.4 (s, 1B); minor signal: δ 30.3 (s). Anal. Calcd for $\text{C}_{10}\text{H}_{25}\text{B}_9\text{O}_2\text{S}$: C, 39.17; H, 8.22. Found: C, 39.61; H, 8.11.

Method B. A solution of methyl ester **3[3]b** (0.88 g, 2.74 mmol) and NaOH (0.44 g, 11 mmol) in MeOH (20 mL) was refluxed for 6 hrs. The solvent was evaporated, water was added followed by 10 % solution of HCl. The resulting precipitated was filtered and dried giving 0.71 g (84% yield) of acid **2[3]**.

*Preparation of ester [closo-1-CB₉H₈-1-COOH-10-(4-C₃H₇C₅H₉S)] and 4-butoxyphenol (**3[3]a**).*

Acid **[2[3]]** (40 mg, 0.13 mmol) was dissolved in anhydrous CH_2Cl_2 (2 mL). $(\text{COCl})_2$ (0.017 mL, 0.197 mmol) and a catalytic amount of *N,N*-dimethylformamide were added, the reaction mixture was stirred for 1 hr, and evaporated to dryness *in vacuo*. The residue was dissolved in anhydrous CH_2Cl_2 (5 mL) and NEt_3 (0.11 mL, 0.784 mmol) and 4-butoxyphenol (33 mg, 0.20 mmol) were added. The reaction was stirred overnight. The reaction mixture was washed with 5 % HCl, organic layer dried (Na_2SO_4), and solvent removed. The crude material was passed through a short silica gel plug (CH_2Cl_2 /hexane, 1:1) giving 47 mg (52% yield) of ester **3[3]a** as a white crystalline solid. The resulting ester was purified further by recrystallization from *iso*-octane/toluene: ^1H NMR (CDCl_3) δ 0.6-2.8 (br m, 8H), 0.95 (t, $J = 6.8$ Hz, 3H), 0.99 (t, $J = 7.4$ Hz, 3H), 1.36-1.43 (m, 4H), 1.51 (sextet, $J = 7.5$ Hz, 2H), 1.65-1.83 (m, 4H), 2.26-2.42 (m, 3H), 3.43 (t, $J = 12.6$ Hz, 2H), 3.71 (br d, $J = 12.7$ Hz, 2H), 3.98 (t, $J = 6.5$ Hz, 2H), 6.95 (d, $J = 9.0$ Hz, 2H), 7.24 (d, $J = 9.0$ Hz, 2H); minor signals: δ 2.07-2.14 (m), 2.24-2.35 (m),

3.54-3.61 (m); ^{11}B NMR (CDCl_3) major signals: δ -19.6 (d, J = 146 Hz, 4B), -14.0 (d, J = 160 Hz, 4B), 31.7 (s, 1B); minor signal: δ 30.0 (s). Anal. Calcd. for $\text{C}_{20}\text{H}_{37}\text{B}_9\text{O}_3\text{S}$: C, 52.81; H, 8.20. Found: C, 52.00; H, 8.07.

Preparation of [closo-1-CB₉H₈-1-COOMe-10-(C₅H₁₀S)] (3[0]b).

A solution of ester [closo-1-CB₉H₈-1-COOMe-10-N₂] (**16**, 20 mg, 0.09 mmol), prepared by methylation of dinitrogen acid **10** with CH_2N_2 [9], in thian (1 mL) was heated at 120 °C for 2 hrs. The solvent was removed under reduced pressure (80 °C, 0.2 mmHg), the residue was washed with hexane, and separated using a short silica gel column (hexane/ CH_2Cl_2 , 1:1). The first fraction contained 17.3 mg (64% yield) of pure methyl ester **3[0]b** as a white crystalline solid, which was recrystallized from *iso*-octane: mp 173-174 °C; ^1H NMR δ 1.20 (br q, J = 144 Hz, 4H), 1.69 (dtt, J_1 = 11.6 Hz, J_2 = 11.0 Hz, J_3 = 3.0 Hz, 1H), 1.89-1.95 (m, 1H), 1.90 (br q, J = 157 Hz, 4H), 1.98-2.08 (m, 2H), 2.33 (dm, J = 12.0 Hz, 2H), 3.38 (ddd, J_1 = 12.9 Hz, J_2 = 12.3 Hz, J_2 = 2.5 Hz, 2H), 3.68 (dt, J_1 = 12.4 Hz, J_2 = 2.4 Hz, 2H), 3.96 (s, 3H); ^{11}B NMR δ -20.3 (d, J = 143 Hz, 4H), -14.8 (d, J = 158 Hz, 4H), 32.2 (s, 1H). HRMS, calcd for $\text{C}_8\text{H}_{22}\text{B}_9\text{O}_2\text{S}$ m/z 281.2178; found m/z 281.2198.

The more polar fraction (6.3 mg) was eluted with CH_2Cl_2 : ^1H NMR (CD_3CN) δ major signal 3.96 (s); ^{11}B NMR (CD_3CN) major signals δ -24.5 (d, J = 135 Hz, 4B), -18.5 (d, J = 156 Hz, 4B), 48.0 (s, 1B). HRMS, calcd for $\text{C}_8\text{H}_{22}\text{B}_9\text{O}_2\text{S}$ m/z 281.2175; found m/z 281.2215.

Preparation of [closo-1-CB₉H₈-1-COOMe-10-(4-C₃H₇C₅H₉S)] (3[3]b).

Method A. A solution of methyl ester **16** (250 mg, 1.22 mmol) in 4-propylthiane (**17[3]**, 2.0 mL) was stirred at 120 °C for 3 hrs. Excess thiane was removed and the semisolid

residue was passed through a silica gel plug (hexane/CH₂Cl₂, 1:2). The first fraction containing the product was evaporated giving 192 mg (49% yield) of ester **3[3]b** as a white solid.

Method B. Crude acid **2[3]** (2.40 g, 7.8 mmol), obtained by hydrolysis of the reaction products as described in 4.4. Method A, was dissolved in CH₂Cl₂ (20 mL) and (COCl)₂ (2.60 mL, 30 mmol) was added followed by a catalytic amount of DMF. The mixture was stirred for 1 hr at ambient temperature, volatiles were removed, the resulting acid chloride was dissolved in MeOH (20 mL) and the solution was gently refluxed for 1 hr. MeOH was evaporated and the crude methyl ester **3[3]b** was purified by column chromatography (SiO₂, hexane/CH₂Cl₂, 1:1) to give 1.47 g (58% yield) of **3[3]b** as a white solid, which was recrystallized from hexane/CH₂Cl₂: mp 95-103 °C; ¹H NMR major signals: δ 0.60-2.50 (m, 8H), 0.93 (t, *J* = 7.0 Hz, 3H), 1.27-1.45 (m, 4H), 1.65-1.75 (m, 2H), 2.04-2.15 (m, 1H), 2.33 (dm, *J* = 11.8 Hz, 2H), 3.39 (t, *J* = 11.9 Hz, 2H), 3.74 (dm, *J* = 12.2 Hz, 2H), 3.956 (s, 3H); minor signals: δ 3.47-3.56 (m), 3.960 (s); ¹¹B NMR major signals: δ -20.3 (d, *J* = 141 Hz, 4B), -14.8 (d, *J* = 158 Hz, 4B), 32.6 (1B); minor signal: δ 30.6 (s). Anal. Calcd for C₁₁H₂₇B₉O₂S: C, 41.20; H, 8.49. Found: C, 41.40; H, 8.60.

*Preparation of [closo-2-CB₉H₉-2-COOH]⁻ [NEt₄]⁺ (**4**).*

[Arachno-6-CB₉H₁₃-6-COOH]⁻ [NEt₄]⁺ (**5**, 64.5 g, 0.217 mol) was suspended in a biphasic system of Et₂O (500 mL) and ice-cold 18% HCl (400 mL) in a 2-L Erlenmeyer flask. The mixture was stirred vigorously in an ice-bath and slowly warmed to room temperature until only traces of solid remained (~ 2 hrs). The Et₂O was separated in a 2-L separatory funnel, and the aqueous layer was further extracted with additional Et₂O (3 x

150 mL). Any remaining solid material was drained into the aqueous layer. The Et₂O layers were combined in a 1-L round-bottom flask and evaporated to approximately one-half its volume. A cooled (0 °C) solution of KOH (2.7 M, 645 mL) was then added, and the remaining Et₂O was removed, and the last remnants of Et₂O were removed in vacuum (< 5 mm Hg) until vigorous bubbling was no longer observed. The solution was then poured into a 3-L three-necked flask equipped with an addition funnel and mechanical stirrer and cooled down to ~ 5 °C in an ice-bath. Elemental I₂ (126.5 g, 0.500 mol) was slowly added in ~10 g portions every 5-10 min, or as often as solid iodine was no longer visible. Towards the last few additions, the solution developed a yellow/orange color. The solution was further stirred for 1 hr where the yellow/orange color dissipated after ~30 min. Reaction progress was monitored by following ¹¹B NMR spectrum of an aliquot taken directly from the reaction mixture [¹¹B {¹H} NMR (D₂O) δ -1.2 (1B), -3.8 (1B), -23.3 (1B), -26.5 (2B), -29.4 (2B), -30.3 (2B)]. Solid Na₂S₂O₅ (123.75 g, 0.6510 mol) and [NEt₄]⁺Br⁻ (68.41 g, 0.3255 mol) were then added, and after 15 min, 20% HCl (85 mL) was added slowly *via* the addition funnel until a pH of ~3 was obtained. A white precipitate was filtered, washed with water (5 x 100 mL), press dried, and further dried in air overnight giving 27 g – 37 g (42%–58% yield) of [*closo*-2-CB₉H₉-2-COOH]⁻[NEt₄]⁺ (**4**) in purity greater than 90% by ¹¹B NMR. The filtrate is a yellow solution. ¹¹B NMR was consistent with that reported in the literature [10,11].

*Preparation of [arachno-6-CB₉H₁₃-6-COOH]⁻ [NEt₄]⁺ (**5**).*

Glyoxylic acid (200.0 g, 2.16 mol) was slowly added in 15 g portions to a cooled solution (0 °C) of KOH (251.3 g, 4.48 mol) in water (300 mL) containing 200 g of crushed ice in a 3-L three-necked flask equipped with an addition funnel, mechanical

stirrer, and internal thermometer. Vigorous stirring and slow addition of glyoxylic acid is important to maintain the temperature of the solution below 5 °C. Finely crushed B₁₀H₁₄ (40.0 g, 0.327 mol) was then slowly added in two portions, while maintaining the temperature of the solution around 5 °C. Once all B₁₀H₁₄ had dissolved, the solution was vigorously stirred for an additional 2 hrs (< 5 °C). Reaction progress was monitored by following ¹¹B NMR spectrum of an aliquot taken directly from the reaction mixture [¹¹B {¹H} NMR (D₂O) δ -3.2 (1B), -4.7 (2B), -14.6 (1B), -16.2 (1B), -19.8 (1B), -20.8 (1B), -26.7 (1B), -38.3 (1B), -38.7 (1B)]. Solid [NEt₄]⁺Br⁻ (47.9 g, 0.228 mol) was added, and after 10 min, freezer-cold (-15 °C) 20% solution of HCl (340 mL) was slowly added *via* the addition funnel until a pH of ~3 was obtained. Addition of HCl resulted in vigorous bubbling, foaming, and release of H₂. Occasionally, manual breaking up of large clumps of the product was necessary for thorough neutralization of the product and decomposition of the flammable boron hydride byproducts. At pH ~3, the bubbling and foaming begins to subside. The resulting white precipitate was filtered, washed with H₂O (10 x 100 mL), press dried, and further dried in air overnight giving 64 g – 72 g (66% – 74% yield) [12] of [*arachno*-6-CB₉H₁₃-6-COOH][NEt₄]⁺ (**5**) in purity greater than 90% by NMR: ¹¹B {¹H} NMR (CD₃CN) δ major signals -0.5 (1B), -9.2 (3B), -20.1 (1B), -27.8 (1B), -39.0 (2B); (acetone-*d*₆) δ major signals -0.3 (1B), -9.0 (2B), -9.6 (1B), -19.6 (1B), -27.6 (1B), -38.8 (2B) [lit.[10] (acetone-*d*₆) -0.6 (1B), -9.4 (1B), -10.3 (3B), -19.3 (1B), -27.9 (2B), -39.1 (1B)].

When an acetone solution of **5** is filtered, evaporated, and redissolved in acetone-*d*₆ the spectrum changes: ¹¹B {¹H} NMR (acetone-*d*₆) δ major signals 3.0 (2B), 0.5 (1B), -4.6 (2B), -11.9 (2B), -29.1 (1B), -36.2 (1B).

*Preparation of [closo-2-CB₉H₈-2-COOH-7-I]⁻[NEt₄]⁺ (**6**) [4].*

A red solution of *N*-iodosuccinimide (35.23 g, 0.157 mol) and [closo-2-CB₉H₉-2-COOH][NEt₄]⁺ (**4**, 30.82 g, 0.104 mol) in anhydrous MeCN (150 ml) was stirred vigorously for 1 hr at 0 °C and then stored for 72 hrs in a freezer (-10 to -20 °C). MeCN was removed at 0 °C under reduced pressure (< 10 mm Hg). Solid Na₂S₂O₅ (29.8 g, 0.157 mol) and 10 % HCl (350 mL) were added and the reaction mixture turned green/yellow and a yellow precipitate began to form. If solution does not turn green/yellow, more Na₂S₂O₅ should be added. The mixture was stirred vigorously. Once all red residue dissolved, Et₂O (100 mL) was added and the mixture was vigorously stirred until the yellow precipitate redissolved leaving an orange organic layer. The Et₂O layer was separated and the aqueous layer was further extracted with Et₂O (4x100 mL). The Et₂O layers were combined, and half of the Et₂O was evaporated before adding H₂O (250 mL). The remaining Et₂O was evaporated completely and the aqueous solution was filtered to remove insoluble material. Solid [NEt₄]⁺Br⁻ (32.91 g, 0.157 mol) was added and a white solid began to precipitate after brief stirring. The solid was filtered, washed with H₂O (5x100 mL), press dried and further dried in air overnight giving 28 g – 40 g (68%– 91% yield) of iodo acid **6**. ¹¹B NMR was consistent with that reported in the literature [4]. In addition, NMR revealed that up to 20% of the expected product **6** has undergone rearrangement giving the 1,10 and 1,6 isomers of iodo acid **1** and **7** in about 2:1 ratio. The product was used for the next step.

*Preparation of [closo-1-CB₉H₈-1-COOH-10-NH₃] (**8**) [9].*

Following a literature procedure [9], [closo-1-CB₉H₈-1-COOH-10-I]⁻NMe₄⁺ (**1**, 15.00 g, 0.041 mol) was added to a solution of lithium hexamethyldisilazane (LiHMDS,

618 mL, 0.615 mol, 1.0 M in THF) at ambient temperature under N₂. The light orange suspension was stirred vigorously for 20 min or until the suspension became more fine and disperse. Pd₂dba₃ (0.756 g, 0.83 mmol) and 2-(dicyclohexylphosphino)biphenyl (**A**, 0.985 g, 3.30 mmol) were added, and the reaction was stirred at reflux for 20 hrs. After several minutes at reflux, the reaction mixture turned dark brown. The reaction was cooled to 0 °C, and 10% HCl (1500 mL) was added slowly. The THF was removed in vacuo giving a dark orange solution. The orange solution was extracted with Et₂O (5x200 mL), the Et₂O layers were combined, dried (Na₂SO₄), and evaporated at slightly elevated temperature (~40 °C) to ensure complete removal of trimethylsilanol. ¹¹B NMR of the crude material revealed a 7:3 ratio of amino acid **8** to parent acid **9**.

The crude brown/orange material was redissolved in Et₂O, and water (150 mL) was added. The Et₂O was removed in *vacuo* or until bubbling became less vigorous. The aqueous layer was filtered through Celite, and the process was repeated two more times (the insoluble material presumably contains a B(10)-phosphonium derivative). Water (3x100 mL) was added to the flask and the flask was shaken vigorously to release the remaining amino acid from the insoluble material. The aqueous fractions were filtered as well. The aqueous layers were combined, and [NEt₄]⁺Br⁻ (8.67 g, 0.041 mol) was added resulting in precipitation of a white solid. CH₂Cl₂ (400 mL) was added, and the biphasic system was stirred vigorously overnight until the aqueous layer became clear. The organic layer was separated, and the process was repeated once more. The biphasic system was stirred for 1 hr. The H₂O layer was filtered, reacidified with conc. HCl (75 mL), and extracted with Et₂O (5 x 150 mL). The Et₂O layers were combined, washed with water, dried (Na₂SO₄), and solvent evaporated giving 3.55 g–4.14 g (48%–56%

yield) of amino acid **8** with purity > 90% by ^{11}B NMR. The amino acid was used for the next step without further purification.

*Preparation of [closo-1-CB₉H₈-1-COOH-10-N₂] (**10**) [9].*

Amino acid [closo-1-CB₉H₈-1-COOH-10-NH₃] (**8**, 1.850 g, 10.31 mmol) was suspended in anhydrous CH₃CN (20 mL) and anhydrous pyridine (4.25 mL, 51.5 mmol) was added. The reaction mixture was cooled to -15 °C, and NO⁺[BF₄]⁻ (3.61 g, 30.9 mmol) was added in six portions at 10 min intervals. Once all NO⁺[BF₄]⁻ was added, the reaction was stirred for 1.5 hr at -15 °C.

The reaction mixture was evaporated to dryness (the flask was kept at cold water bath), 10% HCl (200 mL) was added, and the mixture was stirred vigorously until all solids had dissolved (~20 min). The aqueous solution was extracted with Et₂O (4 x 50 mL), the Et₂O layers were combined, washed with water, dried (Na₂SO₄), and evaporated to dryness giving 1.327 g of crude dinitrogen acid **10**. The crude product was passed through a short silica gel plug (CH₃OH/CH₂Cl₂, 1:19, R_f = 0.2) giving 0.97 g–1.29 g (49%–65% yield) of dinitrogen acid **10** as a white solid.

*Preparation of [closo-1-CB₉H₈-1-COOH-10-SCHNMe₂] (**11**) [9].*

A solution of acid [closo-1-CB₉H₈-1-COOH-10-N₂] (**10**, 1.678 g, 8.81 mmol) and freshly distilled Me₂NCHS (11.50 mL, 0.132 mmol) was stirred at 120 °C for 1 hr. As the reaction progressed, bubbling of N₂ became evident. Excess Me₂NCHS was removed by vacuum distillation (120 °C, 1.0 mm Hg) leaving crude product as an off-white crystalline solid. The crude product was washed with toluene giving 2.00 g–2.16 g (91%–98% yield) of crude protected mercaptan **11** containing up to 5% of Me₂NCHS by ^1H NMR.

Preparation of [closo-1-CB₉H₈-1-COOMe-10-(4-C₄H₈S)] (14).

The ester was prepared from **11** and 1,4-dibromobutane followed by treatment with (COCl)₂ and MeOH. Pure ester **14** was isolated as a white solid by chromatography (SiO₂, CH₂Cl₂/hexane, 1:1) followed by recrystallization (CH₂Cl₂/hexane): mp 114-116 °C; ¹H NMR (500 MHz, CDCl₃) δ 1.30 (q, *J* = 142 Hz, 4H), 2.03 (q, *J* = 158 Hz, 4H), 2.28-2.37 (m, 2H), 2.58-2.67 (m, 2H), 3.67-3.76 (m, 2H), 3.78-3.88 (m, 2H), 4.02 (s, 3H); ¹¹B {¹H} NMR δ -20.0, -14.8, 34.1. Anal. Calcd for C₇H₁₉B₉O₂S: C, 31.78; H, 7.24. Found: C, 31.88; H, 7.32.

Preparation of 4-Propylthiane (17[3]) [18].

To a solution of dibromide **12** (9.8 g, 36.0 mmol) [17] in EtOH (80 mL) a solution of Na₂S•9H₂O (13.0 g, 54 mmol) in water (40 mL) was added dropwise during 1 hr at 50 °C. The mixture was stirred at this temperature for 1 hr, then refluxed for 1 hr, and diluted with water. The organic product was extracted with hexanes, extract dried (Na₂SO₄) and solvent evaporated. The oily residue was passed through silica gel plug to give 4.50 g of thiane (87% yield) as a colorless oil. Analytical sample was obtained by bulb-to-bulb distillation (50-55 °C, 0.5 mm Hg; lit. [18] bp. 92 °C /23 mm Hg): ¹H NMR (500 MHz, CDCl₃) δ 0.87 (t, *J* = 7.2 Hz, 3H), 1.16-1.23 (m, 2H), 1.24-1.37 (m, 5H), 1.98 (br d, *J* = 11.9 Hz, 2H), 2.58 (br d, *J* = 11.9 Hz, 2H), 2.65 (t, *J* = 12.6 Hz, 2H).

Preparation of 4-Pentylthiane (17[5]) [18,19].

The thiane was prepared in 85% yield from 1,5-dibromo-3-pentylpentane [17] using method similar to that described for **17[3]**: bp. 52-53 °C, 0.15 mm Hg (lit.[19] bp 101 °C, 2 mm Hg); ¹H NMR (300 MHz, CDCl₃) δ 0.88 (t, *J* = 6.8 Hz, 3H), 1.16-1.45 (m,

11H), 1.99 (br d, $J = 12.1$ Hz, 2H), 2.58-2.66 (m, 4H); ^{13}C NMR (75 MHz, CDCl_3) δ 14.0, 22.6, 26.0, 28.8, 32.05, 34.2, 37.2, 37.3; EI-MS, m/z 172 (M, 49) 115 (100).

3.2.2.5 Acknowledgements

This project was supported by NSF grant (DMR-0907542).

3.2.2.6 References

- [1] D. Brelloch In *Contemporary Boron Chemistry*; Davidson, M. G., Hughes, A. K., Marder, T. B., Wade, K., Eds.; Royal Society of Chemistry: Cambridge, England, 2000, p 212-214.
- [2] B. Brelloch, J. Backovsky, B. Stíbr, T. Jelínek, J. Holub, M. Bakardjiev, D. Hnyk, M. Hofmann, I. Císarová; B. Wrackmeyer, *Eur. J. Inorg. Chem.* (2004) 3605-3611.
- [3] A. Franken, C. A. Kilner, M. Thornton-Pett; J. D. Kennedy, *Inorg. Chem. Comm.* 5 (2002) 581-584.
- [4] B. Ringstrand, A. Balinski, A. Franken; P. Kaszynski, *Inorg. Chem.* 44 (2005) 9561-9566.
- [5] B. Ringstrand, P. Kaszynski, A. Januszko; V. G. Young, Jr., *J. Mater. Chem.* 19 (2009) 9204-9212.
- [6] B. Ringstrand; P. Kaszynski, *J. Mater. Chem.* 21 (2011) 90-95.
- [7] B. Ringstrand; P. Kaszynski, *J. Mater. Chem.* 20 (2010) 9613-9615.
- [8] B. Ringstrand, H. Monobe; P. Kaszynski, *J. Mater. Chem.* 19 (2009) 4805-4812.
- [9] B. Ringstrand, P. Kaszynski, V. G. Young, Jr.; Z. Janousek, *Inorg. Chem.* 49 (2010) 1166-1179.
- [10] A. Franken, M. J. Carr, W. Clegg, C. A. Kilner; J. D. Kennedy, *J. Chem. Soc., Dalton Trans.* (2004) 3552-3561.

- [11] A. Franken, C. A. Kilner; J. D. Kennedy, Chem. Comm. 3 (2004) 328-329.
- [12] The yields of the crude *arachno* acid **5** are not fully reliable. The solid contains boric acid and some other insoluble impurities (upon dissolution in NMR tube with CD₃CN or acetone-*d*₆), and may also be partially hydrated. Therefore, the most reliable yields are obtained by combining the first two processes: insertion and oxidation (30%-40% yield on average).
- [13] The ¹¹B {¹H} NMR spectrum of the unknown pyrophoric product in CD₃CN contained characteristic signals at 9.0, -13.0, -15.5, -18.5, -22.2, -31.2, -35, -39.2 ppm.
- [14] The original paper mistakenly shows only 1 mole of I₂ per mole of *arachno* acid **5**.
- [15] V. T. Abaev; O. V. Serdyuk, Russ. Chem. Rev. 77 (2008) 177-192, and references therein.
- [16] Y. Sevryugina, R. L. Julius; M. F. Hawthorne, Inorg. Chem. 49 (2010) 10627–10634.
- [17] B. Ringstrand, M. Oltmanns, J. Batt; A. Jankowiak, R. P. Denicola, P. Kaszynski, Beilst. J. Org. Chem. 7 (2011) 386-393.
- [18] R. Onesta; G. Castelfranchi, Gazz. Chim. Ital. 89 (1959) 1127-1138.
- [19] N. P. Volynskii; L. P. Shcherbakova, Bul. Acad. Sci. USSR, Div. Chem. Sci. (1979) 1006-1009.

3.3 Synthesis and characterization of 12-pyridinium derivatives of the [*closo*-1-CB₁₁H₁₂]⁻ anion.

3.3.1 Description and contributions

Pyridinium derivatives of the [*closo*-1-CB₁₁H₁₂]⁻ anion (type **1C** and **1F**, see Chapter 1, Table 1) are expected to be effective additives to nematic hosts due to their high longitudinal molecular dipole moment and reasonable solubility in nematic materials. However, lack of suitable synthetic methods for this type of compounds were the major obstacle in accessing this type of materials (See Chapter 1). In the course of my research, I found that the key factors affecting the yield of installing the pyridine at the B(12) position, were the length of the alkyl chain in the 4-alkoxypyridine and the presence of a substituent at the C(1) vertex. At the same time, it was shown that the 12-(4-methoxypyridinium) derivative (**2b**) of the [*closo*-1-CB₁₁H₁₂]⁻ can be obtained in about 50% yield in the same diazotization reactions. We demonstrated that derivative **2b** can be demethylated using LiCl in DMF to yield pyridone **5b**, which, subsequently, can be *O*-alkylated using alkyl triflates. Moreover, both steps, the dealkylation and *O*-alkylation, give the products in nearly quantitative yields. The overall yield for the 3-step process was greatly improved compared to the yield of diazotization of [*closo*-1-CB₁₁H₁₀-1-R-12-NH₂]⁻ in the presence of substituted pyridines containing long alkyl chains. The new method was successfully applied to the synthesis of derivative **1c**, which exhibits a smectic A phase. The 12-(4-methoxypyridinium) derivative **2b** and its isomer, 1-(4-methoxypyridinium) analog **3b** were examined by single-crystal X-ray and UV spectroscopy. We also presented for the first time the formation of the transient

dinitrogen derivative [*closo*-1-CB₁₁H₁₀-1-C₅H₁₁-12-N₂] (**14**) by means of ¹¹B NMR, whose stability is dependent on the substituent on the carbon vertex.

My role in this project was to search for a more efficient route to 12-pyridinium derivatives (type **1F**) of the [*closo*-1-CB₁₁H₁₂]⁻ anion. I was responsible for the synthesis and characterization of all compounds. I also conducted physicochemical studies, which included UV-vis spectroscopy, thermal analysis, and spectroscopy on the temperature-dependent NMR of the putative intermediate **14**. Dr. Bryan Ringstrand contributed to the project by helping with synthesis of starting amines and assisting in preparation of single crystals for X-ray analysis conducted by Prof. Krzysztof Wozniak and Dr. Slawomir Domagala at Warsaw University. Prof. Piotr Kaszynski was responsible for quantum mechanical calculations, which augmented experimental results.

In the following chapter the entire text of the manuscript is included for consistency of the narrative, however, the experimental section contains only experiments performed by me.

3.3.2 The manuscript

Reproduced by permission of American Chemical Society
Pecyna, J.; Ringstrand, B.; Domagala, S.; Kaszynski, P.; Wozniak, K. *Inorg. Chem.* **2011**, *53*, 12617-12626.
Copyright 2014 American Chemical Society. Available online:
<http://pubs.acs.org/doi/abs/10.1021/ic502265g>

3.3.2.1 Introduction

Zwitterionic derivatives **I** and **II** of monocarbaborates [*closo*-1-CB₉H₁₀]⁻ (**A**) and [*closo*-1-CB₁₁H₁₂]⁻ (**B**, Figure 1) possess large longitudinal dipole moments and for this reason are of interest as core elements of polar liquid crystals¹ suitable for electro-optical applications.² In this context, we initially investigated 1-sulfonium derivatives of type **IA**,^{3,4} and later we developed a convenient method for access to 1-pyridinium zwitterions

of anions **A** and **B**.⁵ Although materials of type **IA** and **IB** are effective additives that increase dielectric anisotropy, $\Delta\epsilon$, of a nematic liquid crystal host, these polar materials rarely exhibit liquid crystalline properties themselves, have high melting points, and display limited solubility in nematic hosts.

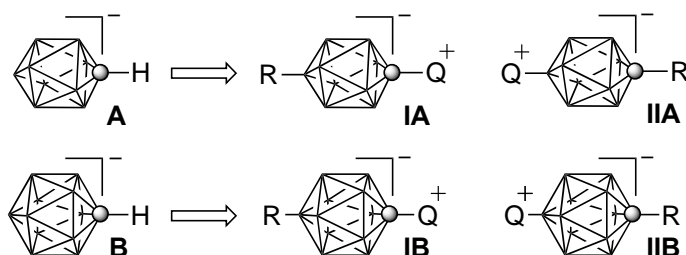


Figure 1. The structures of the $[closo-1-CB_9H_{10}]^-$ and $[closo-1-CB_{11}H_{12}]^-$ anions (**A** and **B**), and their zwitterionic 1,10– (**IA**, **IIA**) and 1,12–disubstituted (**IB**, **IIB**) derivatives. Q^+ represents an onium fragment such as quinuclidinium, sulfonium or pyridinium. Each vertex represents a BH fragment and the sphere is a carbon atom.

We sought to improve the properties of materials derived from monocarbaborates **A** and **B** by focusing on structures **IIA** and **IIB**, in which the onium fragment is attached to the B(10) and B(12) positions of the anions, respectively. Pyridinium and sulfonium zwitterions **IIA**, prepared from relatively stable 10-dinitrogen derivatives of the $[closo-1-CB_9H_{10}]^-$ anion (**A**), showed great promise. These compounds have lower melting points, often form nematic phases, and display greater solubility in nematic hosts relative to structures of type **I**, while maintaining a sizeable longitudinal dipole moment and high $\Delta\epsilon$ values.^{4,6} Although the chemistry of the $[closo-1-CB_9H_{10}]^-$ anion (**A**) is well understood and straightforward,⁷ the $[closo-1-CB_{11}H_{12}]^-$ anion⁸ (**B**) is more accessible^{9,10} and, for this reason, is more attractive as a structural element of molecular materials. Functionalization of the former anion and preparation of zwitterionic materials is

conveniently achieved through dinitrogen derivatives as the key intermediates.¹¹⁻¹³ Unfortunately, analogous dinitrogen derivatives of the [*closo*-1-CB₁₁H₁₂]⁻ anion (**B**) are generally much less stable, and their isolation appears impractical. This limitation significantly reduces access to zwitterionic derivatives of the [*closo*-1-CB₁₁H₁₂]⁻ anion (**B**). Nonetheless, we recently demonstrated that even unstable dinitrogen derivatives of monocarbaborates, such as [*closo*-1-CB₉H₈-1-COOH-6-N₂],¹⁴ can be synthetically useful, when formed *in situ* as transient species during diazotization of the corresponding amines. For example, diazotization of [*closo*-1-CB₁₁H₁₀-1-COOH-12-NH₃] in neat 4-heptyloxy pyridine gave 6% yield of the desired pyridinium acid [*closo*-1-CB₁₁H₁₀-1-COOH-12-(4-C₇H₁₅OC₅H₄N)] (**1a**, Figure 2).¹⁵ Since esters of **1a** and other compounds containing the pyridinium zwitterion are of interest as high Δε additives to liquid crystals, we set out to develop an alternative and more efficient method for the preparation of such compounds.

Here we report a simple and efficient method for the preparation of [*closo*-1-CB₁₁H₁₁-12-(4-C₇H₁₅OC₅H₄N)] (**1b**) and extend it to the preparation of liquid crystalline [*closo*-1-CB₁₁H₁₀-1-C₅H₁₁-12-(4-C₇H₁₅OC₅H₄N)] (**1c**) as a representative of a potentially diverse class of 12-(4-alkoxypyridinium) zwitterionic derivatives of [*closo*-1-CB₁₁H₁₂]⁻ anion (**B**). The synthetic work is accompanied by mechanistic consideration augmented with DFT computational results. We also take advantage of the available **2b** and compare its electronic and molecular structures with its C(1) isomer **3b** using experimental and computational methods.

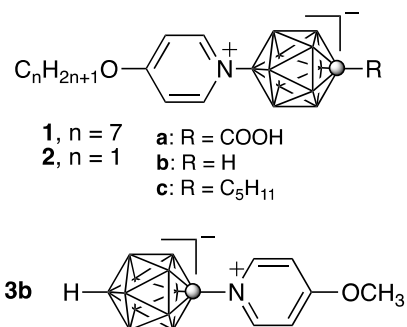


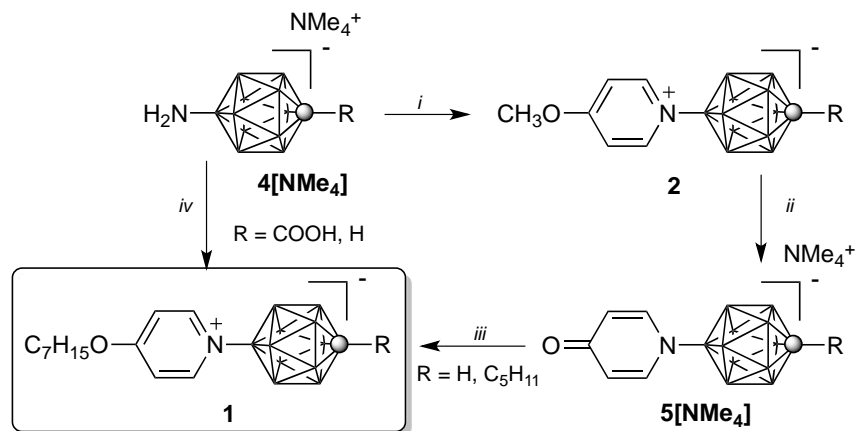
Figure 2. The structures of pyridinium zwitterions.

3.3.2.2 Results and discussion

Synthesis

Diazotization of amine [*closo*-1-CB₁₁H₁₁-12-NH₂]⁺[NMe₄]⁻ (**4b**[NMe₄]) with [NO]⁺[PF₆]⁻ in neat 4-methoxypyridine at -20 °C, according to a general procedure,¹⁴ gave 4-methoxypyridinium derivative **2b** in about 50% yield (Scheme 1). In contrast, diazotization of **4b**[NMe₄] in neat 4-heptyloxypyridine gave zwitterion **1b** in only 15% yield, which is over 3 times lower than that for **2b** and consistent with the 6% yield obtained for acid **1a** under the same conditions.¹⁵

To increase the yield of 4-alkoxypyridinium zwitterions with longer or more diverse alkyl chains, another route to **1b** was explored starting from 4-methoxypyridinium derivative **2b**. Thus, the methyl group in **2b** was removed using LiCl in DMF¹⁶ giving pyridone **5b**[NMe₄] in quantitative yield. Subsequent *O*-alkylation of **5b**[NMe₄] with heptyl triflate⁵ gave **1b** in 80% yield (Scheme 1) or 40% overall yield from amine **4b**[NMe₄], which represents a significant improvement over the single step procedure.

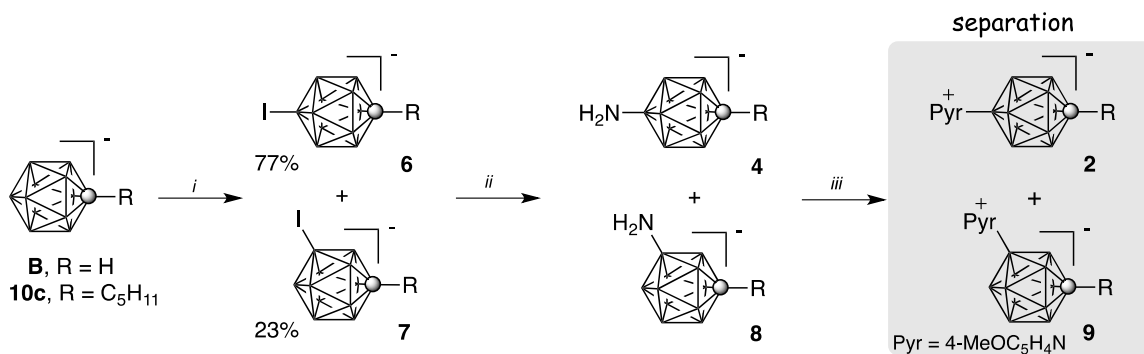


Scheme 1. Synthesis of 4-heptyloxyppyridinium derivatives **1**. Reagents and conditions: *i*) 4-methoxyppyridine, $[\text{NO}]^+[\text{PF}_6]^-$, $-20\text{ }^\circ\text{C}$, 2 hr; *ii*) 1. LiCl, DMF, $80\text{ }^\circ\text{C}$; 2. $[\text{NMe}_4]^+\text{Cl}^-$; *iii*) ROTf, CH_2Cl_2 , rt; *iv*) 4-heptyloxyppyridine, $[\text{NO}]^+[\text{PF}_6]^-$, $-20\text{ }^\circ\text{C}$, 2 hr.

The requisite amine **4b** $[\text{NMe}_4]$ was obtained in about 50% yield by Pd-catalyzed amination^{12,17} of iodo derivative $[\textit{closo-1-CB}_{11}\text{H}_{11-12}\text{-I}]^-\text{Cs}^+$ (**6b** $[\text{Cs}]$), which was prepared by iodination¹⁸ of $[\textit{closo-1-CB}_{11}\text{H}_{12}]^-$ anion (**B**) with I_2 in AcOH (Scheme 2). The iodination reaction leads, however, to a mixture of two regioisomers, the 12- and 7-iodo derivatives **6b** and **7b**, respectively, in about 3:1 ratio. The desired pure 12-iodo isomer, $[\textit{closo-1-CB}_{11}\text{H}_{11-12}\text{-I}]^-$ (**6b**), can be obtained by repeated recrystallization of its Cs^+ salt, **6b** $[\text{Cs}]$, from hot water. This is accomplished, however, with low mass recovery (typically less than 50%) and has significant impact on the overall yield of **1**. Therefore, higher efficiency of preparation of **1** could be achieved by improving the separation of isomers that are formed on early stages of the synthetic sequence.

To avoid losses of the desired **6b** the ionic isomers were carried forward without separation. Therefore, the sequence of amination and diazotization was performed on a 3:1 mixture of isomers **6b** and **7b**. Thus, amination of the mixture with LiHMDS in THF

gave a 3:1 mixture of amines **4b**[NMe₄] and [*closo*-1-CB₁₁H₁₁-7-NH₂]⁻[NMe₄]⁺ (**8b**[NMe₄]), which was diazotized in 4-methoxypyridine giving a mixture of 12-(4-methoxypyridinium) and 7-(4-methoxypyridinium) isomers, **2b** and **9b**, respectively (Scheme 2). The desired **2b** was easily and quantitatively separated from the more polar 7-isomer [*closo*-1-CB₁₁H₁₁-7-(4-MeOC₅H₄N)]⁻ (**9b**) by column chromatography.

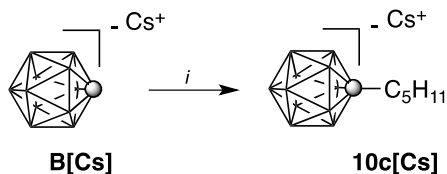


Scheme 2. Synthesis of 12-pyridinium derivatives. Reagents and conditions: *i*) I₂, AcOH, 50 °C, 72 hr; *ii*) Pd₂dba₃, 2-(Chx₂P)biphenyl, LiHMDS, THF, reflux, 72 hr; *iii*) 4-methoxypyridine, [NO]⁺[PF₆]⁻, -20 °C, 2 hr.

The two protocols were used in tandem for the preparation of the 1-pentyl derivative **1c** from the parent anion [*closo*-1-CB₁₁H₁₂]⁻ (**B**). Thus, following a general literature procedure,¹⁸ Cs⁺ salt of anion **B** was treated with *n*-BuLi in the presence of TMEDA and subsequently with 1-iodopentane to afford [*closo*-1-CB₁₁H₁₁-1-C₅H₁₁]⁻Cs⁺ (**10c**[Cs]) in 85% yield (Scheme 3). Iodination of **10c**[Cs] with I₂ in AcOH gave a mixture of isomers **6c** and **7c** in 77% yield, which upon amination with LiHMDS provided a mixture of isomers **4c**[NMe₄] and **8c**[NMe₄] in 81% yield (Scheme 2). Subsequent diazotization of the amines gave a mixture of the pyridinium derivatives **2c** and **9c**, out of which the desired [*closo*-1-CB₁₁H₁₀-1-C₅H₁₁-12-(4-MeOC₅H₄N)]⁻ (**2c**) was

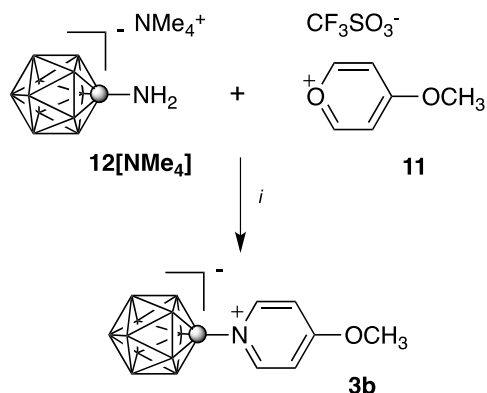
isolated in 45% yield. Thus, the overall yield for the synthesis is 12% based on anion **B**. No enrichment of a particular isomer was observed in this sequence of reactions.

Removal of the methyl group in **2c** gave pyridone [*closo*-1-CB₁₁H₁₀-1-C₅H₁₁-12-(4-OC₅H₄N)]⁻[NMe₄]⁺ (**5c**[NMe₄]), which upon treatment with heptyl triflate⁵ yielded **1c** in nearly quantitative yield for the two-step process (Scheme 1).



Scheme 3. Synthesis of pentyl derivative **10c**[Cs]. Reagents and conditions: *i*) 1. *n*-BuLi, TMEDA, THF, -78 °C; 2. *n*-C₅H₁₁I, 0 °C → rt.

Finally, for comparison purposes, 4-methoxypyridinium derivative **3b** was conveniently obtained by reacting 4-methoxypyrylium triflate (**11**) with amine [*closo*-1-CB₁₁H₁₁-1-NH₂]⁻[NMe₄]⁺ (**12**[NMe₄]) in 16% yield, according to a previously reported method (Scheme 4).⁵ During recrystallization of **3b** from EtOH/H₂O, partial exchange of the methyl group for ethyl was observed. This suggests that the C(1) 4-methoxypyridinium derivative is also susceptible to demethylation and may provide means to more efficient preparation of higher C(1) 4-alkoxypyridinium homologs. These reactions were not pursued at this time.



Scheme 4. Preparation of 4-methoxypyridinium derivative **3b**. Reagents and conditions: *i*) THF, rt, 12 hr.

Thermal properties

Differential scanning calorimetry (DSC, Figure 3) and polarizing optical microscopy (POM, Figure 4) revealed that **1c** exhibits crystal polymorphism and an enantiotropic SmA phase between 111 °C and 143 °C. This is in contrast to its constitutional isomer **13**:⁵ exchanging positions of the substituents on the {1-CB₁₁} cluster in **1c** leads to a substantial increase of the melting point and elimination of liquid crystalline properties (Figure 5). However, extension of the pentyl chain in **13** to decyl results in induction of a SmA phase with the isotropic transition at 200 °C.⁵ The difference in thermal behavior of the two isomers is related to the stability of the crystalline phase governed by the magnitude of the molecular dipole moment: $\mu = 12.2$ D for **1c** and $\mu = 18.2$ D for **13**, according to B3LYP/6-31G(d,p) calculations in vacuum.

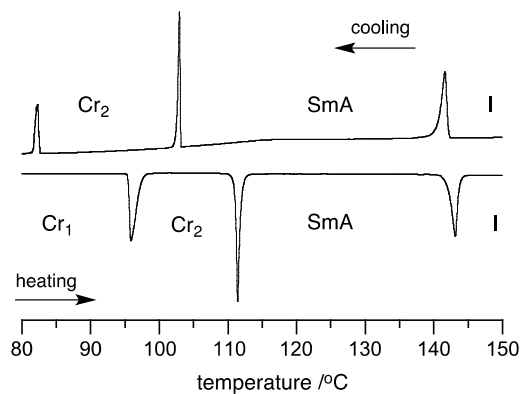


Figure 3. A DSC trace of **1c**. Cr - crystal; SmA - smectic A; I - isotropic. The heating and cooling rates are 5 K min⁻¹.

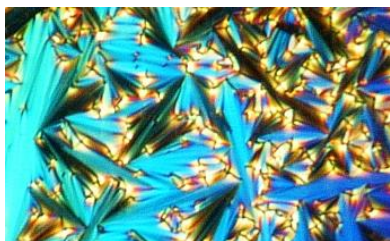
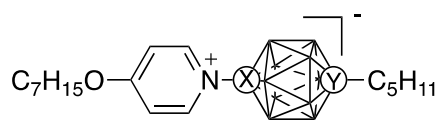


Figure 4. Optical texture of a SmA phase observed for **1c** at 130 °C on cooling from the isotropic phase.



1c, X = B, Y = C: Cr₁ 96 (5.0) Cr₂ 111 (5.4) SmA 143 (4.5) I
13, X = C, Y = B: Cr 205 (26.6) I

Figure 5. A comparison of thermal properties for two isomers **1c** and **13**. Data for **13** was taken from ref ⁵.

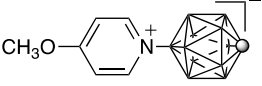
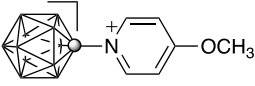
Comparative analysis of isomers 2b and 3b

To gain a better understanding of the effect of substitution position of the pyridine ring on electronic and molecular structures of the zwitterions, two isomers, the 12-(4-methoxypyridinium) and 1-(4-methoxypyridinium) derivatives **2b** and **3b**, respectively, were investigated in detail.

Electronic Structures NBO population analysis of the B3LYP/6-31G(d,p) wavefunction demonstrates differences in electron density distribution in both isomers, mainly at the ring–cage connection (Table 1). Thus, substitution of the pyridine for H atom on the cage results in depletion of electron density by about 0.3e at the substituted atom, either B(12) or C(1). In **2b** the nitrogen atom connected to the boron atom has higher electron density (−0.44e) than in the **3b** isomer (−0.28e), which is connected to the carbon atom. This results in different polarization of the B–N bond and leads to significant differences in the calculated molecular dipole moment and thermodynamic stability of the two isomers: substitution of the pyridine fragment on the C(1) atom of the cluster increases the dipole moment by about 50% to 16.7 D and decreases stability by nearly 43 kcal mol^{−1} in vacuum (Table 1). Electron density of the MeO group is essentially the same in both isomers.

The difference in electron distribution in the two isomers affects the chemical shifts in NMR spectroscopy, and the “organic” H atoms in **2b** are generally more shielded relative to those in **3b**. For instance, hydrogen atoms in positions 2/6 of the pyridine ring are more shielded in the B(12) isomer by 0.36 ppm than in the C(1) isomer **3b** (Table 1). Similarly, the distant Me group is more shielded in **2b**, although the effect is appropriately weaker.

Table 1. Selected electronic parameters for **2b** and **3b**.

		
	2b	3b
$q_{C(1)}^a$	-0.71	-0.36
$q_{B(12)}^a$	+0.17	-0.14
q_N^a	-0.44	-0.28
q_{Me}^a	-0.337	-0.338
μ / D^b	11.6	16.7
$\Delta H / kcal\ mol^{-1}$	0.0	+42.7
$\delta (H_{2,6}) / ppm^c$	8.47	8.83
$\delta (H_{3,5}) / ppm^c$	7.18	7.24
$\delta (Me) / ppm$	4.01 ^c (58.4) ^d	4.10 ^c (59.4) ^d

^a Atomic charge from the NBO analysis of the B3LYP/6-31G(d,p) wavefunction. ^b Dipole moment in vacuum. ^c ¹H NMR chemical shift of the pyridine fragment (CD₃CN). ^d ¹³C NMR chemical shift (CD₃CN).

Electronic Absorption Spectroscopy. Both isomers **2b** and **3b** exhibit a single absorption band in the UV region with maximum around 250 nm ($\log \epsilon \approx 4.3$) in MeCN (Figure 6). The maximum for the C(1) isomer (**3b**) is shifted to lower energies by 9.5 nm or 187

meV relative to the B(12) derivative **2b**. TD-DFT computational analysis of both compounds in MeCN dielectric medium reproduced well the experimental spectra. The electronic excitation energy for **2b** is calculated at 239 nm ($f = 0.40$) and involves mainly the HOMO, localized on the cluster, to the LUMO, localized on the pyridine fragment, transition (Figure 7). Similar TD-DFT analysis for the C(1)-pyridinium isomer **3b**, demonstrated that the absorption band at 257 nm is composed of two transitions at 245 nm (HOMO→LUMO, $f = 0.27$) and 231 nm (HOMO-4→LUMO, $f = 0.20$) both involving the {1-CB₁₁} to pyridine excitation.¹⁰

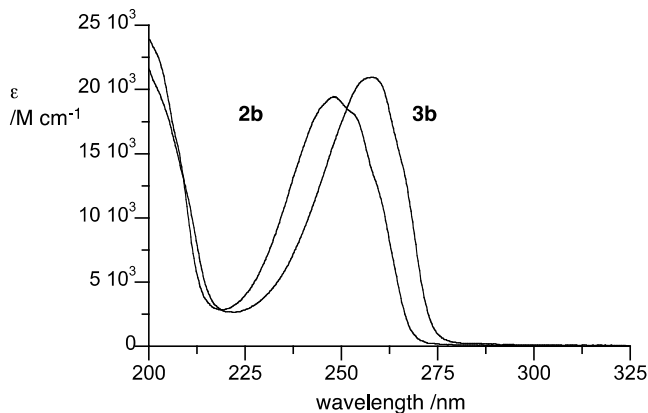


Figure 6. Electronic absorption spectra for **2b** and **3b** (CH₃CN).

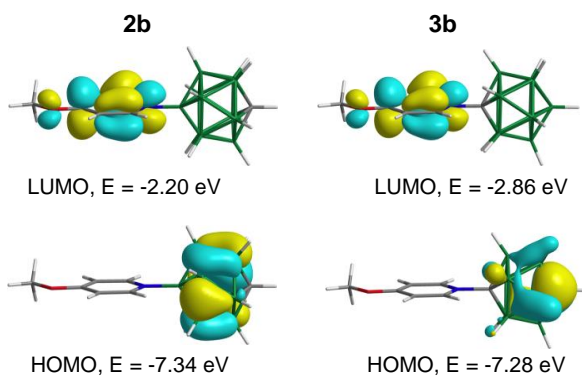


Figure 7. B3LYP/6-31G(d,p)-derived contours and energies of molecular orbitals relevant to low energy excitations in **2b** and **3b** in vacuum.

X-ray Crystallography. Colorless crystals of **2b** and **3b** were obtained by slow evaporation of CH₂Cl₂/MeOH solutions and their solid-state structures were determined by low temperature single crystal X-ray analysis. Results are shown in Tables 2 and 3 and in Figure 8.

B(12)–pyridinium derivative **2b** crystallizes in a *Pc* monoclinic space group, whereas the C(1)–pyridinium isomer **3b** crystallizes in a *P*-1 triclinic space group. Both crystal structures contain two molecules in the asymmetric part of the unit cell. In the C(1) isomer **3b**, the C(1)–N bond length is 1.476(1) Å in molecule A and 1.477(1) Å in molecule B, which compares to 1.485 Å calculated at the B3LYP/6-31G(d,p) level of theory. In the B(12) isomer **2b**, the pyridine–{CB₁₁} bonding distance is longer: 1.548(2) Å and 1.545(2) Å in the two unique molecules (calculated 1.561 Å). In both isomers, the pyridine ring nearly eclipses the B–H bond; the ring–{1-CB₁₁} torsional angle is 11.8° and 11.3° (calcd 7.4°) in **3b**, and 3.6° and 12.9° (calcd 9.1°) in **2b**.

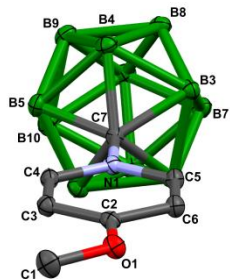
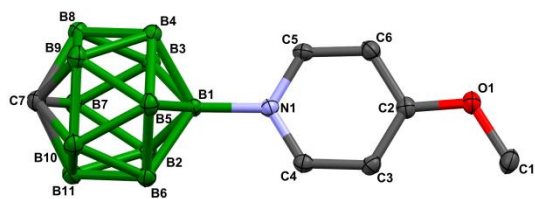
Table 2. Crystallographic data for **2b** and **3b**.^a

	2b	3b
empirical formula	C ₇ H ₁₈ B ₁₁ NO	C ₇ H ₁₈ B ₁₁ NO
fw	251.13	251.13
space group	<i>Pc</i>	<i>P</i> -1
<i>a</i> , Å	7.8904(1)	10.1946(3)
<i>b</i> , Å	10.4796(2)	11.9855(3)

c , Å	17.1104(3)	12.0919(3)
α , deg	90	87.461(2)
β , deg	91.521(2)	77.206(2)
γ , deg	90	77.472(2)
V , Å ³	1414.32(4)	1406.47(7)
Z	4	4
ρ (calcd), g/cm ³	1.179	1.186
μ , mm ⁻¹	0.061	0.062
R_{int}	0.0313	0.0341
R^b ($I > 2\sigma(I)$)	0.0414	0.0464
R_w^c ($I > 2\sigma(I)$)	0.1076	0.1359
R (all data)	0.0513	0.0574
R_w (all data)	0.1149	0.1483
goodness of fit on F^2	1.061	1.079

^aTemperature 100K, $\lambda = 0.71073$ Å; ^b $R = \sum||F_o| - |F_c||/\sum|F_o|$. ^c $R_w = [\sum[w(F_o^2 - F_c^2)^2]/\sum[w(F_o^2)^2]]^{1/2}$.

Analysis of data in Table 3 indicates that the position of the pyridine ring in the cluster has small, but noticeable effect on the {1-CB₁₁} cluster geometry. Thus, substitution of the pyridine ring at the B(12) position lowers the Y–B(12)–B angle from 121.7(1)^o in **3b** (Y = H) to 120.5(1)^o in **2b** (Y = N). On the other hand, the Y–C(1)–B angle slightly expands upon substitution with the pyridine fragment from 117.2(2)^o in **2b** (Y = H) to 118(1)^o in **3b** (Y = H). Consequently, the C(1)···B(12) distance is shorter for **2b** (3.186(4) Å) than in the C(1) isomer **3b** (3.243(6) Å).



a)

b)

Figure 8. Thermal ellipsoid diagram of (a) 12-(4-methoxypyridinium)-1-carbadodecaborate (**2b**) and (b) 1-(4-methoxypyridinium)-1-carbadodecaborate (**3b**). Hydrogen atoms are omitted for clarity. Pertinent molecular dimensions are listed in Table 3.

Table 3. Selected interatomic distances and angles for **2b** and **3b**.^a

	2b	3b
N–X	1.547(2) (X=B)	1.476(1) (X = C)
C(1)–B	1.705(5)	1.722(4)
B(2)–B(3)	1.782(2)	1.791(4)
B(2)–B(7)	1.775(3)	1.773(4)
B(7)–B(8)	1.795(4)	1.786(4)
B(12)–B	1.773(7)	1.785(3)
C(1)···B(12)	3.186(4)	3.243(6)
B–B(12)–Y	120.5(1) (Y=N)	121.7(1) (Y=H)
B–C(1)–Y	117.2(2) (Y=H)	118(1) (Y=N)

^a Average values were calculated for both unique molecules in the unit cell.

Mechanistic considerations

The transformation of amine **4** to pyridinium derivative **2** is a multistep process, similar to that reported¹⁴ earlier for [*closo*-1-CB₉H₈-1-COOH-6-NH₃]. The proposed mechanism involves the formation of 12-dinitrogen zwitterion **14**, heterolysis of the B–N bond with loss of N₂, and trapping of the resulting 12-boronium ylide **15** with a nucleophile, such as 4-methoxypyridine, and formation of **2** (Figure 9).

Previous MP2/6-31+G(d,p)//MP2/6-31G(d,p) level calculations in 50% aqueous EtOH dielectric medium demonstrated^{12,14} that the 12-ammonium group in the parent [*closo*-1-CB₁₁H₁₁-12-NH₃] (**4b[H]**) is more acidic than the 10-ammonium group in

[*closo*-1-CB₉H₉-10-NH₃], whose carboxylic acid derivative, [*closo*-1-CB₉H₈-1-COOH-10-NH₃], has been diazotized successfully in pyridine solutions giving an isolable stable dinitrogen acid [*closo*-1-CB₉H₈-1-COOH-10-N₂].¹² This suggests that amine **4b**[H] can also undergo partial deprotonation in pyridine solutions to the extent sufficient for effective diazotization and formation of transient dinitrogen derivative **14b**.

In agreement with experimental observations, DFT computational analysis indicates that dinitrogen [*closo*-1-CB₁₁H₁₁-12-N₂] (**14b**) is unstable against loss of N₂ (Table 4). The formation of the ylide **15b** is only +24.8 kcal mol⁻¹ endothermic ($\Delta G_{298} = +14.1$ kcal mol⁻¹), which is similar to that calculated for [*closo*-1-CB₉H₈-1-COO-6-N₂] in pyridine solutions (24.1 kcal mol⁻¹) and 11.3 kcal mol⁻¹ lower than that obtained for [*closo*-1-CB₉H₈-1-COO-10-N₂] at the same level of theory in pyridine dielectric medium. This difference is apparently sufficiently large to render [*closo*-1-CB₉H₈-1-COOH-10-N₂] an isolable stable compound,¹² while the two other dinitrogen compounds (including **14b**) exist only as transient species.¹⁴ The subsequent reaction of ylide **15b** with 4-methoxypyridine is strongly exothermic ($\Delta H = -68.6$ kcal mol⁻¹), which is typical for boronium ylides of the 10-vertex analogues.¹²

Further DFT calculations indicate that the stability of the dinitrogen species **14** depends on the nature of the antipodal substituent. Interestingly, substitution of the C(1) position with a COO⁻ group, present during diazotization of the amino acid **4a**[H] in pyridine solutions, moderately increases propensity of **14d** to loss of N₂, presumably due to electrostatic reasons. In contrast, a moderately electron donating alkyl group, such as ethyl, and electron withdrawing COOH stabilize the dinitrogen species **14e** and **14a**, respectively, by about 1 kcal mol⁻¹ relative to the parent **14b**.

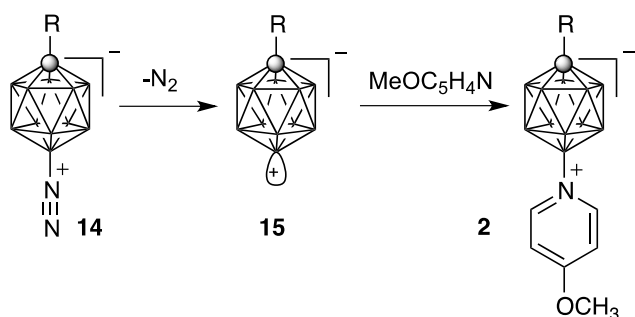


Figure 9. Proposed mechanism for the formation of **2**.

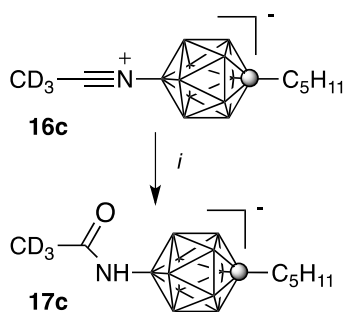
Table 4. Thermodynamic parameters (kcal mol⁻¹) for transformation of **14** to **2**.^a

R	14 → 15	15 → 2
	ΔH (ΔG_{298})	ΔH (ΔG_{298})
a COOH	26.0 (15.3)	-70.9 (-58.5)
b H	24.8 (14.1)	-68.6 (-56.7)
d COO ⁻	24.5 (13.6)	-65.1 (-51.8)
e C ₂ H ₅	25.8 (14.7)	-69.0 (-56.2)

^a In pyridine dielectric medium (B3LYP/6-31G(d,p) with PCM model). For structures see Figure 9.

Interestingly, ¹¹B NMR analysis of the crude reaction mixture taken during the conversion of amine **4c** to pyridinium **2c** and diluted with CD₃CN revealed the presence of a single species, presumably the transient 12-dinitrogen derivative [*closo*-1-CB₁₁H₁₀-1-

C_5H_{11} -12- N_2] (**14c**), with the characteristic signal at $\delta -9.3$ ppm (Figure 9). At -40 °C, the signal was slowly converting to the signal at $+3.6$ ppm, characteristic for the expected **2c**, and the process was much faster at ambient temperature. Monitoring of the originally taken NMR sample revealed that the signal related to **2c** and a new signal at $+0.2$ ppm were evolving at the expense of the signal at -9.3 ppm (Figure 10). This new signal at $+0.2$ ppm was attributed to [*closo*-1- $CB_{11}H_{10}$ -1- C_5H_{11} -12- $NCCD_3$] (**16c**), an adduct of ylide **15c** to acetonitrile- d_3 , which upon treatment with H_2O gave the acetamide derivative **17c** with the B(12) signal shifted to -1.8 ppm (Scheme 5). This structural assignment is supported by HRMS analysis of the hydrolyzed NMR sample. Similar adducts were observed in thermolysis of dinitrogen derivatives of [*closo*-1- CB_9H_8 -1-COOH-10- N_2],¹² [*closo*-1- CB_9H_9 -1- N_2],¹¹ and [*closo*- $B_{10}H_8$ -1,10-(N_2)₂]¹⁹ in organic nitriles. If correct, derivative **14c** would represent the first experimentally observed dinitrogen derivative of 12-vertex *closo*-borates.



Scheme 5. Formation of **17c**. Reagents and conditions: *i*) H_2O .

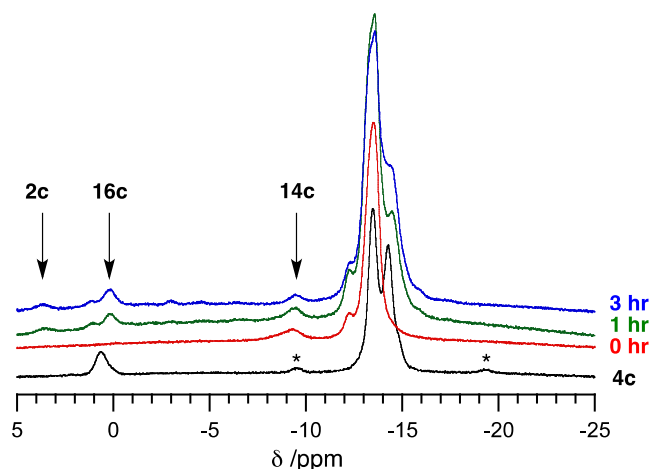


Figure 10. A sequence of ^{11}B NMR spectra showing the transformation of amine **4c**[NMe₄] (black line) to CD₃CN adduct **16c**. The asterisks indicate trace impurities in the amine. The sample was taken at $-40\text{ }^{\circ}\text{C}$, dissolved in CD₃CN at $-40\text{ }^{\circ}\text{C}$, and placed in the spectrometer at ambient temperature before immediate recording of the spectra.

The origin for this propensity towards loss of molecular nitrogen (dediazonation) by some dinitrogen zwitterions lays in the nature of the N–B bond, which is best analyzed for the parent derivatives at the MP2 level of theory. Thus, computational analysis of [*closo*-1-CB₁₁H₁₁-12-N₂] (**14b**) in MeCN dielectric medium, revealed that its bonding situation is similar to that found for [*closo*-1-CB₉H₉-6-N₂] (**18**), and significantly different from the presumably much more stable [*closo*-1-CB₉H₉-10-N₂] (**19**, Table 5).¹⁴ In compounds **14b** and **18** the B–N bond is long ($d_{\text{BN}} = 1.507\text{ \AA}$ and 1.491 \AA , respectively) with low bond order (WBI = 0.74 and 0.76), while the N–N bond is short ($d_{\text{NN}} = 1.133$ and 1.136 \AA) with high bond order (WBI = 2.54 and 2.50). This, weak bonding in **14b** and **18** is related to the small negative charge ($q_{\text{B}} = -0.05$ and -0.08) at the B(12) and B(6) atom, respectively. In consequence, both compounds have predicted low thermodynamic stability against loss of N₂ ($\Delta\text{H} = 30.5\text{ kcal/mol}$ and 28.8 kcal/mol ,

respectively), which renders them unstable at ambient temperature. In contrast, bonding situation in **19** is significantly better: the B(10)–N bond is markedly shorter ($d_{\text{BN}} = 1.459$ Å), has higher electron density (WBI = 0.80), and the B(10) atom has higher negative charge ($q_B = -0.13$). This results in increased thermodynamic stability of the species with the highest enthalpy for dediazonation, ($\Delta H = 41.8$ kcal/mol) among the three zwitterions (Table 5).

Table 5. Bonding properties of selected dinitrogen derivatives.^a

	14b	19^b	18^b
$d_{B-N} / \text{\AA}$	1.507	1.459	1.491
$d_{N-N} / \text{\AA}$	1.133	1.138	1.136
WBI_{B-N}	0.74	0.80	0.76
WBI_{N-N}	2.54	2.47	2.50
B^c	$sp^{6.5}$	$sp^{6.0}$	$sp^{6.0}$
N^c	$sp^{0.64}$	$sp^{0.65}$	$sp^{0.65}$
q_B	-0.05	-0.13	-0.08
q_N	+0.15	+0.14	+0.13
$\Delta H / \text{kcal/mol}^d$	30.5	41.8	28.8

^a NBO analysis of the MP2/6-31G(d,p) wavefunction in MeCN dielectric medium (IPCM model): d –distance, WBI –Wiberg bond index, q –charge, ΔH –energy of dediazonation. ^b Partial data from ref.¹⁴ ^c Hybridization of the orbital forming the B–N bond. ^d Heterolytic cleavage of the B–N bond.

3.3.2.3 Summary and conclusions

We have developed a method for the efficient preparation of B(12)-substituted pyridinium zwitterions derived from the [*closo*-1-CB₁₁H₁₂]⁻ anion (**B**). This new method represents an approximately 3-fold improvement in yield over the previously employed methodology. The improved process involves synthesis of a 4-methoxypyridinium zwitterion followed by demethylation and re-alkylation with an alkyl triflate. The method was demonstrated for the heptyl substituent, although more complex alkyl groups, such as *trans*-4-pentylcyclohexylmethyl, should work equally well opening up convenient access to a potentially broad class of polar materials. Overall, polar pyridinium derivatives, such as **1**, are available in 8 steps and about 12% yield from commercial B₁₀H₁₄.

A comparison of the two 4-methoxypyridinium isomers, **2b** and **3b**, demonstrated that they generally have similar spectroscopic properties and molecular structures. Detailed analysis revealed that the pyridine ring in **3b** is more deshielded, **3b** has lower cage-to-pyridine excitation energy and 50% higher molecular dipole moment. The latter causes these C(1) zwitterions (e.g. **3** and **13**) to be more crystalline (higher melting), while the isomeric derivatives **1**, such as **1c**, have lower melting points and some exhibit liquid crystalline behavior.

We also computationally assessed the reaction mechanism for the formation of the B(12)-substituted pyridinium derivatives of [*closo*-1-CB₁₁H₁₂]⁻ anion. The calculations confirmed that dinitrogen derivatives of the [*closo*-1-CB₁₁H₁₂]⁻ anion are generally unstable and therefore difficult to isolate. Nonetheless, ¹¹B NMR evidence for the existence of the dinitrogen derivative **14c** as a transient species was presented.

The findings reported here represent further development and understanding of the fundamental chemistry of the [*closo*-1-CB₁₁H₁₂]⁻ anion and contribute to our ongoing program in designing liquid crystalline materials incorporating boron clusters.

3.3.2.4 Computational details

Quantum-mechanical calculations were carried out using Gaussian 09 suite of programs.²⁰ Geometry optimizations for unconstrained conformers of **1c** and **13** with the most extended molecular shapes were undertaken at the B3LYP/6-31G(d,p) level of theory using default convergence limits. The alkyl groups were set in all-*trans* conformation in the input structure.

Calculations involving reactive intermediates were carried out with the B3LYP and MP2(fc) methods with 6-31G(d,p) basis set. Geometry optimizations were undertaken using appropriate symmetry constraints and tight convergence limits. Vibrational frequencies were used to characterize the nature of the stationary points and to obtain thermodynamic parameters. Zero-point energy (ZPE) corrections were scaled by 0.9806.²¹ Hybridization parameters, Wiberg Bond Index (WBI) matrix, and natural charges were obtained using the NBO algorithm supplied in the Gaussian 09 package. Population analysis of the MP2 wavefunction (MP2//MP2) was performed using the DENSITY(MP2) keyword. The IPCM solvation model²² was used with default parameters and $\epsilon = 36.64$ for MeCN. The PCM model²³ was implemented using the SCRF(Solvent=Pyridine) keyword.

3.3.2.5 Experimental section

General. Reagents and solvents were obtained commercially. Reactions were carried out under Ar, and subsequent manipulations were conducted in air. NMR spectra were obtained at 128 MHz (^{11}B) and 400 MHz (^1H) in CD_3CN or CDCl_3 . ^1H NMR spectra were referenced to the solvent and ^{11}B NMR chemical shifts to an external boric acid sample in CH_3OH (18.1 ppm). Optical microscopy and phase identification were performed using a polarized microscope equipped with a hot stage. Thermal analysis was obtained using a TA Instruments DSC using small samples of about 0.5-1.0 mg. Transition temperatures (onset) and enthalpies were obtained on heating using small samples (0.5-1 mg) and a heating rate of 5 K min^{-1} under a flow of nitrogen gas unless specified otherwise.

X-Ray data collection

Single-crystal X-ray measurement for **2b** was performed with a Supernova Dual diffractometer equipped with an Atlas detector whereas for **3b** it was performed with a SuperNova diffractometer equipped with an Eos detector. Both measurements were conducted at 100K using the MoK_α radiation. The crystals were positioned at $\sim 50\text{ mm}$ from the CCD detectors. A total number of 501 frames were collected at 1° intervals with a counting time of 25 s for **2b**, whereas 1328 frames were collected for **3b** with a counting time of 15s. The data were corrected for Lorentzian and polarization effects. Data reduction and analysis were carried out with the CrysAlis program.²⁴ Both structures were solved by direct methods using SHELXS-97 and refined using SHELXL-97²⁵ within the Olex2 program.²⁶ The refinement was based on F^2 for all reflections except those with very negative F^2 . Weighted R factors (wR) and all goodness-of-fit (GooF) values are

based on F^2 . Conventional R factors are based on F with F set to zero for negative F^2 . The $F_o^2 > 2\sigma(Fo^2)$ criterion was used only for calculating the R factors and it is not relevant to the choice of reflections for the refinement. The R factors based on F^2 are about twice as large as those based on F . Scattering factors were taken from the International Tables for Crystallography.²⁷ All hydrogen atoms were placed in idealized geometrical positions. The structures have been deposited at CCDC (1025212 and 1025213).

12-(4-Heptyloxyppyridinium)-1-carbadodecaborate (1b).

Method A. Pure [*closo*-1-CB₁₁H₁₁-12-NH₂]⁺[NMe₄]⁺ (**4b**[NMe₄], 100 mg, 0.63 mmol) was dissolved in freshly distilled 4-heptyloxyppyridine (4 mL) and the solution was cooled to -20 °C. Solid [NO]⁺[PF₆]⁻ (0.66 g, 3.77 mmol) was added in 4 portions in 10 min intervals to the vigorously stirred mixture. The reaction mixture was allowed to warm to rt and stirred for 2 hr. The brown suspension was washed with hexane (5 x 10 mL) and then dissolved in 10% HCl (30 mL). The aqueous layer was extracted with Et₂O (4 x 10 mL), the organic layer dried (Na₂SO₄), and solvents were evaporated. The crude product was purified by column chromatography (SiO₂, CH₂Cl₂/hexane, 1:2) to give 31 mg (15% yield) of pure **1b**, which was recrystallized from *iso*-octane (2x) giving a white crystalline solid: mp 99 °C; ¹H NMR (400 MHz, CD₃CN) δ 0.90 (t, $J = 6.8$ Hz, 3H), 1.0-2.5 (br m, 10H), 1.25-1.49 (m, 8H), 1.81 (quint, $J = 7.0$ Hz, 2H), 2.59 (br s, 1H), 4.23 (t, $J = 6.6$ Hz, 2H), 7.14 (d, $J = 7.5$ Hz, 2H), 8.43 (d, $J = 7.2$ Hz, 2H); ¹³C NMR (125.8 MHz, CD₃CN) δ 14.7, 23.6, 26.3, 29.4, 29.9, 32.8, 47.2 (br), 71.9, 113.8, 148.2; ¹¹B NMR (128 MHz, CD₃CN) δ -16.5 (d, $J = 158$ Hz, 5B), -13.6 (d, $J = 140$ Hz, 5B), 4.8 (s, 1B). Anal. Calcd. for C₁₃H₃₀B₁₁NO: C, 46.57; H, 9.02; N, 4.18. Found: C, 46.56; H, 9.21; N, 4.18.

Method B. Pyridone **5b**[NMe₄] (35 mg, 0.11 mmol) was dissolved in CH₂Cl₂ (1 mL) and heptyl triflate⁵ (28 mg, 0.11 mmol) was added drop-wise while stirring. Reaction progress was monitored by TLC (CH₂Cl₂). After 1 hr the organic layer was passed through a short silica gel plug (CH₂Cl₂), solvents removed, and the residue was washed with cold pentane to give 30 mg (80% yield) of **1b** as colorless crystals.

12-(4-Heptyloxy pyridinium)-1-pentyl-1-carbadodecaborate (1c).

Pyridone **5c**[NMe₄] (30 mg, 0.08 mmol) was dissolved in CH₂Cl₂ (1 mL) and heptyl triflate⁵ (28 mg, 0.09 mmol) in CH₂Cl₂ (0.5 mL) was added drop-wise, while stirring. Reaction progress was monitored by TLC (CH₂Cl₂). After 2 hr the reaction mixture was passed through a short silica gel plug (CH₂Cl₂). Solvents were removed giving 32 mg (100% yield) of crude **1c** as a white solid, which was recrystallized twice from *iso*-octane: ¹H NMR (400 MHz, CD₃CN) δ 0.86 (t, *J* = 7.2 Hz, 3H), 0.90 (t, *J* = 6.9 Hz, 3H), 1.0-2.5 (br m, 10H), 1.10-1.20 (m, 2H), 1.21-1.48 (m, 12H), 1.75-1.82 (m, 2H), 1.85 (br t, *J* = 8.5 Hz, 2H), 4.22 (t, *J* = 6.6 Hz, 2H), 7.12 (d, *J* = 7.5 Hz, 2H), 8.41 (d, *J* = 7.4 Hz, 2H); ¹¹B NMR (128 MHz, CD₃CN) δ -13.7 (d, *J* = 146 Hz, 10B), 3.6 (s, 1B). Anal. Calcd. for C₁₈H₄₀B₁₁NO: C, 53.33; H, 9.94; N, 3.45. Found: C, 53.45; H, 9.87; N, 3.52.

12-(4-Methoxy pyridinium)-1-carbadodecaborate (2b).

Amine [*closo*-1-CB₁₁H₁₁-12-NH₂][NMe₄]⁺ (**4b**[NMe₄], 290 mg, 1.25 mmol) containing about 22% of the 7-isomer **8b**[NMe₄] was dissolved in freshly distilled 4-methoxy pyridine (8 mL), and the solution was cooled to -20 °C. Solid [NO]⁺[PF₆]⁻ (1.32 g, 7.56 mmol) was added in 6 portions in 10 min intervals, with vigorous mechanical stirring. After each addition, the solution turned green. The reaction was warmed to rt and

stirred for 2 hr. The brown suspension was washed with hexane (5 x 10 mL) and then dissolved in 10% HCl (50 mL). The aqueous layer was extracted with Et₂O (4 x 10 mL), the organic layer dried (Na₂SO₄), and solvents were evaporated giving 377 mg of crude material. Separation by column chromatography (SiO₂, CH₂Cl₂/hexane, 3:2) gave 130 mg (53% yield based on pure **4b**[NMe₄]) of pure **2b** (R_f = 0.61), which was recrystallized twice from *iso*-octane/toluene giving colorless needles: mp 221 °C; ¹H NMR (400 MHz, CD₃CN) δ 1.0-2.5 (br m, 10H), 2.60 (br s, 1H), 4.01 (s, 3H), 7.18 (d, *J* = 7.5 Hz, 2H), 8.47 (d, *J* = 6.8 Hz, 2H); ¹³C NMR (125.8 MHz, CD₃CN) δ 47.1 (br), 58.4, 113.5, 148.3, 171.8; ¹¹B NMR (128 MHz, CD₃CN) δ -16.5 (d, *J* = 156 Hz, 5B), -13.6 (d, *J* = 141 Hz, 5B), 4.8 (s, 1B). Anal. Calcd. for C₇H₁₈B₁₁NO: C, 33.48; H, 7.22; N, 5.58. Found: C, 33.70; H, 7.29; N, 5.62.

The more polar fraction contained the 7-(4-methoxypyridinium) isomer **9b** (SiO₂, CH₂Cl₂/hexane, 3:2, R_f = 0.46): ¹H NMR (400 MHz, CD₃CN) δ 1.0-2.5 (br m, 10H), 2.72 (br s, 1H), 4.05 (s, 3H), 7.24 (d, *J* = 7.5 Hz, 2H), 8.64 (d, *J* = 6.8 Hz, 2H); ¹¹B NMR (128 MHz, CD₃CN) δ -18.6 (d, *J* = 141 Hz, 1B), -16.4 (d, *J* = 155 Hz, 4B), -13.6 (d, *J* = 130 Hz, 4B), -6.7 (d, *J* = 138 Hz, 1B), 0.6 (s, 1B); HRMS, calcd for [M-Me+H] C₆H₁₅B₁₁NO: *m/z* = 238.2184; found: *m/z* = 238.2213.

12-(4-Methoxypyridinium)-1-pentyl-1-carbadodecaborate (2c).

Following the procedure for preparation of **2b**, amine [*closo*-1-CB₁₁H₁₀-12-NH₂-1-C₅H₁₁][NMe₄]⁺ (**4c**[NMe₄]), 250 mg, 0.83 mmol, 23% of the 7-isomer **8c**[NMe₄]) in 4-methoxypyridine (5 mL) was treated with [NO]⁺[PF₆]⁻ (0.87 g, 4.97 mmol). The resulting brown crude product was separated by column chromatography (SiO₂, CH₂Cl₂/hexane, 1:1) giving 87 mg (45% yield based on pure **4c**[NMe₄]) of **2c**. Recrystallization from *iso*-

octane/toluene (2x) gave **2c** as colorless needles: mp 165 °C; ¹H NMR (400 MHz, CD₃CN) δ 0.86 (t, *J* = 7.2 Hz, 3H), 1.0-2.5 (br m, 10H), 1.10-1.20 (m, 2H), 1.21-1.35 (m, 4H), 1.85 (br t, *J* = 8.5 Hz, 2H), 4.0 (s, 3H), 7.16 (d, *J* = 7.5 Hz, 2H), 8.44 (d, *J* = 7.3 Hz, 2H); ¹¹B NMR (128 MHz, CD₃CN) δ -13.7 (d, *J* = 146 Hz, 10B), 3.6 (s, 1B). Anal. Calcd. for C₁₂H₂₈B₁₁NO: C, 44.86; H, 8.79; N, 4.36. Found: C, 45.13; H, 8.90; N, 4.38.

Further elution of the column gave the 7-isomer **9c**: ¹H NMR (400 MHz, CD₃CN) δ 0.87 (t, *J* = 7.2 Hz, 3H), 1.0-2.5 (br m, 10H), 1.10-1.20 (m, 2H), 1.21-1.35 (m, 4H), 1.88 (br t, *J* = 8.6 Hz, 2H), 4.0 (s, 3H), 7.23 (d, *J* = 7.5 Hz, 2H), 8.63 (d, *J* = 7.1 Hz, 2H); ¹¹B NMR (128 MHz, CD₃CN) δ -15.6 (1B), -13.4 (d, *J* = 126 Hz, 8B), -9.67 (d, *J* = 140 Hz, 1B), 0.64 (s, 1B); HRMS, calcd for [M-Me+H] C₁₁H₂₆B₁₁NO: *m/z* = 309.3045; found: *m/z* = 309.3027.

1-(4-Methoxyppyridinium)-1-carbadodecaborate (3b).

Amine **12**[NMe₄] (200 mg, 0.86 mmol) was dissolved in THF (3 mL) and crude 4-methoxyppyrylium salt (**11**, 269 mg, 1.0 mmol, prepared by methylation of 4-pyrone with CF₃SO₃Me in THF according to a general procedure⁵) in THF (1 mL) was added. The reaction mixture was stirred overnight at rt, solvents were removed and the brown residue was purified by column chromatography (SiO₂, CH₂Cl₂) to give the 35 mg (16% yield) of **3b**. The product was washed with hot toluene and then recrystallized twice from CH₃OH containing few drops of CH₃CN: mp > 260 °C; ¹H NMR (400 MHz, CD₃CN) δ 1.0-2.9 (br m, 10H), 4.10 (s, 3H), 7.24 (d, *J* = 7.8 Hz, 2H), 8.83 (d, *J* = 7.8 Hz, 2H); ¹³C NMR (125.8 MHz, CD₃CN) δ 59.4, 84.8 (br), 114.1, 146.2, 173.4; ¹¹B NMR (128 MHz, CD₃CN) δ -13.7 (d, *J* = 130 Hz, 5B), -12.9 (d, *J* = 126 Hz, 5B), -8.1 (d, *J* = 137 Hz, 1B).

Anal. Calcd. for C₇H₁₈B₁₁NO: C, 33.48; H, 6.90; N, 5.58. Found: C, 33.90; H, 6.90; N, 5.68.

[*closo*-1-CB₁₁H₁₁-12-NH₂]⁻[NMe₄]⁺ (**4b**[NMe₄]).¹⁷

[*closo*-1-CB₁₁H₁₁-12-I]⁻[Cs]⁺ (**6b**[Cs]),¹⁸ 670 mg, 1.67 mmol) containing 23% of the 7 isomer **7b**[Cs] was added to a solution of lithium hexamethyldisilazane (LiHMDS, 35 mL, 35 mmol, 1.0 M in THF) at rt under N₂. The light-orange suspension was then stirred for 15 min. Pd₂dba₃ (91 mg, 0.1 mmol) and 2-(dicyclohexylphosphino)biphenyl (41 mg, 0.40 mmol) were quickly added, and the reaction mixture was stirred at reflux for 16 hr. After cooling to 0 °C, 20% HCl (80 mL) was added slowly to quench unreacted LiHMDS. THF was removed *in vacuo* giving a dark orange liquid, which was extracted with Et₂O (3 x 50 mL). The organic extracts were dried (Na₂SO₄), and solvents were removed. The resulting brown residue was redissolved in Et₂O, H₂O was added (10 mL), and the Et₂O was removed *in vacuo*. The aqueous layer was filtered and the process was repeated four more times to remove phosphonium by-products. The aqueous layers were combined and [NEt₄]⁺Br⁻ (350 mg, 1.67 mmol) was added resulting in a white precipitation. The suspension was filtered through Celite, the filtrate was acidified with conc. HCl (5 mL), and extracted with Et₂O (3 x 50 mL). The organic layers were combined, dried (Na₂SO₄), and solvents were evaporated giving 90 mg (40% yield) of an off-white solid: {¹H}¹¹B NMR (128 MHz, CD₃CN) δ major isomer **4b**[Cs] (77%) -16.6 (5B), -13.9 (5B), -0.8 (1B); minor isomer **8b**[Cs] (23%) δ -19.0, -12.5, -6.9, -5.4. The solid was treated with an aqueous solution of [NMe₄]⁺[OH]⁻•5H₂O (453 mg, 2.50 mmol), and the resulting suspension was extracted into CH₂Cl₂ (3 x 20 mL). The organic layer was dried (Na₂SO₄) and CH₂Cl₂ was removed *in vacuo* to give a white crystalline solid of

4b[NMe₄] containing 23% of the 7-isomer **8b[NMe₄]**: ¹H/¹¹B NMR (128 MHz, CD₃CN) δ major isomer -17.2 (5B), -13.4 (5B), 2.8 (1B); minor isomer δ -22.2, -14.6, -6.5, 0.2.

[closo-1-CB₁₁H₁₀-1-C₅H₁₁-12-NH₂][NMe₄]⁺ (4c[NMe₄]**).**

[*closo*-1-CB₁₁H₁₀-1-C₅H₁₁-12-I]⁻[Cs]⁺ (**6c[Cs]**, 784 mg, 1.66 mmol) containing 23% of the 7 isomer **7c[Cs]** was reacted with lithium hexamethyldisilazane (LiHMDS, 33 mL, 33 mmol, 1.0 M in THF) in the presence of Pd₂dba₃ (91 mg, 0.1 mmol) and 2-(dicyclohexylphosphino)biphenyl (141 mg, 0.40 mmol) as described for the synthesis of the parent **6b[Cs]**. The ethereal extract of the crude product was evaporated giving a brown solid, which was purified by column chromatography (CH₂Cl₂ then 10% CH₃CN in CH₂Cl₂). The solvents were evaporated, and the resulting brown solid was washed with hot hexane giving 370 mg (97% yield) of crude amine **4c[H]** contaminated with about 23% of the 7-isomer **8c[H]**: ¹H NMR (400 MHz, CD₃CN) δ major isomer 0.85 (t, *J* = 7.3 Hz, 3H), 1.0-2.5 (br m, 10H), 1.1-1.2 (m, 2H), 1.21-1.32 (m, 4H), 1.80 (br t, *J* = 10.7 Hz, 2H); ¹¹B NMR (128 MHz, CD₃CN) δ -13.9 (d, *J* = 147 Hz, 10B), -2.2 (s, 1B); minor isomer δ -16.1, -10.0, -5.4.

The brown solid was treated with a solution of NMe₄OH•5H₂O, and the resulting precipitation was extracted into CH₂Cl₂. The organic layers were combined, dried (Na₂SO₄), and solvents were evaporated giving 400 mg (81% yield) of **4c[NMe₄]** as a tan solid contaminated with the 7-isomer **8c[NMe₄]**.

Major isomer **4c[NMe₄]**: ¹H NMR (400 MHz, CD₃CN) δ 0.85 (t, *J* = 7.3 Hz, 3H), 1.0-2.5 (br m, 10H), 1.09-1.18 (m, 2H), 1.20-1.32 (m, 4H), 1.80 (br t, *J* = 8.5 Hz, 2H),

3.1 (s, 12H); ^{11}B NMR (128 MHz, CD_3CN) δ -14.3 (d, $J = 127$ Hz, 5B), -13.5 (d, $J = 118$ Hz, 5B), 0.7 (s, 1B).

Minor isomer **8c**[NMe₄], characteristic signals: ^1H NMR (400 MHz, CD_3CN) δ 0.86 (t, $J = 7.3$ Hz, 3H); $\{^1\text{H}\}^{11}\text{B}$ NMR (128 MHz, CD_3CN) δ -19.2, -9.6. HRMS, calcd for $\text{C}_6\text{H}_{23}\text{B}_{11}\text{N}$: $m/z = 228.2927$; found: $m/z = 228.2959$.

12-(4-Pyridon-1-yl)-1-carbadodecaborate NMe₄ salt (5b[NMe₄]).

[*closo*-1-CB₁₁H₁₁-12-(4-CH₃OC₅H₄N)] (**2b**, 100 mg, 0.40 mmol) was dissolved in dry DMF (5 mL), LiCl (50 mg, 1.2 mmol) was added, and the resulting mixture was stirred at 80 °C for 16 hr. The reaction mixture was cooled to rt, DMF was removed *in vacuo*, water (5 mL) containing NMe₄Cl (130 mg, 1.2 mmol) and CH₂Cl₂ (5 mL) were added, and the resulting biphasic system was stirred for 2 hr. The organic layer was separated, dried (Na₂SO₄), and solvents were removed. The oily yellow residue was washed with Et₂O (3 x 5 mL) and dried to give 122 mg (99% yield) of **5b**[NMe₄] as a white crystalline solid which was recrystallized twice from a toluene/CH₃CN mixture: mp 251 °C; ^1H NMR (400 MHz, CD_3CN) δ 1.0-2.5 (br m, 10H), 2.43 (br s, 1H) 3.10 (s, 12H), 6.10 (d, $J = 7.5$ Hz, 2H), 7.61 (d, $J = 6.7$ Hz, 2H); ^{13}C NMR (125.8 MHz, CD_3CN) δ 45.6 (br), 56.2 (t, $J = 8.5$ Hz), 117.1, 144.9, 178.0; ^{11}B NMR (128 MHz, CD_3CN) δ -17.0 (d, $J = 151$ Hz, 5B), -13.7 (d, $J = 139$ Hz, 5B), 5.4 (s, 1B); HRMS, calcd for $\text{C}_6\text{H}_{15}\text{B}_{11}\text{NO}$: $m/z = 238.2184$; found: $m/z = 238.2186$. Anal. Calcd. for $\text{C}_{10}\text{H}_{27}\text{B}_{11}\text{N}_2\text{O}$: C, 38.71; H, 8.77; N, 9.03. Found: C, 38.99; H, 8.93; N, 8.96.

1-Pentyl-12-(4-pyridon-1-yl)-1-carbadodecaborate NMe₄ salt (5c[NMe₄]).

[*closo*-1-CB₁₁H₁₀-12-(4-CH₃OC₅H₄N)-1-C₅H₁₁] (**2c**, 80 mg, 0.25 mmol) was converted to pyridone **5c**[NMe₄] using LiCl (32 mg, 0.75 mmol) in DMF (3 mL) as

described above for **5b**[NMe₄]. Double recrystallization from EtOAc/hexane gave pure **5c**[NMe₄] as colorless crystals: mp 223.5 °C; ¹H NMR (400 MHz, CD₃CN) δ 0.86 (t, *J* = 7.2 Hz, 3H), 1.0-2.5 (br m, 10H), 1.10-1.20 (m, 2H), 1.21-1.37 (m, 4H), 1.85 (br t, *J* = 8.5 Hz, 2H), 3.1 (s, 12H), 5.95 (d, *J* = 7.6 Hz, 2H), 7.48 (d, *J* = 6.3 Hz, 2H); {¹H}¹¹B NMR (128 MHz, CD₃CN) δ -13.9 (10B), 4.0 (1B). Anal. Calcd. for C₁₅H₃₇B₁₁N₂O: C, 47.36; H, 9.80; N, 7.36. Found: C, 47.09; H, 9.96; N, 7.40.

[*closo*-1-CB₁₁H₁₁-1-C₅H₁₁-12-I]⁺Cs⁺ (6c**[Cs]).**

Following a modified general procedure,¹⁸ [*closo*-1-CB₁₁H₁₁-1-C₅H₁₁][Cs]⁺ (**10c**[Cs], 930 mg, 2.69 mmol) was dissolved in AcOH (15 mL), iodine (682 mg, 2.69 mmol) was added and the reaction mixture was stirred at 50 °C. Reaction progress was monitored by ¹¹B NMR, and more iodine was added when necessary (up to 1.23 g, 4.84 mmol in total). AcOH was removed *in vacuo*, and the residue was treated with 10% HCl (30 mL) followed by Na₂S₂O₅ to reduce the remaining I₂. The resulting yellow aqueous solution was extracted with Et₂O (4 x 30 mL). The organic layers were combined, H₂O (30 mL) was added, and the Et₂O was removed *in vacuo*. Solid [NEt₄]⁺Br⁻ (565 mg, 2.69 mmol) was added, and the resulting white precipitation was filtered and dried giving 1.06 g (77% yield) of **6c**[NEt₄] contaminated with about 22% of the 7-isomer **7c**[NEt₄]. The product was suspended in 10% HCl (50 mL) and extracted with Et₂O. Water (25 mL) was added to the combined organic layers and Et₂O was removed *in vacuo*. The aqueous solution was treated with an excess CsOH•H₂O to ensure basicity of the solution, and the resulting white precipitation was extracted into Et₂O (5 x 30 mL). The organic layers were combined, dried (Na₂SO₄), and solvents evaporated giving 912 mg of mixture of isomers **6c**[NEt₄] and **7c**[NEt₄]. Isomerically pure **6c**[Cs]

was obtained by repeated recrystallization from hot water: mp 225-226 °C; ^1H NMR (400 MHz, CD_3CN) δ 0.84 (t, $J = 7.3$ Hz, 3H), 1.0-2.5 (br m, 10H), 1.15-1.18 (m, 2H), 1.19-1.30 (m, 4H), 1.68 (br t, $J = 8.4$ Hz, 2H); ^{13}C NMR (125.8 MHz, CD_3CN) δ 14.4, 23.2, 30.9, 32.6, 40.3, 71.7 (br); ^{11}B NMR (128 MHz, CD_3CN) δ -19.0 (s, 1B), -13.0 (d, $J = 172$ Hz, 5B), -11.6 (d, $J = 159$ Hz, 5B). Anal. Calcd. for $\text{C}_6\text{H}_{21}\text{B}_{11}\text{CsI}$: C, 15.27; H, 4.49. Found: C, 15.66; H, 4.50.

[*closo*-1-CB₁₁H₁₁-1-C₅H₁₁]⁻Cs⁺ (10c**[Cs]).**

Pure [*closo*-1-CB₁₁H₁₂]⁻[Cs]⁺ (1.88 g, 6.81 mmol) was dissolved in freshly distilled THF (100 mL), freshly distilled dry TMEDA (1.0 mL, 6.81 mmol) was added and the solution was cooled down to -78 °C. *n*-BuLi (6.8 mL, 17.0 mmol, 2.5 M in hexanes) was added drop-wise to the solution. The reaction mixture was stirred at -78 °C for 15 min and then allowed to warm up to rt. The resulting white suspension was stirred for 1.5 hr at rt, cooled to 0 °C, and pentyl iodide (4.0 mL, 30.7 mmol) was added slowly. After stirring overnight, water (15 mL) was added to the mixture and THF was removed *in vacuo*. The aqueous solution was acidified with conc. HCl (3 mL) and extracted with Et₂O (3 x 30 mL). Water (20 mL) was added to the ethereal extract and Et₂O was removed *in vacuo*. The aqueous solution was treated with an excess CsOH•H₂O to ensure basicity of the solution, and the resulting white suspension was extracted with Et₂O (5 x 30 mL). The organic layers were combined, dried (Na_2SO_4), and solvents evaporated giving 2.22 g (94% yield) of **10c**[Cs] as a slightly yellow solid. The crude product (containing about 8% of the starting Cs⁺ salt by ^{11}B NMR) was recrystallized from hot water (2x) to give 1.98 g (84% yield) of pure **10c**[Cs] as a colorless crystalline solid: mp 209 °C; ^1H NMR (400 MHz, CD_3CN) δ 0.85 (t, $J = 7.3$ Hz, 3H), 1.0-2.5 (br m, 10H), 1.1-

1.18 (m, 2H), 1.2-1.34 (m, 4H), 1.78 (br t, $J = 8.5$ Hz, 2H); ^{11}B NMR (128 MHz, CD_3CN) δ -13.2 (d, $J = 143$ Hz, 10B), -9.9 (d, $J = 134$ Hz, 1B). Anal. Calcd. for $\text{C}_6\text{H}_{22}\text{B}_{11}\text{Cs}$: C, 20.82; H, 6.41. Found: C, 21.08; H, 6.67.

12-(d_3 -acetylamino)-1-pentyl-1-carbadodecaborate (17c).

It was formed by decomposition of the putative 12-dinitrogen **14c** in CD_3CN solvent at ambient temperature during 24 hr followed by treatment with water and extraction into CH_2Cl_2 : ^{11}B NMR (128 MHz, CD_3CN) δ characteristic signal at -1.8; HRMS, calcd for $\text{C}_8\text{H}_{22}\text{D}_2\text{B}_{11}\text{NO}$: $m/z = 271.3080$; found: $m/z = 271.3087$.

3.3.2.6 Acknowledgements

This work was supported by the NSF grant (DMR-1207585).

3.3.2.7 References

- (1) Kaszynski, P. In *Boron Science: New Technologies & Applications*; Hosmane, N., Ed.; CRC Press: 2012, p 305-338.
- (2) Kirsch, P.; Bremer, M. *Angew. Chem. Int. Ed.* **2000**, *39*, 4216-4235.
- (3) Ringstrand, B.; Kaszynski, P.; Januszko, A.; Young, V. G., Jr. *J. Mater. Chem.* **2009**, *19*, 9204-9212.
- (4) Pecyna, J.; Kaszynski, P.; Ringstrand, B.; Bremer, M. *J. Mater. Chem. C* **2014**, *2*, 2956-2964.
- (5) Pecyna, J.; Pocięcha, D.; Kaszynski, P. *J. Mater. Chem. C* **2014**, *2*, 1585-1519.
- (6) Ringstrand, B.; Kaszynski, P. *J. Mater. Chem.* **2010**, *20*, 9613-9615.
- (7) Ringstrand, B.; Kaszynski, P. *Acc. Chem. Res.* **2013**, *46*, 214-225.
- (8) Körbe, S.; Peter J. Schreiber, P. J.; Michl, J. *Chem. Rev.* **2006**, *106*, 5208-5249.

- (9) A recently published optimized procedure provides [*closo*-1-CB₁₁H₁₂]⁻[NEt₄]⁺ in two steps and 66% yield from commercial B₁₀H₁₄: Franken, A.; Kennedy, J. D.; Clapper, J.; Sneddon, L. G. *Inorg. Synth.* **2014**, *36*, 180–191.
- (10) For more details see the ESI.
- (11) Ringstrand, B.; Kaszynski, P.; Franken, A. *Inorg. Chem.* **2009**, *48*, 7313-7329.
- (12) Ringstrand, B.; Kaszynski, P.; Young, V. G., Jr.; Janoušek, Z. *Inorg. Chem.* **2010**, *49*, 1166-1179.
- (13) Pecyna, J.; Denicola, R. P.; Ringstrand, B.; Jankowiak, A.; Kaszynski, P. *Polyhedron* **2011**, *30*, 2505-2513.
- (14) Ringstrand, B.; Kaszynski, P.; Young, V. G., Jr. *Inorg. Chem.* **2011**, *50*, 2654-2660.
- (15) Pecyna, J.; Denicola, R. P.; Gray, H. M.; Ringstrand, B.; Kaszynski, P. *Liq. Cryst.* **2014**, *41*, 1188-1198.
- (16) Bernard, A. M.; Ghiani, M. R.; Piras, P. P.; Rivoldini, A. *Synthesis* **1989**, 287-289.
- (17) Konieczka, S. Z.; Himmelpach, A.; Hailmann, M.; Finze, M. *Eur. J. Inorg. Chem.* **2013**, 134-146.
- (18) Valášek, M.; Štursa, J.; Pohl, R.; Michl, J. *Inorg. Chem.* **2010**, *49*, 10255-10263.
- (19) Knoth, W. H. *J. Am. Chem. Soc.* **1966**, *88*, 935-939.
- (20) Frisch MJ, Trucks GW, Schlegel HB, Scuseria GE, Robb MA, *et al* Gaussian 09, Revision A.02, Gaussian, Inc., Wallingford CT, 2009.
- (21) Scott, A. P.; Radom, L. *J. Phys. Chem.* **1996**, *100*, 16502-16513.
- (22) Foresman, J. B.; Keith, T. A.; Wiberg, K. B.; Snoonian, J.; Frisch, M. J. *J. Phys. Chem.* **1996**, *100*, 16098-16104.

- (23) Cossi, M.; Scalmani, G.; Rega, N.; Barone, V. *J. Chem. Phys.* **2002**, *117*, 43-54
and references therein.
- (24) Agilent, CrysAlis PRO, Agilent Technologies, Yarnton, England, 2012.
- (25) Sheldrick, G. M. *Acta Crystallogr. A* **2008**, *64*, 112–122.
- (26) Dolomanov, O. V.; Bourhis, L. J.; Gildea, R. J.; Howard, J. A. K.; Puschmann, H.
J. Appl. Crystallogr. **2009**, *42*, 339–341.
- (27) International Tables for Crystallography; Schmueli, U., Ed.; Springer: New York,
2006.

Chapter 4. High $\Delta\epsilon$ materials – synthesis and characterization

4.1 Introduction

Polar liquid crystals based on the monocarba-*closo*-borates substituted at the antipodal positions with one onium fragment (sulfonium, pyridinium or quinuclidinium) and one electrically neutral are attractive materials for electro-optical switching devices due to their high longitudinal dipole moment, and, consequently, sensitivity to the external electric field. Sulfonium derivatives of the [*closo*-1-CB₉H₁₀][−] anion substituted at B(10) vertex (type **2E**, see Table 1) are of special interest as they were previously shown to be compatible with nematic hosts, and to increase the $\Delta\epsilon$ of the hosts. Pyridinium zwitterions based on the [*closo*-1-CB₉H₁₀][−] and [*closo*-1-CB₁₁H₁₂][−] anions (Chapter 1, Table 1) are also attractive materials for electro-optical applications as they exhibit substantial dipole moment and reasonable solubility. Access to such materials, however, was hindered due to mechanistic issues in the former, and instability of the key intermediate in the latter.

The first section in this chapter provides details on the synthesis and investigation of thermal and electro-optical properties of polar materials based on sulfonium derivatives of the [*closo*-1-CB₉H₁₀][−] anion (type **2E**, see Chapter 1, Table 1). In the second section, properties of 1-pyridinium derivatives of the [*closo*-1-CB₉H₁₀][−] (type **2C**) and [*closo*-1-CB₁₁H₁₂][−] (type **1C**) anions were synthesized and their thermal and dielectric properties were measured and analyzed.

4.2 Investigation of high $\Delta\epsilon$ derivatives of the $[\textit{closo-1-CB}_9\text{H}_{10}]^-$ anion for liquid crystal display applications.

4.2.1 Description and contributions

In search of new materials possessing enhanced dielectric and mesogenic properties, we prepared and examined 18 esters **4[n]** and three derivatives **3[n]**. We performed extensive structure-property relationship studies, which includes the effect of the length of the alkyl chain on the mesogenic and electrooptical properties. Nine phenols and two alcohols were used for the synthesis of ester **4[n]**. Binary mixtures of selected esters were prepared in two nematic hosts. We determined thermal (transition temperatures and enthalpies) and electro-optical (ϵ_{\parallel} , ϵ_{\perp} , $\Delta\epsilon$, K_{11} , V_{th}) characteristics of **4[n]** and **3[n]**. It was found that all these derivatives improve dielectric anisotropy, $\Delta\epsilon$, of the nematic host due to significant longitudinal dipole moment and, consequently, large extrapolated $\Delta\epsilon$ values.

In this work, I was responsible for all aspects of the synthesis of esters **4[n]**, including intermediates such as acids, phenols, alcohols. Dr. Bryan Ringstrand synthesized three derivatives **3[n]**. My role was also to investigate thermal properties of all esters **4[n]** and to prepare and analyze thermal and electro-optical properties of binary mixtures of selected esters **4[n]** and derivatives **3[n]** in two nematic hosts. I also determined electro-optical parameters of the esters and their virtual temperatures based on the collected data. Experimental data was supported by quantum mechanical calculations performed by Prof. Piotr Kaszynski.

In the following chapter the entire text of the manuscript is included for consistency of the narrative, however, the experimental section contains only experiments performed by me.

4.2.2 The manuscript

Reproduced by permission of the Royal Society of Chemistry
Pecyna, J.; Ringstrand, B.; Bremmer, M.; Kaszynski, P. *J. Mater. Chem.* **2014**, *2*, 2956-2964.
Copyright 2014 Royal Society of Chemistry. Available online:
<http://pubs.rsc.org/en/content/articlelanding/2014/te/c4tc00230j>

4.2.2.1 Introduction

Polar liquid crystals and polar compounds compatible with nematic materials are important for adjusting dielectric anisotropy, $\Delta\epsilon$, and hence modifying electrooptical properties of materials used in liquid crystal display (LCD) technology.^{1,2} In this context, we have been investigating zwitterionic derivatives of the [*closo*-1-CB₉H₁₀]⁻ cluster (**A**, Fig. 1) as potential additives to liquid crystalline hosts. Recently, we demonstrated that polar derivatives, **1[6]**, **2[n]** and **3[6]a** (CHART I), of type **IA** (Fig. 1) significantly increase $\Delta\epsilon$ of a nematic host and have high virtual N-I transitions, $[T_{NI}]$, although they themselves rarely are mesogenic.^{3,4} Unfortunately, these compounds have limited solubility in nematic materials, and their high $\Delta\epsilon$ values were extrapolated from infinite dilutions. Subsequent investigation of zwitterionic esters of type **IIA** (Fig. 1), containing a sulfonium group (**4[5]a** and **4[5]b**, CHART I) or a pyridinium fragment (**5**,^{5,6} CHART I) revealed that they form nematic phases, have satisfactory solubility in nematic hosts, and possess $\Delta\epsilon$ between 30 and 40. For the 4-cyanophenol ester in series **5** a record high $\Delta\epsilon$ of 113 was measured in a nematic host.^{5,6}

In continuation of our search for new polar compounds with improved

mesogenic and dielectric properties, we investigated derivatives **3[n]** and esters **4[n]** (CHART I). Here, we report the synthesis and thermal and dielectric characterization of the two series of compounds in the pure form as well as in binary mixtures. Dielectric data is analyzed with the Maier-Meier relationship and augmented with DFT computational results.

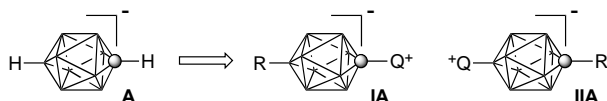


Figure 1. The structure of the $[closo-1-CB_9H_{10}]^-$ cluster (**A**) and its polar derivatives **IA** and **IIA**. Each vertex represents a BH fragment, the sphere is a carbon atom, and Q^+ stands for an onium group such as an ammonium, sulfonium or pyridinium.

CHART I

4.2.2.2 Results

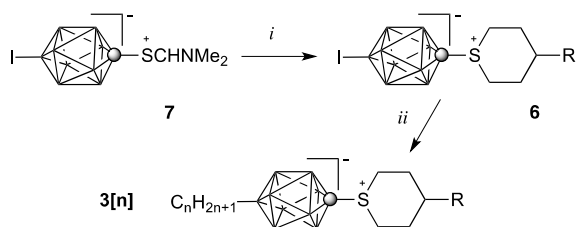
Synthesis

Compounds **3[3]b**, **3[5]b**, and **3[6]c** were prepared by Negishi coupling of the appropriate organozinc reagent with iodide **6**⁷ in the presence of Pd_2dba_3 and $[HPCy_3]^+[BF_4]^-$ in a THF/NMP mixture (Scheme 1).³ The iodides **6** were obtained from protected mercaptans **7**³ upon reactions with an appropriate dibromides **8**⁷ under hydrolytic conditions as described before.³

Aromatic esters **4[n]a–4[n]l** were prepared by reacting acid chlorides of sulfonium acids **9[n]** with appropriate phenols **10** in the presence of NEt_3 (Scheme 2). The two aliphatic esters, **4[3]e** and **4[3]f**, were obtained from the corresponding acid chloride and excess cyclohexanols **11** in neat pyridine. The sulfonium acids **9[3]**,⁸ **9[5]**,⁵ and **9[7]** were prepared by thermolysis of the methyl ester of diazonium acid **12**^{8,9} in the presence of the appropriate thiane **13[n]**⁸ followed by hydrolysis of the

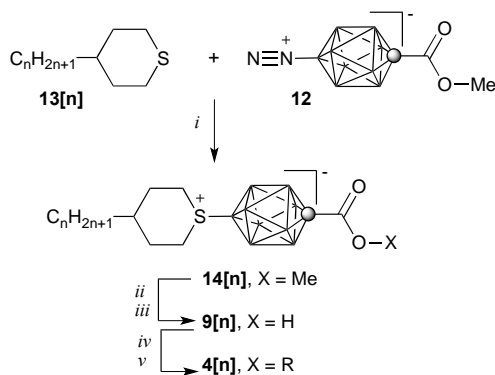
resulting methyl ester **14[n]** (Scheme 2).

Scheme 1.^a Synthesis of series **3[n]**



^a Reagents and conditions: *i*) $\text{RCH}(\text{CH}_2\text{CH}_2\text{Br})_2$ (**8**), $[\text{NMe}_4]^+[\text{OH}]^-$ or Cs_2CO_3 , MeCN ref.³; *ii*) $\text{C}_n\text{H}_{2n+1}\text{ZnCl}$, Pd_2dba_3 , $[\text{HPCy}_3]^+[\text{BF}_4]^-$, THF/NMP, rt, 12h, ~90%.

Scheme 2.^a Synthesis of esters **4[n]**

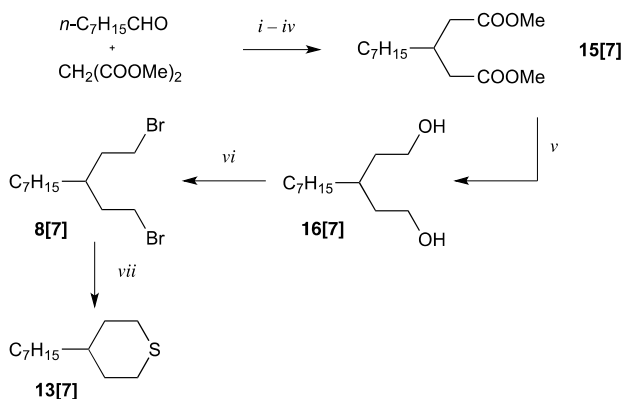


^a Reagents and conditions: *i*) 120 °C, 2h; *ii*) NaOH or KOH, MeOH, reflux; *iii*) HCl dil.; *iv*) $(\text{COCl})_2$, DMF (cat), CH_2Cl_2 ; *v*) ROH (**10**), NEt_3 , CH_2Cl_2 , rt, 12h or ROH (**11**), Pyridine, 90 °C.

Thiane **13[7]** was prepared in reaction of dibromide **8[7]** with Na_2S in EtOH/ H_2O (Scheme 3).⁸ Dibromide **8[7]**¹⁰ was obtained following a previously established procedure for dibromide **8[5]**.⁷ Thus, octanal and dimethyl malonate were converted to dimethyl 3-heptylglutarate (**15[7]**) in 4 steps and 65% overall yield

(Scheme 3). Subsequently, the ester was reduced to diol **16**[7] and converted to dibromide **8**[7].

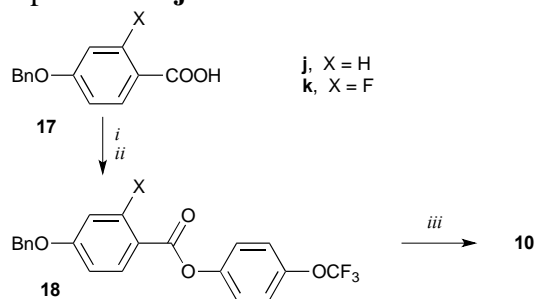
Scheme 3.^a Synthesis of thiane **13**[7]



^a Reagents and conditions: *i*) piperidine (cat), benzene, reflux; *ii*) HCl conc. reflux; *iii*) SOCl_2 , reflux; *iv*) MeOH, reflux; *v*) LiAlH_4 , THF; *vi*) HBr conc., H_2SO_4 , 120 °C; *vii*) $\text{Na}_2\text{S}\cdot 9\text{H}_2\text{O}$, EtOH, 50 °C, 1h, 89%.

Phenols **10j** and **10k** were prepared from the corresponding 4-benzyloxybenzoic acids **17**. The acids were converted into esters **18** after which the protecting benzyl group was removed under reductive conditions (Scheme 4).

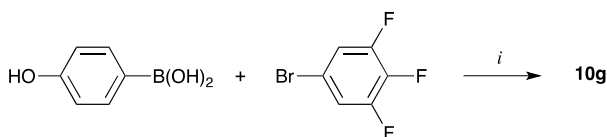
Scheme 4.^a Synthesis of phenols **10j** and **10k**.



^a Reagents and conditions: *i*) (COCl)₂, DMF (cat), CH₂Cl₂; *ii*) 4-HOC₆H₄OCF₃, NEt₃, CH₂Cl₂; *iii*) H₂, Pd/C, EtOH/THF or AcOEt/EtOH, rt, 12h, >90%.

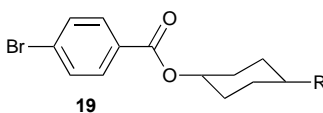
Phenol **10g**¹¹ was obtained using a ligand-free Suzuki coupling reaction¹² (Scheme 5). Phenols **10h**,¹³ **10i**,^{14,15} and **10l**¹⁶ were obtained as reported in the literature.

Scheme 5.^a Synthesis of phenol **10g**



^a Reagents and conditions: *i*) PdCl₂, K₂CO₃, EtOH/H₂O (1:1), rt, 1h, 79%.

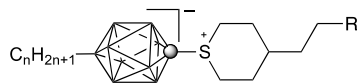
trans-4-Alkylcyclohexanols **11**¹⁷ were isolated from a mixture of stereoisomers by recrystallization of their 4-bromobenzoate esters **19**, followed by hydrolysis.

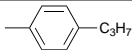
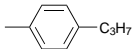



Thermal analysis

Transition temperatures and enthalpies of compounds **3[n]** and **4[n]** were determined by differential scanning calorimetry (DSC). Phase structures were assigned by optical microscopy in polarized light, and the results are shown in Tables 1–3.

Table 1. Transition temperatures ($^{\circ}\text{C}$) and enthalpies (kJ/mol, in italics) for **3[n]**^a

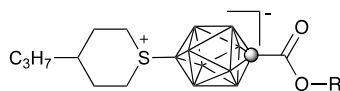


n	R	Cr ₁	Cr ₂
3	b 	Cr ₁ 185 (3.0)	Cr ₂ 224 (20.5) I
5	b 	Cr ₁ 189 (5.2)	Cr ₂ 199 (13.9) I
6	a $-\text{CH}_2\text{CH}_3$	Cr ₁ ^b 66 (21.9)	Cr ₂ 209 (10.9) I ^c
6	c 	Cr ₁ 230 (9.8)	Cr ₂ 253 (11.6) I

^a Determined by DSC (5 K min^{-1}) on heating: Cr – crystal, N – nematic, I – isotropic. ^b Additional Cr–Cr transition at $133 \text{ }^{\circ}\text{C}$ (14.6). ^c Ref.³

Compounds in series **3[n]** display only crystalline polymorphism and melt at or above $200 \text{ }^{\circ}\text{C}$, which is consistent with behavior of the previously reported derivative **3[6a]**.³ Extension of the sulfonium substituent in **3[6a]** by the cyclohexylethyl fragment in **3[6c]** increased the melting point by 44 K. Analogous comparison of **3[3b]** and **3[5b]** shows that extension of the alkyl group at the B(10) position by two methylene groups lowered the melting point by 25 K. Thus, in contrary to expectations, elongation of the core in **3[6a]** did not induce mesogenic behavior or reduce the melting point.

Table 2. Transition temperatures ($^{\circ}\text{C}$) and enthalpies (kJ/mol, in italics) for **4[3]**^a



R		
b		Cr 111 (29.3) (N 96 (1.1)) I ^b [N 19] ^c
c		Cr 135 (31.6) I
d		Cr ₁ 102 (6.3) Cr ₂ 140 (21.0) I [N -34] ^c [N 21] ^d
e		Cr ₁ 140 (3.2) Cr ₂ 158 (19.9) I [N -1] ^c [N -4] ^d
f		Cr ₁ 101 (2.6) Cr ₂ 137 (15.7) I
g		Cr 225 (40.8) I
h		Cr 187 (36.4) N 231 (0.7) I [N 161] ^d
i		Cr 175 (27.7) N 201 (3.8) I
j		Cr ^e 160 (23.7) N 244 (1.3) I
k		Cr ^f 183 (29.9) N 234 (1.7) I
l		Cr 183 (36.1) N 278 (1.5) I [N 331] ^d

^a Determined by DSC (5 K min^{-1}) on heating: Cr – crystal, N – nematic, I – isotropic. ^b Ref.⁸. ^c Virtual $[T_{\text{NI}}]$ obtained in **CinnCN**; typical error about $\pm 5 \text{ K}$. ^d Virtual $[T_{\text{NI}}]$

obtained in **CI Ester**; typical error about ± 2 K. ^e Cr–Cr transition at 137 °C (27.6); another crystalline polymorph melts at 165 °C. ^f Cr–Cr transitions at 81 °C (18.2 kJ/mol).

TABLE 3

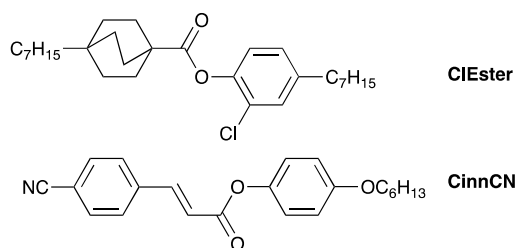
Esters in series **4[3]** generally have lower melting points than compounds in series **3[n]** and some exhibit nematic behavior. Among the single-ring phenol and alcohol derivatives, **4[3]b–4[3]f**, only the 4-butoxyphenol ester **4[3]b** displays a monotropic nematic phase and has the lowest melting point in the entire series (111 °C, Table 2). Extension of the phenol core by another ring generally increases the melting point, and also induces nematic behavior. The only exception is the 3,4,5-trifluorophenol derivative **4[3]d**, in which the addition of the benzene ring does increase the melting point by 85 K in **4[3]g** but fails to induce a mesophase. However, another biaryl derivative, phenylpyrimidinol ester **4[3]h** with a terminal hexyl group, does exhibit a 44 K wide nematic phase. Insertion of a $-\text{C}_6\text{H}_4\text{COO}-$ fragment into the 4-trifluoromethoxyphenyl ester **4[3]c** only moderately increases the melting point (by 25 K) in **4[3]j** and induces a wide-range enantiotropic nematic phase ($T_{\text{NI}} = 244$ °C) along with rich crystalline polymorphism. Substitution of a lateral fluorine into the benzoate fragment of **4[3]j** lowered the nematic phase stability by 10 K, and, contrary to expectations, markedly increased the melting temperature in **4[3]k**. Finally, insertion of a fluorophenylethyl fragment into the cyclohexyl ester **4[3]f** increased the melting point by 38 K and induced a 26 K wide nematic phase in **4[3]i**. Similar insertion of a fluorinated biphenylethyl fragment into **4[3]f** resulted in appearance of a nematic phase in **4[3]l** ($T_{\text{NI}} = 278$ °C).

The effect of alkyl chain extension at the thiane ring on thermal properties was

investigated for select esters **4[3]** (Table 3). Thus, extending the C₃H₇ chain in **4[3]b** to C₅H₁₁ in **4[5]b** lowered the melting point by 10 K, and had no impact on nematic phase stability. Further extension of the terminal chain to C₇H₁₅ lowered T_{NI} by 4 K in **4[7]b**. The same alkyl chain extension in the phenylpyrimidinol ester **4[3]h** had little effect on the melting temperature, however, it lowered T_{NI} by 10 K in the pentyl analogue **4[5]h** and by an additional 22 K in the heptyl derivative **4[7]h**. More significant melting point reduction, by about 25 K, is observed in derivatives **4[3]c** and **4[3]j** upon extension of C₃H₇ to C₇H₁₅ in **4[7]c** and **4[7]j**, respectively. In addition, the chain extension in **4[3]j** lowered the T_{NI} by 18 K to 226 °C in **4[7]j**.

Binary mixtures

To assess the new materials for formulation of LCD mixtures, selected compounds were investigated as low concentration additives to nematic host **CI Ester**, which is an ambient temperature nematic characterized by a small negative $\Delta\epsilon$ of –0.56. In addition, solutions of 3 compounds in **CinnCN** were prepared to establish their virtual clearing temperatures [T_{NI}].



Analysis of **CI Ester** solutions demonstrated that most derivatives **3[n]** and **4[n]** dissolve in the isotropic phase in concentrations up to about 10 mol%. However, solutions stable at ambient temperature for at least 24 hr are limited to about 4-5 mol%. For instance, compound **4[3]c** forms stable 5.5 mol% solutions in **CI Ester**. On the other hand, compound **3[5]b** and ester **4[3]g** were found to be least soluble in

ClEster, and the latter precipitates even from a 1.3 mol% solution at ambient temperature after several hours. In contrast, **4[3]d**, the shorter analogue of **4[3]g** containing only one benzene ring, is soluble at a concentration of 3.0 mol%. Extending the alkyl chain at the thiane ring does not significantly improve solubility of the esters **4[n]** in **ClEster**. As might be expected, the most soluble compounds are those with more flexible fragments such as **4[3]i**, **4[3]j**, and **4[7]j**.

Thermal analysis of the binary mixtures established virtual N-I transition temperatures [T_{NI}] in both **ClEster** and **CinnCN** hosts by extrapolation of the mixture's N-I transition peak temperatures to pure additive (Fig. 2). Analysis of results in Table 2 demonstrates that extrapolated [T_{NI}] values are typically lower than those measured for pure compounds. This suggests phase stabilization in pure **4[n]** by dipole-dipole interactions. For instance, [T_{NI}] for pyrimidine derivative **4[3]h** is 70 K lower in **ClEster**, while for butoxyphenol **4[3]b**, [T_{NI}] is 77 K lower in **CinnCN**. The only exception is the five-ring mesogen **4[3]l** for which the extrapolated [T_{NI}] is 53 K higher than measured for the pure compound. Further analysis of the data demonstrates significant dependence of [T_{NI}] on the host for trifluorophenol derivative **4[3]d**, while for cyclohexanol ester **4[3]e** such dependence essentially is not observed.

In general, three-ring esters destabilize the host's nematic phase, whereas 4- and 5-ring derivatives stabilize the host's nematic phase.

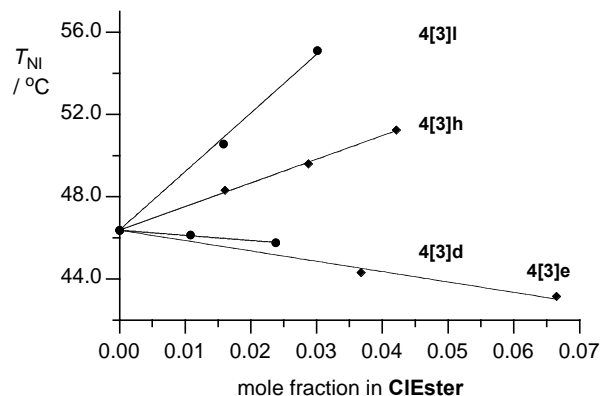


Figure 2. Plot of peak temperatures of the N-I transition vrs concentration in **CIEster**.

Dielectric measurements

Analysis of selected binary mixtures in **CIEster** revealed linear dependence of dielectric parameters on concentration, which, after extrapolation, established dielectric values for pure additives (Fig. 3). Analysis of the data in Table 4 demonstrates that for esters **4[5]a** and **4[3]e**, having no additional polar groups, extrapolated dielectric anisotropy, $\Delta\epsilon$, values are about 23. A lower $\Delta\epsilon$ value, less than 18, was estimated for **4[3]i** on the basis of $\Delta\epsilon < 0$ for its 3 mol% solution in **CIEster**. Substituting a polar group, such as OCF_3 (in **4[3]c**) or three fluorine atoms (in **4[3]d**) into the benzene ring substantially increases the extrapolated $\Delta\epsilon$ value to 70 and 60, respectively. Extension of **4[3]c** by insertion of a $-\text{C}_6\text{H}_4\text{COO}-$ fragment (in **4[3]j**) or a $-\text{C}_6\text{H}_3\text{FCOO}-$ fragment (in **4[3]k**) essentially does not affect the dielectric parameters of the material. Interestingly, by extending the length of the alkyl chain at the thiane ring in the former diester (**4[3]j**) by $-(\text{CH}_2)_4-$, $\Delta\epsilon$ increases in **4[7]j** by 6%. Incorporation of the pyrimidinyl substituent as a second polar group in **4[3]h** has a modest effect on dielectric anisotropy, and an extrapolated $\Delta\epsilon$ value of 50 was

obtained. It appears, however, that unlike for other esters, dielectric parameters for solutions of **4[3]h** deviate from linearity at higher concentrations.

Dielectric values for sulfonium **3[5]b** extrapolated from two concentrations (2.5 mol% and 3.7 mol%) in **ClEster** are modest and about half of those previously obtained at infinite dilution for the **3[6]a** analogue, which indicates significant aggregation of the additive in solutions.

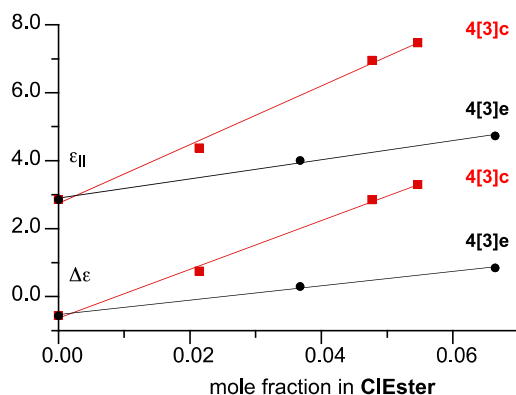


Figure 3. Dielectric parameters of binary mixtures of **4[3]e** (black) and **4[3]c** (red) in **ClEster** as a function of concentration.

Analysis of dielectric data

Dielectric parameters extrapolated for pure additives were analyzed using the Maier-Meier relationship (eq 1),^{18,19} which includes molecular and phase parameters.²⁰ Using experimental $\epsilon_{||}$ and $\Delta\epsilon$ values and DFT-calculated parameters μ , α , and β (Table 5), equations 2 and 3 are used to calculate the apparent order parameter, S_{app} ,²⁰ and Kirkwood factor, g (Table 4). The effect of the additive was ignored in the determination of field parameters F and h in equations 2 and 3; F and h were calculated using the experimental dielectric and optical data for pure **ClEster** host.^{21,22}

$$\Delta\varepsilon = \frac{NFh}{\varepsilon_0} \left\{ \Delta\alpha - \frac{F\mu_{eff}^2}{2k_B T} (1 - 3\cos^2\beta) \right\} S \quad \text{eq 1}$$

$$S = \frac{2\Delta\varepsilon\varepsilon_0}{NFh[2\Delta\alpha + 3\bar{\alpha}(1 - 3\cos^2\beta)] - 3(\bar{\varepsilon} - 1)\varepsilon_0(1 - 3\cos^2\beta)} \quad \text{eq 2}$$

$$g = \frac{[(\varepsilon_{\parallel} - 1)\varepsilon_0 - \bar{\alpha}NFh - \frac{2}{3}\Delta\alpha NFhS]3k_B T}{NF^2 h\mu^2 [1 - (1 - 3\cos^2\beta)S]} \quad \text{eq 3}$$

The molecular electric dipole moment, μ , and polarizability, α , required for the Maier-Meier analysis were obtained at the B3LYP/6-31G(d,p) level of theory in the dielectric medium of **ClEster**.²² While molecules in series **3[n]** are essentially conformationally stable with a strong preference for the *trans* isomer in the diequatorial form,⁵ sulfonium esters **4[n]** exist as a dynamic mixture of interconverting stereoisomers *trans* and *cis* in about 4:1 ratio (Fig. 4).⁵ Therefore, their molecular parameters were obtained as a weighted sum of values calculated for the two stereoisomers **4[n]-trans** and **4[n]-cis** and the composite numbers for **4[n]** are shown in Table 5.²²

Table 4. Extrapolated experimental (upper) and predicted (lower in italics) dielectric data and results of Maier-Meier analysis for selected compounds. ^a

Compound d	ε_{\parallel}	ε_{\perp}	$\Delta\varepsilon$	$\Sigma_{\alpha\pi\pi}$	γ
3[5]b	46	9	37	0.69	0.25
	<i>84.9</i>	<i>15.9</i>	<i>69.0</i>	<i>0.65</i> <i>b</i>	<i>0.50</i> <i>b</i>
3[6]a ^c	84	23	61	0.52	0.49
	<i>95.2</i>	<i>18.2</i>	<i>77.0</i>	<i>0.65</i> <i>b</i>	<i>0.50</i> <i>b</i>

4[5]a ^d	35.0	9.7	25.3	0.60	0.57
	32.6	8.2	24.4	0.65 <i>b</i>	0.50 <i>b</i>
4[3]c	87	17	70	0.62	0.77
	58.5	11.3	47.2	0.65 <i>b</i>	0.50 <i>b</i>
4[3]d	78	18	60	0.58	0.61
	68.2	13.0	55.2	0.65 <i>b</i>	0.50 <i>b</i>
4[3]e	32	11	21	0.51	0.55
	32.6	8.1	24.5	0.65 <i>b</i>	0.50 <i>b</i>
4[3]g	<i>e</i>	<i>e</i>	<i>e</i>	—	—
	59.5	11.4	48.1	0.65 <i>b</i>	0.50 <i>b</i>
4[3]h	61	11	50	0.68	0.69
	44.1	9.3	34.8	0.65 <i>b</i>	0.50 <i>b</i>
4[3]j	86	17	69	0.62	0.73
	61.8	11.5	50.3	0.65 <i>b</i>	0.50 <i>b</i>
4[7]j	89	15	74	0.67	0.78
	56.8	10.9	45.9	0.65 <i>b</i>	0.50 <i>b</i>
4[3]k	87	16	71	0.63	0.67
	67.4	12.0	55.4	0.65 <i>b</i>	0.50 <i>b</i>
4[3]l	<i>f</i>	<i>f</i>	<18 ^f	—	—
	25.4	7.6	17.8	0.65 <i>b</i>	0.50 <i>b</i>

4[3]m	^e	^e	^e	–	–
	99.3	17.9	81.4	0.65	0.50
				_b	_b

^a Values predicted for assumed $\Sigma_{\alpha\pi\pi} = 0.65$ and $g = 0.5$. For details see text and the ESI. Typical error of experimental extrapolated dielectric parameters ± 1 . ^b Assumed value. ^c Experimental data from ref ³. ^d Experimental data from ref ⁵. ^e Not measured; see text. ^f $\Delta\varepsilon < 0$ for a 3.0 mol% mixture.

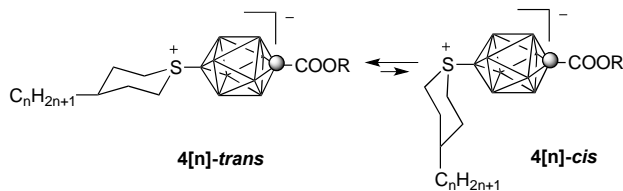


Figure 4. Interconversion of the *trans* and *cis* isomers of ester **4[n]**.

Results in Table 5 demonstrate that replacement of the pentyl chain in **3[6]a** with the 4-propylphenethyl group in **3[5]b** essentially has no effect on the molecular dipole moment ($\mu \approx 16.5$ D), however it increases anisotropy of polarizability by about 50% from $\Delta\alpha = 24.8 \text{ \AA}^3$ in **3[6]a** to $\Delta\alpha = 36.2 \text{ \AA}^3$ in **3[5]b**.

The dipole moment of esters **4[n]** with a non-polar alcohol and phenol (e.g. **4[3]a** and **4[3]e**, Table 5) is about 6 D lower than for compounds in series **3[n]**. It can be increased by introduction of additional polar groups into the molecular structure of **4[n]**. Hence, replacement of the pentyl chain in **4[3]a** with a polar group, such as OCF_3 (**4[3]c**), 3 fluorine atoms (**4[3]d**), or CN (**4[3]m**, CHART I) increases the longitudinal dipole moments by 3.5 D, 4.2 D and 6.7 D, respectively. Extending the molecular core in ester **4[3]d** by another benzene ring in **4[3]g** has negligible effect on the dipole moment, but it does increase anisotropy of polarizability by about 50% from $\Delta\alpha = 30.4 \text{ \AA}^3$ in the former to $\Delta\alpha = 47.6 \text{ \AA}^3$ in the latter with a modest increase

in average polarizability α (~ 25%). Similar extension of **4[3]c** with a weakly polar – C₆H₄COO– fragment in **4[3]j** increases the longitudinal dipole moment by 2.2 D and significantly increases $\Delta\alpha$ (53%) and α (28%). Placement of a fluorine atom on the – C₆H₄COO– group in **4[3]j** further increases the dipole moment in **4[3]k** by 1 D, with a minimal impact on polarizability.

Table 5. Calculated molecular parameters for selected compounds. ^a

Compound	$\mu_{ }$ /D	μ_{\perp} /D	μ /D	β^b /°	$\Delta\alpha$ /Å ³	α_{avg} /Å ³
3[5]d	16.3	2.38	16.5	8.3	36.1	62.4
b	9		7		8	0
3[6]a	16.1	2.95	16.3	10.4	24.8	53.3
	0		7		4	4
4[3]a	10.3	2.42	10.6	13.2	36.4	61.3
	9		6		5	2
4[5]a	10.3	2.96	10.7	16.1	37.5	65.0
	0		2		0	5
4[3]c	13.9	1.95	14.1	7.9	32.9	53.9
	9		2		1	2
4[3]d	14.6	2.16	14.8	8.4	30.4	51.5
	6		1		9	4
4[3]e	9.77	2.64	10.1	15.1	27.0	56.8
			2		2	3
4[3]g	14.7	1.90	14.8	7.1	47.6	64.1
	7		9		0	9
4[3]h	12.9	2.33	13.1	10.2	57.7	75.8
	4		4		4	6
4[3]j	16.1	1.68	16.2	5.9	50.2	69.0
	5		4		3	8

4[7]j	16.1	2.05	16.2	7.2	52.1	76.5
	6		9		2	9
4[3]k	17.1	0.67	17.1	2.2	52.7	69.7
	6		8		3	7
4[3]l	10.5	4.13	11.3	21.4	61.4	89.2
	6		4		7	1
4[3]m	17.1	2.25	17.3	7.5	39.1	54.8
	8		3		4	6

^a Obtained at the B3LYP/6-31G(d,p) level of theory in **ClEster** dielectric medium. For esters **4[n]** calculated for an average molecule at the equilibrium (*[cis]* = 21 mol%). For details see text and the ESI. ^b Angle between the net dipole vector μ and $\mu_{||}$.

The longitudinal dipole moment in esters **4[n]** was also increased by incorporation of a pyrimidine fragment; compounds possessing such a fragment are known to exhibit substantial dielectric anisotropies.²³ Thus, the ester of 2-(4-hexylphenyl)pyrimidin-5-ol, derivative **4[3]h**, has a calculated dipole moment $\mu = 13.14$ D, which is about 2.5 D higher than that of 4-pentylphenol **4[3]a**.

Lateral fluorination has no effect on the magnitude of the longitudinal molecular dipole moment component, $\mu_{||}$. Thus, results for **4[3]l** show that $\mu_{||}$ remains nearly the same as in the 4-pentylphenol ester **4[3]a**. However, the transverse component, μ_{\perp} , of the molecular dipole moment increases by 1.7 D, changing the orientation of the net dipole moment vector with respect to the main molecular axis from $\beta = 13.1^{\circ}$ in **4[3]a** to $\beta = 21.3^{\circ}$ in **4[3]l**.

Analysis of the computational results for the **4[3]-trans** isomers shows that, with the exception of **4[3]l**, the net dipole moment is nearly parallel with the long molecular axis, and the angle β ranges from 2° in **4[3]k** to 14° in **4[3]e** (avrg 7.8°

$\pm 3.7^\circ$). In the **4[3]-cis** isomers the angle β is larger by an average of $4.6^\circ \pm 1.7^\circ$ relative to the *trans* analogues. The molecular shape also affects anisotropy of polarizability $\Delta\alpha$, which is larger for the linear **4[3]-trans** molecules than for the bent **4[n]-cis** analogues by an average of $4.6 \pm 0.5 \text{ \AA}^3$.

The effectiveness of these compounds as high $\Delta\epsilon$ additives to **CI Ester** was investigated using the Maier-Meier formalism. Following a frequently used approach in designing of polar liquid crystals, the analysis initially assumed the order parameter of the additives to be the same as for the **CI Ester** host ($S = 0.65$), and Kirkwood factor (g) was set at 0.5.^{24,25} Results in Table 4 demonstrate that esters **4[n]** of non-polar phenols or alcohols exhibit expected $\Delta\epsilon$ values of about 24 (**4[5]a** and **4[3]e**). The lowest $\Delta\epsilon$ value of 17.8 is predicted for **4[3]l**, which is the largest molecule investigated in this series. This low value is due, in part, to the low number of molecules in the unit volume (low N number).

Esters of phenols with polar substituents are expected to have higher $\Delta\epsilon$ values. Thus, OCF_3 , F, and additional COO groups enhance the longitudinal dipole moment, which results in $\Delta\epsilon$ of about 50 (e.g. **4[3]c**, **4[3]d**, and **4[3]j**). A particularly large $\Delta\epsilon$ of 81 is predicted for ester **4[3]m** containing a CN group (CHART I). Surprisingly, the least effective dipole moment booster is the pyrimidine fragment in **4[3]h**, with a predicted relatively low $\Delta\epsilon$ of 35.

Compounds in series **3[n]** have predicted higher $\Delta\epsilon$ values (~ 70) than those for esters **4[n]**. However, these values are observed only at infinitely low concentrations. At higher concentration (~ 2 mol%) molecular aggregation significantly reduces $\Delta\epsilon$.

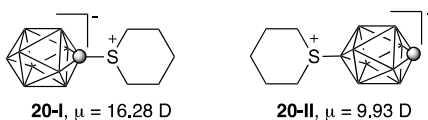
Experimental $\Delta\epsilon$ for **4[n]** are in general agreement with theoretical predictions,

mainly due to fairly high and uniform S_{app} values. Analysis of data in Table 4 demonstrates that experimental S_{app} of 0.61 ± 0.02 for the compounds are comparable with the order parameter of **ClEster** ($S = 0.65$). The only exceptions are **4[3]e** ($S_{\text{app}} = 0.51$), **4[3]h** ($S_{\text{app}} = 0.68$), and **4[7]j** ($S_{\text{app}} = 0.67$). These outlying S_{app} values for the first two compounds are consistent with the extreme virtual clearing temperatures, $[T_{\text{NI}}] = -4$ °C for **4[3]e** and $[T_{\text{NI}}] = 161$ °C for **4[3]h**, and demonstrate low compatibility of the former (**4[3]e**) and higher compatibility of the latter (**4[3]h**) with the host.

The Kirkwood parameter, g , has a broader range for esters **4[n]** between 0.55 for **4[3]e** and 0.78 for **4[7]j** and reflects different degrees of molecular association of the additive in solutions. In general, the observed values for g are higher than that initially assumed ($g = 0.5$). Perhaps most gratifying is that compounds **4[3]j**, **4[7]j**, and **4[3]k** with the highest values of $|\mu|$ show little association ($g = 73$, 78 , and 67 , respectively). Particularly interesting is the observed decreased association (increased g) upon alkyl chain extension in **4[n]j**. This demonstrates that molecular structure containing several polar groups placed in the semi-rigid core provide a successful design for preparation of high $\Delta\epsilon$ materials. On the other hand, analysis of compounds in series **3[n]** gives low g values (e.g. $g = 0.25$ for **3[5]b**), which shows that these materials are prone to excessive aggregation in solutions. This is also consistent with their low solubility and non-linear dependence of dielectric parameters versus concentration.

4.2.2.3 Discussion

The centerpiece of polar materials presented here is the sulfonium zwitterion **20** of the [*closo*-1-CB₉H₁₀]⁻ cluster with calculated ground-state electric dipoles of 16.3 D and 9.9 D for zwitterions **20-I** and **20-II**, respectively, in **ClEster** dielectric medium. The observed difference in the dipole moments originates from the strong polarization of electron density towards the carbon atom in the boron cluster. Elongation of the molecular core by substitution in the antipodal positions of the [*closo*-1-CB₉H₁₀]⁻ cluster and the thiane ring in **20-I** and **20-II** helps to induce liquid crystalline behavior and increases compatibility with nematic hosts. In general, compounds with a total of 2 or 3 rings in both series **3[n]** and **4[n]** do not form liquid crystalline phases; the only exception thus far is the 4-butoxyphenol ester **4[n]b**.



The calculated longitudinal dipole moment, $\mu_{||}$, in compounds **3[n]** is about 16 D and originates solely from **20-I**. Esters **4[n]** can achieve the same magnitude of $\mu_{||}$ by combining the moderate dipole moment of **20-II** with that of a polar substituent. Examples include diesters **4[n]j** and benzonitrile **4[3]m**, in which the net dipole moments are calculated to be 16.2 and 17.3 D, respectively (Table 5). In contrast to **3[n]**, compounds **4[n]** with several polar groups exhibit lower melting points, higher solubility in nematic hosts, and display mesogenic behavior. These qualities are quantified in the Maier-Meier analysis and reflected in high order, S_{app} , and Kirkwood, g , parameters, as shown for diesters **4[n]j** and **4[3]k** (Table 4).

Results in Table 4 indicate that small polar compounds are more effective additives due to their higher density of dipoles in the unit volume (larger number density N). For instance, ester **4[3]c** and its “extended” analogue diester **4[3]j** have essentially the same experimental dielectric parameters ($\Delta\epsilon \approx 70$) in spite of a larger dipole moment in the latter by about 2 D (Table 5). Benzonitrile derivative **4[3]m**, although not prepared in this investigation, is expected to exhibit a relatively large dielectric anisotropy, on the basis of its small size and large dipole moment.

Finally, it should be emphasized that analysis of experimental dielectric data using the Maier-Meier formalism provides informative insight into the behavior of additives in nematic solutions and has become an important tool in our investigation of polar compounds.²⁰

4.2.2.4 Conclusions

We have reported a diverse library of two series of polar compounds derived from an inorganic boron cluster, which act as effective additives to nematic materials for modulating dielectric anisotropy, $\Delta\epsilon$, and hence electrooptical properties. Compounds **3[n]** do not display liquid crystalline behavior or enhanced solubility even with elongated molecular cores up to 3 rings. However, they have high extrapolated $\Delta\epsilon$ values, but are hampered by limited solubility in nematic materials. On the other hand, esters **4[n]** have significantly improved compatibility with nematic hosts and exhibit liquid crystalline behavior. However, compounds with a total of 2 or 3 rings in **4[n]** generally do not form liquid crystalline phases. Esters **4[n]** have more modest extrapolated $\Delta\epsilon$ values due to smaller zwitterion’s dipole moment, but incorporation of additional polar substituents into the molecular structure can increase

$\Delta\epsilon$ values, while maintaining solubility on the order of several mol%. The most effective additives for increasing $\Delta\epsilon$ of **CI Ester** appear to be **4[3]c** and **4[n]j**. These materials exhibit good compatibility with the host (reasonable solubility, high g and S_{app} values) and a large $\Delta\epsilon$ of about 70.

Additional structure-property relationship studies are needed to further increase compatibility of these polar compounds with nematic hosts. Enhanced solubility would make these classes of compounds, especially esters **4[n]**, more useful as additives in formulation of LCD mixtures.

4.2.2.5 Computational details

Quantum-mechanical calculations were carried out using Gaussian 09 suite of programs.²⁶ Geometry optimizations for unconstrained conformers of **3[5]b**, **3[6]a**, and **4[n]** with the most extended molecular shapes were undertaken at the B3LYP/6-31G(d,p) level of theory using default convergence limits. Dipole moments and exact electronic polarizabilities for **3[5]b**, **3[6]a**, and **4[n]** for analysis with the Maier-Meier relationship were obtained in **CI Ester** dielectric medium using the B3LYP/6-31G(d,p)//B3LYP/6-31G(d,p) method and the PCM solvation model²⁷ requested with the SCRF(Solvent=Generic, Read) keyword and “eps=3.07” and “epsinf=2.286” parameters (single point calculations). The reported values for dipole moment components and dielectric permittivity tensors are at Gaussian standard orientation of each molecule (charge based), which is close to the principal moment of inertia coordinates (mass based).

4.2.2.6 Experimental Part

General. NMR spectra were obtained at 128 MHz (¹¹B), 100 MHz (¹³C), and 400

MHz (^1H) in CDCl_3 or CD_3CN . Chemical shifts were referenced to the solvent (^1H , ^{13}C) or to an external sample of $\text{B}(\text{OH})_3$ in MeOH (^{11}B , $\delta = 18.1$ ppm). Optical microscopy and phase identification were performed using a PZO “Biopolar” polarized microscope equipped with a HCS400 Instec hot stage. Thermal analysis was obtained using a TA Instruments 2920 DSC. Transition temperatures and enthalpies were typically obtained using small samples (~ 0.5 mg) and a heating rate of 5 K min^{-1} .

Preparation of Esters 4[n]. General procedure.

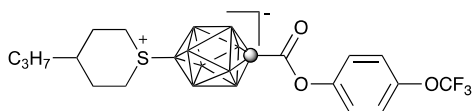
Method A. Esters of phenols. The sulfonium acid (0.16 mmol) was suspended in CH_2Cl_2 (1 mL) and was treated with $(\text{COCl})_2$ (3 eq) and anhydrous DMF (catalytic amount). The suspension began to bubble and became homogenous and was stirred vigorously for 30 min at rt. The light yellow solution was evaporated to dryness. The residue was redissolved in anhydrous CH_2Cl_2 (1 mL) and the appropriate phenol **10** (1.1 eq) and freshly distilled NEt_3 (3 eq) were added. The mixture was stirred at rt overnight. The reaction mixture was washed with 5% HCl , dried (Na_2SO_4) and evaporated to dryness. The product was isolated by column chromatography (SiO_2), the eluent was filtered through a cotton plug and the solvent evaporated to give the desired ester in about 60% yield. The resulting esters were purified further by repeated recrystallization.

Method B. Esters of cyclohexanols. The acid chloride derived from the sulfonium acid was generated as in Method A. The crude acid chloride, excess alcohol **11** (5 eq), and freshly distilled pyridine (5 eq) were stirred and heated for 3 days at $90 \text{ }^\circ\text{C}$, protected from moisture. At times, the reaction was cooled to rt, and minimal amount of anhydrous

CH₂Cl₂ was added to wash the sides of the flask. The product was purified as in Method A.

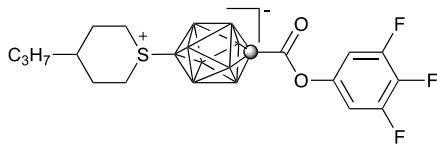
* NMR spectra of all esters **4[n]** recorded at ambient temperature show the presence of minor quantities (about 20%) of the *cis* isomer, (**4[n]-cis**) with characteristic signals at 2.08-2.15 (m), 2.28-2.35 (m) and 3.55-3.65 (m) ppm in the ¹H NMR spectra. The B(10) signals of the *cis* isomers are shifted upfield by about 1 ppm relative to the *trans* isomers in ¹¹B NMR spectra. In addition, in compounds **4[n]h** the pyrimidine ring of the *cis* isomer is shifted downfield by about 0.01 ppm relative to the *trans* isomer **4[n]h-trans**.

Ester **4[3]c**.



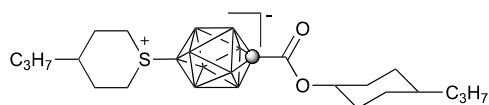
The ester was obtained in 65% yield, purified by column chromatography (CH₂Cl₂/hexane, 1:3) followed by recrystallization from *iso*-octane/toluene (2x) and then methanol/water (2x) to give a white crystalline solid: ¹H NMR (400 MHz, CDCl₃) δ 0.6-2.8 (br m, 8H), 0.96 (t, *J* = 5.6 Hz, 3H), 1.39-1.43 (m, 5H), 1.67-1.79 (m, 2H), 2.38 (br d, *J* = 11.6 Hz, 2H), 3.44 (br t, *J* = 10.4, 2H), 3.72 (br d, *J* = 10.0 Hz, 2H), 7.29 (d, *J* = 6.8 Hz, 2H), 7.37-7.40 (m, 2H); {¹H}¹¹B NMR (128 MHz, CDCl₃) δ -19.6 (4B), -14.0 (4B), 32.0 (1B). Anal. Calcd. for C₁₇H₂₈B₉F₃O₃S: C, 43.75; H, 6.05. Found: C, 43.94; H, 6.07.

Ester **4[3]d**.



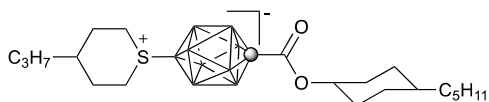
The ester was obtained in 58% yield, purified by column chromatography (CH_2Cl_2) followed by recrystallization from *iso*-octane/toluene (2x) and then methanol/water (2x) to give a white crystalline solid: ^1H NMR (400 MHz, CDCl_3) δ 0.6-2.8 (br m, 8H), 0.96 (t, $J = 5.6$ Hz, 3H), 1.39-1.43 (m, 5H), 1.67-1.79 (m, 2H), 2.33 (br d, $J = 11.2$ Hz, 2H), 3.44 (br t, $J = 10.4$ Hz, 2H), 3.71 (br d, $J = 10.8$ Hz, 2H), 7.07 (t, $J = 5.6$ Hz, 2H); $\{^1\text{H}\}^{11}\text{B}$ NMR (128 MHz, CDCl_3) δ -19.6 (4B), -13.9 (4B), 32.4 (1B). Anal. Calcd. for $\text{C}_{16}\text{H}_{26}\text{B}_9\text{F}_3\text{O}_2\text{S}$: C, 44.00; H, 6.00. Found: C, 44.03; H, 6.07.

Ester 4[3]e.



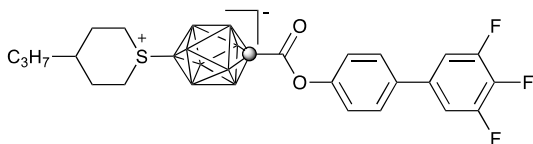
The ester was obtained in 77% yield, purified by column chromatography (CH_2Cl_2 /hexane, 1:2) followed by recrystallization from *iso*-octane/toluene (2x) to give a white crystalline solid: ^1H NMR (400 MHz, CDCl_3) δ 0.6-2.8 (br m, 8H), 0.89 (t, $J = 5.8$ Hz, 3H), 0.96 (t, $J = 5.6$ Hz, 3H), 1.05-1.12 (m, 2H), 1.18-1.23 (m, 2H), 1.28-1.32 (m, 3H), 1.39-1.43 (m, 5H), 1.47-1.59 (m, 2H), 1.67-1.79 (m, 2H), 1.83 (br d, $J = 10.4$ Hz, 2H), 2.18 (d, $J = 8.4$ Hz, 2H), 2.33 (br d, $J = 11.2$ Hz, 2H), 3.44 (br t, $J = 10.4$ Hz, 2H), 3.71 (br d, $J = 10.8$ Hz, 2H), 4.98-5.06 (m, 1H); $\{^1\text{H}\}^{11}\text{B}$ NMR (128 MHz, CDCl_3) δ -19.7 (4B), -14.3 (4B), 30.4 (1B). Anal. Calcd. for $\text{C}_{19}\text{H}_{41}\text{B}_9\text{O}_2\text{S}$: C, 52.96; H, 9.59. Found: C, 53.24; H, 9.72.

Ester 4[3]f.



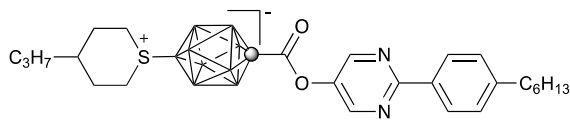
The ester was prepared by method B in 59% yield, purified by column chromatography (CH₂Cl₂) followed by recrystallization from *iso*-octane/toluene (2x) to give a white crystalline solid: ¹H NMR (400 MHz, CDCl₃) δ 0.6-2.8 (br m, 8H), 0.89 (t, *J* = 7.12 Hz, 3H), 0.95 (t, *J* = 6.7 Hz, 3H), 1.04-1.13 (m, 2H), 1.15-1.30 (m, 7H), 1.35-1.43 (m, 5H), 1.45-1.59 (m, 2H), 1.64-1.76 (m, 2H), 1.84 (d, *J* = 12.9 Hz, 2H), 2.18 (d, *J* = 9.0 Hz, 2H), 2.33 (br d, *J* = 12.8 Hz, 2H), 3.41 (br t, *J* = 12.8 Hz, 2H), 3.69 (br d, *J* = 12.9 Hz, 2H), 4.98-5.06 (m, 1H); {¹H}¹¹B NMR (128 MHz, CDCl₃) δ -19.8 (4B), -14.5 (4B), 31.0 (1B). Anal. Calcd. for C₂₁H₄₅B₉O₂S: C, 54.96; H, 9.88. Found: C, 55.08; H, 9.82.

Ester 4[3]g.



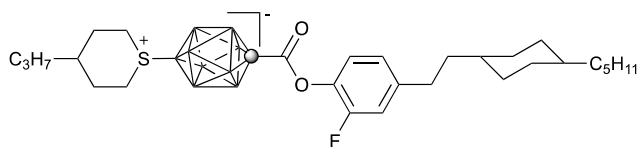
The ester was obtained in 64% yield, purified by column chromatography (CH₂Cl₂) followed by recrystallization from *iso*-octane/toluene (2x) and then CH₃CN (2x) to give a white crystalline solid: ¹H NMR (400 MHz, CDCl₃) δ 0.6-2.8 (br m, 8H), 0.96 (t, *J* = 6.5 Hz, 3H), 1.41-1.42 (m, 5H), 1.67-1.77 (m, 2H), 2.36 (br d, *J* = 14.0 Hz, 2H), 3.44 (br t, *J* = 10.4 Hz, 2H), 3.72 (br d, *J* = 12.7 Hz, 2H), 7.21 (t, *J* = 7.6 Hz, 2H), 7.43 (d, *J* = 8.6 Hz, 2H), 7.58 (d, *J* = 8.6 Hz, 2H); {¹H}¹¹B NMR (128 MHz, CDCl₃) δ -19.6 (4B), -13.9 (4B), 32.0 (1B). Anal. Calcd. for C₂₂H₃₀B₉F₃O₂S: C, 51.53; H, 5.90. Found: C, 51.70; H, 6.00.

Ester 4[3]h.



The ester was obtained in 66% yield, purified by column chromatography (CH_2Cl_2 /hexane, 2:1) followed by recrystallization from *iso*-octane/toluene (2x) to give a white crystalline solid: ^1H NMR (400 MHz, CDCl_3) δ 0.6-2.8 (br m, 8H), 0.89 (t, $J = 6.9$ Hz, 3H), 0.96 (t, $J = 6.6$ Hz, 3H), 1.25-1.45 (m, 9H), 1.65-1.79 (m, 6H), 2.41 (br d, $J = 11.2$ Hz, 2H), 2.69 (t, $J = 7.8$ Hz, 2H), 3.44 (br t, $J = 10.4$, 2H), 3.71 (br d, $J = 10.8$ Hz, 2H), 7.30 (t, $J = 8.2$ Hz, 2H), 8.36 (s, 2H); $\{^1\text{H}\}^{11}\text{B}$ NMR (128 MHz, CDCl_3) δ -19.5 (4B), -13.9 (4B), 32.9 (1B). Anal. Calcd. for $\text{C}_{26}\text{H}_{43}\text{B}_9\text{N}_2\text{O}_2\text{S}$: C, 57.30; H, 7.95; N, 5.14. Found: C, 57.44; H, 8.07; N, 5.19.

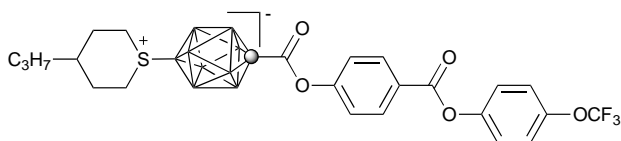
Ester 4[3]i.



The ester was obtained in 88% yield, purified by column chromatography (CH_2Cl_2) followed by recrystallization from *iso*-octane/toluene (2x) and then methanol with few drops of acetone (2x) to give a white crystalline solid: ^1H NMR (400 MHz, CDCl_3) δ 0.6-2.8 (br m, 8H), 0.88 (t, $J = 7.2$ Hz, 3H), 0.96 (t, $J = 6.5$ Hz, 3H), 1.14-1.16 (m, 4H), 1.21-1.29 (m, 8H), 1.39-1.41 (m, 5H), 1.50-1.54 (m, 2H), 1.69-1.73 (m, 8H), 2.39 (br d, $J = 12.9$ Hz, 2H), 2.63 (t, $J = 8.1$ Hz, 2H), 3.43 (br t, $J = 11.5$ Hz, 2H), 3.73 (br d, $J = 10.4$ Hz, 2H), 6.98 (d, $J = 8.1$ Hz, 1H), 7.03 (d, $J = 12.6$ Hz, 1H), 7.23 (d, $J =$

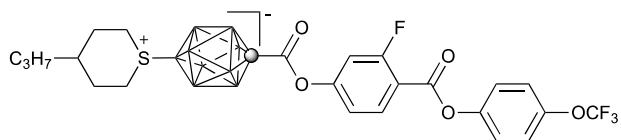
8.1 Hz, 1H); $\{^1\text{H}\}^{11}\text{B}$ NMR (128 MHz, CDCl_3) δ -19.6 (4B), -13.9 (4B), 32.0 (1B). Anal. Calcd. for $\text{C}_{29}\text{H}_{52}\text{B}_9\text{FO}_2\text{S}$: C, 59.94; H, 9.02. Found: C, 59.93; H, 8.91.

Ester 4[3]j.



The ester was obtained in 57% yield, purified by column chromatography (CH_2Cl_2) followed by recrystallization from *iso*-octane/toluene (2x) then CH_3OH (2x) to give a white crystalline solid: ^1H NMR (400 MHz, CDCl_3) δ 0.6-2.8 (br m, 8H), 0.94 (t, J = 6.8 Hz, 3H), 1.37-1.43 (m, 5H), 1.65-1.80 (m, 2H), 2.39 (br d, J = 12.2 Hz, 2H), 3.44 (br t, J = 12.8 Hz, 2H), 3.72 (br d, J = 12.6 Hz, 2H), 7.27 (s, 4H), 7.52 (d, J = 8.8 Hz, 2H), 8.29 (d, J = 8.8 Hz, 2H); $\{^1\text{H}\}^{11}\text{B}$ NMR (128 MHz, CDCl_3) δ -19.3 (4B), -13.7 (4B), 32.4 (1B). Anal. Calcd. for $\text{C}_{24}\text{H}_{32}\text{B}_9\text{F}_3\text{O}_5\text{S}$: C, 49.12; H, 5.50. Found: C, 49.20; H, 5.51.

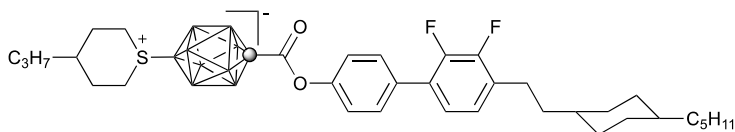
Ester 4[3]k.



The ester was prepared by method A in 66% yield, purified by column chromatography (CH_2Cl_2 then CH_3CN) followed by recrystallization from hexane/ethyl acetate (2x) to give a white crystalline solid: ^1H NMR (CD_3CN , 400 MHz) δ 0.6-2.8 (br m, 8H) 0.94 (t, J = 6.8 Hz, 3H). 1.30-1.43 (m, 5H), 1.62-1.80 (m, 2H), 2.34 (br d, J = 11.9 Hz, 2H), 3.43 (br t, J = 12.0 Hz, 2H), 3.78 (d, J = 12.0 Hz, 2H), 7.36-7.45 (m, 6H), 8.27 (t, J = 8.6 Hz, 1H); ^1H NMR (CDCl_3 , 400 MHz) δ 0.6-2.8 (br m, 8H) 0.96 (t, J = 6.5 Hz, 3H). 1.35-1.46 (m, 5H), 1.63-1.82 (m, 2H), 2.40 (d, J = 11.9 Hz, 2H), 3.44 (t, J =

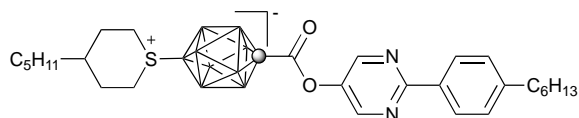
12.9 Hz, 2H), 3.73 (d, $J = 13.0$ Hz, 2H), 7.28-7.36 (m, 6H), 8.20 (t, $J = 8.4$ Hz, 1H); $\{^1\text{H}\}^{11}\text{B}$ NMR (CD_3CN , 128 MHz) δ -20.0 (4B), -14.2 (4B), 34.0 (1B); $\{^1\text{H}\}^{11}\text{B}$ NMR (CDCl_3 , 128 MHz) δ -19.5 (4B), -13.8 (4B), 32.6 (1B). Anal. Calcd. for $\text{C}_{24}\text{H}_{31}\text{B}_9\text{F}_4\text{O}_5\text{S}$: C, 47.66; H, 5.17. Found: C, 47.61; H, 5.32.

Ester 4[3]l.



The ester was obtained in 61% yield, purified by column chromatography (CH_2Cl_2) followed by recrystallization from *iso*-octane/toluene (2x) and then CH_3CN (2x) to give a white crystalline solid: ^1H NMR (400 MHz, CDCl_3) δ 0.6-2.8 (br m, 8H), 0.88 (t, $J = 7.2$ Hz, 3H), 0.96 (t, $J = 6.5$ Hz, 3H), 1.14-1.16 (m, 4H), 1.21-1.29 (m, 8H), 1.39-1.41 (m, 5H), 1.50-1.54 (m, 2H), 1.69-1.73 (m, 8H), 2.39 (br d, $J = 12.9$ Hz, 2H), 2.63 (t, $J = 8.1$ Hz, 2H), 3.43 (br t, $J = 11.5$ Hz, 2H), 3.73 (br d, $J = 10.4$ Hz, 2H), 6.99 (t, $J = 7.4$ Hz, 1H), 7.13 (t, $J = 6.7$ Hz, 1H), 7.42 (d, $J = 7.6$ Hz, 2H), 7.62 (d, $J = 8.6$ Hz, 2H); $\{^1\text{H}\}^{11}\text{B}$ NMR (128 MHz, CDCl_3) δ -19.5 (4B), -13.9 (4B), 32.1 (1B). Anal. Calcd. for $\text{C}_{35}\text{H}_{55}\text{B}_9\text{F}_2\text{O}_2\text{S}$: C, 62.26; H, 8.21. Found: C, 62.26; H, 8.11.

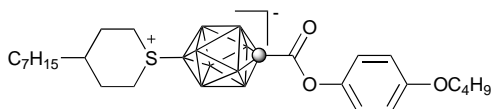
Ester 4[5]h.



The ester was obtained in 91% yield, purified by column chromatography (CH_2Cl_2) followed by recrystallization from hexane (2x) to give a white crystalline solid: ^1H NMR (400 MHz, CDCl_3) δ 0.6-2.8 (br m, 8H), 0.90 (t, $J = 7.0$ Hz, 3H), 0.92 (t, $J =$

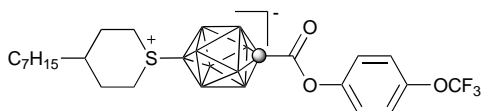
6.7 Hz, 3H), 1.30-1.40 (m, 13H), 1.67-1.77 (m, 6H), 2.40 (br d, $J = 12.5$ Hz, 2H), 2.69 (t, $J = 7.5$ Hz, 2H), 3.45 (br t, $J = 13.2$ Hz, 2H), 3.73 (br d, $J = 12.5$ Hz, 2H), 7.31 (d, $J = 8.2$ Hz, 2H), 8.35 (d, $J = 8.2$ Hz, 2H), 8.86 (s, 2H); $\{^1\text{H}\}^{11}\text{B}$ NMR (128 MHz, CDCl_3) δ -19.5 (4B), -13.8 (4B), 32.9 (1B). Anal. Calcd. for $\text{C}_{28}\text{H}_{47}\text{B}_9\text{N}_2\text{O}_2\text{S}$: C, 58.69; H, 8.27; N, 4.89. Found: C, 58.95; H, 8.19; N, 4.84.

Ester 4[7]b.



The ester was prepared in 81% yield, purified by column chromatography (CH_2Cl_2) followed by recrystallization from *iso*-octane/toluene (2x) and then CH_3OH (2x) to give a white crystalline solid: ^1H NMR (400 MHz, CDCl_3) δ 0.6-2.8 (br m, 8H), 0.90 (t, $J = 6.5$ Hz, 3H), 0.99 (t, $J = 7.4$ Hz, 3H), 1.25-1.38 (m, 13H), 1.49-1.51 (m, 2H), 1.72-1.80 (m, 4H), 2.37 (br d, $J = 12.5$ Hz, 2H), 3.43 (br t, $J = 11.3$ Hz, 2H), 3.71 (br d, $J = 12.5$ Hz, 2H), 3.98 (t, $J = 6.5$ Hz, 2H), 6.93 (d, $J = 9.0$ Hz, 2H), 7.23 (d, $J = 9.0$ Hz, 2H); $\{^1\text{H}\}^{11}\text{B}$ NMR (128 MHz, CDCl_3) δ -19.7 (4B), -14.2 (4B), 32.5 (1B). Anal. Calcd. for $\text{C}_{24}\text{H}_{45}\text{B}_9\text{O}_3\text{S}$: C, 56.41; H, 8.88. Found: C, 56.84; H, 8.89.

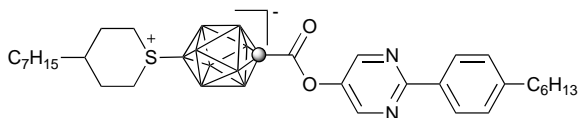
Ester 4[7]c.



The ester was obtained in 79% yield, purified by column chromatography (CH_2Cl_2) followed by recrystallization from *iso*-octane/toluene (2x) and then CH_3OH (2x) to give a white crystalline solid: ^1H NMR (400 MHz, CDCl_3) δ 0.6-2.8 (br m, 8H), 0.91 (t, $J = 6.3$ Hz, 3H), 1.30-1.39 (m, 11H), 1.70-1.77 (m, 4H), 2.49 (br d, $J = 13.9$ Hz,

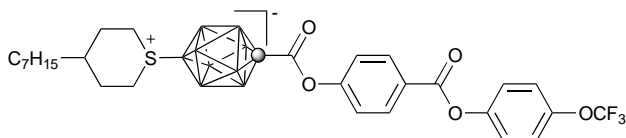
2H), 3.44 (br t, $J = 13.0$ Hz, 2H), 3.72 (br d, $J = 12.4$ Hz, 2H), 7.30 (d, $J = 8.6$ Hz, 2H), 7.39 (d, $J = 9.0$ Hz, 2H); $\{^1\text{H}\}$ ^{11}B NMR (128 MHz, CDCl_3) δ -19.7 (4B), -14.0 (4B), 32.4 (1B). Anal. Calcd. for $\text{C}_{21}\text{H}_{36}\text{B}_9\text{F}_3\text{O}_3\text{S}$: C, 48.24; H, 6.94. Found: C, 47.39; H, 6.96.

Ester 4[7]h.



The ester was obtained in 63% yield, purified by column chromatography (CH_2Cl_2) followed by recrystallization from *iso*-octane/toluene (2x) and then CH_3OH (2x) to give a white crystalline solid: ^1H NMR (400 MHz, CDCl_3) δ 0.6-2.8 (br m, 8H), 0.87-0.92 (m, 6H), 1.25-1.38 (m, 17H), 1.62-1.77 (m, 6H), 2.39 (br d, $J = 12.6$ Hz, 2H), 2.68 (t, $J = 7.6$ Hz, 2H), 3.44 (br t, $J = 13.1$ Hz, 2H), 3.72 (br d, $J = 12.9$ Hz, 2H), 7.31 (d, $J = 8.2$ Hz, 2H), 8.35 (d, $J = 8.2$ Hz, 2H), 8.86 (s, 2H); $\{^1\text{H}\}$ ^{11}B NMR (128 MHz, CDCl_3) δ -19.5 (4B), -13.8 (4B), 32.8 (1B). Anal. Calcd. for $\text{C}_{30}\text{H}_{51}\text{B}_9\text{N}_2\text{O}_2\text{S}$: C, 59.95; H, 8.55; N, 4.66. Found: C, 59.66; H, 8.41; N, 4.59.

Preparation of ester 4[7]j.

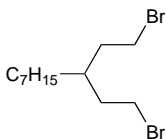


The ester was prepared by method A in 82% yield, purified by column chromatography (CH_2Cl_2) followed by recrystallization from *iso*-octane/toluene (2x) and then CH_3OH (2x) to give a white crystalline solid: ^1H NMR (400 MHz, CDCl_3) δ 0.6-2.8 (br m, 8H), 0.90 (t, $J = 6.6$ Hz, 3H), 1.30-1.39 (m, 11H), 1.70-1.77 (m, 4H), 2.49 (br d, $J = 14.2$ Hz, 2H), 3.44 (br t, $J = 12.7$ Hz, 2H), 3.71 (br d, $J = 12.0$ Hz, 2H), 7.29 (s, 4H),

7.52 (d, $J = 8.7$ Hz, 2H). 8.29 (d, $J = 8.7$ Hz, 2H); $\{^1\text{H}\} \text{ }^{11}\text{B}$ NMR (128 MHz, CDCl_3) δ -19.4 (4B), -13.7 (4B), 32.0 (1B). Anal. Calcd. for $\text{C}_{28}\text{H}_{40}\text{B}_9\text{F}_3\text{O}_5\text{S}$: C, 52.31; H, 6.27. Found: C, 52.48; H, 6.36.

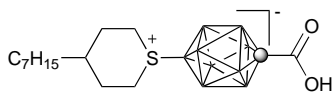
Intermediates

Preparation of 1,5-dibromo-3-heptylpentane (**8[7]**).²



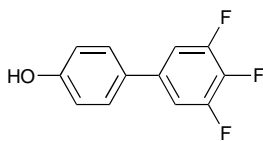
Following a general literature procedure,³ a biphasic mixture of the 3-heptylpentane-1,5-diol, 47% aqueous HBr (15 eq) and an equal volume of conc. H_2SO_4 (relative to HBr) was stirred at 120 °C overnight. The black reaction mixture was cooled to rt, diluted by the addition of half its volume of H_2O and extracted with CH_2Cl_2 . The organic layers were combined, dried (MgSO_4) and evaporated to leave black oil. The oil was passed through a short silica gel plug (hexanes) to give crude dibromide **8[7]** as a slightly brown oil. The dibromide was purified further by short-path distillation (135 °C, 0.7 mmHg) to give 15.4 g (54% yield) of **8[7]** as a colorless oil: ^1H NMR (400 MHz, CDCl_3) δ 0.88 (t, $J = 7.0$ Hz, 3H), 1.27 (m, 12H), 1.71-1.74 (m, 1H), 1.77-1.90 (m, 4H), 3.41 (t, $J = 7.3$ Hz, 4H); ^{13}C NMR (100 MHz, CDCl_3) δ 14.0, 22.6, 26.0, 29.2, 29.7, 31.2 (2C), 31.8, 32.4, 35.4, 36.6 (2C). Anal. Calcd. for $\text{C}_{14}\text{H}_{24}\text{Br}_2$: C, 43.93; H, 7.37. Found: C, 43.63; H, 7.38.

Preparation of sulfonium acid **9**[7].



The methyl ester **14**[7] (230 mg; 0.61 mmol) was hydrolyzed using KOH (0.17 g, 3.05 mmol) in CH₃OH (3 mL) under reflux overnight. The solvent was evaporated and 10% HCl (5 mL) was added. The solution was extracted with CH₂Cl₂ (3x10 mL). The extracts were dried (Na₂SO₄), evaporated and washed with hot hexane to give 193 mg (87% yield) of a white solid. The crude acid was recrystallized from *iso*-octane/toluene (2x) and then cold CH₃CN (2x) to give acid **9**[7] as a white crystalline solid: mp 175-176 °C; ¹H NMR (400 MHz, CDCl₃) δ major signals 0.5-2.8 (br m, 8H), 0.89 (t, *J* = 6.7 Hz, 3H), 1.25-1.37 (m, 13H), 1.65-1.78 (m, 2H), 2.38 (br d, *J* = 14.0 Hz, 2H), 3.42 (br t, *J* = 12.9 Hz, 2H), 2.69 (br d, *J* = 12.7 Hz, 2H) (*cis* isomer δ 2.09-2.15 (m), 2.28-2.35 (m), 3.52-3.64 (m)); {¹H} ¹¹B NMR (128 MHz, CDCl₃) δ -19.6 (4B), -14.0 (4B), 32.1 (1B). Anal. Calcd. for C₁₄H₃₃B₉O₂S: C, 46.35; H, 9.17. Found: C, 46.79; H, 9.15.

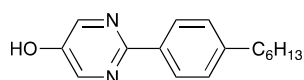
Preparation of phenol **10g**.⁴



The phenol was prepared via ligand-free Suzuki coupling⁵ by reacting 4-hydroxyphenylboronic acid (490 mg, 3.55 mmol) and 1-bromo-3,4,5-trifluorobenzene (500 mg, 2.37 mmol) in 50% EtOH (10 mL) in the presence of PdCl₂ (32.5 mg, 0.5 mol %) and K₂CO₃ (320 mg, 5.7 mmol). The reaction mixture was stirred for 1 hr at rt. The mixture was washed with brine (15 mL), extracted with diethyl ether (3x10 mL), dried (MgSO₄), concentrated under vacuum and the product was purified by column

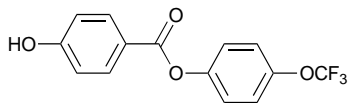
chromatography (EtOAc) to give 420 mg (79% yield) of the product that was further purified by recrystallization (EtOH/H₂O) to give **10g** as a white fluffy solid: mp 110.5 °C (lit.⁴ mp 237 °C); ¹H NMR (400 MHz, CDCl₃) δ 4.79 (s, 1H), 6.90 (d, *J* = 8.7 Hz, 2H), 7.08-7.16 (m, 2H), 7.38 (d, *J* = 8.7 Hz, 2H) [lit.⁴ ¹H NMR (CDCl₃) δ 4.90 (s, 1H), 6.91 (d, *J* = 8.4 Hz, 2H), 7.12 (t, *J* = 7.96 Hz, 2H), 7.38 (dd, *J* = 8.44 Hz, 2H)]; ¹³C NMR (100 MHz, CDCl₃) δ 110.4 (dd, *J*₁ = 15.8 Hz, *J*₂ = 5.9 Hz), 115.9, 128.1, 131.0, 136.8 (td, *J*₁ = 7.8 Hz, *J*₂ = 4.6 Hz), 138.8 (dt, *J*₁ = 249 Hz, *J*₂ = 15.4 Hz), 151.3 (ddd, *J*₁ = 247.6 Hz, *J*₂ = 9.9 Hz, *J*₃ = 4.2 Hz), 155.7.

Phenol 10h.⁶



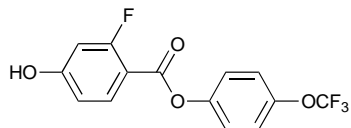
Mp 144-144.5 °C (lit.⁶ mp 126-128 °C); ¹H NMR (400 MHz, CD₃CN) δ 0.89 (t, *J* = 7.0 Hz, 3H), 1.28-1.40 (m, 6H), 1.65 (quint, *J* = 7.5 Hz, 2H), 2.67 (t, *J* = 7.7 Hz, 2H), 7.30 (d, *J* = 8.2 Hz, 2H), 7.6 (br s, 1H), 8.22 (d, *J* = 8.3 Hz, 2H), 8.42 (s, 2H); ¹H NMR (400 MHz, CDCl₃) δ 0.87 (t, *J* = 6.9 Hz, 3H), 1.22-1.40 (m, 6H), 1.63 (quint, *J* = 7.5 Hz, 2H), 2.65 (t, *J* = 7.7 Hz, 2H), 7.1 (br s, 1H), 7.27 (d, *J* = 8.6 Hz, 2H), 8.17 (d, *J* = 8.2 Hz, 2H), 8.41 (s, 2H); ¹³C NMR (100 MHz, CDCl₃) δ 14.1, 22.6, 28.9, 31.1, 31.7, 35.8, 127.5, 128.9, 134.0, 144.9, 145.5, 149.9, 157.4. Anal. Calcd. for C₁₆H₂₀N₂O: C, 74.97; H, 7.86; N, 10.93. Found: C, 74.71; H, 7.76; N, 10.74.

Preparation of phenol **10j**.



4-(Trifluoromethoxy)phenyl 4-benzyloxybenzoate (**18j**, 3.20 g, 8.24 mmol) was dissolved in a mixture of ethanol/THF (200 mL). Pd/C (10 %, 0.44 g) was added and H₂ was purged through the reaction mixture overnight. The reaction mixture was filtered and the solvent was evaporated to give 2.40 g (97% yield) of phenol **10j** as a white crystalline solid. Analytical sample of **10j** was prepared by recrystallization from *iso*-octane/toluene (2x): mp 146.5 °C; ¹H NMR (400 MHz, CDCl₃) δ 5.41 (br s, 1H), 6.93 (d, *J* = 8.8 Hz, 2H), 7.23-7.29 (m, 4H), 8.11 (d, *J* = 8.8 Hz, 2H); ¹³C NMR (100 MHz, CDCl₃) δ 115.5 (2C), 121.3, 122.0 (q), 122.1 (2C), 123.0 (2C), 132.6 (2C), 146.5, 149.1, 160.6, 164.9. Anal. Calcd. for C₁₄H₉F₃O₄: C, 56.39; H, 3.04. Found: C, 56.63; H, 3.03.

Preparation of phenol **10k**.

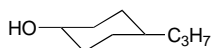


4-(Trifluoromethoxy)phenyl 4-benzyloxy-2-fluorobenzoate (**18k**, 252 mg, 0.62 mmol) was dissolved in a mixture of EtOAc and EtOH. Pd/C (10%, 66 mg) was added and H₂ was purged through the reaction for 12 hr. The reaction mixture was filtered and the solvent evaporated to give 190 mg (97% yield) of crude phenol **10k**. Analytical sample of **10k** was prepared by recrystallization from cold methanol to give a white crystalline solid: mp 172.5 °C; ¹H NMR (400 MHz, CD₃CN) δ 6.72 (dd, *J*₁ = 12.8 Hz, *J*₂ = 2.3 Hz, 1H), 6.80 (dd, *J*₁ = 8.8 Hz, *J*₂ = 2.4 Hz, 1H), 7.32 (d, *J* = 9.2 Hz, 2H), 7.39 (d, *J*

= 8.7 Hz, 2H), 8.00 (t, $J = 8.7$ Hz, 1H), 8.1 (br s, 1H). Anal. Calcd. for $C_{14}H_{18}F_4O_4$: C, 53.18; H, 2.55. Found: C, 53.30; H, 2.54.

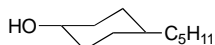
trans-4-Alkylcyclohexanol (11). 4-Bromobenzoate **19** was hydrolyzed in a solution of KOH in MeOH at 50 °C. Water was added and most MeOH was evaporated. The mixture was extracted with CH_2Cl_2 (3x), the extract was dried and evaporated and distilled to give the desired *trans*-alcohol **11**.

trans-4-Propylcyclohexanol (11e).⁷



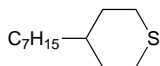
1H NMR (500 MHz, $CDCl_3$) δ 0.87 (t, $J = 7.7$ Hz, 3H), 0.92-0.97 (m, 2H), 1.13-1.25 (m, 5H), 1.30 (sext, $J = 5.9$ Hz, 2H), 1.37 (br s, 1H), 1.75 (d, $J = 12.0$ Hz, 2H), 1.95 (br d, $J = 10.2$ Hz, 2H), 3.50-3.58 (m, 1H); ^{13}C NMR (100 MHz, $CDCl_3$) δ 14.1, 19.9, 31.1, 35.1, 36.2, 38.8, 70.4.

trans-4-Pentylcyclohexanol (11f).^{7,8}



1H NMR (400 MHz, $CDCl_3$) δ 0.89 (t, $J = 7.2$ Hz, 3H), 0.89-0.98 (m, 2H), 1.13-1.35 (m, 11H), 1.75 (br d, $J = 11.4$ Hz, 2H), 1.93 (br d, $J = 12.4$ Hz, 2H), 3.48-3.58 (m, 1H).

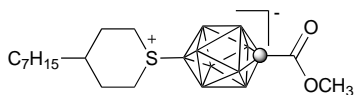
Preparation of 4-heptylthiane (13[7]).



Following an analogous procedure for **13[3]**,¹ to a solution of 1,5-dibromo-3-heptylpentane (**8[7]**, 15.4 g, 0.047 mol) in EtOH (100 mL) a solution of $Na_2S \cdot 9H_2O$ (16.9 g, 0.07 mol) in water (50 mL) was added dropwise during 1 h at 50 °C. The mixture was stirred at this temperature for 1 h, then refluxed for 1 h, and diluted with water. The

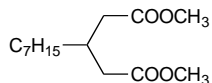
organic product was extracted with hexanes, the extract dried (Na_2SO_4) and the solvent evaporated. The yellow oily residue was passed through a silica gel plug (hexanes) to give 8.4 g (89% yield) of thiane **13[7]** as a colorless oil. Analytical sample of **13[7]** was obtained by short-path distillation (130 °C, 0.7 mm Hg): ^1H NMR (400 MHz, CDCl_3) δ 0.86 (t, $J = 7.1$ Hz, 3H), 1.18-1.35 (m, 15H), 1.96 (br d, $J = 12.1$ Hz, 2H), 2.54-2.67 (m, 4H); ^{13}C NMR (100 MHz, CDCl_3) δ 14.0, 22.6, 26.3, 28.7 (2C), 29.2, 29.7, 31.8, 34.2 (2C), 37.1, 37.3. Anal. Calcd. for $\text{C}_{12}\text{H}_{24}\text{S}$: C, 71.93; H, 12.07. Found: C, 71.85; H, 12.08.

Preparation of methyl ester **14[7]**.



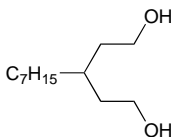
A solution of ester **12**^{9,10} (150 mg, 0.73 mmol) in thiane **13[7]** (5 mL) was heated at 120 °C for 1 hr. The solvent was removed under reduced pressure (110 °C, 0.7 mmHg), the residue was washed with hexane, and purified on a short silica gel plug (CH_2Cl_2 /hexane, 1:1) to give 241 mg (87% yield) of ester **14[7]** as an off-white solid. The ester was recrystallized from *iso*-octane (2x): mp 88 °C (DSC); ^1H NMR (400 MHz, CDCl_3) δ 0.5-2.8 (br m, 8H), 0.89 (t, $J = 6.6$ Hz, 3H), 1.25-1.42 (m, 13H), 1.65-1.77 (m, 2H), 2.37 (br d, $J = 12.6$ Hz, 2H), 3.40 (br t, $J = 13.4$ Hz, 2H), 3.69 (br d, $J = 12.7$ Hz, 2H), 4.02 (s, 3H), (minor signal for the *cis* isomer: δ 2.06-2.12 (m), 2.25-2.32 (m), 3.50-3.60 (m)); $\{^1\text{H}\}^{11}\text{B}$ NMR (128 MHz, CDCl_3) δ -19.8 (4B), -14.4 (4B), 31.2 (1B) (minor signal for the *cis* isomer: δ 29.4). Anal. Calcd. for $\text{C}_{15}\text{H}_{35}\text{B}_9\text{O}_2\text{S}$: C, 47.82; H, 9.36. Found: C, 48.09; H, 9.44.

Preparation of dimethyl 3-heptylglutarate (**15[7]**).



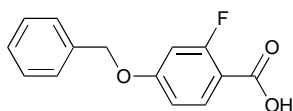
Following a procedure for **15[5]**,¹ a mixture of dimethyl malonate (45.8 g, 0.35 mol), octanal (20.5 g, 0.16 mol), benzene (50 mL), piperidine (0.85 mL) and NEt₃ (2.5 mL) was stirred at rt for 2 hr and then heated overnight under reflux. A Dean-Stark trap was used to collect water produced in the reaction. The mixture was washed with dilute HCl, dried and excess dimethyl malonate was removed under vacuum (up to 80 °C, 0.05 mmHg). The oily residue was heated overnight under reflux with conc. HCl (250 mL), the aqueous HCl acid was removed under reduced pressure and the oily residue was short-path distilled (150-170 °C, 1 mmHg) to give crude 3-heptylglutaric acid (33.1 g). Without further purification, the diacid was heated with SOCl₂ (42 mL) for 2 hr, excess SOCl₂ was removed under reduced pressure and the resulting dark acid chloride was heated under reflux with CH₃OH (200 mL) for 2 hr. Excess CH₃OH was evaporated and the crude diester **15[7]** was distilled (135 °C, 1 mmHg) to give 18.7 g (63% overall yield) of dimethyl 3-heptylglutarate (**15[7]**) as a colorless oil: ¹H NMR (400 MHz, CDCl₃) δ 0.86 (t, *J* = 7.1 Hz, 3H), 1.24-1.35 (m, 12H), 2.30-2.35 (m, 5H), 3.64 (s, 6H); ¹³C NMR (100 MHz, CDCl₃) δ 14.0, 22.5, 26.5, 29.0, 29.4, 31.7, 32.0, 33.5, 38.3(2C), 51.4(2C), 173.0(2C). Anal. Calcd. for C₁₄H₂₆O₄: C, 65.09; H, 10.14. Found: C, 64.94; H, 9.95.

Preparation of 3-heptylpentane-1,5-diol (**16[7]**).



Dimethyl 3-heptylglutarate (**15[7]**, 18.7 g, 0.10 mol) was reduced with LiAlH₄ (5.7 g, 0.15 mol) in anhydrous THF. The reaction mixture was carefully quenched with H₂O (30 mL) and then 2M KOH (20 mL). After 30 minutes, the white precipitate was removed by filtration and then washed with Et₂O (200 mL). The filtrate was dried (MgSO₄), filtered and evaporated to give 17.9 g (86% yield) of 3-heptylpentane-1,5-diol (**16[7]**) as a slightly yellow oil which was used without further purification: ¹H NMR (400 MHz, CDCl₃) δ 0.87 (t, *J* = 7.0 Hz, 3H), 1.22-1.32 (m, 12 H), 1.48-1.68 (m, 5H), 3.62-3.75 (m, 4H); ¹³C NMR (100 MHz, CDCl₃) δ 14.0, 22.6, 26.5, 29.2, 29.9, 31.1, 31.8, 34.5, 36.5(2C), 60.7(2C).

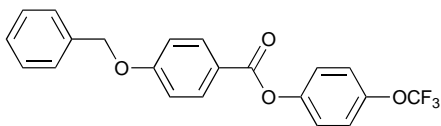
Preparation of 4-(benzyloxy)-2-fluorobenzoic acid (**17k**).



A mixture of 2-fluoro-4-hydroxybenzoic acid (500 mg, 3.20 mmol), potassium hydroxide (395 mg, 7.05 mmol) and benzyl bromide (603 mg, 3.52 mmol) in EtOH/H₂O (22 mL, 10:1) was heated under reflux for 20 hr. Aqueous potassium hydroxide (20%, 10 mL) was added and the mixture was heated under reflux for additional 2 hr. The reaction mixture was cooled, water was added, and the solution was acidified with 10% HCl. The precipitate was filtered and dried to give 530 mg (67% yield) of acid **17k** as an off-white solid. Analytical sample was prepared by recrystallization from *iso*-octane/toluene (2x) and then cold CH₃CN (2x) to give acid **17k** as colorless crystals: mp 168 °C; ¹H NMR

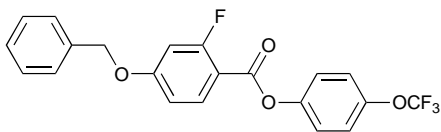
(400 MHz, CDCl₃) δ 5.12 (s, 2H), 6.74 (dd, $J_1 = 12.7$ Hz, $J_2 = 2.4$ Hz, 1H), 6.83 (dd, $J_1 = 8.8$ Hz, $J_2 = 2.4$ Hz, 1H), 7.34-7.42 (m, 5H), 7.98 (t, $J = 8.7$ Hz, 1H). Anal. Calcd. for C₁₄H₁₁FO₃: C, 68.29; H, 4.50. Found: C, 68.28; H, 4.42.

Preparation of 4-(trifluoromethoxy)phenyl 4-(benzyloxy)benzoate (18j).



4-Benzyloxybenzoic acid (**17j**, 2.0 g, 8.76 mmol) was suspended in anhydrous CH₂Cl₂ (15 mL) and was treated with (COCl)₂ (2.25 mL, 26.3 mmol) and anhydrous DMF (catalytic amounts). The suspension began to bubble and became homogenous and was stirred vigorously for 30 min at rt. The light yellow solution was evaporated to dryness. The residue was redissolved in anhydrous CH₂Cl₂ (15 mL) and the 4-trifluoromethoxyphenol (1.64 g, 9.20 mmol) and NEt₃ (3.66 mL, 26.3 mmol) were added. The mixture was stirred overnight at rt. The reaction mixture was washed with 5% HCl (15 mL), the organic layer was dried (Na₂SO₄) and evaporated to dryness. The product was purified by column chromatography (CH₂Cl₂). The eluent was filtered through a cotton plug and evaporated to give 3.2 g (93% yield) of **18j** as a white crystalline solid. Analytical sample was prepared by recrystallization from *iso*-octane/toluene (2x): mp 174 °C; ¹H NMR (CD₃CN, 400 MHz) δ 5.18 (s, 2H), 7.07 (d, $J = 8.9$ Hz, 2H), 7.24 and 7.27 (AB, $J = 9.2$ Hz, 4H), 7.37-7.47 (m, 5H), 8.15 (d, $J = 8.8$ Hz, 2H). Anal. Calcd. for C₂₁H₁₅F₃O₄: C, 64.95; H, 3.89. Found: C, 64.67; H, 3.77.

Preparation of 4-(trifluoromethoxy)phenyl 4-(benzyloxy)-2-fluorobenzoate (**18k**).

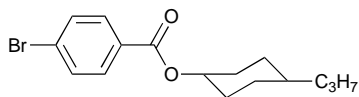


The ester was prepared in 97% yield according to the procedure for **18j**, and purified by column chromatography (SiO_2 , CH_2Cl_2) to give white crystalline solid. Analytical sample of **18k** was prepared by recrystallization from methanol to give colorless crystals: mp 164 °C; ^1H NMR (400 MHz, CD_3CN) δ 5.21 (s, 2H), 6.92 (dd, $J_1 = 13.1$ Hz, $J_2 = 2.4$ Hz, 1H), 6.97 (dd, $J_1 = 8.8$ Hz, $J_2 = 2.4$ Hz, 1H), 7.33 (d, $J = 9.2$ Hz, 2H), 7.39-7.51 (m, 7H), 8.08 (t, $J = 8.8$ Hz, 1H). Anal. Calcd. for $\text{C}_{21}\text{H}_{14}\text{F}_4\text{O}_4$: C, 62.08; H, 3.47; Found: C, 62.19; H, 3.59.

Preparation of *trans*-4-pentylcyclohexyl and *trans*-4-propylcyclohexyl 4-bromobenzoate (**19**).

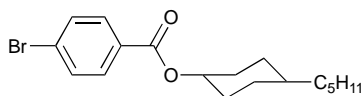
4-Bromobenzoic acid (0.06 mol) was treated with oxalyl chloride (0.18 mol) in CH_2Cl_2 in the presence of catalytic amounts of DMF. Volatiles were removed and the crude 4-bromobenzoyl chloride was added to a mixture of isomeric 4-pentylcyclohexanols (obtained from 4-alkylcyclohexanone and NaBH_4) and dry pyridine (0.18 mol). The mixture was stirred overnight at 50 °C, cooled and poured into dil. HCl. The organic layer was separated, washed with NaHCO_3 , dried (MgSO_4), and solvent removed. The residue was passed through a short silica gel plug (CH_2Cl_2), solvent removed and the residue was crystallized (3x) from pentane at -20 °C (*trans*-4-pentylcyclohexyl 4-bromobenzoate, **19f**) or cold hexanes (2x) (*trans*-4-propylcyclohexyl 4-bromobenzoate, **19e**) to give colorless plates of the desired ester.

***trans*-4-Propylcyclohexyl 4-bromobenzoate (19e).**



Mp 83 °C; ¹H NMR (400 MHz, CDCl₃) δ 0.89 (t, *J* = 7.3 Hz, 3H), 1.06 (dq, *J*₁ = 3.3 Hz, *J*₂ = 13.4 Hz, 2H), 1.15-1.34 (m, 5H), 1.46 (dq, *J*₁ = 3.5 Hz, *J*₂ = 12.5 Hz, 2H), 1.84 (br d, *J* = 12.3 Hz, 2H), 2.08 (br d, *J* = 14.2 Hz, 2H), 4.89 (tt, *J*₁ = 11.0 Hz, *J*₂ = 4.4 Hz, 1H), 7.56 (d, *J* = 8.6 Hz, 2H), 7.89 (d, *J* = 8.6 Hz, 2H); ¹³C NMR (100 MHz, CDCl₃) δ 14.3, 20.2, 30.9 (2C), 31.7 (2C), 36.3, 31.7, 36.3, 38.8, 74.6, 127.1, 129.8, 131.1 (2C), 131.6 (2C), 165.4. Anal. Calcd. for C₁₈H₂₅BrO₂: C, 59.09; H, 6.51. Found: C, 59.27; H, 6.59.

***trans*-4-Pentylcyclohexyl 4-bromobenzoate (19f).**



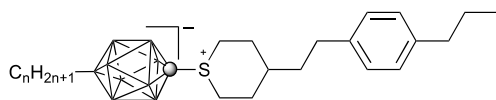
Mp: 69 °C; ¹H NMR (400 MHz, CDCl₃) δ 0.89 (t, *J* = 7.2 Hz, 3H), 1.06 (dq, *J*₁ = 3.3 Hz, *J*₂ = 13.4 Hz, 2H), 1.15-1.34 (m, 9H), 1.46 (dq, *J*₁ = 3.5 Hz, *J*₂ = 12.5 Hz, 2H), 1.84 (d, *J* = 13.0 Hz, 2H), 2.07 (br d, *J* = 12.7 Hz, 2H), 4.89 (tt, *J*₁ = 11.1 Hz, *J*₂ = 4.4 Hz, 1H), 7.56 (d, *J* = 8.6 Hz, 2H), 7.89 (d, *J* = 8.6 Hz, 2H). Anal. Calcd. for C₁₈H₂₅BrO₂: C, 61.19; H, 7.13. Found: C, 61.29; H, 7.34.

Binary mixtures

Preparation of binary mixtures for dielectric studies. Solutions of compounds **3[n]** or **4[n]** in host **ClEster** (15-20 mg) in dry CH₂Cl₂ (~0.5 mL) were heated at ~60 °C for 2 hr in an open vial to assure homogeneity of the sample. The sample was degased under vacuum (0.2 mmHg), left at ambient temperature for 2 hr and analyzed by polarized

optical microscopy (POM). After a minimum of several days, the mixtures were inspected again for inhomogeneity and partial crystallization.

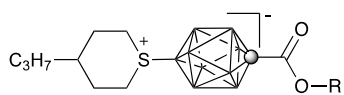
Table S1. Solubility data for 3[n]b ^a



n	Highest soluble tried ^b	Lowest Insoluble tried ^c
3	3.67 ^d	6.52
5	3.26	6.19

^a Concentration in mole %. ^b Stable homogenous solution after 24 hrs or longer. ^c Partial crystallization upon cooling to ambient temperature. ^d Partial crystallization after 24 hrs or longer.

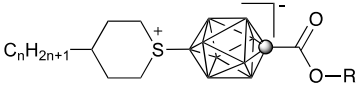
Table S2. Solubility data for selected esters 4[3]^a

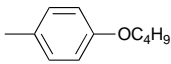
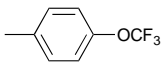
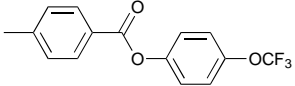


R	Highest soluble tried ^b	Lowest insoluble tried ^c
b	2.2	6.6
c	3.6	?
d	3.0	6.0
e	4.1	6.6
g	?	1.1
h	4.2 ^d	5.6
i	4.3	6.5
j	5.6	12.1
k	4.1	?
l	3.0	?

^a concentration in mole %. ^b Stable homogenous solution after 24 hrs or longer. ^c Partial crystallization upon cooling to ambient temperature. ^d Partial crystallization after 24 hrs or longer.

Table S3. Transition temperatures ($^{\circ}\text{C}$) and enthalpies (kJ/mol, in italics) for 4[n]. ^a



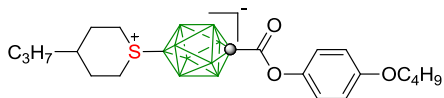
R	n = 5		n = 7	
	highest soluble tried ^b	lowest insoluble tried ^c	highest soluble tried ^b	lowest insoluble tried ^c
^b 	5.5	11.3	–	–
^c 	–	–	9.9	?
^j 	–	–	6.0	11.5

^a concentration in mole %. ^b Stable homogenous solution after 24 hrs or longer. ^c Partial crystallization upon cooling to ambient temperature. ^d Partial crystallization after 24 hrs or longer.

Thermal analysis Virtual N-I transition temperatures [T_{NI}] were determined for selected compounds in **CI Ester** and **CinnCN** hosts. The clearing temperature for each homogenous mixture, prepared as above, was determined by DSC as the peak of the transition using small samples (~0.5 mg) and a heating rate of $5 \text{ K}\cdot\text{min}^{-1}$. The results are shown in Tables S4-S8. The virtual N-I transition temperatures, [T_{NI}], were determined by line extrapolation of the data for peak of the transition to pure substance ($x = 1$). To minimize the error, the intercept in the fitting function was set as the peak T_{NI} for the pure host.

Results for esters **4[3]c**, **4[3]j**, and **4[3]k** show non-linear dependence of T_{NI} on concentration or scattered data and were not analyzed.

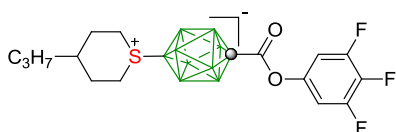
Table S4. T_{NI} for solutions of **4[3]b** in **CinnCN**.



$T_{NI}/^{\circ}\text{C}$	Mole fraction, x			
	0.00 (host)	0.0228	0.0432	0.0689
Onset		–	132.89	130.57
Peak	139.5	–	133.62	131.57

$$[T_{NI}] = 19 \pm 6 \text{ }^{\circ}\text{C}, r^2 = 0.983$$

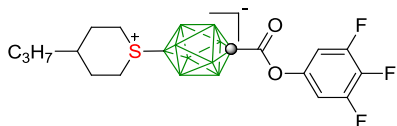
Table S5. T_{NI} for solutions of **4[3]d** in **ClEster**.



$T_{NI}/^{\circ}\text{C}$	Mole fraction, x			
	0.00 (host)	0.0108	0.02375	0.0299 not used
Onset		45.72	45.23	44.97
Peak	46.36	46.13	45.75	45.42

$$[T_{NI}] = 21 \pm 1 \text{ }^{\circ}\text{C}, r^2 = 0.990$$

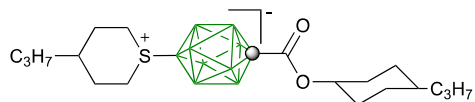
Table S6. T_{NI} for solutions of **4[3]d** in **CinnCN**.



$T_{NI}/^{\circ}\text{C}$	Mole fraction, x			
	0.00 (host)	0.0205	0.0321	0.0895
Onset		133.43	135.59	121.09
Peak	139.5	136.10	134.76	123.67

$$[T_{NI}] = -34 \pm 5 \text{ }^{\circ}\text{C}, r^2 = 0.994$$

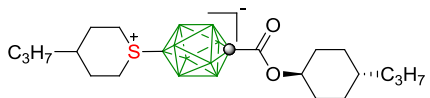
Table S7. T_{NI} for solutions of **4[3]e** in **ClEster**.



$T_{NI}/^{\circ}\text{C}$	Mole fraction, x			
	0.00 (host)	0.0368	0.0665	—
Onset		42.4	40.3	—
Peak	46.36	44.29	43.13	—

$$[T_{NI}] = -4 \pm 2 \text{ }^{\circ}\text{C}, r^2 = 0.989$$

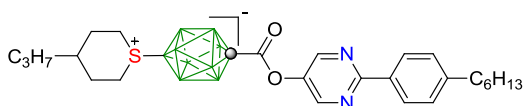
Table S8. T_{NI} for solutions of **4[3]e** in **CinnCN**.



$T_{NI}/^{\circ}\text{C}$	Mole fraction, x			
	0.00 (host)	0.0215	0.0381	–
Onset		135.62	133.42	–
Peak	139.5	136.16	134.52	–

$$[T_{NI}] = 1 \pm 6 \text{ }^{\circ}\text{C}, r^2 = 0.987$$

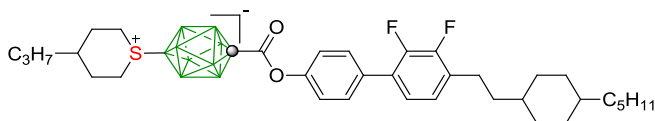
Table S9. T_{NI} for solutions of **4[3]h** in **ClEster**.



$T_{NI}/^{\circ}\text{C}$	Mole fraction, x			
	0.00 (host)	0.0161	0.0288	0.04215
Onset		47.62	48.81	50.00
Peak	46.36	48.3	49.59	51.23

$$[T_{NI}] = 161 \pm 3 \text{ }^{\circ}\text{C}, r^2 = 0.999$$

Table S10. T_{NI} for solutions of **4[3]I** in **CI Ester**.



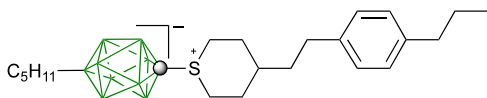
$T_{NI}/^{\circ}\text{C}$	Mole fraction, x			
	0.00 (host)	0.0158	0.0182	0.0301
Onset		49.27	49.49	53.3
Peak	46.36	50.56	50.58	55.1

$$[T_{NI}] = 331 \pm 7 \text{ }^{\circ}\text{C}, r^2 = 0.997$$

Dielectric measurements. Dielectric properties of solutions of selected esters in **CI Ester** were measured by a Liquid Crystal Analytical System (LCAS - Series II, LC Vision, Inc.) using GLCAS software version 0.13.14, which implements literature procedures for dielectric constants.⁵ The instrument was calibrated using a series of capacitors (11.30 pF – 3292 pF). The homogenous binary mixtures were loaded into ITO electro-optical cells by capillary forces with moderate heating supplied by a heat gun. The cells (about 10 μm thick, electrode area 1.00 cm^2 and anti-parallel rubbed polyimide layer) were obtained from LC Vision, Inc. The filled cells were heated to an isotropic phase and cooled to room temperature before measuring of dielectric properties. Default parameters were used for measurements: triangular shaped voltage bias ranging from 0.1-20 V at 1 kHz frequency. The threshold voltage V_{th} was measured at a 5% change. For each mixture the measurement was repeated 10 times manually for two cells. The results were averaged to calculate the mixture's parameters. Results are shown in Tables S11–S18. All

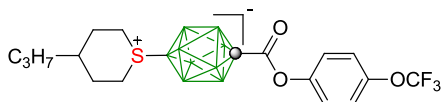
measurements were run at 25 °C. Error in concentration is estimated at about 1.5%. The dielectric values obtained for each concentration were fitted to a linear function in which the intercept was set at the value extrapolated for the pure host. The resulting extrapolated values for pure additives are shown in Table 4 in the main text.

Table S11. Dielectric parameters for **3[5]b** in **ClEster** at 25 °C.



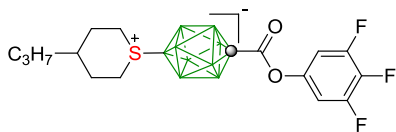
Parameter	Mole fraction, x			
	0.00 (host)	0.0246	0.0374	–
ϵ_{\parallel}	2.86 ± 0.01	4.00 ± 0.01	4.40 ± 0.01	–
ϵ_{\perp}	3.42 ± 0.01	3.55 ± 0.01	3.60 ± 0.01	–
$\Delta\epsilon$	-0.56 ± 0.01	0.45 ± 0.01	0.80 ± 0.01	–

Table S12. Dielectric parameters for **4[3]c** in **ClEster** at 25 °C.



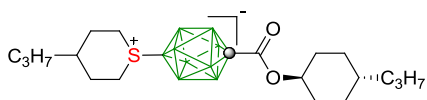
Parameter	Mole fraction, x			
	0.00 (host)	0.0215	0.0478	0.0547
ϵ_{\parallel}	2.86 ± 0.01	4.37 ± 0.01	6.95 ± 0.05	7.47 ± 0.1
ϵ_{\perp}	3.42 ± 0.01	3.62 ± 0.01	4.10 ± 0.05	4.20 ± 0.1
$\Delta\epsilon$	-0.56 ± 0.01	0.75 ± 0.01	2.84 ± 0.01	3.30 ± 0.1

Table S13. Dielectric parameters for **4[3]d** in **ClEster** at 25 °C.



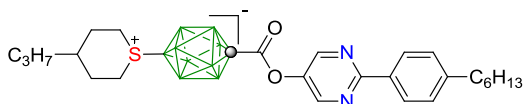
Parameter	Mole fraction, x			
	0.00 (host)	0.0153	0.0279	0.0361
ϵ_{\parallel}	2.86±0.01	4.01±0.01	4.98±0.01	5.55±0.02
ϵ_{\perp}	3.42±0.01	3.62±0.02	3.78±0.01	3.96±0.06
$\Delta\epsilon$	-0.56±0.01	0.40±0.01	1.19±0.01	1.59±0.06

Table S14. Dielectric parameters for **4[3]e** in **ClEster** at 25 °C.



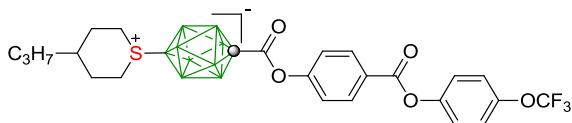
Parameter	Mole fraction, x			
	0.00 (host)	0.0368	0.0665	—
ϵ_{\parallel}	2.86±0.01	4.01±0.01	4.73±0.04	—
ϵ_{\perp}	3.42±0.01	3.71±0.01	3.89±0.02	—
$\Delta\epsilon$	-0.56±0.01	0.31±0.01	0.84±0.02	—

Table S15. Dielectric parameters for **4[3]h** in **ClEster** at 25 °C.



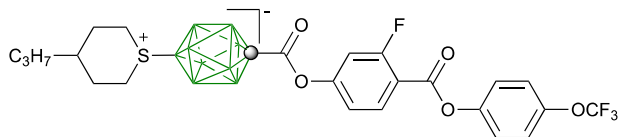
Parameter	Mole fraction, x			
	0.00 (host)	0.0261	0.0353	—
ϵ_{\parallel}	2.86±0.01	4.41±0.01	4.91±0.04	—
ϵ_{\perp}	3.42±0.01	3.63±0.01	3.69±0.04	—
$\Delta\epsilon$	-0.56±0.01	0.78±0.01	1.22±0.01	—

Table S16. Dielectric parameters for **4[3]j** in **ClEster** at 25 °C.



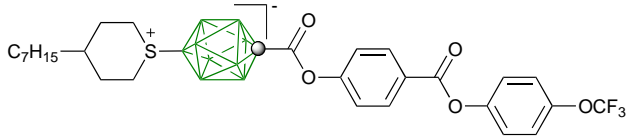
Parameter	Mole fraction, x			
	0.00 (host)	0.0172	0.0278	0.0375
ϵ_{\parallel}	2.86±0.01	4.36±0.01	5.33±0.02	5.85±0.05
ϵ_{\perp}	3.42±0.01	3.67±0.01	3.80±0.01	3.90±0.01
$\Delta\epsilon$	-0.56±0.01	0.69±0.01	1.53±0.01	1.945±0.06

Table S17. Dielectric parameters for **4[3]k** in **ClEster** at 25 °C.



Parameter	Mole fraction, x			
	0.00 (host)	0.01876	0.0231	0.0405
ϵ_{\parallel}	2.86±0.01	4.57±0.01	4.98±0.02	6.13±0.06
ϵ_{\perp}	3.42±0.01	3.65±0.01	3.75±0.01	3.92±0.03
$\Delta\epsilon$	-0.56±0.01	0.92±0.01	1.23±0.02	2.21±0.04

Table S18. Dielectric parameters for **4[7]j** in **ClEster** at 25 °C.



Parameter	Mole fraction, x			
	0.00 (host)	0.0165	0.0258	0.0309
ε_{\parallel}	2.86±0.01	4.20±0.02	5.12±0.01	5.52±0.01
ε_{\perp}	3.42±0.01	3.60±0.01	3.73±0.01	3.77±0.01
$\Delta\varepsilon$	-0.56±0.01	0.61±0.01	1.39±0.01	1.75±0.01

Background for calculations in the nematic phase

The equations derived from the Maier-Meier theory¹¹ used in this work were adopted from literature¹² and had the following form:

$$\Delta\varepsilon = \frac{NFh}{\varepsilon_0} \left\{ \Delta\alpha - \frac{F\mu_{eff}^2}{2k_B T} (1 - 3\cos^2 \beta) \right\} S \quad (1)$$

$$\varepsilon_{\parallel} = 1 + \frac{NFh}{\varepsilon_0} \left\{ \bar{\alpha} + \frac{2}{3} \Delta\alpha S + \frac{F\mu_{eff}^2}{3k_B T} [1 - (1 - 3\cos^2 \beta) S] \right\} \quad (2)$$

$$\varepsilon_{\perp} = 1 + \frac{NFh}{\varepsilon_0} \left\{ \bar{\alpha} + \frac{1}{3} \Delta\alpha S + \frac{F\mu_{eff}^2}{3k_B T} [1 - (1 - 3\cos^2 \beta) S] \right\} \quad (3)$$

All quantities were in SI units as defined in the ESI in previous publications.¹³

- Dielectric permittivity of vacuum:

$$\varepsilon = 1.114 \cdot 10^{-10} / 4\pi = 8.865 \cdot 10^{-12} \text{ F} \cdot \text{m}^{-1}$$

- The diagonal values of the electronic polarizabilities tensors matrix α_{xx} , α_{yy} , α_{zz} expressed in a.u. units were converted to $F \cdot m^2$ units by multiplying with $1.482 \cdot 4\pi\epsilon \cdot 10^{-31} = 1.651 \cdot 10^{-41}$
- Computed dipole moments μ_x , μ_y , μ_z in Debye were converted to dipole moments in $C \cdot m$ units using the conversion $1D = 3.3356 \cdot 10^{-30} C \cdot m$
- Number density N is expressed in molecules per m^3

Field parameters $F = 1.2090$ and $h = 1.28754$ in equations 1–3 were assumed to be of pure host, **CI Ester**, and obtained from literature dielectric and optical data¹⁴ according to equation 4 and 5. Permittivity ϵ_s was assumed to be experimental average permittivity ($\epsilon = 3.07$) for the pure host, **CI Ester**. The density of the hosts **CI Ester** at 25 °C was taken as 1.02 g/cm^3 according to a literature report.¹⁴

$$F = \frac{1}{1 - \alpha \cdot f} \quad \text{where } f = \frac{2(\overline{\epsilon_s} - 1)}{2\overline{\epsilon_s} + 1} \cdot \frac{N}{3\epsilon_0} \quad (4)$$

$$h = \frac{3\epsilon_s}{(2\epsilon_s + 1)} \quad (5)$$

Procedures for Maier-Meier analysis.

The order parameter S and the Kirkwood factor g for the additives were obtained by solving simultaneously equations for $\Delta\epsilon$ and ϵ_{\parallel} (equation 1 and 2). The unknown g from the expression for $\Delta\epsilon$ (equation 1) was substituted into the expression for ϵ_{\parallel} (equation 2) and solved for S (equation 6). In this form, order parameter S does not depend on the dipole moment μ , but depends on the dielectric permittivity components ϵ_{\parallel} and ϵ_{\perp} . The obtained value S was substituted to the expression for parameter g (equation 7).

$$S = \frac{\Delta\epsilon\epsilon_0}{\Delta\alpha NFh + (1 - 3\cos^2 \beta)[\Delta\epsilon\epsilon_0 - \frac{3}{2}(\epsilon_{\parallel}\epsilon_0 - \epsilon_0 - \overline{\alpha}NFh)]} \quad (6)$$

$$g = \frac{2(\Delta\alpha NFhS - \Delta\epsilon\epsilon_0)k_B T}{NF^2 h \mu^2 (1 - 3\cos^2 \beta)S} \quad (7)$$

The protocol was verified by substituting the computed parameters S and g into equation 1–3 and calculating back the dielectric parameters.

Quantum mechanical calculation

Quantum-mechanical calculations were carried out using Gaussian 09 suite of programs.¹⁵ Geometry optimizations for unconstrained conformers of with the most extended molecular shapes were undertaken at the B3LYP/6-31G(d,p) level of theory using default convergence limits. The alkyl groups were set in all-*trans* conformation in the input structures. No conformational search was attempted. The nature of the stationary point was verified by frequency calculations.

Calculations in solvent media using the PCM model¹⁶ were requested with the SCRF(Solvent=Generic,Read) keyword and eps=3.07 and epsinf=2.286 input parameters. Exact polarizabilities were obtained with the POLAR keyword.

References

- 1 B. Ringstrand, M. Oltmanns, J. Batt, A. Jankowiak, R. P. Denicola, P. Kaszynski *Beilstein J. Org. Chem.* 2011, **7**, 386.
- 2 J. Thomas, D. Clough *journal of Pharmacy and Pharmacology* 1963, **15**, 167.
- 3 D. Landini, F. Montanari, F. Rolla *Synthesis* 1978, **10**, 771.
- 4 N. Aziz, S. M. Kelly, W. Duffy, M. Goulding *Liq. Cryst.* 2008, **35**, 1279.
- 5 J. Qiu, L. Wang, M. Liu, Q. Shen, J. Tang *Tetrahedron Lett.* 2011, **52**, 6489.

- 6 T. A. Kizner, M. A. Mikhaleva, E. S. Serebryakova *Chem. Heteroc. Comp.* 1990, **26**, 668.
- 7 S. Hayashi, S. Takenaka, S. Kusabayashi *Bull. Chem. Soc. Jpn* 1984, **57**, 283.
- 8 J. C. Liang, R. Hubbard *Mol. Cryst. Liq. Cryst.* 1985, **128**, 89.
- 9 B. Ringstrand, P. Kaszynski, V. G. Young, Jr., Z. Janoušek *Inorg. Chem.* 2010, **49**, 1166.
- 10 J. Pecyna, R. P. Denicola, B. Ringstrand, A. Jankowiak, P. Kaszynski *Polyhedron* 2011, **30**, 2505.
- 11 W. Maier, G. Meier *Z. Naturforsch.* 1961, **16A**, 262.
- 12 S. Urban, in *Physical Properties of Liquid Crystals: Nematics*, (Eds.: D. A. Dunmur, A. Fukuda, and G. R. Luckhurst) IEE, London, **2001**, pp 267-276.
- 13 B. Ringstrand, P. Kaszynski *J. Mater. Chem.* 2011, **21**, 90.
- 14 R. Dabrowski, J. Jadzyn, S. Czerkas, J. Dziaduszek, A. Walczak *Mol. Cryst. Liq. Cryst.* 1999, **332**, 61.
- 15 Gaussian 09, Revision A.02, M. J. Frisch, G. W. Trucks, H. B. Schlegel, G. E. Scuseria, M. A. Robb, J. R. Cheeseman, G. Scalmani, V. Barone, B. Mennucci, G. A. Petersson, H. Nakatsuji, M. Caricato, X. Li, H. P. Hratchian, A. F. Izmaylov, J. Bloino, G. Zheng, J. L. Sonnenberg, M. Hada, M. Ehara, K. Toyota, R. Fukuda, J. Hasegawa, M. Ishida, T. Nakajima, Y. Honda, O. Kitao, H. Nakai, T. Vreven, J. A. Montgomery, Jr., J. E. Peralta, F. Ogliaro, M. Bearpark, J. J. Heyd, E. Brothers, K. N. Kudin, V. N. Staroverov, R. Kobayashi, J. Normand, K. Raghavachari, A. Rendell, J. C. Burant, S. S. Iyengar, J. Tomasi, M. Cossi, N. Rega, J. M. Millam, M. Klene, J. E. Knox, J. B. Cross, V. Bakken, C. Adamo, J. Jaramillo, R. Gomperts, R. E. Stratmann, O. Yazyev, A. J.

Austin, R. Cammi, C. Pomelli, J. W. Ochterski, R. L. Martin, K. Morokuma, V. G. Zakrzewski, G. A. Voth, P. Salvador, J. J. Dannenberg, S. Dapprich, A. D. Daniels, O. Farkas, J. B. Foresman, J. V. Ortiz, J. Cioslowski, and D. J. Fox, Gaussian, Inc., Wallingford CT, 2009.

16 M. Cossi, G. Scalmani, N. Rega, V. Barone *J. Chem. Phys.* 2002, **117**, 43.

4.2.2.7 Acknowledgements

This work was supported by NSF grant DMR-1207585. We are grateful to Professor Roman Dąbrowski of the Military University of Technology (Warsaw, Poland) for the gift of **CI Ester**.

4.2.2.8 References

1 D. Pauluth, K. Tarumi *J. Mater. Chem.* 2004, **14**, 1219-1227.

2 M. Bremer, P. Kirsch, M. Klasen-Memmer, K. Tarumi *Angew. Chem. Int. Ed.* 2013, **52**, 8880-8896.

3 B. Ringstrand, P. Kaszynski, A. Januszko, V. G. Young, Jr. *J. Mater. Chem.* 2009, **19**, 9204-9212.

4 J. Pecyna, D. Pocięcha, P. Kaszynski *J. Mater. Chem. C* 2014, **2**, DOI 10.1039/C1033TC32351J.

5 B. Ringstrand, P. Kaszynski *J. Mater. Chem.* 2011, **21**, 90-95.

6 B. Ringstrand, P. Kaszynski *J. Mater. Chem.* 2010, **20**, 9613-9615.

7 B. Ringstrand, M. Oltmanns, J. A. Batt, A. Jankowiak, R. P. Denicola, P. Kaszynski *Beilstein J. Org. Chem.* 2011, **7**, 386-393.

8 J. Pecyna, R. P. Denicola, B. Ringstrand, A. Jankowiak, P. Kaszynski *Polyhedron* 2011, **30**, 2505-2513.

- 9 B. Ringstrand, P. Kaszynski, V. G. Young, Jr., Z. Janoušek *Inorg. Chem.* 2010, **49**, 1166-1179.
- 10 J. Thomas, D. Clough *J. Pharm. Pharmacol.* 1963, **15**, 167-177.
- 11 N. Aziz, S. M. Kelly, W. Duffy, M. Goulding *Liq. Cryst.* 2008, **35**, 1279-1292.
- 12 J. Qiu, L. Wang, M. Liu, Q. Shen, J. Tang *Tetrahedron Lett.* 2011, **52**, 6489-6491.
- 13 T. A. Kizner, M. A. Mikhaleva, E. S. Serebryakova *Chem. Heteroc. Comp.* 1990, **26**, 668-670.
- 14 B. Ringstrand, A. Jankowiak, L. E. Johnson, P. Kaszynski, D. Pocięcha, E. Górecka *J. Mater. Chem.* 2012, **22**, 4874-4880.
- 15 S. M. Kelly *Helv. Chim. Acta* 1989, **72**, 594-607.
- 16 A. Jankowiak, B. Ringstrand, A. Januszko, P. Kaszynski, M. D. Wand *Liq. Cryst.* 2013, **40**, 605-615.
- 17 S. Hayashi, S. Takenaka, S. Kusabayashi *Bull. Chem. Soc. Jpn* 1984, **57**, 283-284.
- 18 W. Maier, G. Meier *Z. Naturforsch.* 1961, **16A**, 262-267 and 470-477.
- 19 S. Urban *Physical Properties of Liquid Crystals: Nematics* 2001, 267-276.
- 20 P. Kaszyński, A. Januszko, K. L. Glab *J. Phys. Chem. B* 2014, **118**, 000.
- 21 R. Dabrowski, J. Jadzyn, S. Czerkas, J. Dziaduszek, A. Walczak *Mol. Cryst. Liq. Cryst.* 1999, **332**, 61-68.
- 22 For details see the Electronic Supplementary Information.
- 23 A. I. Pavluchenko, N. I. Smirnova, V. F. Petrov, Y. A. Fialkov, S. V. Shelyazhenko, L. M. Yagupolsky *Mol. Cryst. Liq. Cryst.* 1991, **209**, 225-235.
- 24 P. Kędziora, J. Jadzyn *Mol. Cryst. Liq. Cryst.* 1990, **192**, 31-37.
- 25 P. Kędziora, J. Jadzyn *Acta Phys. Polon.* 1990, **A77**, 605-610.

26 Gaussian 09, Revision A.02, M. J. Frisch, G. W. Trucks, H. B. Schlegel, G. E. Scuseria, M. A. Robb, J. R. Cheeseman, G. Scalmani, V. Barone, B. Mennucci, G. A. Petersson, H. Nakatsuji, M. Caricato, X. Li, H. P. Hratchian, A. F. Izmaylov, J. Bloino, G. Zheng, J. L. Sonnenberg, M. Hada, M. Ehara, K. Toyota, R. Fukuda, J. Hasegawa, M. Ishida, T. Nakajima, Y. Honda, O. Kitao, H. Nakai, T. Vreven, J. A. Montgomery, Jr., J. E. Peralta, F. Ogliaro, M. Bearpark, J. J. Heyd, E. Brothers, K. N. Kudin, V. N. Staroverov, R. Kobayashi, J. Normand, K. Raghavachari, A. Rendell, J. C. Burant, S. S. Iyengar, J. Tomasi, M. Cossi, N. Rega, J. M. Millam, M. Klene, J. E. Knox, J. B. Cross, V. Bakken, C. Adamo, J. Jaramillo, R. Gomperts, R. E. Stratmann, O. Yazyev, A. J. Austin, R. Cammi, C. Pomelli, J. W. Ochterski, R. L. Martin, K. Morokuma, V. G. Zakrzewski, G. A. Voth, P. Salvador, J. J. Dannenberg, S. Dapprich, A. D. Daniels, O. Farkas, J. B. Foresman, J. V. Ortiz, J. Cioslowski, and D. J. Fox, Gaussian, Inc., Wallingford CT, 2009.

27 M. Cossi, G. Scalmani, N. Rega, V. Barone *J. Chem. Phys.* 2002, **117**, 43-54 and references therein.

28 S.-T. Wu, D. Coates, E. Bartmann *Liq. Cryst.* 1991, **10**, 635-646.

4.3 Zwitterionic pyridinium derivatives of [*closo*-1-CB₉H₁₀]⁻ and [*closo*-1-CB₁₁H₁₂]⁻ clusters as polar liquid crystals for LCD applications.

4.3.1 Description and contributions

The goal of this project was to develop an efficient and practical route to 1-pyridinium derivatives of both [*closo*-1-CB₉H₁₀]⁻ and [*closo*-1-CB₁₁H₁₂]⁻ clusters. It was found that amines **7** and **8** are converted to pyridinium zwitterions using pyrylium salts **5** in 35-50% yield. Two of the zwitterions display a SmA phase driven by dipolar interactions, which was supported by comparing their mesogenic properties with the nonpolar analogue. The investigated compounds were found to be effective additives to nematic hosts and to have high dielectric anisotropy. The new method provides means for introduction of a variety of alkoxy substituents on the pyridinium ring, which allows for manipulation with the structure and properties of the derivatives.

I was responsible for the entire synthetic part in this project. I also investigated thermal and optical properties of the zwitterions. My work included preparation and thermal and electro-optical characterization of binary mixtures of three compounds in a nematic host. Powder X-ray analysis was performed by Dr. Damian Pocięcha at Warsaw University, and quantum mechanical calculations were provided by Prof. Piotr Kaszynski.

In the following chapter the entire text of the manuscript is included for consistency of the narrative, however, the experimental section contains only experiments performed by me.

4.3.2 The manuscript

Reproduced by permission of the Royal Society of Chemistry
Pecyna, J.; Pocięcha, D.; Kaszynski, P. *J. Mater. Chem. C* **2014**, 2, 1585-1519.
Copyright 2014 Royal Society of Chemistry. Available online:
<http://pubs.rsc.org/en/content/articlelanding/2014/tc/c3tc32351j>

4.3.2.1 Introduction

Polar liquid crystals and additives enable electro-optical switching¹ and are essential components of materials for liquid crystal display (LCD) applications.² Recently, we have demonstrated that zwitterionic derivatives of the [*closo*-1-CB₉H₁₀]⁻ cluster (**A**, Fig. 1) have high dielectric anisotropy $\Delta\epsilon$ and are useful additives to nematic materials for LCD. In this context, we developed synthetic methodology and prepared 1-sulfonium^{3,4} and 1-quinuclidinium,³ and also 10-sulfonium⁴⁻⁶ and 10-pyridinium⁷ zwitterions, compounds of the general structure **IIA** and **IA**. Some of them exhibit nematic behavior and $\Delta\epsilon$ reaching a record high $\Delta\epsilon$ value of 113.5(!) in nematic solutions.⁷ The preparation of 1-pyridinium derivatives of the [*closo*-1-CB₉H₁₀]⁻ (**A**) and [*closo*-1-CB₁₁H₁₂]⁻ (**B**) clusters however, was very inefficient due to mechanistic issue in the former,⁸ and instability of the key intermediate in the later case.⁹ Such pyridinium derivatives **IIA** and **IIB** (Fig. 1, Q = Pyr) are predicted to have significant longitudinal dipole moments, and, consequently, high positive $\Delta\epsilon$. In addition, they are expected to have lower melting points and be more soluble than the quinuclidinium analogues.

Here we demonstrate a simple method for preparation of 1-pyridinium zwitterions of anions **A** and **B** and their use as high $\Delta\epsilon$ additives to liquid crystal materials for LCD applications.

4.3.3.2 Results and discussion

Synthesis

Compounds **1[n]**, 10-vertex derivatives of type **IIA**, and **2[n]**, 12-vertex derivatives of type **IIB**, were obtained by adapting a general method for converting

pyrylium salts to *N*-substituted pyridinium derivatives¹⁰ and following a single example of using 4-alkoxyppyrylium in this context.¹¹ Thus, a reaction of 1-amino derivatives **3[n]** and **4[n]** with 4-alkoxyppyrylium salts **5** in anhydrous THF gave **1[n]** and **2[n]**, respectively, in 35–50% yields (Scheme1). 4-Alkoxyppyryliums are very rare,¹² however triflate salts **5** were conveniently obtained by alkylation of 4*H*-pyran-4-one with appropriate alkyl triflate **6**. In addition to three primary alkoxy derivatives **5a**, **5b** and **5d**, the new method was demonstrated also for a secondary alkoxy derivative. Thus, (*S*)-2-octanol was converted to triflate **6c** and subsequently to pyrylium salt **5c** with apparent partial racemization (*ee* = 35%), as evident from the analysis of the pyridinium product **1[6]c**. This indicates that the electrophilic *O*-alkylation of 4*H*-pyran-4-one with **6c** proceeds through an ion pair and partial scrambling of the stereocenter. Triflate **6c** was significantly more reactive than primary alkyl triflates and synthesis of **1[6]c** and **2[6]c** was performed at lower temperatures.

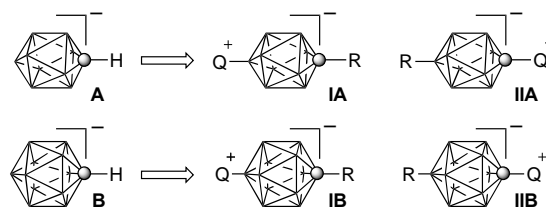
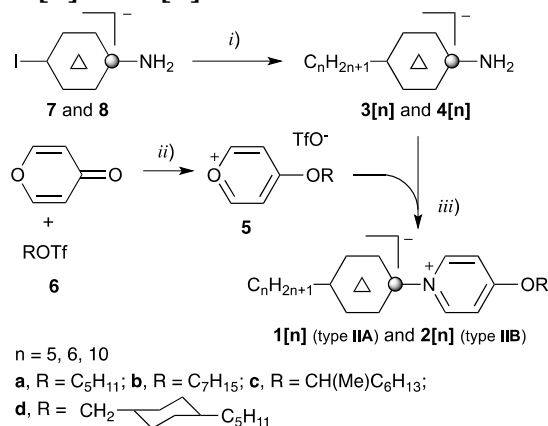


Figure 1. The structures of the $[closo-1-CB_9H_{10}]^-$ and $[closo-1-CB_{11}H_{12}]^-$ anions (**A** and **B**), and their zwitterionic 1,10- (**IA**, **IIA**) and 1,12-disubstituted (**IB**, **IIB**) derivatives. Q^+ represents an onium fragment such as ammonium, sulfonium or pyridinium. Each vertex represents a BH fragment and the sphere is a carbon atom.

The requisite alkyl amines **3[n]** and **4[n]** were obtained by alkylation of the corresponding iodo amines **7** and **8** under Pd-catalyzed coupling conditions using either RMgBr or RZnCl reagents. The synthesis of 10-hexyl amine **3[6]** was reported

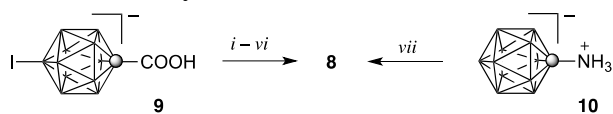
previously¹³ and some **4[n]** are reported elsewhere.⁹ The iodo amine **8** was prepared from iodo acid **9** following the procedure described for iodo amine **7** (Scheme 2),¹³ or alternatively obtained by iodination of [*closo*-1-CB₁₁H₁₁-1-NH₃]⁻ (**10**).⁹

Scheme 1. Synthesis of **1[n]** and **2[n]**.^a



^a Reagents and conditions: *i*) C_nH_{2n+1}MgBr or C_nH_{2n+1}ZnCl, Pd(0); *ii*) 60 °C, 1 hr; *iii*) THF, rt;

Scheme 2.^a Synthesis of iodo amine **8**.



^a Reagents and conditions: *i*) (COCl)₂, CH₂Cl₂, rt; *ii*) Me₃SiN₃, ZnCl₂, CH₂Cl₂, 0 °C→rt; *iii*) 80 °C, MeCN; *iv*) *t*-BuOH, MeCN, 80 °C; *v*) HCl, MeOH, rt; *vi*) [NMe₄]⁺ OH⁻, H₂O; *vii*) ICl, AcOH, 60 °C.

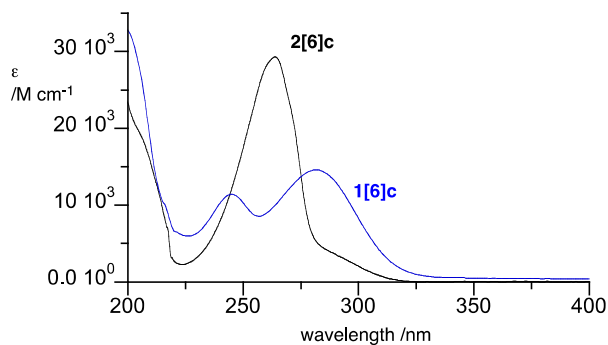


Figure 2. Electronic absorption spectra of **1[6]c** and **2[6]c** in MeCN.

Electronic absorption

Pyridinium derivatives **1[n]** and **2[n]** are colorless solids. Spectroscopic analysis demonstrated that the 12-vertex derivative **2[6]c** is more transparent in the UV region than its analogue **1[6]c**, however both compounds exhibit relatively strong $\pi \rightarrow \pi^*$ absorption bands at λ_{\max} 265 nm (calcd. at 260 nm, $f = 0.16$)¹⁴ for **2[6]c** and at λ_{\max} at 282 nm (calcd at 309 nm, $f = 0.25$) for **1[6]c** (Fig. 2). The origin of this absorption is an efficient intramolecular charge transfer from the HOMO, localized on the cluster, to the LUMO on the pyridinium fragment as shown for **1[6]b** and **2[6]b** in Fig. 3.⁸ Interestingly, the HOMO of the latter has lower energy and significantly greater contribution from the B-alkyl chain than observed in the 10-vertex analogue **1[6]b**.

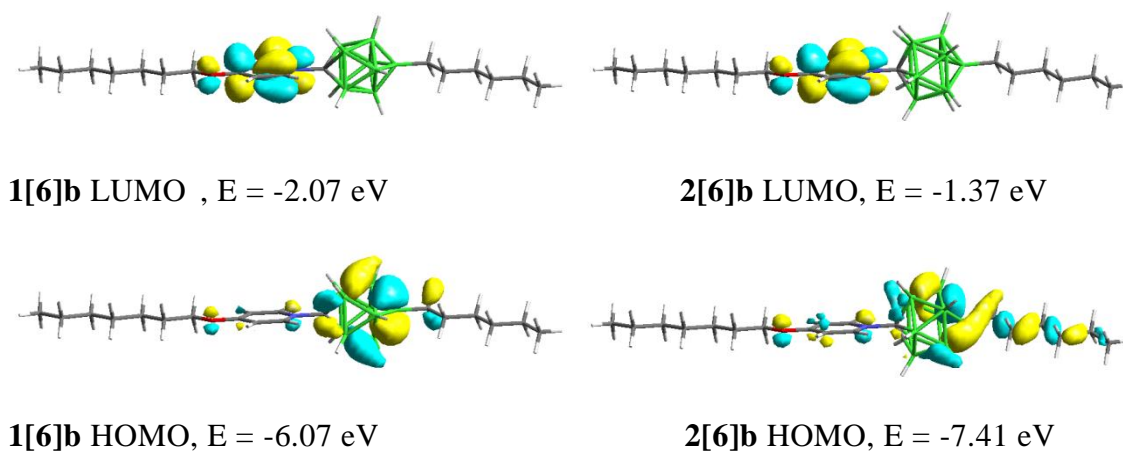


Figure 3. B3LYP/6-31G(d,p) derived contours and energies of FMOs involved in low energy excitations in **1[6]b** (left) and **2[6]b** (right).

Thermal analysis

All six compounds melt above 100 °C (Table 1). The lowest melting points were observed for the branched (2-octyloxy)pyridinium derivatives **[6]c**, which is in agreement with results obtained for bis-zwitterionic derivatives of the [*closo*-B₁₀H₁₀]²⁻ cluster.¹⁵ It is considered that the branching methyl group close to the pyridinium ring disrupts efficient packing in the solid state driven by coulombic interactions.¹⁵ The highest melting point among the six compounds (216 °C) is exhibited by three-ring derivative **1[6]d**. Data in Table 1 also suggests that derivatives of the [*closo*-1-CB₉H₁₀]⁻ cluster (**A**) have lower melting points than the 12-vertex analogues (e.g. **1[6]c** vs **2[6]c**), which is in agreement with general trends in mesogenic derivatives of 10- and 12-vertex carboranes.^{16,17}

Table 1. Transition temperatures ($^{\circ}\text{C}$) and enthalpies (kJ/mol, in italics) for **1[n]** and **2[n]**
 a

compo und	n	R	
1[n]	a	6	C_5H_{11} Cr 122 (33.7) I
	c	6	$\text{CH}(\text{Me})\text{C}_6\text{H}_{13}$ Cr 101 (21.5) I
	d	6	$\text{CH}_2\text{C}_6\text{H}_{10}$ Cr 217 (33.5) SmA > C_5H_{11} 270 I ^b
2[n]	b	5	C_7H_{15} Cr 205 (26.6) I
	b	10	C_7H_{15} Cr ^c 184 (16.2) SmA 200 (9.1) I
	c	6	$\text{CH}(\text{Me})\text{C}_6\text{H}_{13}$ Cr 130 (23.7) I

^a Determined by DSC (5 K min^{-1}) in the heating mode: Cr = crystal; SmA = smectic A; I = isotropic. ^b decomp. ^c Cr–Cr transition at $117 \text{ }^{\circ}\text{C}$ (9.7 kJ/mol).

Polarizing optical microscopy (POM) and differential scanning calorimetry (DSC) revealed that **2[10]b** and **1[6]d** exhibit an enantiotropic SmA phase with the clearing temperature of $202 \text{ }^{\circ}\text{C}$ and above $270 \text{ }^{\circ}\text{C}$, respectively (Table 1, Fig. 4).

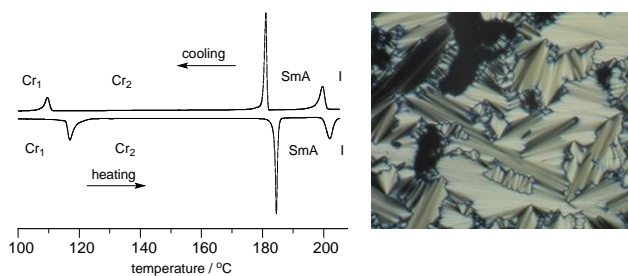


Figure 4. Left: DSC trace of **2[10]b**. The heating and cooling rates are 5 K min^{-1} . Right: The optical texture of **2[10]b** obtained at $190 \text{ }^{\circ}\text{C}$ on cooling from the isotropic phase.

XRD data

The formation of the SmA phase was confirmed by powder XRD measurements for **2[10]b**. A diffractogram of the mesophase obtained at $195 \text{ }^{\circ}\text{C}$

showed a series of sharp commensurate reflections consistent with the lamellar structure with layer spacing of 25.61 Å (Fig. 5). Considering the calculated molecular length of 31.75 Å,¹⁴ the observed layer spacing indicates 19% of interdigitation. The wide-angle region of the diffractogram shows an unsymmetric broad halo, which can be deconvoluted into two signals with the maxima 4.5 Å and 5.4 Å. The diffused signals correlate with the mean distance between the molten alkyl chains (former) and the mean separation between the carborane cages (latter).

Temperature dependence studies demonstrated that the SmA phase has a negative thermal expansion coefficient, $\kappa = -0.0030(1)$ Å/K, while thermal expansion coefficient of the Cr₂ phase is positive ($\kappa = +0.00598(3)$ Å/K).¹⁴

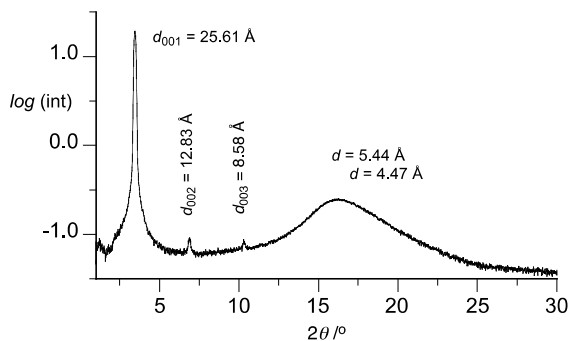
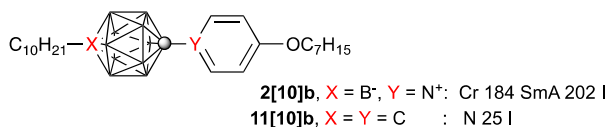


Figure 5. XRD pattern for **2[10]b** at 195 °C.

Smectic behavior of boron cluster-derived mesogens is very rare¹⁶ even for polar compounds,^{6,7} and the observed high-temperature SmA phase for **2[10]b** and **1[6]d** results presumably from strong lateral dipole-dipole interactions of the zwitterions. This is supported by a comparison of **2[10]b** with its non-polar isosteric analogue⁷ **11[10]b**, a low temperature nematogen ($T_{NI} = 25$ °C) derived from *p*-caraborane.



Binary mixtures

Three of the new compounds were investigated as additives to **CI Ester**, which forms a nematic phase at ambient temperature characterized by a small negative $\Delta\epsilon$. Results demonstrated that the two-ring zwitterions are more soluble in the host than the three-ring derivative **1[6]d**, and **2[10]b** forms stable 6 mol% solutions in the host.¹⁴ Extrapolation of the virtual $[T_{NI}]$ for **2[10]b** from the solution data gives the N-I transition at 82 ± 4 °C, which is significantly lower than the SmA-I transition at 202 °C. This difference further supports the notion that SmA stability originates from dipolar interactions between the zwitterions. The branched derivative **1[6]c** significantly disrupt the nematic order of the host and its extrapolated $[T_{NI}]$ is below -100 °C.

Dielectric measurements

Dielectric permittivity values change non-linearly with the concentration of the additives in **CI Ester** as shown for **2[10]b** in Fig. 6. This indicates some aggregation of the polar molecules in the solution, which is similar, albeit to lesser extent, to that previously observed for sulfonium (**1-Sulf**) and quinuclidinium (**1-Quin**) derivatives of type **IIA**.³ Therefore, dielectric parameters for the pure additives were extrapolated from dilute about 3 mol% solutions and results are shown in Table 2.

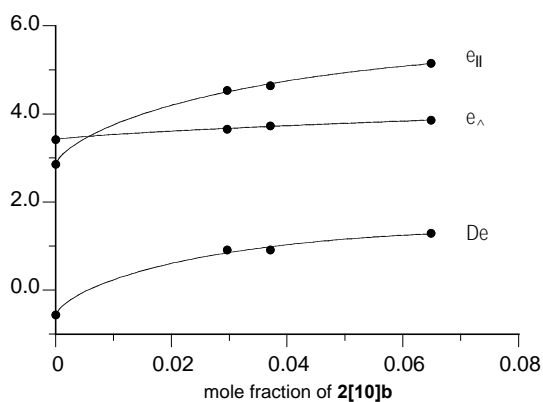
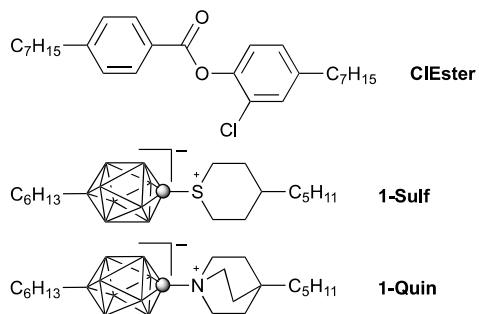


Figure 6. Dielectric parameters as a function of concentration of **2[10]b** in **ClEster**.

Analysis of data in Table 2 demonstrates that all three pyridinium derivatives exhibit substantial dielectric anisotropy. Zwitterions **1[6]d** and **2[6]b** have $\Delta\epsilon$ values 54 and 49, respectively, which, for comparable concentrations, are higher by about 10 than those for the previously investigated **1-Sulf** and **1-Quin** derivatives.³ The value $\Delta\epsilon = 35$ extrapolated for **1[6]c** with the branched alkyl chain is the lowest in the series, which is presumably related to the low order parameter as evident from dramatic destabilization of the nematic phase of the host.

Table 2. Extrapolated dielectric data for selected compounds.^a

Compound d	mol %	$\Delta\epsilon$	ϵ_{\parallel}
1[6]c	3.7	35	49
1[6]d	2.7	54	67
2[10]b	3.0	49	60
1-Sulf	2.5 ^b	44 ^c	54 ^c
1-Quin	3.3 ^b	39	45
	2.7	43 ^c	48 ^c

^a 10 μm cell. ^b Ref. 3. ^c 4 μm cell.

Computational results for **1[6]b** and **2[6]b** in Table 3 indicate that the value and orientation of the calculated dipole moment for both series of pyridinium zwitterions are essentially the same: 20 D oriented about 6° relative to the long molecular axis. Consequently, assuming a typical order parameter $S = 0.65$ and the Kirkwood factor $g = \mu_{\text{eff}}^2 / \mu^2 = 0.50$, the calculated dielectric anisotropy values in **ClEster** are $\Delta\epsilon = 115$ ($\epsilon_{\parallel} = 140$) for **1[6]b** and $\Delta\epsilon = 107$ ($\epsilon_{\parallel} = 130$) for **2[6]b**, according to the Maier-Meier relationship between molecular and bulk parameters of the nematic phase.¹⁸ Thus, the observed differences in the extrapolated dielectric parameters for the pyridinium zwitterions in Table 2 reflect different compatibility with the host: degree of aggregation (Kirkwood factor g) and impact on the order parameter (S_{app}).

Table 3. Calculated molecular parameters for selected compounds. ^a

Compound	$\mu_{ }$ /D	μ_{\perp} /D	μ /D	$\beta \square^b$ /°	$\Delta\alpha$ /Å ³	α_{avr} g /Å ³
1[6]b	20.1	2.36	20.3	6.7	37.	57.
	8		2		0	1
2[6]b	20.0	2.26	20.1	6.4	33/	59.
	3		5		4	1
1-Sulf	16.1	2.95	16.3	10.	24.	53.
	0		7	4	8	3
1-Quin	16.7	3.31	17.0	11.	23.	53.
	7		9	2	4	3

^a Dipole moments and polarizabilities obtained at the B3LYP/6-31G(d,p) level of theory in **ClEster** dielectric medium. Polarizability values calculated from diagonal polarizability tensors were converted from a.u. to Å³ using the factor 0.1482. ^b Angle between the net dipole vector μ and $\mu_{||}$.

In comparison, the same calculations for **1-Sulf** and **1-Quin**, with assumed $S = 0.65$ and $g = 0.50$, give the predicted values significantly lower, $\Delta\epsilon = 77$ ($\epsilon_{||} = 95$) and $\Delta\epsilon = 81$ ($\epsilon_{||} = 100$), respectively. Trends in computational results are consistent with the extrapolated experimental dielectric parameters in Table 2.

4.3.2.3 Conclusions

We have developed a method for efficient preparation of two types of 1-pyridinium zwitterions derived from the [*closo*-1-CB₉H₁₀]⁻ (**A**) and [*closo*-1-CB₁₁H₁₂]⁻ anions (**B**), that exhibit mesogenic properties and are suitable for low concentration, high $\Delta\epsilon$ additives to nematic hosts. The method appears to be general and opens access to a variety of derivatives of the general structure **II** where Q = 4-alkoxy-pyridine (Fig. 1). The method permits manipulation with the structure of R group and the alkoxy substituent for tuning properties of the compounds, especially

for improving solubility in the nematic hosts. Dielectric measurements indicate that the pyridinium zwitterions **1[n]** and **2[n]** are significantly more effective dipolar additives to nematic hosts than those previously investigated (**1-Sulf** and **1-Quin**).

4.3.2.4 Computational details

Quantum-mechanical calculations were carried out using Gaussian 09 suite of programs.¹⁹ Geometry optimizations for unconstrained conformers of **1[6]b** and **2[6]b** with the most extended molecular shapes were undertaken at the B3LYP/6-31G(d,p) level of theory using default convergence limits. The alkoxy group was set in all-*trans* conformation co-planar with the pyridine ring in the input structure. The orientation of the alkyl substituents on the alicyclic ring and carborane cage in the input structure was set according to conformational analysis of the corresponding 1-ethyl derivatives. No conformational search for the global minimum was attempted.

Calculations in solvent media using the PCM model²⁰ were requested with the SCRF(Solvent=Generic,Read) keyword and eps=3.07 and epsinf=2.286 input parameters.

Electronic excitation energies for **1[6]b** and **2[6]b** in MeCN dielectric medium were obtained at the B3LYP/6-31G(d,p) level using the time-dependent DFT method²¹ supplied in the Gaussian package. Solvent calculations using the PCM model²⁰ were requested with the SCRF(solvent=CH3CN) keyword. Selected molecular orbitals involved in these transitions are shown in Figures S5 and S6.

4.3.2.5 Experimental part

General. Reactions were carried out under Ar and subsequent manipulations were conducted in air. NMR spectra were obtained at 128 MHz (¹¹B) and 400 MHz (¹H) in

CDCl₃ or CD₃CN. ¹¹B chemical shifts were referenced to the solvent (¹H) or to an external sample of B(OH)₃ in MeOH (¹¹B, δ = 18.1 ppm). Optical microscopy and phase identification were performed using a polarized microscope equipped with a hot stage. Thermal analysis was obtained using a TA Instruments DSC using small samples of about 0.5-1.0 mg.

Binary mixtures preparation. Solutions of the pyridinium derivatives **1[n]** or **2[n]** in **CI Ester** host (15-20 mg of the host) were prepared in an open vial. The mixture of the compound and host in CH₂Cl₂ was heated for 2 hr at 60 °C to remove the solvent. The binary mixtures were analyzed by polarized optical microscopy (POM) to ensure that the mixtures were homogenous. The mixtures were then allowed to stand for 2 hr at room temperature before thermal and dielectric measurements.

Dielectric measurements. Dielectric properties of solutions of selected pyridinium **1[n]** or **2[n]** and **1-Quin** in **CI Ester** were measured by a Liquid Crystal Analytical System (LCAS - Series II, LC Vision, Inc.) using GLCAS software version 0.13.14, which implements literature procedures for dielectric constants.⁶ The homogenous binary mixtures were loaded into ITO electro-optical cells by capillary forces with moderate heating supplied by a heat gun. The cells (about 4 μm thick, electrode area 0.581 cm² or about 10 μm thick, electrode area 1.000 cm², and anti-parallel rubbed polyimide layer) were obtained from LC Vision, Inc. The filled cells were heated to an isotropic phase and cooled to room temperature before measuring dielectric properties. Default parameters were used for measurements: triangular shaped voltage bias ranging from 0.1-20 V at 1 kHz frequency. The threshold voltage V_{th} was measured at a 5% change. For each mixture the measurement was repeated 10 times

for two independent cells. The results were averaged to calculate the mixture's parameters. Results are shown in Tables S4–S6. All measurements were run at 25 °C. Error in concentration is estimated at about 1.5%. The dielectric values obtained for each concentration were fitted to a linear function in which the intercept was set at the value for the pure host measured in a 4 μm thick cell and homeotropic alignment. The resulting extrapolated values for pure additives are shown in Table 2.

General procedure for preparation of pyridinium derivatives 1[n] and 2[n]. A mixture of amine 3[n] or 4[n] (1 mmol) and the appropriate crude pyrylium triflate 5 [freshly prepared from 4-pyrone (1.2 mmol) and alkyl triflate 6] in THF (1 mL) under Ar was stirred overnight at rt. The solvent was evaporated to dryness to give a dark solid. Pure product 1[n] or 2[n] obtained as white crystalline solid in 34-51% yield by column chromatograph (CH₂Cl₂/hexane, 1:1) followed by recrystallization from *iso*-octane/toluene and then EtOH.

1[6]a. ¹H NMR (CDCl₃, 400 MHz) δ 0.3-2.8 (br m, 8H), 0.92 (t, *J* = 7.0 Hz, 3H), 0.99 (t, *J* = 7.1 Hz, 3H), 1.37-1.54 (m, 8H), 1.60 (quint, *J* = 14.6 Hz, 2H), 1.88-2.00 (m, 4H), 2.08 (pseudo t, *J* = 8.1 Hz, 2H), 4.35 (t, *J* = 6.5 Hz, 2H), 7.29 (d, *J* = 7.5 Hz, 2H), 9.14 (d, *J* = 7.5 Hz, 2H); ¹¹B NMR (CDCl₃, 128 MHz) δ -24.8 (d, *J* = 143 Hz, 4B), -15.4 (d, *J* = 137 Hz, 4B), 47.7 (s, 1B). Anal. Calcd. for C₁₇H₃₆B₉NO: C, 55.52; H, 9.87; N, 3.81. Found: C, 55.96; H, 9.91; N, 3.78%.

1[6]c. *ee* = 35% (AD-H Chiral, 15% EtOH in hexane), [α]_D²⁴ = +8° (c = 1.0, MeCN); ¹H NMR (CDCl₃, 400 MHz) δ 0.3-2.8 (br m, 8H), 0.90 (t, *J* = 6.9 Hz, 3H), 0.92 (t, *J* = 7.0 Hz, 3H) 1.30-1.49 (m, 12H), 1.51 (d, *J* = 6.1 Hz, 3H), 1.60 (quint, *J* = 7.1 Hz, 2H), 1.74-1.81 (m, 1H), 1.86-1.96 (m, 3H), 2.08 (pseudo t, *J* = 8.1 Hz, 2H), 4.77

(sextet, $J = 6.1$ Hz, 1H), 7.27 (d, $J = 6.5$ Hz, 2H), 9.16 (d, $J = 7.6$ Hz, 2H); ^{11}B NMR (CDCl_3 , 128 MHz) δ -24.9 (d, $J = 143$ Hz, 4B), -15.4 (d, $J = 139$ Hz, 4B), 47.2 (s, 1B); UV (MeCN), λ_{max} (log ϵ) 245 (4.06), 282 (4.16). Anal. Calcd. for $\text{C}_{20}\text{H}_{42}\text{B}_9\text{NO}$: C, 58.61; H, 10.33; N, 3.42. Found: C, 58.57; H, 10.26; N, 3.46%.

1[6]d. ^1H NMR (CDCl_3 , 400 MHz) δ 0.3-2.8 (br m, 8H), 0.90 (t, $J = 7.2$ Hz, 3H), 0.92 (t, $J = 7.0$ Hz, 3H), 1.01 (t, $J = 10.6$ Hz, 2H), 1.10-1.46 (m, 15H), 1.60 (quint, $J = 7.2$ Hz, 2H), 1.86-1.96 (m, 7H), 2.08 (pseudo t, $J = 8.0$ Hz, 2H), 4.14 (d, $J = 5.9$ Hz, 2H), 7.30 (d, $J = 7.6$ Hz, 2H), 9.16 (d, $J = 7.5$ Hz, 2H); $\{^1\text{H}\}^{11}\text{B}$ NMR (CDCl_3 , 128 MHz) δ -24.8 (4B), -15.4 (4B), 47.7 (1B). Anal. Calcd. for $\text{C}_{24}\text{H}_{48}\text{B}_9\text{NO}$: C, 62.13; H, 10.43; N, 3.02. Found: C, 62.35; H, 10.39; N, 3.03%.

2[5]b. ^1H NMR (CDCl_3 , 400 MHz) δ 0.66 (br s, 2H), 0.85 (t, $J = 7.0$ Hz, 3H), 0.89 (t, $J = 6.8$ Hz, 3H), 1.0-2.8 (br m, 10H), 1.20-1.40 (m, 12H), 1.41-1.49 (m, 2H), 1.89 (quint, $J = 7.0$ Hz, 2H), 4.26 (t, $J = 6.5$ Hz, 2H), 7.10 (d, $J = 7.8$ Hz, 2H), 8.86 (d, $J = 8.9$ Hz, 2H); $\{^1\text{H}\}^{11}\text{B}$ NMR (CDCl_3 , 128 MHz) δ -14.2 (5B), -11.6 (5B), 4.4 (1B). Anal. Calcd. for $\text{C}_{18}\text{H}_{40}\text{B}_{11}\text{NO}$: C, 53.30; H, 9.94; N, 3.45. Found: C, 53.52; H, 9.88; N, 3.40%.

2[10]b. ^1H NMR (CDCl_3 , 400 MHz) δ 0.66 (br s, 2H), 0.87 (t, $J = 7.0$ Hz, 3H), 0.89 (t, $J = 6.8$ Hz, 3H), 1.0-2.8 (br m, 10H), 1.23-1.28 (m, 16H), 1.31-1.39 (m, 2H), 1.42-1.49 (m, 2H), 1.89 (quint, $J = 7.0$ Hz, 2H), 4.26 (t, $J = 6.48$ Hz, 2H), 7.09 (d, $J = 7.8$ Hz, 2H), 8.87 (t, $J = 7.8$ Hz, 2H); ^{11}B NMR (CDCl_3 , 400 MHz) δ -14.1 (d, $J = 142$ Hz, 5B), -11.6 (d, $J = 137$ Hz, 5B), 4.8 (s, 1B). Anal. Calcd. for $\text{C}_{23}\text{H}_{50}\text{B}_{11}\text{NO}$: C, 58.09; H, 10.60; N, 2.95. Found: C, 58.13; H, 10.45; N, 2.99%.

2[6]c. ^1H NMR (CDCl_3 , 400 MHz) δ 0.66 (br s, 2H), 0.84-0.91 (m, 6H), 1.0-2.8 (br m, 10H), 1.24-1.37 (m, 16H), 1.44 (d, $J = 6.2$ Hz, 3H), 1.67-1.76 (m 1H), 1.79-1.84 (m, 1H), 4.67 (sextet, $J = 6.1$ Hz, 1H), 7.05 (d, $J = 7.8$ Hz, 2H), 8.84 (d, $J = 7.8$ Hz, 2H); $\{^1\text{H}\}$ ^{11}B NMR (CDCl_3 , 128 MHz) δ -14.2 (5B), -11.7 (5B), 4.34 (1B); UV (MeCN), λ_{max} ($\log \epsilon$) 264 (4.47). Anal. Calcd. for $\text{C}_{20}\text{H}_{44}\text{B}_{11}\text{NO}$: C, 55.42; H, 10.23; N, 3.23. Found: C, 55.71; H, 10.17; N, 3.28%.

General methods for preparation of pyrylium salts 5. Method A. A neat mixture of 4*H*-pyran-4-one (1 mmol) and alkyl triflate **6** (1 mmol) was stirred at 60 °C for 1 hr under Ar resulting in a brown oil. The mixture was cooled to rt and used without further purification.

Method B. A modified Method A by using CH_2Cl_2 (1 mL) as a solvent. After 1 hr, the solvent was removed *in vacuo* and the product was used without further purification.

Method C. A modified Method B by conducting the reaction at 0 °C to prevent decomposition of the secondary alkyl triflate. ^1H NMR data is provided in the ESI.

General methods for preparation of alkyl triflates 6.

Method A. Following a general method for alkyl triflates,²² to a vigorously stirred solution of triflic anhydride (1.2 mmol) in CH_2Cl_2 (15 mL) at 0 °C, a solution of pyridine (1 mmol) and primary alcohol (1 mmol) in CH_2Cl_2 (10 mL) was added dropwise over a 15-min period and the mixture was stirred for an additional 1 hr at 0 °C. The solution was washed with ice-cold H_2O , dried (Na_2SO_4) and evaporated to dryness to give the appropriate alkyl triflate **6** as a colorless liquid that quickly began to darken. The resulting mixture was filtered through a cotton plug and used without further purification.

Method B. To a vigorously stirred mixture of a secondary alcohol (1 mmol) and pyridine (1 mmol) at -78 °C in CH₂Cl₂ (25 mL) was added dropwise triflic anhydride (1 mmol). The mixture was stirred for 10 minutes at -78 °C and then kept at 0 °C until the alcohol was consumed (by TLC). The mixture was washed with ice-cold water, dried (Na₂SO₄) and the solvent was removed *in vacuo* at 0 °C. The resulting triflate **6** was kept at 0 °C and quickly used in the next step. ¹H NMR data is provided in the ESI.

Preparation of 1-decyl-12-(4-heptyloxyphenyl)-p-carborane (11[10]b). A solution of 1-decyl-12-(4-hydroxyphenyl)-p-carborane (**12[10]**, 125 mg, 0.318 mmol), heptyl tosylate (104 mg, 0.382 mmol), K₂CO₃ (132 mg, 0.956 mmol) and NBu₄Br (10 mg, 0.032 mmol) in anhydrous CH₃CN (5 mL) was refluxed overnight. The mixture was cooled down to rt and filtered. The residue was washed with CH₂Cl₂ (3x10 mL), dried (Na₂SO₄) and evaporated to dryness. The crude product was purified by column chromatography (hexane/CH₂Cl₂, 2:1) to give 160 mg of **11[10]b** as a colorless liquid, which was crystallized from CH₃CN containing a few drops of EtOAc at -80 °C: ¹H NMR (CDCl₃, 400 MHz) δ 0.88 (t, *J* = 7.1 Hz, 6H), 1.0-2.6 (br m, 10H), 1.12-1.42 (m, 24H), 1.64 (pseudo t, *J* = 8.1 Hz, 2H), 1.73 (quintet, *J* = 6.6 Hz, 2H), 3.87 (t, *J* = 6.5 Hz, 2H), 6.65 (d, *J* = 9.0 Hz, 2H), 7.09 (t, *J* = 9.0 Hz, 2H); ¹¹B NMR (CDCl₃, 128 MHz) δ -12.3 (d, *J* = 164 Hz). Anal. Calcd. for C₂₅H₅₀B₁₀O: C, 63.25; H, 10.62. Found: C, 63.99; H, 10.73%.

1-Decyl-12-(4-methoxyphenyl)-p-carborane (11[10]e). A solution of (4-methoxyphenyl)-p-carborane²³ (200 mg, 0.80 mmol) in Et₂O (3 mL) was treated with BuLi (0.8 mL, 1.90 mmol, 2.5M in hexanes) at -78 °C. The mixture was stirred for 15

minutes and then warmed up to rt and stirred for 2 hr. THF (1.0 mL) was added to the mixture and the solution was stirred for 1 hr at rt. The reaction was cooled to 0 °C and a solution of 1-iododecane (236 mg, 0.88 mmol) in Et₂O were added to the mixture. The reaction was allowed to warm up to rt and stirred overnight. The solvent was removed in *vacuo* and the residue was dissolved in CH₂Cl₂ and passed through a short silica gel plug. The solvent was evaporated and the resulting mixture was separated by column chromatography (hexane). The desired product **11[10]e** was isolated as the second fraction (122 mg, 40% yield) as a colorless film. The product was crystallized from CH₃CN containing a few drops of EtOAc and then cold EtOAc containing a few drops of hexane at -80 °C: mp 38-40 °C (no mesophase was detected upon cooling to -20 °C); ¹H NMR (CDCl₃, 400 MHz) δ 0.88 (t, *J* = 7.1 Hz, 3H), 1.0-2.6 (br m, 10H), 1.12-1.35 (m, 16H), 1.65 (pseudo t, *J* = 8.1 Hz, 2H), 3.74 (s, 3H), 6.67 (d, *J* = 9.0 Hz, 2H), 7.11 (d, *J* = 9.0 Hz, 2H); ¹¹B NMR (CDCl₃, 128 MHz) δ -12.3 (d, *J* = 164 Hz); Anal. Calcd. for C₁₉H₃₈B₁₀O: C, 58.42; H, 9.81. Found: C, 58.84; H, 9.39%.

The first oily fraction (27 mg), obtained in the chromatographic separation of **11[10]e**, was identified as **1-decyl-12-(3-decyl-4-methoxyphenyl)-*p*-carborane** which apparently resulted from *ortho*-lithiation of (4-methoxyphenyl)-*p*-carborane under the reaction conditions: ¹H NMR (CDCl₃, 400 MHz) δ 0.88 (t, *J* = 6.9 Hz, 3H), 0.89 (t, *J* = 7.7 Hz, 3H), 1.05-1.35 (m, 30H), 1.44-1.52 (m, 2H), 1.64 (br t, *J* = 8.2 Hz, 2H), 2.48 (t, *J* = 7.7 Hz, 2H), 3.74 (s, 3H), 6.58 (d, *J* = 8.7 Hz, 1H), 6.94 (d, *J* = 2.6 Hz, 1H), 6.98 (dd, *J*₁ = 8.6 Hz, *J*₂ = 2.6 Hz, 1H); ¹¹B NMR (CDCl₃, 128 MHz) δ -12.3 (d, *J* = 163 Hz, 10B); HRMS, Calcd for C₂₉H₅₉B₁₀O: *m/z* = 533.5496, found *m/z* = 533.5507.

1-Decyl-12-(4-hydroxyphenyl)-p-carborane (12[10]). A solution of 1-decyl-12-(4-methoxyphenyl)-p-carborane (**11[10]e**, 187 mg, 0.478 mmol) in CH₂Cl₂ (5 mL) was treated with BBr₃ (360 mg, 1.44 mmol, 1.0M in CH₂Cl₂,) at 0 °C and the reaction was allowed to warm up to rt and stirred overnight. Water (10 mL) was added to the mixture and the organic layer was separated, dried (Na₂SO₄) and evaporated to dryness to give the crude product as a colorless film, which was purified by column chromatography (CH₂Cl₂) to give 145 mg (78% yield) of a white solid. The product was recrystallized at -80 °C from CH₃CN containing a few drops of EtOAc and then EtOAc containing a few drops of hexane to give phenol **12[10]** as a colorless film: ¹H NMR (CDCl₃, 400 MHz) δ 0.88 (t, *J* = 7.1 Hz, 3H), 1.0-2.6 (br m, 10H), 1.10-1.30 (m, 16H), 1.64 (pseudo t, *J* = 8.1 Hz, 2H), 4.71 (s, 1H), 6.59 (d, *J* = 8.9 Hz, 2H), 7.06 (d, *J* = 8.8 Hz, 2H); ¹¹B NMR (CDCl₃, 128 MHz) δ -12.3 (d, *J* = 164 Hz). Anal. Calcd. for C₁₈H₃₆B₁₀O: C, 57.41; H, 9.64. Found: C, 57.18; H, 9.33%.

4.3.2.6 Acknowledgements

This work was supported by the NSF grant DMR-1207585. We are grateful to Professor Roman Dąbrowski of Military University of Technology (Warsaw, Poland) for the gift of CIEster.

4.3.2.7 References

- 1 L. M. Blinov, V. G. Chigrinov *Electrooptic Effects in Liquid Crystal Materials*; Springer-Verlag: New York, 1994.
- 2 P. Kirsch, M. Bremer *Angew. Chem., Int. Ed.* 2000, **39**, 4216.
- 3 B. Ringstrand, P. Kaszynski, A. Januszko, V. G. Young, Jr. *J. Mater. Chem.* 2009, **19**, 9204.

- 4 J. Pecyna, B. Ringstrand, M. Bremer, P. Kaszynski *in preparation*.
- 5 J. Pecyna, R. P. Denicola, B. Ringstrand, A. Jankowiak, P. Kaszynski *Polyhedron* 2011, **30**, 2505.
- 6 B. Ringstrand, P. Kaszynski *J. Mater. Chem.* 2011, **21**, 90.
- 7 B. Ringstrand, P. Kaszynski *J. Mater. Chem.* 2010, **20**, 9613.
- 8 B. Ringstrand, P. Kaszynski, A. Franken *Inorg. Chem.* 2009, **48**, 7313.
- 9 J. Pecyna, B. Ringstrand, S. Pakhomov, A. G. Douglass, P. Kaszynski *in preparation*.
- 10 A. R. Katritzky *Tetrahedron* 1980, **36**, 679.
- 11 H. Ishino, S. Tokunaga, H. Seino, Y. Ishii, M. Hidai *Inorg. Chem.* 1999, **38**, 2489.
- 12 P. Mäding, J. Steinbach, B. Johannsen *J. Labelled Compd Radiopharm.* 2000, **43**, 565.
- 13 B. Ringstrand, H. Monobe, P. Kaszynski *J. Mater. Chem.* 2009, **19**, 4805.
- 14 For details see the Electronic Supplementary Information.
- 15 A. Jankowiak, A. Baliński, J. E. Harvey, K. Mason, A. Januszko, P. Kaszyński, V. G. Young, Jr., A. Persoons *J. Mater. Chem. C* 2013, **1**, 1144.
- 16 P. Kaszynski In *Boron Science: New Technologies & Applications*; Hosmane, N., Ed.; CRC Press: 2012, p 305.
- 17 B. Ringstrand, A. Jankowiak, L. E. Johnson, P. Kaszynski, D. Pocięcha, E. Górecka *J. Mater. Chem.* 2012, **22**, 4874.
- 18 W. Maier, G. Meier *Z. Naturforsch.* 1961, **16A**, 262.
- 19 Gaussian 09, Revision A.02, M. J. Frisch, G. W. Trucks, H. B. Schlegel, G. E. Scuseria, M. A. Robb, J. R. Cheeseman, G. Scalmani, V. Barone, B. Mennucci, G. A. Petersson, H. Nakatsuji, M. Caricato, X. Li, H. P. Hratchian, A. F. Izmaylov, J. Bloino, G. Zheng, J. L. Sonnenberg, M. Hada, M. Ehara, K. Toyota, R. Fukuda, J. Hasegawa, M.

Ishida, T. Nakajima, Y. Honda, O. Kitao, H. Nakai, T. Vreven, J. A. Montgomery, Jr., J. E. Peralta, F. Ogliaro, M. Bearpark, J. J. Heyd, E. Brothers, K. N. Kudin, V. N. Staroverov, R. Kobayashi, J. Normand, K. Raghavachari, A. Rendell, J. C. Burant, S. S. Iyengar, J. Tomasi, M. Cossi, N. Rega, J. M. Millam, M. Klene, J. E. Knox, J. B. Cross, V. Bakken, C. Adamo, J. Jaramillo, R. Gomperts, R. E. Stratmann, O. Yazyev, A. J. Austin, R. Cammi, C. Pomelli, J. W. Ochterski, R. L. Martin, K. Morokuma, V. G. Zakrzewski, G. A. Voth, P. Salvador, J. J. Dannenberg, S. Dapprich, A. D. Daniels, O. Farkas, J. B. Foresman, J. V. Ortiz, J. Cioslowski, and D. J. Fox, Gaussian, Inc., Wallingford CT, 2009.

20 M. Cossi, G. Scalmani, N. Rega, V. Barone *J. Chem. Phys.* 2002, **117**, 43.

21 R. E. Stratmann, G. E. Scuseria, M. J. Frisch *J. Chem. Phys.* 1998, **109**, 8218.

22 S. Wang, A. Zhang *Org. Prep. Proc. Int.* 2008, **40**, 293.

23 M. A. Fox, J. A. H. MacBride, R. J. Peace, K. Wade *J. Chem. Soc., Dalton Trans.* 1998, 401.

Chapter 5. Isostructural polar/non-polar liquid crystals for probing polarity effects in liquid crystals.

5.1 Introduction

Dipole moment and its orientation play a significant role when designing molecules for electro-optical applications. However, little was known about how the dipole moment affects the stability of a mesophase due to the lack of proper experimental models. Moreover, any change in molecular dipole moment is typically associated with the change in molecular geometry. Recently, however, it was discovered that the replacement of a C–C bond in [*closo*-1,10-C₂B₈H₁₀] derivatives with isosteric and isoelectronic N⁺–B[–] fragment in derivatives of the [*closo*-1-CB₉H₁₀][–] anion could serve as a tool to assess the influence of molecular dipole moment on the stability of a mesophase.¹ Such replacement results in a significant change of the molecular dipole moment with a negligible change in the molecular geometry.

The following chapter constitutes an important contribution to the fundamental understanding of the liquid crystal phenomena. The studies described in the following section explain the role of the dipole moment in the stabilization of a mesophase using carefully designed pairs of polar and nonpolar derivatives of the [*closo*-1-CB₁₁H₁₂][–] and [*closo*-C₂B₁₀H₁₂] clusters, respectively.

References

- (1) Ringstrand, B.; Kaszynski, P., How much can an electric dipole moment stabilize a nematic phase? Polar and non-polar isosteric derivatives of [*closo*-1-CB₉H₁₀][–] and [*closo*-1,10-C₂B₈H₁₀]. *J. Mater. Chem.* **2010**, *20*, 9613-9615.

5.2 The effect of molecular polarity on nematic stability in 12-vertex carboranes.

5.2.1 Description and contributions

The goal of this project was to validate the findings for the 10-vertex polar – nonpolar pairs that a uniform change in dipole moment does not correspond to a uniform change in clearing temperature T_{NI} . The [*closo*-1-CB₁₁H₁₂]⁻ and [*closo*-C₂B₁₀H₁₂] clusters were chosen for this purpose since they are structurally the closest analogues of the 10-vertex clusters that were previously investigated.

A series of esters based on pyridinium acid [*closo*-1-CB₁₁H₁₀-1-COOH-12-(4-C₇H₁₅OC₅H₄N)] (**4[12]**) and its non-polar analogue, acid [*closo*-1,12-C₂B₁₀H₁₀-1-COOH-12-(4-C₇H₁₅OC₆H₄)] (**3[12]**) were synthesized and their mesogenic properties were analyzed. The results of thermal analysis of the esters confirmed the previous findings for the 10-vertex analogues that the uniform increase in molecular dipole moment does not correspond to a uniform change in the clearing temperature. Quantum computational calculations confirmed that the replacement of C–C fragment with the N⁺–B⁻ increased the dipole moment, while essentially unaffected the molecular geometry significantly.

My role in this project was to synthesize the two acids and their esters **3[12]** and **4[12]**, and to obtain their full characterization. I also performed thermal analysis of the compounds. Rich Denicola and Harrison Gray, undergraduate students, contributed to the project by synthesizing small quantities of the acids in the early stage of this work. Dr. Bryan Ringstrand assisted in purification of a several esters. Prof. Piotr Kaszynski performed quantum mechanical calculations.

In the following chapter the entire text of the manuscript is included for consistency of the narrative, however, the experimental section contains only experiments performed by me.

5.2.2 The manuscript

Reproduced by permission of Taylor & Francis Online

Pecyna, J.; Denicola, R. O.; Gray, H. M.; Ringstrand, B.; Kaszynski, P. *Liq. Cryst.* **2014**, *41*, 1188-1198.

Copyright 2014 Taylor & Francis Online. Available online:

<http://www.tandfonline.com/doi/abs/10.1080/02678292.2014.911371>

5.2.2.1 Introduction

The molecular dipole moment and its orientation with respect to the main rotational axis are important parameters considered in the design of liquid crystals for electrooptical applications.[1,2] These two parameters give rise to dielectric anisotropy $\Delta\epsilon$ which allows for electrooptical switching of the molecules.[3,4] Despite its significance, there is little known about how the molecular dipole moment, as the *only* variable, impacts phase structure and stability. Typically, modification of the molecular dipole moment is associated with changes of the molecular geometry and dynamics, and experimental studies of the effect are hindered by lack of appropriate molecular models.

Recently, we used the concept of the isosteric polar replacement of the C–C fragment with the N⁺–B[–] fragment[5] and investigated pairs of structurally analogous and essentially geometrically identical derivatives of the [*closo*-1,10-C₂B₈H₁₀] and [*closo*-1-CB₉H₁₀][–] clusters ([**10**] Figure 1) that display nematic behavior.[6] The exchange of C–C for N⁺–B[–] resulted in a uniform increase of the longitudinal dipole moment $\mu_{||}$ by about 12 D in the pairs of non-polar (**1**[**10**]) and polar (**2**[**10**]) derivatives. Surprisingly, the uniform increase of $\mu_{||}$ did not result in a uniform

change of the clearing temperature T_{NI} in the series. This result was rationalized by differential dielectric screening of the dipole-dipole interactions by the ester molecular subunits. It is worth mentioning that one of the compounds, ester **2**[**10**]e, was found to have a record high dielectric anisotropy $\Delta\epsilon$ of 113,[7] and for this reason polar mesogens of structure **2** are of interest for practical applications. In order to verify the general validity of findings for the 10-vertex clusters and search for new high $\Delta\epsilon$ materials, we expanded our investigations to the 12-vertex analogues [**12**] (Figure 1).

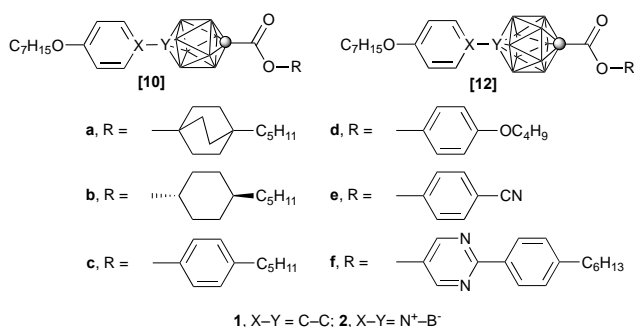


Figure 1. Structures of nematics derived from 10-vertex ([**10**]) and 12-vertex ([**12**]) clusters. Each vertex represents a BH fragment and the sphere is a carbon atom.

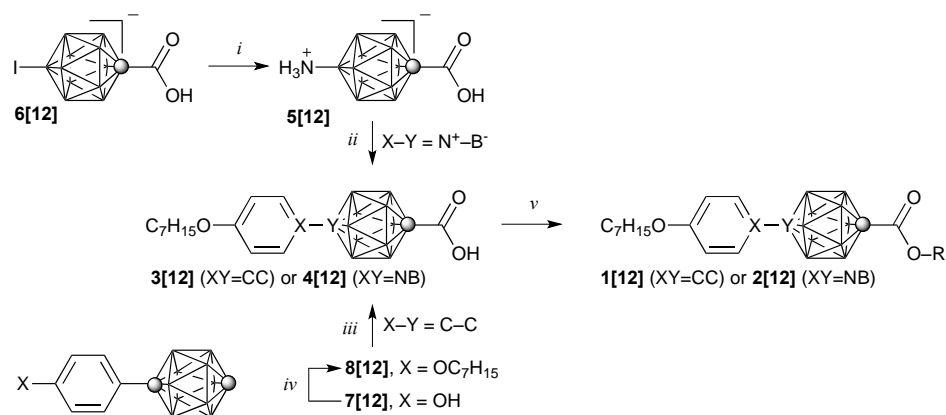
Here, we report a series of non-polar (**1**) – polar (**2**) isosteric pairs of nematic 12-vertex cluster derivatives, [**12**]b–[**12**]f, in which the non-polar C–C fragment is replaced with the polar N⁺–B⁻ fragment. We analyzed the effect of the increase of the dipole moment within the 12-vertex series itself, and also considered the effect of the cluster size (12-vertex *vs* 10-vertex) on phase stability.

5.2.2.2 Results

Synthesis

Colorless esters **[12]b**–**[12]f** were obtained from carboxylic acid **3[12]** (series **1[12]**) or **4[12]** (series **2[12]**) and the appropriate phenol or cyclohexanol through acid chloride (Scheme 1). Ester **[12]a** was not prepared due to low yield of the process.[6] The preparation of acid **4[12]** expanded on our previous results obtained for diazotization of [*closo*-1-CB₉H₈-1-COOH-6-NH₃] and [*closo*-1-CB₁₁H₁₁-12-NH₃] in 4-methoxypyridine solutions, which directly leads to the corresponding 6-pyridinium acid [*closo*-1-CB₉H₈-1-COOH-6-(4-MeOC₅H₄N)] and [*closo*-1-CB₁₁H₁₁-12-(4-MeOC₅H₄N)], through an unstable diazonium intermediates.[8,9] Thus, diazotization of amino acid [*closo*-1-CB₁₁H₁₀-1-COOH-12-NH₃] (**5[12]**) with [NO]⁺[PF₆]⁻ in a neat solution of 4-heptyloxypyridine gave acid **4[12]** in 6% yield. The prerequisite amino acid **5[12]** was obtained in 40% yield by Pd-catalyzed amination of iodo acid [*closo*-1-CB₁₁H₁₀-1-COOH-12-I]⁻ (**6[12]**)[10] using conditions described for the 10-vertex analogue.[11,12]

Acid **3[12]**[13] was prepared in three steps from 1-(4-hydroxyphenyl)-*p*-carborane[14] (**7[12]**, Scheme 1). Thus, phenol **7[12]** was *O*-alkylated with heptyl tosylate to facilitate separation of the resulting heptyloxyphenyl derivative **8[12]** from the alkylating reagent, giving the desired product **8[12]** in higher yield (89%) compared to direct arylation of *p*-carborane with 1-heptyloxy-4-iodobenzene.[15] Carboxylic acid **4[12]** was obtained by direct carboxylation of **8[12]** in 92% yield, which is more convenient than a two-step preparation through its methyl ester.[13]



Scheme 1. Synthesis of esters **1[12]** and **2[12]**. Reagents and conditions: *i*) Pd₂dba₃, 2-(Chx₂P)biphenyl, LiHMDS, THF, reflux, 72 h; *ii*) 4-heptyloxypyridine, [NO]⁺[PF₆]⁻, -15 °C, 8 h; *iii*) 1. *n*-BuLi, THF, -78 °C; 2. CO₂. 3. H₃O⁺; *iv*) C₇H₁₅OTs, K₂CO₃, [NBu₄]⁺[Br]⁻, CH₃CN, reflux, 12 h; *v*) 1. (COCl)₂, 2. ROH, Pyr.

Thermal analysis

Transition temperatures and enthalpies of the mesogens were obtained by differential scanning calorimetry (DSC). Phase structures were assigned by polarizing optical microscopy and the results are shown in Table 1.

Table 1. Transition temperatures for [12]b–[12]f and [10]f.^a

	X–Y	Cr		N		I
[12]b	C–C	•	72 (23.9)	•	114 (1.3)	•
	N ⁺ –B ⁻	•	154 (28.8)	•	176 (0.9)	•
[12]c	C–C	•	51 (30.5)	•	100 (1.3)	•
	N ⁺ –B ⁻	•	134 (15.0) ^b	(•	133 (0.7) ^c)	•
[12]d	C–C	•	54 (28.5)	•	130 (1.7)	•
	N ⁺ –B ⁻	•	142 (19.2)	•	172 (0.9)	•
[12]e	C–C	•	99 (31.9)	•	124 (0.9)	•
	N ⁺ –B ⁻	•	155 (29.3) ^d	(•	151 (0.4) ^e)	•
[12]f	C–C	•	81 (37.1)	•	211 (1.4) ^e	•
	N ⁺ –B ⁻	•	184 (32.9)	•	263 (1.5) ^e	•
[10]f	C–C	•	100 (29.0) ^f	•	214 (1.1) ^e	•
	N ⁺ –B ⁻	•	159 (31.1) ^g	•	262 (0.4) ^e	•

^a Cr-crystal, N-nematic, I-isotropic. Temperatures obtained on heating at 5 K min⁻¹. ^b Cr₁ 125 (16.8) Cr₂. ^c Obtained on cooling. ^d Cr₁ 137 (3.0) Cr₂. ^e Heating rate 10 K min⁻¹. ^f Cr₁ 45 (1.8) Cr₂. ^g Cr₁ 147 (8.7) Cr₂.

Optical and thermal analysis demonstrated that all derivatives [12]b–[12]f exhibit only a nematic phase (Table 1), which is consistent with findings for the [10]a–[10]e series.[6] In general, polar nematics **2** have significantly higher transition temperatures than the non-polar analogues **1**. Consistent with our previous findings for [10],[6] the lowest clearing temperature is observed for the pentylphenol esters [12]c and the highest for pyrimidinol esters [12]f in both series **1** and **2**.

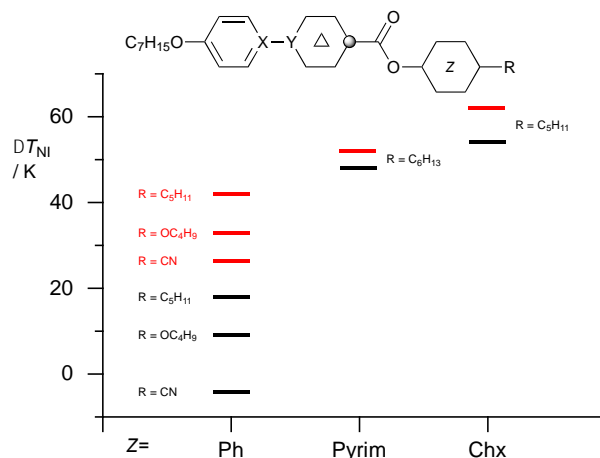


Figure 2. A plot of the ΔT_{NI} for series [10] (black) and for series [12] (red). ΔT_{NI} represents the difference between T_{NI} of polar (2) and T_{NI} of non-polar (1) mesogen in each series.

A comparison of the two series of 12-vertex derivatives, **1**[12] and **2**[12], shows that the difference in the clearing temperatures ΔT_{NI} , defined as $T_{NI}(2) - T_{NI}(1)$, is not uniform for all five pairs; the largest difference in clearing temperatures of $\Delta T_{NI} = 62$ is observed for pair [12]**b** (pentylcyclohexanol esters) and the lowest, $\Delta T_{NI} = 27$, for pair [12]**e** (cyanophenol esters). A plot of ΔT_{NI} values for pairs [12] demonstrates the same trend as observed previously for series [10] (Figure 2). The ΔT_{NI} values are systematically larger for series [12] than those for the 10-vertex analogues. Moreover, the data reveals a reasonable linear correlation for ΔT_{NI} in both series [10] and series [12] (Figure 3). This suggests that the remote substituent has a strong and consistent impact on intermolecular interactions and hence phase stability in both series.

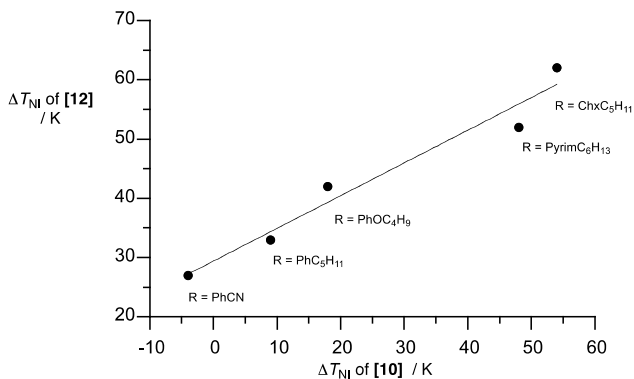


Figure 3. A plot of ΔT_{NI} for the [10] series versus the ΔT_{NI} of the [12] analogues; slope = 0.55, $r^2 = 0.96$.

The available data also permits the analysis of the effect of cluster size on nematic phase stability in the two series. Thus, a comparison of T_{NI} of polar mesogens **2**[10] with **2**[12] shows an excellent linear correlation (Figure 4). Similar relationship was found for the non-polar analogues, although the datapoint for the cyclohexyl ester **1b** falls outside the correlation. In general, the data indicates higher nematic phase stability for series [10] in the non-polar derivatives **1**, while 12-vertex derivatives exhibit higher mesophase stability for polar compounds **2**. These trends result in the observed uniformly higher ΔT_{NI} values for the 12-vertex series than for series [10], as demonstrated in Figures 2 and 4.

Molecular structure and properties

For a better understanding of the impact on the molecular level of the replacement of the C–C fragment in series **1** with the $N^+–B^-$ fragment in series **2**, molecular dimensions and electronic properties of the two series of nematics [12]**b**–[12]**f** were calculated in their most extended conformations at the B3LYP/6-31G(d,p) level of theory in the gas phase. Analysis of the data in Table 2 shows that

replacement of C–C with N⁺–B[−] results in a significant change of the molecular dipole moment and negligible change in electronic polarizability and geometry (Table 3). Thus, the replacement increases the longitudinal component of the dipole $\mu_{||}$ by 11.3 ± 0.2 D and the transverse component μ_{\perp} by an average of 1.4 D (Table 2). At the same time, electronic polarizability $\alpha_{||}$ increases by about 0.2 \AA^3 or about 0.4%, while the average α slightly decreases by 0.06 \AA^3 . The polar molecules are longer by 5.2 ± 1 pm or $\sim 0.2\%$ as a result of minor expansion of the aryl–cage bond and the {*closo*-1-CB₁₁} cage by 4.5 ± 0.04 pm and 6.2 ± 0.1 pm, respectively, and contraction of the aryl ring and cage–COO bond by -3.3 ± 0.04 pm and -0.5 ± 0.04 pm, respectively (Table 3).

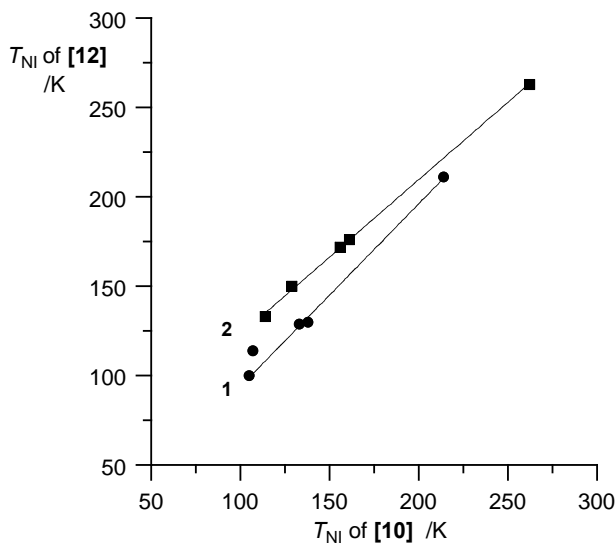


Figure 4. A plot of T_{NI} of the [10] series *vs* the T_{NI} of the [12] analogues for the non-polar (circles) and polar (diamonds) derivatives. Best fit functions: $T_{\text{NI}}[\mathbf{12}] = 1.03 \times T_{\text{NI}}[\mathbf{10}] - 11.2$, $r^2 = 0.998$ for series 1 (excluding **1b**); $T_{\text{NI}}[\mathbf{12}] = 0.87 \times T_{\text{NI}}[\mathbf{10}] + 36.3$, $r^2 = 0.999$ for series 2.

Table 2. Calculated molecular parameters for **[12]b**–**[12]f**.^a

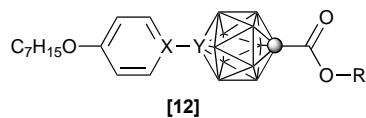
Compound	$\mu_{ }$	μ_{\perp}	μ	$\alpha_{ }$	α_{\perp}	α	$\Delta\alpha$
	/D	/D	/D	/Å ³	/Å ³	/Å ³	/Å ³
1[12]b	1.11	1.42	1.80	89.5	47.5	42.1	61.5
2[12]b	12.16	3.02	12.53	89.6	47.7	41.9	61.7
1[12]c	1.60	1.16	1.97	94.6	46.0	48.6	62.2
2[12]c	12.77	3.13	13.14	94.6	46.2	48.4	62.3
1[12]d	0.80	1.72	1.89	94.6	44.8	49.9	61.4
2[12]d	12.07	3.42	12.54	94.4	45.0	49.5	61.4
1[12]e	7.71	0.53	7.73	88.9	39.8	49.1	56.2
2[12]e	18.99	1.88	19.08	88.7	40.0	48.6	56.2
1[12]f	3.73	1.79	4.14	121.8	52.4	69.4	75.5
2[12]f	15.38	2.38	15.56	121.5	52.6	68.9	75.5

^a Obtained at the B3LYP/6-31G(d,p) level of theory.

To shed more light on the origin of the increased nematic phase stability in polar derivatives, we assessed the interaction energy of a non-polar pair **1[12]d** and compared it to that of its polar analogue **2[12]d**. The calculations were conducted using the M06-2x functional, which reasonably well reproduces non-covalent interactions.[16] Thus, two molecules of **1[12]d** at equilibrium geometry were set antiparallel at a distance of about 4 Å in vacuum and the geometry of the system was optimized. Subsequently, the C–C fragment in **1[12]d** was replaced with the N⁺–B[−] fragment giving two molecules of **2[12]d**, and the geometry was fully optimized again. The resulting equilibrium geometry of **2[12]d–2[12]d** is essentially the same as of the non-polar pair of **1[12]d–1[12]d**. In the resulting molecular complex, the {*closo*-1-CB₁₁} clusters sit above the pyridine rings with the closest B[−]⋯N

intermolecular distance of about 3.6 Å. A comparison of the energies for isolated molecules and the dimeric associates gives the interaction energy of $\Delta H = -9.7$ kcal mol⁻¹ for **1[12]d–1[12]d** and $\Delta H = -22.7$ kcal mol⁻¹ for **2[12]d–2[12]d** (or $\Delta G_{298} = +12.4$ kcal mol⁻¹ and $\Delta G_{298} = +0.1$ kcal mol⁻¹, respectively) in gas phase. Thus, significantly higher association energy (by 13 kcal mol⁻¹) for the polar derivatives corresponds to a higher melting point by nearly 90 K and higher mesophase stability by 42 K of **2[12]d** when compared to **1[12]d**. This significant difference in energy is presumably smaller in the dielectric medium of the condensed phase.

Table 3. Selected structural parameters for [12]b–[12]f.^a



Compound	X–Y	$d_{C...X}$ /Å	d_{X-Y} /Å	$d_{Y...C}$ /Å	d_{C-COO} /Å	L^b /Å
1[12]b	C–C	2.827	1.514	3.130	1.524	31.56
2[12]b	N ⁺ –B ⁻	2.793	1.559	3.193	1.519	31.60
1[12]c	C–C	2.827	1.514	3.131	1.521	31.00
2[12]c	N ⁺ –B ⁻	2.794	1.559	3.192	1.516	31.07
1[12]d	C–C	2.827	1.514	3.130	1.521	31.48
2[12]d	N ⁺ –B ⁻	2.794	1.559	3.192	1.517	31.53
1[12]e	C–C	2.827	1.514	3.129	1.518	27.20
2[12]e	N ⁺ –B ⁻	2.794	1.558	3.190	1.513	27.24
1[12]f	C–C	2.827	1.514	3.129	1.517	36.67
2[12]f	N ⁺ –B ⁻	2.794	1.559	3.190	1.512	36.73
average Δd		-0.033	0.045	0.062	-0.005	0.052
		± 0.0004	± 0.0004	± 0.001	± 0.0004	± 0.013

^a Obtained at the B3LYP/6-31G(d,p) level of theory. Distances in Å. ^b Molecular length measured as a distance between two terminal hydrogen atoms on the alkyl chains or H...N for [12]e.

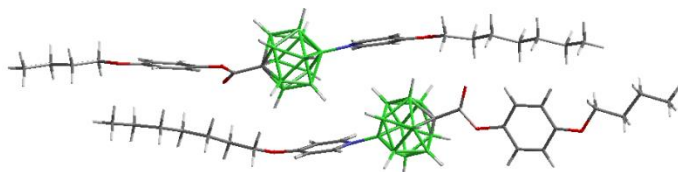


Figure 5. Optimized geometry of two molecules of **2[12]d** obtained at the M06-2x/3-21G* level of theory in gas phase.

5.2.2.3 Discussion and conclusions

The isoelectronic pairs of *p*-carboranes and monocarbaborates offer a unique opportunity to investigate the effect of the molecular dipole moment on phase stability and assist in the development of new materials for display applications. Although the preparation of pyridinium acid **4[12]**, the key intermediate to polar mesogens **2[12]**, is low yield at the moment, its successful synthesis permits studies of fundamental aspects of the liquid crystalline state. The preparation of amino acid **5[12]**, the precursor to **4[12]**, from B₁₀H₁₄ is accomplished in 5 steps and about 10% yield, which compares to 6 steps and 6% overall yield for the synthesis of 10-vertex amino acid **5[10]**.^[11] While the subsequent transformation of **5[10]** to pyridinium acid **4[10]** is accomplished in two steps and about 50% yield,^[6] the single step diazotization of **5[12]** gives the desired **4[12]** in poor yield of 6%. Thus, improving the yield of the last transformation (**5[12]**→**4[12]**) would make compounds **2[12]** more attractive for practical applications.

Mesogenic behavior of compounds in series **[12]** is consistent with findings for 10-vertex series **[10]**: only nematic phases are found in both series and observed trends in T_{NI} are identical. Quantum-mechanical modeling demonstrated that replacement of the non-polar C–C fragment with the polar N⁺–B⁻ group in either series, **[12]** or **[10]**,^[6] practically does not change either the geometry (within 0.2 %) or the conformational properties of the molecules, but significantly increases the dipole moment oriented along the long molecular axis by about 11.3 D and 12 D, respectively. Similar to the findings for the 10-vertex series **[10]**,^[6] the uniform increase of the dipole moment does not correspond to a uniform change in the

clearing temperature, T_{NI} . Since the trends are the same in both series, the observed effect of the remote substituent on the ΔT_{NI} for each pair of compounds appears to be general.

The increase of molecular polarity, resulting from the C–C for N⁺–B[–] replacement, increases the energy of intermolecular association. As calculated for two pairs of molecules, non-polar **1**[**12**]**d**–**1**[**12**]**d** and polar **2**[**12**]**d**–**2**[**12**]**d**, this additional stabilization of 13 kcal mol^{–1} for the polar molecules is substantial and consistent with higher transition temperatures generally observed in series **2**. Although not calculated, it can be assumed that this association energy can be affected by remote substituents (ester residues) either through steric (molecular overlap, *c.f.* Figure 5) or electronic (dipolar interactions, dielectric screening, etc.) factors. However, one should remember that the difference in the association energy was calculated in vacuum without dielectric medium of the condensed phase and without conformational search.

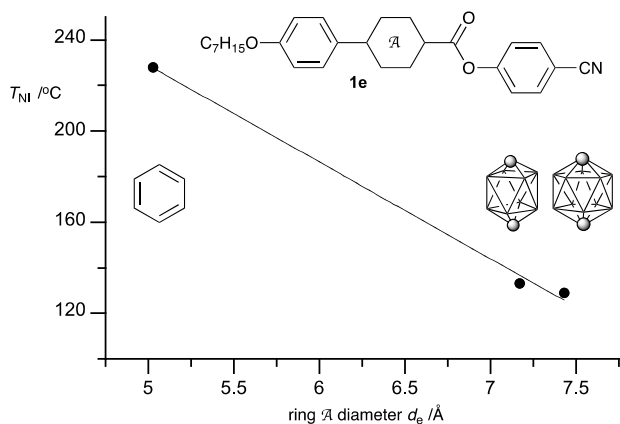


Figure 6. N–I transition temperature (T_{NI}) as a function of the diameter of ring A in **1e**.

Finally, results presented here demonstrate once again that the phase stability depends on the size of the structural elements in the rigid core.[17,18] A comparison

of three isostructural mesogens **1e** shows a linear decrease of T_{NI} with increasing size of the core element A (Figure 6). Thus, **1[Ph]e**,[19] in which benzene ring has the smallest effective Van der Waals diameter d_e ,[20] possesses the highest nematic phase stability. Conversely, **1[12]e** with the largest core element has the lowest T_{NI} . It appears that the bulky carborane cluster near the center of the molecule provides sufficient disruption of molecular packing arrangements and destabilizes the nematic phase relative to benzene analogues. It also completely suppresses formation of smectic phases in series **2**, which, in general, are very seldom observed in carborane-containing mesogens.[18]

Overall, analysis of series **[12]** confirmed our previous findings for 10-vertex series **[10]**, and provided additional rare experimental data for further theoretical analysis of the fundamental issue of molecular dipole moment impact on mesophase stability.

5.2.2.4 Computational details

Quantum-mechanical calculations were carried out using Gaussian 09 suite of programs.[21] Geometry optimizations for unconstrained conformers of **[12]b–[12]f** with the most extended molecular shapes were undertaken at the B3LYP/6-31G(d,p) level of theory using default convergence limits. The alkoxy group was set in all-*trans* conformation co-planar with the aromatic ring in the input structure. The aromatic ring and the carboxyl group were set staggered with the carborane cage as found experimentally and computationally in related structures. The orientation of the alkyl and carbonyloxy substituents on the alicyclic ring was set according to conformational analysis of the corresponding 1-ethyl and 1-acetoxy derivatives of cyclohexane. Optimized structures of the non-polar compounds served as starting

points for optimization of the polar analogues after replacing the two carbon atoms with B and N.

Interaction energy in a binary system of **1[12]d** was obtained using the M06-2x functional [16] with 3-21G* basis set. Two molecules of **1[12]d** at equilibrium geometry (M06-2x/3-21G*) were aligned antiparallel about 4 Å apart in the input structure, and the geometry of the pair was minimized. The resulting energy was corrected for basis set superposition error (BSSE) by running single point calculations (M06-2x/3-21G**/M06-2x/3-21G*) at the equilibrium geometry with the keyword COUNTERPOISE=2.[22] The optimized geometry of the non-polar pair **1[12]d-1[12]d** served as the starting point for calculations involving the polar pair **2[12]d-2[12]d**, after replacement of the C-C fragments with the B-N. Conformational search was not attempted.

5.2.2.5 Experimental

General

Reagents and solvents were obtained commercially. Reactions were carried out under Ar, and subsequent manipulations were conducted in air. NMR spectra were obtained at 128 MHz (¹¹B) and 400 MHz (¹H) in CD₃CN or CDCl₃. ¹H NMR spectra were referenced to the solvent, and ¹¹B NMR chemical shifts were referenced to an external boric acid sample in CH₃OH that was set to 18.1 ppm. Optical microscopy and phase identification were performed using a polarized microscope equipped with a hot stage. Thermal analysis was obtained using a TA Instruments DSC using small samples of about 0.5-1.0 mg. Transition temperatures (onset) and enthalpies were obtained on heating using small samples (0.5-1 mg) and a heating rate of 5 K min⁻¹ under a flow of nitrogen gas unless specified otherwise.

General Procedure for Preparation of Esters [12]b–[12]f

Method A. A mixture of carboxylic acid (0.25 mmol) and anhydrous CH_2Cl_2 (1 mL) was treated with $(\text{COCl})_2$ (0.75 mmol) and a drop of dry DMF at rt. The mixture began to bubble, and the reaction became homogeneous within a few minutes. After 30 mins, the light yellow solution was evaporated to dryness, redissolved in anhydrous CH_2Cl_2 (1.5 mL), and phenol (0.30 mmol) and a freshly distilled NEt_3 (52 μL , 0.37 mmol) were added. The reaction was stirred overnight at rt, evaporated to dryness, passed through a short silica gel plug (CH_2Cl_2), filtered through a cotton plug, and recrystallized.

Method B. The acid chloride derived from carboxylic acid (0.25 mmol) was generated as in Method A. The crude acid chloride, excess *trans*-4-pentylcyclohexanol [23] (~1 mmol), and dry pyridine (0.1 mL) as solvent were added. The mixture was heated for 3 days at 90 °C protected from moisture. At times, the reaction was cooled to rt, and minimal amounts of anhydrous CH_2Cl_2 was added to wash the sides of the flask. The product was purified as described in Method A.

Ester of 12-(4-heptyloxyphenyl)-p-carborane-1-carboxylic acid and 4-trans-pentylcyclohexanol (1[12]b). It was obtained using Method B in 36% yield after chromatography (CH_2Cl_2). The ester was purified by recrystallization from EtOAc/ CH_3CN (3x) at –40 °C and then pentane (3x) at –20 °C to give a white crystalline solid: ^1H NMR (400 MHz, CDCl_3) δ 0.88 (t, J = 7.0 Hz, 3H), 0.89 (t, J = 7.0 Hz, 3H), 0.91-1.02 (m, 2H), 1.12-1.45 (m, 18H), 1.69-1.81 (m, 5H), 1.5-3.5 (br m, 10H), 1.82-1.90 (m, 2H), 3.88 (t, J = 6.5 Hz, 2H), 4.47-4.57 (m, 1H), 6.66 (d, J = 9.0 Hz, 2H), 7.07 (d, J = 8.9 Hz, 2H); $\{^1\text{H}\}^{11}\text{B}$ NMR (128 MHz, CDCl_3) δ –13.2 (5B), –

12.5 (5B). Anal. Calcd. For $C_{27}H_{50}B_{10}O_3$: C, 61.10; H, 9.49. Found: C, 61.30; H, 9.31. *Ester of 12-(4-heptyloxyphenyl)-p-carborane-1-carboxylic acid and 4-pentylphenol (1[12]c)*. It was obtained using Method A in 78% yield after chromatography (CH_2Cl_2). The ester was purified by recrystallization from EtOAc/ CH_3CN (3x) at -40 °C and then pentane (3x) at -20 °C to give a white crystalline solid: 1H NMR (400 MHz, $CDCl_3$) δ 0.88 (t, $J = 7.1$ Hz, 3H), 0.89 (t, $J = 7.0$ Hz, 3H), 1.20-1.45 (m, 10H), 1.45-1.62 (m, 4H), 1.74 (quint, $J = 7.1$ Hz, 2H), 1.5-3.5 (br m, 10H), 2.58 (t, $J = 7.7$ Hz, 2H), 3.89 (t, $J = 6.6$ Hz, 2H), 6.68 (d, $J = 9.0$ Hz, 2H), 6.89 (d, $J = 8.5$ Hz, 2H), 7.10 (d, $J = 8.9$ Hz, 2H), 7.14 (d, $J = 8.5$ Hz, 2H); $\{^1H\}^{11}B$ NMR (128 MHz, $CDCl_3$) δ -13.2 (5B), -12.2 (5B). Anal. Calcd. For $C_{27}H_{44}B_{10}O_3$: C, 61.80; H, 8.45. Found: C, 61.84; H, 8.30.

Ester of 12-(4-heptyloxyphenyl)-p-carborane-1-carboxylic acid and 4-butoxyphenol (1[12]d). It was obtained using Method A in 62% yield after chromatography (CH_2Cl_2). The ester was purified by recrystallization EtOAc/ CH_3CN (3x) at -40 °C and then pentane (3x) at -20 °C to give a white crystalline solid: 1H NMR (400 MHz, $CDCl_3$) δ 0.88 (t, $J = 6.9$ Hz, 3H), 0.96 (t, $J = 7.4$ Hz, 3H), 1.30-1.55 (m, 10H), 1.57-1.77 (m, 4H), 1.5-3.5 (br m, 10H), 3.87 (t, $J = 6.5$ Hz, 2H), 3.91 (t, $J = 6.5$ Hz, 2H), 6.67 (d, $J = 8.9$ Hz, 2H), 6.81 (d, $J = 9.2$ Hz, 2H), 6.88 (d, $J = 9.2$ Hz, 2H), 7.08 (d, $J = 8.9$ Hz, 2H); $\{^1H\}^{11}B$ NMR (128 MHz, $CDCl_3$) δ -13.2 (5B), -12.3 (5B). Anal. Calcd. For $C_{26}H_{42}B_{10}O_4$: C, 59.29; H, 8.04. Found: C, 59.46; H, 8.21.

Ester of 12-(4-heptyloxyphenyl)-p-carborane-1-carboxylic acid and 4-cyanophenol (1[12]e). It was obtained using Method A in 77% yield after chromatography (CH_2Cl_2). The ester was purified by recrystallization from CH_3OH (3x) at -40 °C and

then *iso*-octane (3x) at $-40\text{ }^{\circ}\text{C}$ to give a white crystalline solid: ^1H NMR (400 MHz, CDCl_3) δ 0.89 (t, $J = 6.7$ Hz, 3H), 1.26-1.45 (m, 8H), 1.74 (quint, $J = 6.4$ Hz, 2H), 1.5-3.5 (br m, 10H), 3.89 (t, $J = 6.6$ Hz, 2H), 6.69 (d, $J = 9.0$ Hz, 2H), 7.08 (d, $J = 9.0$ Hz, 2H), 7.15 (d, $J = 8.8$ Hz, 2H), 7.67 (d, $J = 8.8$ Hz, 2H); $\{^1\text{H}\}^{11}\text{B}$ NMR (128 MHz, CDCl_3) δ -13.2 (5B), -12.2 (5B). Anal. Calcd. For $\text{C}_{23}\text{H}_{33}\text{B}_{10}\text{NO}_3$: C, 57.60; H, 6.94; N, 2.92. Found: C, 57.34; H, 6.79; N, 2.79.

Ester of 12-(4-heptyloxyphenyl)-p-carborane-1-carboxylic acid and 2-(4-hexylphenyl)-5-hydroxypyrimidine (I[12]f). It was obtained using Method A in 72% yield after chromatography (CH_2Cl_2). The ester was purified by recrystallization from CH_3CN /toluene (3x) at $-40\text{ }^{\circ}\text{C}$ and then *iso*-octane (3x) at $-40\text{ }^{\circ}\text{C}$ to give a white crystalline solid: ^1H NMR (400 MHz, CDCl_3) δ 0.881 (t, $J = 7.0$ Hz, 3H), 0.884 (t, $J = 7.0$ Hz, 3H), 1.23-1.45 (m, 14H), 1.64 (quint, $J = 7.5$ Hz, 2H), 1.74 (quint, $J = 7.0$ Hz, 2H), 1.5-3.5 (br m, 10H), 2.66 (t, $J = 7.7$ Hz, 2H), 3.89 (t, $J = 6.5$ Hz, 2H), 6.69 (d, $J = 9.0$ Hz, 2H), 7.08 (d, $J = 9.0$ Hz, 2H), 7.28 (d, $J = 8.2$ Hz, 2H), 8.28 (d, $J = 8.2$ Hz, 2H), 8.52 (s, 2H); $\{^1\text{H}\}^{11}\text{B}$ NMR (128 MHz, CDCl_3) δ -13.2 (5B), -12.1 (5B). Anal. Calcd. For $\text{C}_{32}\text{H}_{48}\text{B}_{10}\text{N}_2\text{O}_3$: C, 62.31; H, 7.84; N, 4.54. Found: C, 62.58; H, 7.85; N, 4.56.

Ester of 10-(4-heptyloxyphenyl)-p-carborane(10v)-1-carboxylic acid and 2-(hexylphenyl)-5-hydroxypyrimidine (I[10]f). It was obtained using Method A in 89% yield after chromatography (CH_2Cl_2). The ester was purified by recrystallization from CH_3CN /toluene (2x) and CH_3OH /EtOAc (2x) to give a white crystalline solid: ^1H NMR (400 MHz, CDCl_3) δ 0.88 (t, $J = 6.9$ Hz, 3H), 0.91 (t, $J = 6.7$ Hz, 3H), 1.22-1.44 (m, 12H), 1.49 (quint, $J = 7.3$ Hz, 2H), 1.5-3.4 (br m, 8H), 1.67 (quint, $J = 8.3$

Hz, 2H), 1.83 (quint, $J = 7.0$ Hz, 2H), 2.69 (t, $J = 7.7$ Hz, 2H), 4.04 (t, $J = 6.5$ Hz, 2H), 6.98 (d, $J = 8.7$ Hz, 2H), 7.32 (d, $J = 8.2$ Hz, 2H), 7.71 (d, $J = 8.7$ Hz, 2H), 8.36 (d, $J = 8.2$ Hz, 2H), 8.86 (s, 2H); $\{^1\text{H}\}^{11}\text{B}$ NMR (128 MHz, CDCl_3) $\delta -9.7$ (8B). Anal. Calcd. for $\text{C}_{32}\text{H}_{46}\text{B}_8\text{N}_2\text{O}_3$: C, 64.79; H, 7.82; N, 4.72. Found: C, 65.06; H, 7.90; N, 4.57.

Ester of [closo-1-CB₁₁H₁₀-1-COOH-12-(1-(4-C₇H₁₅O-C₅H₄N))] and *4-trans-pentylcyclohexanol (2[12]b)*. It was obtained using Method A in 46% yield after chromatography (CH_2Cl_2). The ester was purified by recrystallization from toluene/*iso*-octane (3x) and then CH_3OH at -20 °C (3x) to give a white crystalline solid: ^1H NMR (400 MHz, CDCl_3) δ 0.87 (t, $J = 7.1$ Hz, 3H), 0.89 (t, $J = 6.8$ Hz, 3H), 0.92-1.02 (m, 2H), 1.10-1.40 (m, 16H), 1.4-2.8 (br m, 10H), 1.41-1.51 (m, 2H), 1.75 (br d, $J = 12.3$ Hz, 2H), 1.81-1.95 (m, 5H), 4.16 (t, $J = 6.5$ Hz, 2H), 4.53-4.61 (m, 1H), 7.00 (d, $J = 7.4$ Hz, 2H), 8.43 (d, $J = 7.4$ Hz, 2H); $\{^1\text{H}\}^{11}\text{B}$ NMR (128 MHz, CDCl_3) $\delta -13.7$ (10B), 5.5 (1B). Anal. Calcd. For $\text{C}_{25}\text{H}_{50}\text{B}_{11}\text{NO}_3$: C, 56.48; H, 9.48; N, 2.63. Found: C, 56.40; H, 9.55; N, 2.68.

Ester of [closo-1-CB₁₁H₁₀-1-COOH-12-(1-(4-C₇H₁₅O-C₅H₄N))] with *p*-pentylphenol (2[12]c). It was obtained using Method A in 74% yield after chromatography (CH_2Cl_2). The ester was purified by recrystallization from toluene/*iso*-octane (3x) and then CH_3OH at -20 °C (5x) to give a white crystalline solid: ^1H NMR (400 MHz, CDCl_3) δ 0.88 (t, $J = 7.0$ Hz, 3H), 0.90 (t, $J = 6.8$ Hz, 3H), 1.23-1.40 (m, 10H), 1.4-2.8 (br m, 10H), 1.41-1.50 (m, 2H), 1.58 (quint, $J = 7.3$ Hz, 2H), 1.86 (quint, $J = 7.0$ Hz, 2H), 2.56 (t, $J = 7.7$ Hz, 2H), 4.17 (t, $J = 6.5$ Hz, 2H), 6.94 (d, $J = 8.5$ Hz, 2H), 7.03 (d, $J = 7.5$ Hz, 2H), 7.12 (d, $J = 8.5$ Hz, 2H), 8.45 (d, $J = 7.4$ Hz, 2H); $\{^1\text{H}\}^{11}\text{B}$

NMR (128 MHz, CDCl₃) δ -13.5 (10B), 5.9 (1B). Anal. Calcd. For C₂₅H₄₄B₁₁NO₃: C, 57.13; H, 8.44; N, 2.67. Found: C, 57.27; H, 8.36; N, 2.71.

Ester of [closo-1-CB₁₁H₁₀-1-COOH-12-(1-(4-C₇H₁₅O-C₅H₄N))] and 4-butoxyphenol (2[12]d). It was obtained using Method A in 69% yield after chromatography (CH₂Cl₂). The ester was purified by recrystallization from toluene/*iso*-octane (2x), EtOH at -20 °C (2x) and then CH₃OH at -20 °C (4x) to give a white crystalline solid: ¹H NMR (400 MHz, CDCl₃) δ 0.90 (t, *J* = 6.8 Hz, 3H), 0.96 (t, *J* = 7.4 Hz, 3H), 1.24-1.40 (m, 6H), 1.4-2.8 (br m, 10H), 1.41-1.52 (m, 4H), 1.74 (quint, *J* = 7.0 Hz, 2H), 1.86 (quint, *J* = 7.0 Hz, 2H), 3.92 (t, *J* = 6.5 Hz, 2H), 4.17 (t, *J* = 6.5 Hz, 2H), 6.82 (d, *J* = 9.1 Hz, 2H), 6.94 (d, *J* = 9.1 Hz, 2H), 7.03 (d, *J* = 7.5 Hz, 2H), 8.45 (d, *J* = 7.4 Hz, 2H); {¹H}¹¹B NMR (128 MHz, CDCl₃) δ -13.5 (10B), 5.9 (1B). Anal. Calcd. For C₂₄H₄₂B₁₁NO₄: C, 54.65; H, 8.03; N, 2.66. Found: C, 54.84; H, 8.20; N, 2.65.

Ester of [closo-1-CB₁₁H₁₀-1-COOH-12-(1-(4-C₇H₁₅O-C₅H₄N))] and 4-cyanophenol (2[12]e). It was obtained using Method A in 69% yield after chromatography (CH₂Cl₂). The ester was purified by recrystallization from EtOAc/hexane (2x), toluene/*iso*-octane (2x) and then CH₃OH at -20 °C to give a white crystalline solid: ¹H NMR (400 MHz, CDCl₃) δ 0.90 (t, *J* = 6.8 Hz, 3H), 1.25-1.40 (m, 6H), 1.4-2.8 (br m, 10H), 1.41-1.51 (m, 2H), 1.86 (quint, *J* = 7.0 Hz, 2H), 4.18 (t, *J* = 6.5 Hz, 2H), 7.04 (d, *J* = 7.4 Hz, 2H), 7.20 (d, *J* = 8.8 Hz, 2H), 7.65 (d, *J* = 8.7 Hz, 2H), 8.44 (d, *J* = 7.4 Hz, 2H); {¹H}¹¹B NMR (128 MHz, CDCl₃) δ -13.3 (10B), 6.1 (1B). Anal. Calcd. For C₂₁H₃₃B₁₁N₂O₃: C, 52.50; H, 6.92; N, 5.83. Found: C, 52.76; H, 6.73; N, 5.75.

Ester of [closo-1-CB₁₁H₁₀-1-COOH-12-(1-(4-C₇H₁₅O-C₅H₄N))] and 2-(4-hexylphenyl)-5-hydroxypyrimidine (2[12f]). It was obtained using Method A in 84% yield after chromatography (CH₂Cl₂). The ester was purified by recrystallization from toluene/CH₃CN (4x) to give a white crystalline solid: ¹H NMR (400 MHz, CDCl₃) δ 0.88-0.91 (m, 6H), 1.22-1.40 (m, 12H), 1.41-1.50 (m, 2H), 1.65 (quint, *J* = 7.3 Hz, 2H), 1.4-2.8 (br m, 10H), 1.86 (quint, *J* = 6.9 Hz, 2H), 2.66 (t, *J* = 7.6 Hz, 2H), 4.18 (t, *J* = 6.5 Hz, 2H), 7.04 (d, *J* = 7.2 Hz, 2H), 7.27 (d, *J* = 8.3 Hz, 2H), 8.29 (d, *J* = 8.1 Hz, 2H), 8.44 (d, *J* = 7.1 Hz, 2H), 8.58 (s, 2H); {¹H}¹¹B NMR (128 MHz, CDCl₃) δ –13.3 (10B), 6.1 (1B). Anal. Calcd. For C₃₀H₄₈B₁₁N₃O₃: C, 58.34; H, 7.83; N, 6.80. Found: C, 58.47; H, 7.62; N, 6.76.

Ester of [closo-1-CB₉H₈-1-COOH-10-(1-(4-C₇H₁₅O-C₅H₄N))] and 2-(hexylphenyl)-5-hydroxypyrimidine (2[10f]). It was obtained using Method A in 77% yield after chromatography. The ester was purified by recrystallization from *iso*-octane/toluene (2x) and then EtOAc/hexane (2x) to give a white crystalline solid: ¹H NMR (400 MHz, CDCl₃) δ 0.75-2.60 (br m, 8H), 0.89 (t, *J* = 6.6 Hz, 3H), 0.92 (t, *J* = 6.8 Hz, 3H), 1.23-1.47 (m, 12H), 1.53 (quint, *J* = 7.3 Hz, 2H), 1.67 (quint, *J* = 7.3 Hz, 2H), 1.95 (quint, *J* = 7.0 Hz, 2H), 2.69 (t, *J* = 7.7 Hz, 2H), 4.31 (t, *J* = 6.5 Hz, 2H), 7.31 (pseudo t, *J* = 7.3 Hz, 4H), 8.36 (d, *J* = 8.1 Hz, 2H), 8.88 (s, 2H), 9.09 (d, *J* = 7.0 Hz, 2H); {¹H}¹¹B NMR (128 MHz, CDCl₃) δ –20.5 (4B), –15.4 (4B), 43.0 (1B). Anal. Calcd. for C₃₀H₄₆B₉N₃O₃: C, 60.66; H, 7.81; N, 7.07. Found: C, 60.88; H, 7.58; N, 7.04.

Preparation of 12-(4-heptyloxyphenyl)-p-carborane-1-carboxylic acid (3[12]).[13]

A solution of 1-(4-heptyloxyphenyl)-*p*-carborane[15] (**8[12]**, 1.39 g, 4.16 mmol) in anhydrous THF (20 mL) at 0 °C was treated with *n*-BuLi (6.6 mL, 12.5 mmol, 1.9 M in hexanes). The reaction mixture was warmed to rt, and subsequently cooled back to 0 °C, and dry CO₂ was bubbled through the solution for 30 min. The reaction mixture was evaporated to dryness and the residue washed with pentane. Et₂O (20 mL) and 10% HCl (20 mL) were added, and the Et₂O layer was separated. The aqueous layer was further extracted with Et₂O (3 x 20 mL). The organic layers were combined, washed with H₂O, dried (Na₂SO₄), and evaporated to dryness. The tacky white solid was washed with hot H₂O (2x) to remove residual valeric acid and dried in vacuo providing 1.45 g (92% yield) of crude acid 3[12]. The acid was further purified by recrystallization from aq. MeOH, CH₃CN, and *iso*-octane (2x): mp 175 °C; ¹H NMR (400 MHz, CDCl₃) δ 0.88 (t, *J* = 6.8 Hz, 3H), 1.22-1.45 (m, 8H), 1.73 (quint, *J* = 7.0 Hz, 2H), 1.5-3.5 (br m, 10H), 3.87 (t, *J* = 6.6 Hz, 2H), 6.66 (d, *J* = 9.0 Hz, 2H), 7.05 (d, *J* = 9.0 Hz, 2H); ¹¹B NMR (128 MHz, CDCl₃) δ -13.3 (5B), -12.3 (5B). Anal. Calcd. for C₁₆H₃₀B₁₀O₃: C, 50.77; H, 7.99. Found: C, 50.82; H, 7.92.

Preparation of [*closo*-1-CB₁₁H₁₀-1-COOH-12-(4-C₇H₁₅OC₅H₄N)] (4[12]).

A slightly yellow solution of [*closo*-1-CB₁₁H₁₀-1-COOH-10-NH₃] (**5[12]**, 1.02 g; 5.00 mmol) and 4-heptyloxypyridine[24] (30 mL) was stirred at -20 °C. [NO]⁺[PF₆]⁻ (5.42 g, 31 mmol) was added in 6 portions every 10-15 min and the solution was allowed to warm to rt and stirred for 8 hr. As the reaction progressed, the solution became a yellow suspension and heat was produced. The suspension was

saturated with hexanes (3 x 30 mL) to remove excess 4-heptyloxypyridine and decanted. The yellow residue was treated with 10% HCl (30 mL) and the solution was extracted with Et₂O (3 x 20 mL). The Et₂O extracts were combined, dried (Na₂SO₄), and evaporated to give crude acid **4[12]** as yellowish solid. The crude acid was passed through a short silica gel plug (CH₃OH/CH₂Cl₂, 1:9) giving 120 mg (6% yield) of pure acid as an off-white solid. An analytical sample of **4[12]** was prepared by recrystallization from toluene/CH₃CN (3x): mp 189 °C; ¹H NMR (400 MHz, CD₃CN) δ 0.90 (t, *J* = 6.9 Hz, 3H), 1.26-1.50 (m, 8H), 1.4-2.8 (br m, 10H), 1.81 (quint, *J* = 7.0 Hz, 2H), 4.23 (t, *J* = 6.6 Hz, 2H), 7.15 (d, *J* = 7.5 Hz, 2H), 8.40 (d, *J* = 7.4 Hz, 2H); {¹H}¹¹B NMR (128 MHz, CD₃CN) δ -14.4 (5B), -13.6 (5B), 5.9 (1B). Anal. Calcd. For C₁₄H₃₀B₁₁NO₃: C, 44.33; H, 7.97; N, 3.69. Found: C, 44.31; H, 7.83; N, 3.49.

Preparation of [*closo*-1-CB₁₁H₁₀-1-COOH-12-NH₃] (5[12]).

[*closo*-1-CB₁₁H₁₀-1-COOH-12-I]⁻[NEt₄]⁺ (**6[12]**,[10] 7.03 g, 15.8 mmol) was dissolved in a 1 M solution of LiHMDS in THF (300 mL, 0.24 mol) at rt under Ar. The mixture was stirred for 15 min before Pd₂dba₃ (0.97 g, 1.06 mmol) and 2-(dicyclohexylphosphino)biphenyl (0.70 g, 1.98 mmol) were added. The reaction turned brown and was stirred at reflux for 72 hr. The reaction was cooled to 0 °C and quenched with ice-cold 20% HCl (100 mL). THF was removed removed *in vacuo* and the aqueous layer was extracted with Et₂O (3 x 75 mL). The organic layers were dried (Na₂SO₄) and evaporated to dryness giving crude product as a brown oil.

The crude product was redissolved in Et₂O (30 mL), H₂O (75 mL) was added, and the Et₂O evaporated *in vacuo*. The aqueous layer was filtered, and the insoluble residue was redissolved in Et₂O. This process was repeated two times in order to

ensure complete extraction of boron cluster containing material to water. The aqueous layers were combined and treated with $[\text{NEt}_4]^+[\text{Br}]^-$ (1.67 g, 7.95 mmol) to precipitate any deiodinated starting material, catalyst and ligand by-products. The insoluble materials were filtered, the aqueous layer was acidified with conc. HCl (30 mL) and extracted with Et_2O (3 x 75 mL). The organic layer was dried (Na_2SO_4) and evaporated leaving 1.29 g (40% yield) of amino acid **5[12]** as an off-white solid: $\{^1\text{H}\}^{11}\text{B}$ NMR (128 MHz, CD_3CN) δ -14.5 (5B), -13.8 (5B), 0.4 (1B). HRMS, calcd. for $\text{C}_2\text{H}_{14}\text{B}_{11}\text{NO}_2$ m/z 204.1976; found m/z 204.1969.

Preparation of 1-(4-heptyloxyphenyl)-*p*-carborane (8[12]).[15]

A suspension of 1-(4-hydroxyphenyl)-*p*-carborane[14] (**7[12]**, 1.01 g, 4.26 mmol), heptyl tosylate[25] (4.15 g, 15.3 mmol), anhydrous K_2CO_3 (1.77 g, 12.8 mmol), and $[\text{NBu}_4]^+[\text{Br}]^-$ (0.14 g, 0.43 mmol) was stirred at reflux in anhydrous CH_3CN (50 mL) overnight. Precipitation was filtered off and washed with CH_2Cl_2 . The filtrate was evaporated giving a colorless oil. The crude product was passed through a short silica gel plug (hexane) giving 1.26 g (89% yield) of product **7[12]** as a colorless oil: ^1H NMR (400 MHz, CDCl_3) δ 0.89 (t, $J = 6.8$ Hz, 3H), 1.22-1.46 (m, 8H), 1.73 (quint, $J = 7.0$ Hz, 2H), 1.5-3.5 (br m, 10H), 3.88 (t, $J = 6.5$ Hz, 2H), 6.67 (d, $J = 9.0$ Hz, 2H), 7.10 (d, $J = 9.0$ Hz, 2H); ^{11}B NMR (128 MHz, CDCl_3) δ -14.8 (5B), -12.0 (5B). Anal. Calcd. for $\text{C}_{15}\text{H}_{30}\text{B}_{10}\text{O}$: C, 53.86; H, 9.04. Found: C, 53.59; H, 9.30.

5.2.2.6 Acknowledgements

This work was supported by the NSF grant DMR-1207585.

5.2.2.7 References

- [1] Kirsch P, Bremer M. Nematic Liquid Crystals for Active Matrix Displays: Molecular Design and Synthesis. *Angew. Chem. Int. Ed.* 2000;39:4216-4235.
- [2] Bremer M, Lietzau L. 1,1,6,7-Tetrafluoroindanes: improved liquid crystals for LCD-TV application. *New J. Chem.* 2005;29:72-74.
- [3] Blinov, L. M. In *Handbook of Liquid Crystals*, D. Demus, J. Goodby, G. W. Gray, H.-W. Spiess, and V. Vill, Eds.; Willey-VCH, 1998, Vol 1, pp 477-534.
- [4] L. M. Blinov, V. G. Chigrinov *Electrooptic Effects in Liquid Crystal Materials*; Springer-Verlag: New York, 1994.
- [5] Kaszynski P, Pakhomov S, Gurskii ME, Erdyakov SY, Starikova ZA, Lyssenko KA, Antipin MY, Young VG, Jr., Bubnov YN. 1-Pyridine- and 1-Quinuclidine-1-boradamantane as Models for Derivatives of 1-Borabicyclo[2.2.2]octane. Experimental and Theoretical Evaluation of the B-N Fragment as a Polar Isosteric Substitution for the C-C Group in Liquid Crystal Compounds. *J. Org. Chem.* 2009;74:1709-1720.
- [6] Ringstrand B, Kaszynski P. How Much Can an Electric Dipole Stabilize a Nematic Phase? Polar and Non-Polar Isosteric Derivatives of [*closo*-1-CB₉H₁₀]⁻ and [*closo*-1,10-C₂B₈H₁₀]. *J. Mater. Chem.* 2010;20:9613-9615.
- [7] Ringstrand B, Kaszynski P. High Δε nematic liquid crystals: fluxional zwitterions of the [*closo*-1-CB₉H₁₀]⁻ cluster. *J. Mater. Chem.* 2011;21:90-95.
- [8] Ringstrand B, Kaszynski P, Young VG, Jr. Diazotization of the amino acid [*closo*-1-CB₉H₈-1-COOH-6-NH₃] and reactivity of the [*closo*-1-CB₉H₈-1-COO-6-N₂]⁻ anion. *Inorg. Chem.* 2011;50:2654-2660.

- [9] Pecyna J, Ringstrand B, Kaszynski P. Synthesis of 12-pyridinium derivatives of the $[closo-1-CB_{11}H_{12}]^-$ anion by diazotization of $[closo-1-CB_{11}H_{11}-12-NH_3]$. in preparation.
- [10] Ringstrand B, Jankowiak A, Johnson LE, Kaszynski P, Pocięcha D, Górecka E. Anion-Driven Mesogenicity: A Comparative Study of Ionic Liquid Crystals Based on the $[closo-1-CB_9H_{10}]^-$ and $[closo-1-CB_{11}H_{12}]^-$ Clusters. *J. Mater. Chem.* 2012;22:4874-4880.
- [11] Ringstrand B, Kaszynski P, Young VG, Jr., Janoušek Z. The Anionic Amino Acid $[closo-1-CB_9H_8-1-COO-10-NH_3]^-$ and Dinitrogen Acid $[closo-1-CB_9H_8-1-COOH-10-N_2]$ as Key Precursors to Advanced Materials: Synthesis and Reactivity. *Inorg. Chem.* 2010;49:1166-1179.
- [12] Pd-catalyzed amination of the parent $[closo-1-CB_{11}H_{11}-12-I]^-$ under similar conditions in a MW oven was recently reported: Konieczka SZ, Himmelspach A, Hailmann M, Finze M. Synthesis, Characterization, and Selected Properties of 7- and 12-Ammoniocarba-closo-dodecaboranes *Eur. J. Inorg. Chem.* 2013, 134-146.
- [13] Ohta K, Januszko A, Kaszynski P, Nagamine T, Sasnouski G, Endo Y. Structural Effects in Three-Ring Mesogenic Derivatives of p-Carborane and Their Hydrocarbon Analogs. *Liq. Cryst.* 2004;31:671-682.
- [14] Endo Y, Iijima T, Yamakoshi Y, Fukasawa H, Miyaura C, Inada M, Kubo A, Itai A. Potent estrogen agonists based on carborane as a hydrophobic skeletal structure: A new medicinal application of boron clusters. *Chemistry & Biology.* 2001;8:341-355.
- [15] Douglass AG, Pakhomov S, Reeves B, Janoušek Z, Kaszynski P. Triphenylsilyl as a Protecting Group in the Synthesis of 1,12-Heterodisubstituted p-Carboranes. *J. Org. Chem.* 2000;65:1434-1441.

- [16] Zhao Y, Truhlar DG. The M06 suite of density functionals for main group thermochemistry, thermochemical kinetics, noncovalent interactions, excited states, and transition elements: two new functionals and systematic testing of four M06-class functionals and 12 other functionals. *Theor. Chem. Account* 2008;120:215–241.
- [17] Kaszynski P, Januszko A, Ohta K, Nagamine T, Potaczek P, Young VG, Jr., Endo Y. Conformational Effects on Mesophase Stability: Numerical Comparison of Carborane Diester Homologous Series with Their Bicyclo[2.2.2]octane, Cyclohexane and Benzene Analogues. *Liq. Cryst.* 2008;35:1169-1190.
- [18] Kaszynski P. *closo*-Boranes as Structural Elements for Liquid Crystals. In: Hosmane N, editor. *Boron Science: New Technologies & Applications* CRC Press; 2012, p. 305-338.
- [19] D. M. Gavrilovic, US 3.925.238, 1975; LiqCrys 5.0 database, compound #25521.
- [20] Januszko A, Glab KL, Kaszynski P, Patel K, Lewis RA, Mehl GH, Wand MD. The Effect of Carborane, Bicyclo[2.2.2]octane and Benzene on Mesogenic and Dielectric Properties of Laterally Fluorinated Three-Ring Mesogens. *J. Mater. Chem.* 2006;16:3183-3192.
- [21] Frisch MJ, Trucks GW, Schlegel HB, Scuseria GE, Robb MA, *et al* Gaussian 09, Revision A.02, Gaussian, Inc., Wallingford CT, 2009.
- [22] Simon S, Duran M, Dannenberg JJ. How does basis set superposition error change the potential surfaces for hydrogen-bonded dimers? *J. Chem. Phys.* 1996;105:11024-11031.

- [23] Pecyna J, Kaszynski P, Ringstrand B, Bremer M. Investigation of high $\Delta\epsilon$ derivatives of the [*closo*-1-CB₉H₁₀]⁻ anion for liquid crystal display applications. J. Mater. Chem. submitted.
- [24] Kaszynski P, Huang J, Jenkins GS, Bairamov KA, Lipiak D. Boron Clusters in Liquid Crystals. Mol. Cryst. Liq. Cryst. 1995;260:315-332.
- [25] Burns DH, Miller JD, Chan H-K, Delaney MO. Scope and Utility of a New Soluble Copper Catalyst [CuBr–LiSPh–LiBr–THF]:□ A Comparison with Other Copper Catalysts in Their Ability to Couple One Equivalent of a Grignard Reagent with an Alkyl Sulfonate. J. Am. Chem. Soc. 1997;119:2125-2133.

Part III. Ionic liquid crystals based on the [closo-1-CB₉H₁₀]⁻ cluster

Ionic liquid crystals are a class of compounds that combine the properties of thermotropic liquid crystals and ionic liquids.¹ In comparison with common organic solvents, ionic liquids are characterized by low vapor pressure, which makes them a great candidate to replace organic solvents in chemical reactions. Judicious choice of the cation and the anion allows to modify the properties of ionic liquids like miscibility with water, viscosity, polarity, etc. Some of the properties of ILCs differ significantly from conventional LCs due to the ionic character of the molecules. The most advantageous property is anisotropic ion conductivity.^{2,3} Ionic interactions like ion-ion stacking and electrostatic interactions have the tendency to stabilize lamellar interactions. The presence of ionic species induces new types of mesophases such as nematic columnar phase.

Typical ionic LC molecule consists of a large organic cation, based mostly on ammonium,^{4,5} pyridinium⁶ or imidazolium,^{7,8} and an organic or inorganic anion. Less known, but also common cations include phosphonium,⁹ and pyrylium¹⁰ derivatives. It's the organic cation that carries the mesogenicity. The factors responsible for the induction of mesogenic properties include cation-cation repulsive forces, van der Waals interactions between the hydrophobic alkyl tails and hydrogen bonding between some anions and cations.¹¹

Incorporating boron clusters into ionic LC opens the door to a completely new and unique group of mesogenes. Boron clusters, [closo-1-CB₉H₁₀]⁻ (**2**) and [closo-1-CB₁₁H₁₂]⁻ (**1**), bearing a negative charge have completely changed the typical design of

ionic liquid crystals. As demonstrated, now, it's the anion, not the cation that drives the mesogenic properties.

These unusual properties of ILCs based on both clusters (Chapter 1, Figure 1) have encouraged us to explore this new area of ionic mesogenes. ILCs based on the [*closo*-1-CB₁₁H₁₂]⁻ anion (**1**) are more accessible than their 10-vertex analogues since the synthesis of the 12-vertex cluster is more practical, more efficient and achieved in fewer steps. In the following chapter, a part of our study on ILCs based on the [*closo*-1-CB₉H₁₀]⁻ (**2**) anion will be presented.

References

- (1) Binnemans, K., Ionic liquid crystals. *Chem. Rev.* **2005**, *105*, 4148-4204.
- (2) Yoshio, M.; Mukai, T.; Ohno, H.; Kato, T., One-Dimensional Ion Transport in Self-Organized Columnar Ionic Liquids. *J. Am. Chem. Soc.* **2004**, *126*, 994-995.
- (3) Shimura, H.; Yoshio, M.; Hoshino, K.; Mukai, T.; Ohno, H.; Kato, T., Noncovalent Approach to One-Dimensional Ion Conductors: Enhancement of Ionic Conductivities in Nanostructured Columnar Liquid Crystals. *J. Am. Chem. Soc.* **2008**, *130*, 1759-1765.
- (4) Busico, V.; Cernicchiaro, P.; Corradini, P.; Vacatello, M., Polymorphism in anhydrous amphiphilic systems. Long-chain primary *n*-alkylammonium chlorides. *J. Phys. Chem.* **1983**, *87*, 1631-1635.
- (5) Matsunaga, Y.; Tsujimura, T., The Thermotropic Liquid-Crystalline Behavior of Alkylammonium Naphthalenesulfonates. *Mol. Cryst. Liq. Cryst.* **1991**, *200*, 103-108.

- (6) Fürst, H.; Dietz, H. J. J., *Prakt. Chem.* **1956**, *4*, 147-152.
- (7) Gordon, C. M.; Holbrey, J. D.; Kennedy, A. R.; Seddon, K. R., Ionic liquid crystals: hexafluorophosphate salts. *J. Mater. Chem.* **1998**, *8*, 2627-2636.
- (8) Bowlas, C. J.; Duncan, W. B.; Seddon, K. R., Liquid-crystalline ionic liquids. *Chem. Comm.* **1996**, 1625-1626.
- (9) Gowda, G. A. N.; Chen, H.; Khetrapal, C. L.; Weiss, R. G., Amphotropic Ionic Liquid Crystals with Low Order Parameters. *Chem. Mater.* **2004**, *16*, 2101-2016.
- (10) Saeva, F. D.; Reynolds, G. A.; Kaszczuk, L., Liquid-crystalline cation-radical charge-transfer systems. *J. Am. Chem. Soc.* **1982**, *104*, 3524-3525.
- (11) Yu, W.; Peng, H.; Zhang, H.; Zhou, X., Synthesis and Mesophase Behaviour of Morpholinium Ionic Liquid Crystals. *Chin. J. Chem.* **2009**, *27*, 1471-1475.

6.1 Introduction

The goal of this project was to investigate the effect of the connecting group on mesogenic properties in ionic liquid crystals derived from the $[closo-1-CB_9H_{10}]^-$ (**2**) anion.

6.2 Anion driven ionic liquid crystals: The effect of the connecting group in $[closo-1-CB_9H_{10}]^-$ derivatives on mesogenic properties.

6.2.1 Description and contributions

In continuation of our search for new ionic liquid crystals based on the boron clusters, we investigated the effect of the alkyl chain modification on the mesogenic properties. We synthesized a series of esters **1** containing a hexyl chain attached to the apical position of the clusters. In the next step, we replaced the connecting $-CH_2-$ group in **1a** with oxygen in **1b** and sulphur atom (**1c**) and analyzed properties of the new ion

pairs with pyridinium. The properties of boron clusters based salts were compared with their benzene analogues. The results indicated mesophase destabilization upon replacement of the $-\text{CH}_2-$ with an oxygen atom. Analysis of binary mixtures indicated compatibility and miscibility of the ionic molecules with a nonionic mesogenes, which is important for the design of anisotropic electrolytes.

In this project, I was responsible for the synthesis of several intermediates, including the acids required for the preparation of the esters. Mr. Ajan Sivaramamoorthy, an undergraduate student, synthesized three of the esters, and Dr. Aleksandra Jankowiak assisted in preparation and thermal analysis of the binary mixtures.

In the following chapter the entire text of the manuscript is included for consistency of the narrative, however, the experimental section contains only experiments performed by me.

6.2.2 The manuscript

Reproduced by permission of Taylor & Francis Online
Pecyna, J.; Sivaramamoorthy, A.; Jankowiak, A.; Kaszynski, P. *Liq. Cryst.* **2012**, *39*, 965-971.
Copyright 2012 Taylor & Francis Online. Available online:
<http://www.tandfonline.com/doi/abs/10.1080/02678292.2012.689019>

6.2.2.1 Introduction

Recently we have demonstrated (1,2) that boron clusters [*closo*-1-CB₉H₁₀]⁻ (A, Figure 1) and [*closo*-1-CB₁₁H₁₂]⁻ (B) are effective structural elements of ionic liquid crystals (ILC). We have found that ion pairs that have a total of 4 rigid structural elements (rings and the monocarbaborate cage) exhibit liquid crystalline properties. This includes ion pairs 1a[Pyr] and 2a[Pyr], which exhibit SmA and, the rarely observed in ILC, nematic phases (2).

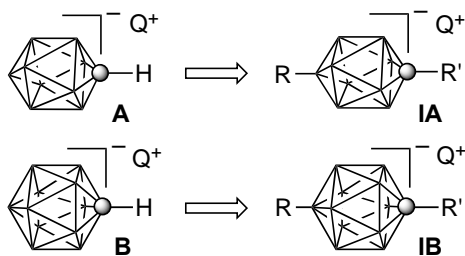


Figure 1. The structures of the [closo-1-CB₉H₁₀]⁻ (**A**) and [closo-1-CB₁₁H₁₂]⁻ (**B**) clusters and ion pairs of their 1,10- (**IA**) and 1,12-disubstituted (**IB**) derivatives with the counterion Q⁺ (metal or an onium ion). Each vertex represents a BH fragment and the sphere is a carbon atom.

In continuing our interest in this class of materials we set out to study the effect of an alkyl chain modification on phase transition. Here we report investigation of an effect of replacing of the connecting CH₂ group in **1a**[Pyr] with an oxygen atom in **1b**[Pyr] on mesogenic properties of ILC derived from the [closo-1-CB₉H₁₀]⁻ cluster (**A**), and our efforts to prepare the sulfur analogue **1c**[Pyr]. The results for the two derivatives, **1a**[Pyr] and **1b**[Pyr], are compared to those in an analogous series of non-ionic benzoate mesogens **3**. Finally, we study binary mixtures of ILC **1**[Pyr] in **2a**[Pyr] and nematogen **3a**.

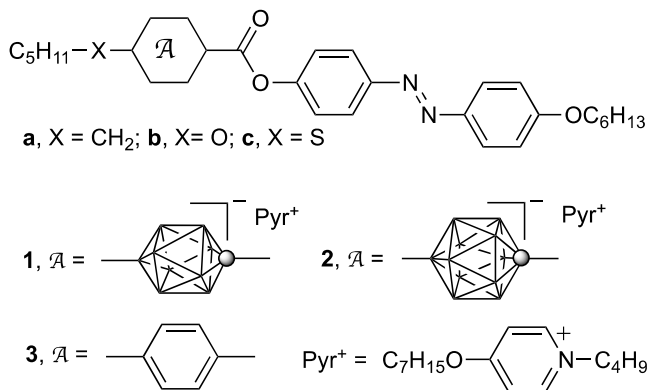
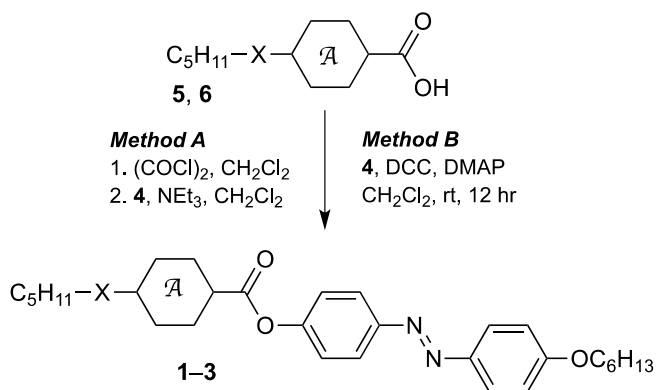


Figure 2. The structures of compounds **1**–**3**

6.2.2.2 Results and discussion

Synthesis

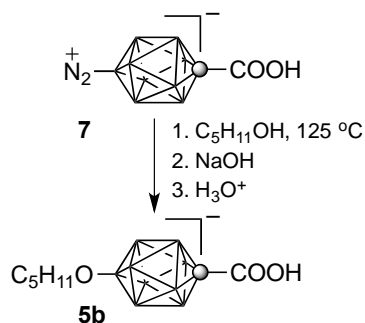
Esters **1–3** were obtained by esterification of 4-hexyloxy-4'-hydroxyazobenzene (**4**) (2) with acid chlorides that were prepared from appropriate carboxylic acids **5** and **6** and (COCl)₂ (Method A, Scheme 1). Ion pair **1b**[NMe₄], obtained from acid **5b**[NMe₄] (**3**), was converted to **1b**[Pyr] by cation exchange in a biphasic CH₂Cl₂/H₂O system, as described before (1). Ester **3c** was prepared directly from carboxylic acid **6c** and phenol **4** in the presence of DCC (Method B).



Scheme 1. Synthesis of esters **1 – 3**.

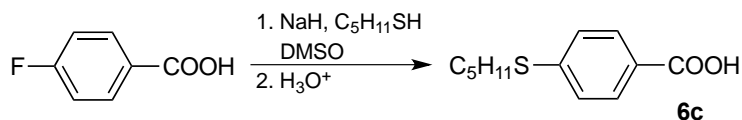
10-Pentyloxy carboxylic acid **5b**[NMe₄] was obtained by thermolysis of dinitrogen acid [*closo*-1-CB₉H₈-1-COOH-10-N₂] (**7**) in dry pentanol followed by basic workup (Scheme 2) (**3**). A similar approach to the preparation of 10-pentylsulfanyl acid [*closo*-1-CB₉H₈-1-COOH-10-SC₅H₁₁] (**5c**[NMe₄]) was unsuccessful. The dinitrogen acid **7** was insoluble in pentanethiol, and its methyl ester [*closo*-1-CB₉H₈-1-COOMe-10-N₂] (**8**) (**4**) was used instead. NMR analysis of the crude reaction mixture demonstrated the presence of several pentyl residues and at least two {*closo*-1-CB₉} species even after basic hydrolysis. In one instance, chromatographic separation of the crude mixture gave a

low yield of the pentyl ester [*closo*-1-CB₉H₈-1-COSC₅H₁₁-10-SC₅H₁₁]⁻, which was characterized by HRMS technique. The results were reproducible in 3 runs, and the preparation of acid **5c** was not pursued further.



Scheme 2. Preparation of [*closo*-1-CB₉H₈-1-COOH-10-OC₅H₁₁]⁻ (**5b**).

4-Pentylsulfanylbenzoic acid (**6c**) (**5**) was prepared in 44% yield by nucleophilic aromatic substitution of 4-fluorobenzoate salt with pentanethiolate in DMSO (Scheme 3), under conditions (6) that promote the S_{RN}1 mechanism (7). This reaction appears to be cleaner than previously reported synthesis of this acid through diazotization of 4-aminobenzoic acid (5), and more straightforward than multistep preparation from 4-bromothiophenol (8).



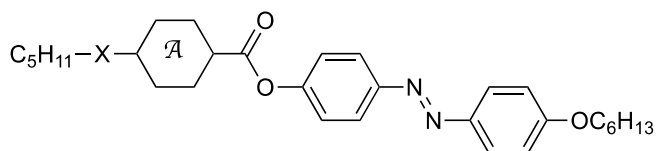
Scheme 3. Synthesis of acid **6c**.

Mesomorphic properties

Transition temperatures and enthalpies of the newly prepared compounds were determined by differential scanning calorimetry (DSC). The phase types were identified by observed microscopic textures in polarized light, and results are shown in Table 1.

Analysis of benzoates **3** demonstrated that all three esters form exclusively a nematic phase. This is consistent with highly nematogenic properties of azobenzene derivatives and exclusive formation of nematic phases by all known (9) alkoxybenzoate esters of alkoxyazophenol, even by those with long alkyl chains (10,11). In series **3** the highest clearing temperature is observed for the pentyloxy derivative **3b** ($T_{NI} = 233$ °C), while replacement of the connecting O atom with a CH₂ group or S atom lowers the T_{NI} by about 30 K. The observed trend in T_{NI} for series **3**, O \gg CH₂ > S, is the same as in another series of structurally similar mesogens **9** (12,13), and is consistent with generally higher clearing temperatures for alkoxy derivatives than for their alkyl analogues. However, an opposite trend is observed in bicyclo[2.2.2]octane derivatives in which 4-butoxybicyclo[2.2.2]octane derivatives have lower T_{NI} values by about 15 K, when compared to the 4-pentylbicyclo[2.2.2]octane analogues (14).

Table 1. Transition temperatures ($^{\circ}\text{C}$) and enthalpies (kJ/mol) for selected compounds.^a



		1	2	3
	A			
	X			
a	-CH ₂ -	Cr ^b 123 SmA 132 N 137 I ^c (43.2) (0.6) (1.3)	Cr 134 (SmA 133) N 144 I ^c (43.2) (0.6) (1.3)	Cr 91 ^d N 206 I (72.8) (1.8)
b	-O-	Cr 107 I (50.0)	NA	Cr ^e 110 N 233 I (34.8) (1.9)
c	-S-	NA	NA	Cr ^f 118 N 200 I (40.7) (1.3)

^a Obtained on heating; Cr-crystal, SmA-smectic A, N-nematic, I-isotropic.

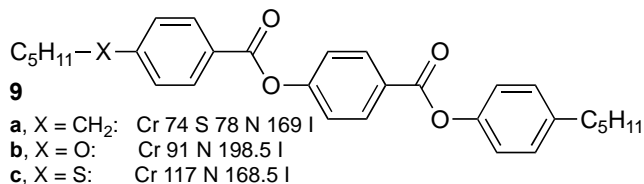
^b Cr – Cr transition at 32 $^{\circ}\text{C}$

^c Ref. (2)

^d Heating rate 0.5 K min^{-1} . For a heating 10 K min^{-1} Cr – Cr transition at 84 $^{\circ}\text{C}$, melting at 86 $^{\circ}\text{C}$, partial crystallization followed by another melting at 91 $^{\circ}\text{C}$.

^e Cr – Cr transition at 76 $^{\circ}\text{C}$ (21.6 kJ mol^{-1})

^f Cr – Cr transition at 109 $^{\circ}\text{C}$ (15.4 kJ mol^{-1})

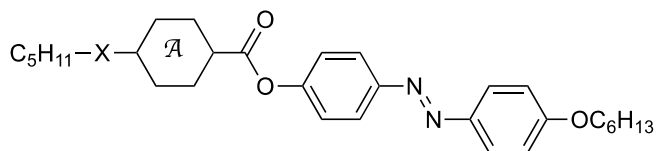


Results for 10-pentyloxy derivative **1b[Pyrr]** were surprising. The ion pair had a lower melting point than the 10-hexyl analogue **1a[Pyrr]** (Table 1) and no mesogenic properties even on cooling by about 35 K below melting. Interestingly, the polymorph obtained from the melt had a lower melting point by 19 K. Mesogenic properties of **1b[Pyrr]** were investigated in binary mixtures with ILC **2a[Pyrr]**, that was previously used in similar studies (2).

Binary mixtures

Virtual transition temperatures for the non-mesogenic ion pair **1b[Pyrr]** and, for comparison purposes, also for **1a[Pyrr]** were extrapolated from low concentration solutions in **2a[Pyrr]**. For both additives the phase transition temperatures changed linearly with respect to the composition of the mixture, as shown in Figure 3, which demonstrates ideal miscibility of the components. The least square fitting lines have high correlation factor ($r^2 > 0.99$), and the extrapolated temperatures have uncertainty of ± 1 K.

Table 2. Virtual transition temperatures (°C) for ionic liquid crystals.^a



χA	1a[<i>Pyr</i>]	1b[<i>Pyr</i>]	2a[<i>Pyr</i>]
host			
2a[<i>Pyr</i>]	[SmA 130 N 135 I]	[SmA 30 N 70 I]	–
3a	[N 145 I]	[N 48 I]	[N 157 I]
None	SmA 132 N 137 I ^b	none	(SmA 133) N 144 I ^b

^a Obtained on heating; SmA-smectic A, N-nematic, I-isotropic.

^b Ref. (2)

The virtual transition temperatures $[T_{N}]$ and $[T_{AN}]$ established for ion pair **1a[*Pyr*]** were 2 K lower than those for enantiotropic transitions in the pure material (Table 2). Results for the pentyloxy ion pair **1b[*Pyr*]** showed that the nematic phase is less stable by 65 K than that in hexyl analogue **1a[*Pyr*]**, while the extrapolated SmA–N transition temperature $[T_{AN}]$ is 100 K lower relative to that in **1a[*Pyr*]**.

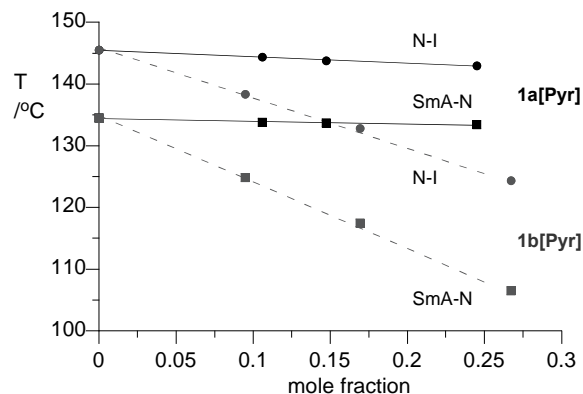


Figure 3. A plot of N-I (dots) and SmA-N (diamonds) transition temperatures for binary mixtures of **1a[Pyr]** (black solid) and **1b[Pyr]** (gray dotted) in **2a[Pyr]** as a function of mole fraction.

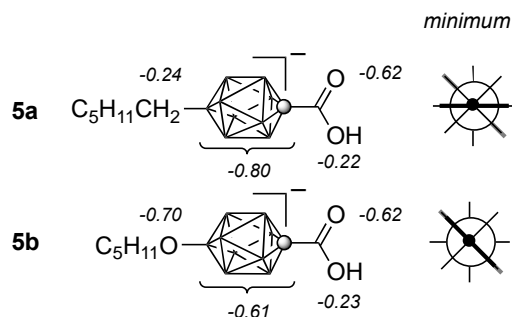


Figure 4. Natural charges for key molecular fragments and extended Newman projection along the long molecular axes of acid **5a** and **5b** showing conformational minima. The bars represent the substituents, and the filled circle is the connecting atom.

The results clearly demonstrated that the $\text{CH}_2 \rightarrow \text{O}$ substitution markedly destabilizes both mesophases in **1b[Pyr]**, and has particularly strong effect on the smectic phase. This effect cannot be attributed only to the difference in conformational properties of acids **5a** and **5b**. Theoretical analysis at the B3LYP/6-31G(d,p) level of theory (15) demonstrated that the C(1)-carboxyl and B(10)-hexyl chain adopt a staggered

orientation with respect to the {*closo*-1-CB₉} cage in the conformational minimum. Consequently, the ideal dihedral angle between the planes of the two substituents is 45°, and all conformers of acid **5a** are chiral (Figure 4). In contrast, DFT analysis of the 10-pentyloxy acid **5b** revealed that the substituent is eclipsed relative to the cage resulting in a C_s-symmetry of the molecule. Such higher symmetry conformational minimum observed in **5b** is expected to have favorable impact on mesophase stability, however, contrary to these expectations, the mesophase in its ester **1b[Pyr]** is significantly destabilized. Thus, the origin of this destabilization likely lies elsewhere, for example in charge distribution in the anions.

Previous studies demonstrated unusually high basicity of the amino group attached to a boron atom in *closo*-carborates (4,16). Similar increase of basicity is observed for pentyloxy derivative **5b**, which easily protonates at the oxygen atom giving a zwitterionic oxonium acid **5b[H]** (3). Analysis of natural charges (17) indeed shows that the cage in acid **5b** has smaller overall negative charge by -0.19e than in acid **5a**, and the B(10)-oxygen atom has a substantial negative charge of -0.70e (Figure 4). This difference in charge distribution and localization of a substantial negative charge on the oxygen atom may lead to strong coulombic interactions with the pyridinium and ion alignment unfavorable for the formation of a mesophase. This is consistent with the observed particularly strong destabilization of the smectic phase (Table 2).

The three ILC, **1a[Pyr]**, **1b[Pyr]** and **2a[Pyr]**, were also investigated as additives to non-ionic hexylbenzoate mesogen **3a** (Table 2 and Figure 5). The ion pairs were fully miscible with the nematic host, and the N-I transition temperature exhibits approximately linear dependence on concentration ($r^2 > 0.97$). For concentrations >8

mol% a SmA phase induction was observed in all three binary systems. It can be estimated that the nematic phase is replaced completely with SmA at concentrations of about 32–35 mol% for the 10-vertex derivatives, **1a[Pyr]** and **1b[Pyr]** (Figure 5), and at even lower concentrations, of about 20 mol%, for **2a[Pyr]**. The N-I transition temperatures extrapolated from mixtures with **3a** are higher than those obtained for pure ion pairs **1a[Pyr]** and **2a[Pyr]** by 8 K and 13 K, respectively, and have uncertainty of ± 4 K. In contrast, the $[T_{NI}]$ extrapolated for **1b[Pyr]** is significantly lower, by 22 K, than that extrapolated from binary mixtures with **2a[Pyr]** (Table 2). These results demonstrate particularly good compatibility of nematic **1a[Pyr]** and **2a[Pyr]** with a non-ionic host, which is consistent with our previous findings for miscibility of ionic and non-ionic smectogens (2). The lower value for $[T_{NI}]$ extrapolated for **1b[Pyr]** from **3a** than from ILC **2a[Pyr]** again indicates significant disruption of molecular organization in the phase, and is consistent with unfavorable cation-anion interactions in **1b[Pyr]** as compared to its close analogue **1a[Pyr]**.

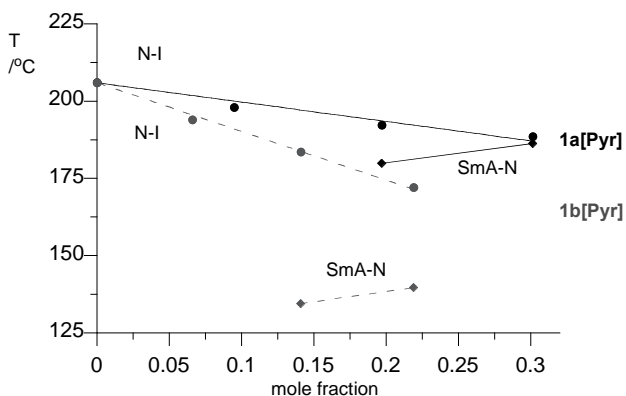


Figure 5. A plot of N–I (dots) and SmA–N (diamonds) transition temperatures for binary mixtures of **1a[Pyr]** (black solid) and **1b[Pyr]** (gray dotted) in **3a** as a function of mole fraction of the ion pair.

6.2.2.3 Conclusions

Results demonstrated that a replacement of the CH₂ connecting group in **1a[Pyr]** with an oxygen atom in **1b[Pyr]** markedly destabilizes the mesophase. The pentyloxy derivative **1b[Pyr]** also has lower than expected [T_{NI}] temperature extrapolated from a non-ionic host, indicating significant disruption of the molecular organization in the nematic phase. Computational analysis suggests that the effect is due to unusually high basicity of the connecting oxygen atom and consequently less favorable interactions between the anion and pyridinium cation. These results indicate that heteroatom connecting and presumably linking groups (such as COO) should be avoided in designing high mesophase stability ILC derived from *closo*-borates.

All three ionic liquid crystals **1a[Pyr]**, **1b[Pyr]** and **2a[Pyr]** are compatible and miscible with non-ionic mesogen **3a**, which is consistent with our previous findings and important for designing anisotropic materials for electrolyte applications.

6.2.2.4 Experimental

Characterization

¹H NMR spectra were obtained at 400 MHz in CDCl₃ and referenced to the solvent, unless specified otherwise. Optical microscopy and phase identification were performed using a PZO “Biolar” polarized microscope equipped with a HCS400 Instec hot stage. Thermal analysis was obtained using a TA Instruments 2920 DSC. Transition temperatures (onset) and enthalpies were obtained using small samples (0.5-1 mg) and a heating rate of 10 K min⁻¹ under a flow of nitrogen gas. For DSC and combustion analyses, each compound was additionally purified by dissolving in CH₂Cl₂, filtering to

remove particles, evaporating and recrystallization. The resulting crystals were dried in vacuum overnight at ambient temperature.

Binary mixtures

Binary mixtures were prepared by dissolving both components in small amounts of dry MeCN, subsequent evaporation of the solvent, and drying the resulting homogenous material at 130 °C for several hours. The hot homogenous mixture was transferred to an aluminum pan and analyzed by DSC. Transition temperatures of the mixtures were taken as peak temperature on the second heating cycle. The transition temperatures were extrapolated to pure additive by fixing the intercept of the fitting line at the peak transition temperature of the host.

Synthesis

4.3.1 Synthesis of esters. General procedures. Method A. Carboxylic acid (1 mmol) was dissolved in anhydrous CH₂Cl₂ (5 mL), (COCl)₂ (0.26 mL, 3 mmol) and a catalytic amount of *N,N*-dimethylformamide were added, the reaction mixture was stirred for 15 min, and evaporated to dryness *in vacuo*. The residue was dissolved in anhydrous CH₂Cl₂ (10 mL) and NEt₃ (0.21 mL, 1.5 mmol) and 4-hydroxy-4'-(hexyloxy)azobenzene (2) (**4**, 328 mg, 1.1 mmol) were added. The reaction was stirred overnight, washed with 10% HCl, organic layer dried (Na₂SO₄), and solvent removed. The crude material was passed through a short silica gel plug (CH₂Cl₂) giving the ester as an orange crystalline solid. The resulting ester was purified further by recrystallization.

Method B. Carboxylic acid (1 mmol) was dissolved in anhydrous CH₂Cl₂ (10 mL). 4-Hydroxy-4'-(hexyloxy)azobenzene (2) (**4**, 328 mg, 1.1 mmol), *N,N'*-dicyclohexylcarbodiimide (DCC, 309 mg, 1.5 mmol) and catalytic amounts of 4-

dimethylaminopyridine were added. The reaction mixture was stirred overnight, washed with 10% HCl, organic layer dried (Na₂SO₄), and solvent removed. The crude material was purified as described in Method A.

Ester of [*closo*-1-CB₉H₈-1-COOH-10-OC₅H₁₁]⁻ acid Pyr salt (1b**[Pyr]).** Ester **1b**[NMe₄], obtained from **5b**[NMe₄] (**3**) using Method A, was dissolved in CH₂Cl₂ and *N*-butyl-4-heptyloxypyridinium bromide (**1**) (1.0 equivalent) was added resulting in a precipitate formation. Water was added, and the biphasic system was stirred vigorously until all the precipitate had dissolved. The CH₂Cl₂ layer was separated, and the aqueous layer was extracted with additional CH₂Cl₂. The CH₂Cl₂ layers were combined, dried (Na₂SO₄), and evaporated giving a yellow crystalline solid of **1b**[Pyr]. Crude product was purified on a silica gel column (CH₂Cl₂/MeCN, 2:1) and then recrystallized repeatedly from AcOEt/hexane. The resulting crystals were dried in vacuum at ambient temperature: ¹H NMR (400 MHz, CD₃CN) δ 0.5-2.5 (m, 8H), 0.91 (t, *J* = 6.9 Hz, 3H), 0.94 (t, *J* = 7.4 Hz, 3H), 0.96 (t, *J* = 7.4 Hz, 3H), 0.98 (t, *J* = 7.3 Hz, 3H), 1.30-1.42 (m, 12H), 1.42-1.58 (m, 8H), 1.78-1.92 (m, 8H), 4.10 (t, *J* = 6.6 Hz, 2H), 4.14 (t, *J* = 6.6 Hz, 2H), 4.29 (t, *J* = 6.6 Hz, 2H), 4.32 (t, *J* = 7.5 Hz, 2H), 7.10 (d, *J* = 9.0 Hz, 2H), 7.34 (d, *J* = 7.5 Hz, 2H), 7.48 (d, *J* = 8.8 Hz, 2H), 7.94 (d, *J* = 9.0 Hz, 2H), 7.99 (d, *J* = 8.8 Hz, 2H), 8.40 (d, *J* = 7.5 Hz, 2H); ¹¹B NMR (128 MHz, CD₃CN) δ -28.4 (d, *J* = 150 Hz, 4B), -20.0 (d, *J* = 162 Hz, 4B), 53.2 (s, 1B). *Anal.* Calc. for C₄₁H₆₈B₉N₃O₅: C, 63.11; H, 8.78; N, 5.39. Found: C, 62.89; H, 8.59; N, 5.36%.

Synthesis of 4-C₅H₁₁SC₆H₄COOH (6c) (5).

1-Pentanethiol (4.42 mL, 0.036 mol) of was added dropwise to a suspension of hexane-washed NaH (1.73 g, 0.072 mol) in anhydrous DMSO (100 mL) under argon.

After 1 hr, 4-fluorobenzoic acid (5.04 g, 0.036 mol) dissolved in DMSO (100 mL) was added slowly. The reaction mixture was stirred at 100 °C overnight. After cooling, the nearly solid reaction mixture was suspended in H₂O and KOH was added to the mixture to ensure basic pH. The solution was filtered, and filtrate acidified. The resulting precipitate was filtered, washed with water and dried to give 5.53 g of an off-white solid. The crude product was recrystallized (aqueous EtOH) to give 3.67 g (46% yield) of acid **6c** as an off-white solid: mp 112-113 °C (lit.(5) mp 113 °C); ¹H NMR (CDCl₃, 400 MHz) δ 0.92 (t, *J* = 7.2 Hz, 3H), 1.36 (sext, *J* = 7.2 Hz, 2H), 1.41-1.48 (m, 2H), 1.72 (quint, *J* = 7.4 Hz, 2H), 3.00 (t, *J* = 7.4 Hz, 2H), 7.31 (d, *J* = 8.6 Hz, 2H), 7.99 (d, *J* = 8.6 Hz, 2H).

6.2.2.5 Acknowledgements

Financial support for this work was received from the National Science Foundation (DMR-0907542). We thank Mr. Bryan Ringstrand for help with the attempted preparation of acid **5c**[NMe₄].

6.2.2.6 References

- (1) Ringstrand, B.; Monobe, H.; Kaszynski, P. *J. Mater. Chem.*, **2009**, *19*, 4805-4812.
- (2) Ringstrand, B.; Jankowiak, A.; Johnson, L. E.; Kaszynski, P.; Pocięcha, D.; Górecka, E. *J. Mater. Chem.*, **2012**, *22*, 4874-4880.
- (3) Pecyna, J.; Ringstrand, B.; Kaszynski, P. *Inorg. Chem.*, **2012**, *51*, 000.
- (4) Ringstrand, B.; Kaszynski, P.; Young, V. G., Jr.; Janoušek, Z. *Inorg. Chem.*, **2010**, *49*, 1166-1179.
- (5) Pettit, L. D.; Sherrington, C. *J. Chem. Soc. A*, **1968**, 3078-3082.
- (6) Jankowiak, A.; Dębska, Ż.; Romański, J.; Kaszyński, P. *J. Sulfur Chem.*, **2012**, *33*, 1-7.

- (7) Rossi, R. A.; de Rossi, R. H. *Aromatic Substitution by the S_{RN1} Mechanism*; ACS: Washington, 1983; Vol. 178.
- (8) Bancroft, S. F.; Thompson, M. J.; Frimpong, N.; Mullins, R. J.; Pugh, C. *Polym. Preprints*, **2007**, *48*, 1001-1002.
- (9) Zäschke, H.; Debacq, J.; Schubert, H. *Z. Chem.*, **1975**, *15*, 100.
- (10) Nessim, R. I.; Naoum, M. M.; Nessim, M. I. *Liq. Cryst.*, **2005**, *32*, 867-876.
- (11) Akutagawa, T.; Hoshino, N.; Matsuda, I.; Matsunaga, Y. *Mol. Cryst. Liq. Cryst.*, **1992**, *214*, 117-123.
- (12) Van Meter, J. P.; Klanderman, B. H. *Mol. Cryst. Liq. Cryst.*, **1973**, *22*, 285-299.
- (13) Van Meter, J. P.; Seidel, A. K. *J. Org. Chem.*, **1975**, *40*, 2998-3000.
- (14) Ayub, K.; Moran, M.; Lazar, C.; Lemieux, R. P. *J. Mater. Chem.*, **2010**, *20*, 6655-6661.
- (15) Frisch, M. J., *et al*, Gaussian 09, Revision A.02, Gaussian, Inc., Wallingford CT, 2009.
- (16) Ringstrand, B.; Kaszynski, P.; Young, V. G., Jr. *Inorg. Chem.*, **2011**, *50*, 2654-2660.
- (17) Obtained from NBO analysis of the SCF wavefunction within Gaussian 09.

7.1 Introduction

Boron *closo*-clusters do not possess classical π bonds in their structure, yet they are often called three-dimensional analogues of benzene, characterized by σ -aromaticity. The clusters have been demonstrated as suitable structural elements of polar and ionic liquid crystals. Design of these functional molecules often requires understanding and control to what extent particular fragments of the molecule interact with each other. In order to better understand these intramolecular electronic interactions with the boron clusters, we have employed analysis of dissociation constants of carboxylic acids derived from the [closo-1-CB₉H₁₀]⁻ and [closo-1-CB₁₁H₁₂]⁻ anions in correlation with Hammett's constants. This section of my dissertation provides details on the study of transmission of electronic effects through the [closo-1-CB₉H₁₀]⁻ and [closo-1-CB₁₁H₁₂]⁻ clusters in a series of carboxylic acids substituted at the antipodal positions.

7.2 Transmission of electronic effects through the {closo-1-CB₉} and {closo-1-CB₁₁} cages: Dissociation constants for a series of [closo-1-CB₉H₈-1-COOH-10-X] and [closo-1-CB₁₁H₁₀-1-COOH-12-X] acids.

7.2.1 Description and contributions

The goal of this project was to investigate to what extent the boron clusters we incorporate as building blocks to polar and ionic liquid crystalline materials conduct electronic effects between the substituents. One of the tools that allows to study these interactions is the analysis of ionization constants of substituted carboxylic acids as a function of the substituent. This kind of study was not conducted before for the [closo-1-CB₉H₁₀]⁻ and [closo-1-CB₁₁H₁₂]⁻ and little was known about the ability of these clusters

1 and **2** to conduct electronic effects. For this purpose, we used a series of eleven carboxylic acids derived from the [*closo*-1-CB₉H₁₀]⁻ and [*closo*-1-CB₁₁H₁₂]⁻ anions, respectively, substituted at the antipodal positions. Most of the acids were intermediates to other functional materials and were available in our laboratory and only several of them required full synthesis. We determined the apparent dissociation constants, *pK_a*, of the acids in an EtOH/H₂O system. The results were correlated with Hammett's constants. The results we obtained were compared to those reported in literature for 4-substituted benzoic, *trans*-cinnamic and bicyclo[2.2.2]octane-1-carboxylic acids in the same solvent system. Analysis of the results showed that efficiency of transmission of electronic effects through the 10- and 12-vertex clusters is 56% and 65%, respectively, of that of benzene. It was suggested that both inductive and resonance effect play significant role in transmission of electronic effects through both clusters. Experimental results were augmented by quantum mechanical calculations, which were consistent with the obtained values.

My role in this project included synthesis of acids **1b**, **1d**, **1e**, **1f**, **1g**, **1h**, **2a**, **2d**, and measurements of the *pK_a* constants of all the acids. Dr. Bryan Ringstrand prepared acids **1a**, **1c**, **2b** and **2c**, and Prof. Piotr Kaszynski performed quantum mechanical calculations.

In the following chapter the entire text of the manuscript is included for consistency of the narrative, however, the experimental section contains only experiments performed by me.

7.2.2 The manuscript

Reproduced by permission of American Chemical Society
Pecyna, J.; Ringstrand, B.; Kaszynski, P. *Inorg. Chem.* **2012**, *51*, 5353-5359.

7.2.2.1 Introduction

Rational design of functional molecules for electronic and photonic applications requires rigid and linear structural elements¹ for which the ability to transmit electronic effects is known.² Some elements must be weakly interacting (electronically insulating), while others are expected to be efficient conduits for electronic effects and also for charge and energy transport. Therefore, the degree of electronic coupling between various structural elements in designing functional molecules is of particular interest.

Benzene (**A**, Figure 1) is the classical structural element of efficient electronic conjugation with π substituents and is generally considered one of the most effective conduits of electronic effects by both resonance and inductive mechanisms. On the other hand, only inductive and field effects are transmitted through the aliphatic bicyclo[2.2.2]octane (BCO, **B**) ring.^{3,4} Other structural elements that may serve as potential conduits for electronic effects include the 10- and 12-vertex *closo*-boranes, such as carboranes **C** and **D**, which are considered to be σ aromatic,^{5,6} possess the ability to interact with π substituents,⁷⁻¹⁰ and exhibit a strong “antipodal” effect (or the A-effect).^{11,12} The strength of these interactions appears to follow the order **A** > **C** > **D** >> **B**.^{8,9}

The first studies of the transmission of electronic effects through boron clusters focused on donor-acceptor derivatives of carborane **D**. Investigations by spectroscopic¹³ and subsequently dipole moment additivity methods¹⁰ concluded that the 12-vertex *p*-carborane (**D**) does indeed transmit electronic effects, although it is a significantly weaker conduit than benzene (**A**). Recent cyclic voltammetry studies of dimetallic

derivatives of *p*-carboranes **C** and **D** demonstrated a substantial separation of 1-electron oxidation potentials for the 10-vertex carborane derivatives compared to the 12-vertex analogues.^{14,15} A similar separation of anodic potentials was found in a cobalt derivative of **D** ($\Delta E^{\circ}_{(\text{ox})} = 0.105 \text{ V}$) that was comparable to that found in the benzene analog ($\Delta E^{\circ}_{(\text{ox})} = 0.110 \text{ V}$).¹⁶ Both results demonstrate significant electronic communication through the carborane cages.

The classic method for studying the degree of transmission of electronic effects through a structural element involves comparing the reactivity of a series of derivatives as a function of a substituent.¹⁷ Most conveniently, an evaluation of ionization constants for a series of substituted carboxylic acids using Hammett's substituent constants¹⁸ $\sigma_p(X)$ provides direct quantitative comparison to benzene as a conduit for electronic effects. Surprisingly, no such systematic investigations for boron clusters have been reported to date,¹⁹ in part due to lack of appropriate derivatives especially of monocarbaborates **E** and **F**.

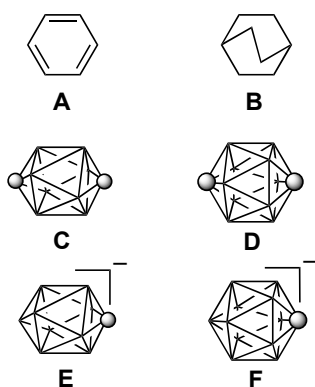
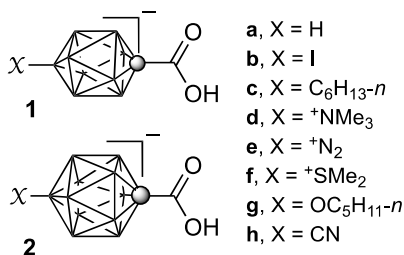


Figure 1. The structures of benzene (**A**), bicyclo[2.2.2]octane (BCO, **B**), 1,10-dicarba-*closo*-decaborane (10-vertex *p*-carborane, **C**), 1,12-dicarba-*closo*-dodecaborane (12-

vertex *p*-carborane, **D**), 1-carba-*closo*-decaborate (**E**), 1-carba-*closo*-dodecaborate (**F**). In **C–F** each vertex corresponds to a BH fragment and the sphere represents a carbon atom.

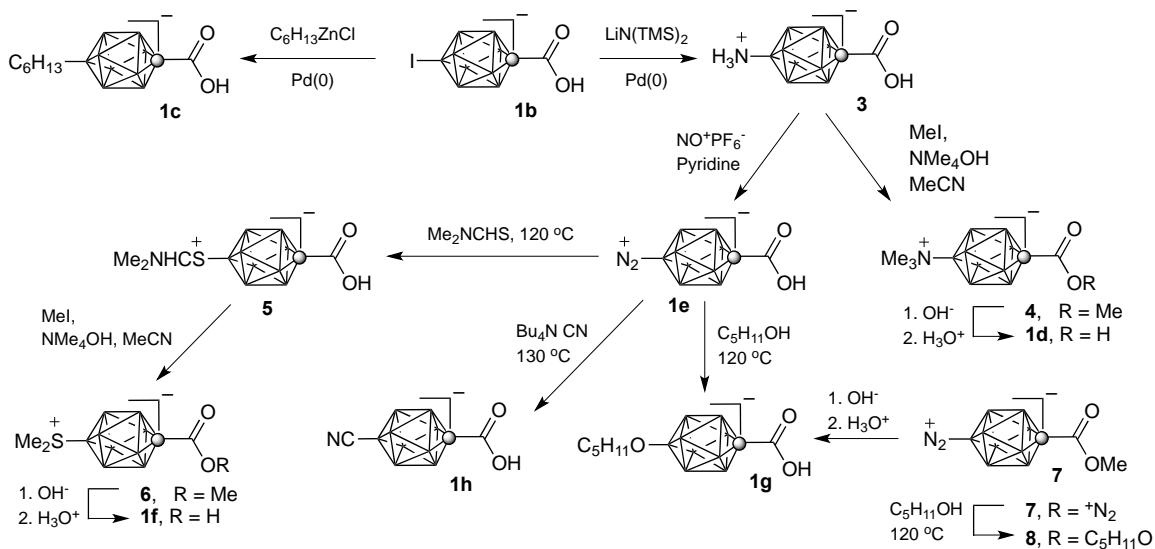
Our recent advances²⁰⁻²⁴ in the chemistry of the [*closo*-1-CB₉H₁₀]⁻ (**E**) and [*closo*-1-CB₁₁H₁₂]⁻ (**F**) clusters and availability of several substituted 1-carboxylic acids derived from these clusters provided an opportunity to determine the extent of transmission of the substituent effect through the cages (Figure 1) by Hammett-type correlation analysis. Here we report ionization constant studies of two series of compounds [*closo*-1-CB₉H₈-1-COOH-10-X]⁻ (**1**) and [*closo*-1-CB₁₁H₁₀-1-COOH-12-X]⁻ (**2**), which are derived from the parent carboxylic acids [*closo*-1-CB₉H₉-1-COOH]⁻ (**1a**) and [*closo*-1-CB₁₁H₁₁-1-COOH]⁻ (**2a**), respectively, by substitution in the antipodal position. The apparent dissociation constants *pK*_a' obtained in EtOH/H₂O (1:1 v/v) were analyzed using substituent constants σ_p(X), and the results were compared to those reported for the corresponding 4-substituted benzoic,²⁵ *trans*-cinnamic,²⁶ and bicyclo[2.2.2]octane-1-carboxylic acids³ in the same solvent. Analysis of experimental data is augmented with DFT results of relative acidity in each series calculated in aqueous medium.



7.2.2.2 Results and discussion

Synthesis

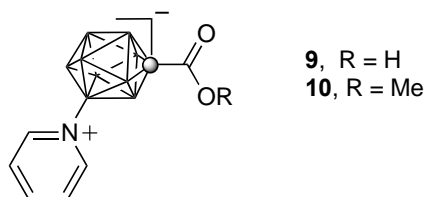
Iodo acid^{20,27} **1b** was a convenient precursor to the remaining acids **1** substituted at the B(10) position (Scheme 1). Thus, a reaction of **1b** with hexylzinc chloride under Negishi conditions gave 10-hexyl acid **1c**.²² Pd-catalyzed amination of **1b** with LiN(TMS)₂ as an ammonia equivalent gave 10-amino acid **3**.^{23,27} Methylation of **3** with MeI resulted in methyl ester **4**, which was hydrolyzed in alcoholic KOH forming 10-trimethylammonium acid **1d**. Dinitrogen acid **1e** was obtained by diazotization of amino acid **3** in the presence of pyridine.^{23,27} Thermolysis of **1e** in Me₂NCHS gave masked mercaptan **5**,^{23,27} which was methylated with MeI. The resulting methyl ester **6** was hydrolyzed giving dimethylsulfonium acid **1f**. Thermolysis of dinitrogen acid **1e** in 1-pentanol resulted in the formation of 10-pentyloxy acid **1g**. Alternatively, acid **1g** was obtained by thermolysis of the dinitrogen acid methyl ester **7**²³ in 1-pentanol followed by hydrolysis of the resulting methyl ester **8** (Scheme 1).



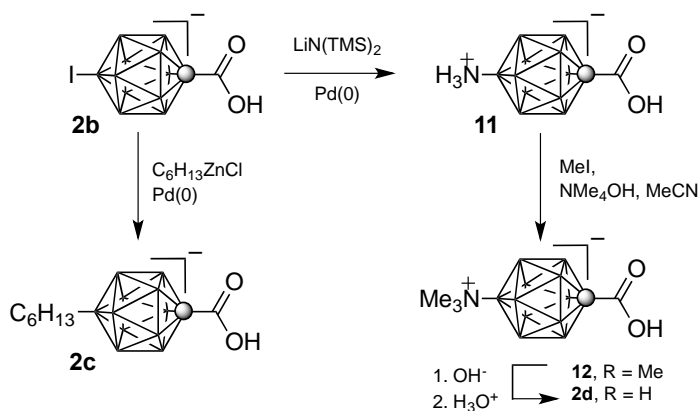
Scheme 1.

The preparation of 10-cyano acid **1h** was plagued by low yields and difficulties with isolation of pure product. Thus, cyanation of iodo acid **1b** with CuCN in NMP at 160 °C gave mostly insoluble materials, while no reaction occurred at lower temperatures. Pd-catalyzed cyanation of **1b** with Zn(CN)₂, according to an analogous general procedure²⁸ and employing the catalyst previously used in Negishi alkylation of **1b**,²³ resulted in recovery of the starting material. A last attempt involved thermolysis of dinitrogen acid **1e** in dry and molten [NBu₄]⁺CN⁻ at 130 °C. The product obtained as an acid extract from Et₂O and constituting about 16% yield is believed to be the desired acid **1h**, according to MS and IR methods.²⁹ The majority of the product was presumably a mixture of zwitterions resulting from insertion of the transient boronium ylide²³ to the C–H bond in one of butyl chains in the [NBu₄]⁺ cation. This is evident from the significantly downfield chemical shift (~50 ppm in ¹¹B NMR), which is consistent with 10-alkyl derivatives of the [*closo*-1-CB₉H₁₀]⁻ anion such as **1c**. Attempts to isolate a pure sample of **1h** as a salt were unsuccessful and the acid was not pursued further.

The parent acid **1a** was isolated as the deiodinated by-product in the amination reaction of **1b**.^{23,27} The dinitrogen acid methyl ester **7** was prepared using a mixture of isomeric iodo acids remaining after separation of pure **1b**.^{23,27} Thus, a 4:5 mixture of 10-iodo acid **1b** and its 6-iodo analog was aminated under the usual conditions²⁷ to give a mixture of amino acids 10-amino **3** and the corresponding 6-isomer. Diazotization of this mixture in pyridine solutions gave both acid **1e** and 6-pyridinium acid **9**,³⁰ which was treated with CH₂N₂. The resulting methyl esters **7** and **10** were conveniently separated using chromatography giving products in 13 % and 10 % overall yields, respectively.²⁹



Access to carboxylic acids **2** derived from the 12-vertex monocarbaborate **F** is limited by the lack of a stable dinitrogen derivative **2e** and rely solely on limited transformations of iodo acid **2b**.^{21,31} Thus, iodo acid **2b** was alkylated forming 12-hexyl acid **2c**²¹ and aminated to give 12-amino acid **11**,²⁴ as described for the {*closo*-1-CB₉} derivatives (Scheme 2). Methylation of **11** with MeI gave 12-trimethylammonium ester **12**, which was hydrolyzed giving acid **2d** in 79% yield. The parent acid **2a** was prepared by lithiation of monocarbaborate [*closo*-1-CB₁₁H₁₂]⁻ (**F**) followed by carboxylation with CO₂.³¹



Scheme 2.

Protonation and deprotonation of acids 1 and 2

Deprotonation of the carboxyl group with [NMe₄]⁺ OH⁻ resulted in upfield shifts of the resonance of the antipodal boron atom: -5 ± 1 ppm for the B(10) nucleus in series **1**

and -3 ± 2 ppm for the B(12) nucleus in series **2**.²⁹ In series **1**, the largest difference was observed for **1c** (-7.0 ppm) and the smallest for **1e** (-3.7 ppm). Replacing the $[\text{NR}_4]^+$ counterion in non-zwitterionic acids with hydronium, H_3O^+ , by extraction of the ion pair from acidic solutions to Et_2O , resulted in minor deshielding of the B(10) in **1** and B(12) in **2** nucleus by less than +0.5 ppm in all acids except for the pentyloxy derivative **1g**. In the latter case, the B(10) was shielded by -5.2 ppm presumably due to protonation of the alkoxy group oxygen atom in **1g** and the formation of a zwitterionic structure. This result is consistent with our findings for amino acid **3** and its methyl ester, which demonstrated high basicity of the nitrogen atom and its preferential protonation resulting in -10 ppm shielding of the B(10) nucleus.²³ Consequently, the diazotization of **3** and formation of **1e** requires basic conditions, such as the presence of pyridine (Scheme 1).

Dissociation constants measurements

Acidity of acids in series **1** and **2** was investigated by potentiometric titration in aqueous EtOH (1:1, v/v), which was previously used as a solvent for the study of substituted benzoic and bicyclo[2.2.2]octane-1-carboxylic acids. Results are shown in Table 1 and presented in Figure 2.

Results in Table 1 show that carboxylic acids derived from the [*closo*-1- $\text{CB}_{11}\text{H}_{12}$] (**F**) are generally more acidic than those derived from the 10-vertex analogue **E**. For four parent acids the acidity decreases in the following order: PhCOOH ($pK_a' = 5.66$) > **2a** ($pK_a' = 6.17$) > **1a** ($pK_a' = 6.53$) > BCO-COOH ($pK_a' = 6.74$)³ in 50% EtOH.

A plot of $\Delta pK_a' = pK_H' - pK_X'$ values for series **1** against standard $\sigma_p(\text{X})$ parameters¹⁸ demonstrated good correlation, and regression analysis of the data gave the reaction constant $\rho = 0.87 \pm 0.04$ ($r^2 = 0.98$). When the most outlying datapoint for hexyl

acid **1c** was removed, the correlation improved ($\rho = 0.86 \pm 0.02$, $r^2 = 0.99$). The higher pK_a ' value for **1c** than expected from the correlation might be due to aggregation of the hydrophobic hexyl chains in the aqueous medium, which affects the ionization constant. Essentially the same value of ρ was obtained for series **1** without including the datapoints for **1c** and **1g**. The slope (reaction constant ρ) depends heavily on the far right datapoint for dinitrogen acid **1e**. When this datapoint was removed from the correlation, the value of ρ increased to 0.93 ± 0.07 , but with a larger error ($r^2 = 0.97$). Overall, the values of ρ for full or partial sets of acids **1** are within 1 standard deviation. The same analysis for the series of 12-vertex carboxylic acids **2** shows a slightly higher reaction constant $\rho = 1.00 \pm 0.09$ ($r^2 = 0.97$) than obtained for the 10-vertex series **1** (either full or comparable data sets).

The reaction constants, ρ , obtained for series **1** and **2** are smaller than that obtained in correlation of ΔpK_a ' values for *p*-substituted benzoic acids at 25 °C with the same set of $\sigma_p(X)$ parameters¹⁸ ($\rho = 1.55 \pm 0.04$, $r^2 = 0.99$).²⁵ Similar analysis for five *p*-substituted *trans*-cinnamic acids (55% EtOH, v/v, 25 °C) gave a ρ value that is about half of benzoic acids ($\rho = 0.70 \pm 0.09$, $r^2 = 0.94$).²⁶ Thus, the results indicate that the effectiveness of the transmission of electronic effects follows the order: benzene (**A**) > [*closo*-1-CB₁₁H₁₂]⁻ (**F**) > [*closo*-1-CB₉H₁₀]⁻ (**E**) > PhCH=CH₂.

A better comparison of the ρ values can be made after normalization for the distance between the carboxyl group and the substituent. According to Hammett, the reaction constant depends on the distance d from the substituent X to the reacting group, temperature T , and reaction type and medium C (1).³²

$$\rho = \frac{1}{d^2 T} C \quad (1)$$

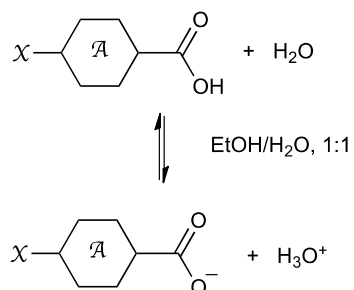
$$\rho' = \rho \times d^2 \quad (2)$$

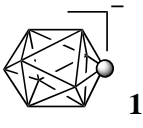
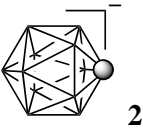
Since the only variable in the considered set of reactions is d , the experimental ρ values were normalized (2) by using the H \cdots C(O) distance that was obtained for each parent acid at the DFT level of theory. Results show that the normalized ρ' values for the boron cluster are significantly lower and very similar ($\rho' = 33.4 \pm 1.5$ for **E** and $\rho' = 35.3 \pm 3.2$ for **F**) than those obtained for benzene (44.6 ± 1.2) and styrene (41.9 ± 5.4). This further demonstrates that both clusters, [*closo*-1-CB₉H₁₀]⁻ and [*closo*-1-CB₁₁H₁₂]⁻, are less efficient conduits for transmission of electronic effects when compared to classical π -systems.

Correlation of $\Delta pK_a'$ values for series **1** and **2** with Swain-Lupton inductive/field parameters¹⁸ $F(X)$ was also investigated. In the case of series **1**, fitting to a function $\Delta pK_a' = \rho F(X)$ had poor correlation factor ($\rho = 0.89 \pm 0.15$, $r^2 = 0.82$), and best fit linear function $\Delta pK_a' = \rho F(X) + \beta$ had an intercept of -0.32 ($\rho = 1.18 \pm 0.15$, $r^2 = 0.92$). Removing the most outlying datapoint for the pentyloxy derivative **1g** improved the correlation ($\rho = 1.11 \pm 0.10$, $\beta = -0.21$, $r^2 = 0.97$). This datapoint is diagnostic for the type of interactions between the substituents and the cage ($\sigma_p(\text{OC}_5\text{H}_{11}) = -0.34$, $F(\text{OC}_5\text{H}_{11}) = +0.29$), and the lack of correlation with the $F(X)$ scale indicates the significance of a resonance-type mechanism in the transmission of electronic effects. For comparison, the available pK_a' data for derivatives of bicyclo[2.2.2]octane-1-carboxylic acid^{3,33} correlate well with the parameters $F(X)$ ($\rho = 1.50 \pm 0.10$, $r^2 = 0.96$), but poorly with parameters $\sigma_p(X)$. This clearly demonstrates that the transmission of electronic effects through the {*closo*-1-CB₉} cage

involves both a type of resonance and inductive/field mechanisms related to the “antipodal” effect observed in boron clusters.

Table 1. Apparent ionization constants pK_a' for selected derivatives of [*closo*-1-CB₉H₈-1-COOH-10-X] (**1**) and [*closo*-1-CB₁₁H₁₀-1-COOH-12-X] (**2**) in 50% EtOH (v/v) at 24 °C



	X \ A	 1	 2
a	H	6.53±0.02 ^a	6.17±0.02 ^a
b	I	6.38±0.02 ^b	5.86±0.02 ^a
c	<i>n</i> -C ₆ H ₁₃	6.87±0.03 ^b	6.36±0.03 ^a
d	⁺ NMe ₃	5.83±0.02	5.38±0.04
e	⁺ N ₂	4.93±0.03	—
f	⁺ SMe ₂	5.68±0.02	—
g	<i>n</i> -C ₅ H ₁₁ O	6.90±0.03 ^a	—

^a The [NEt₄]⁺ counterion. ^b The [NMe₄]⁺ counterion.

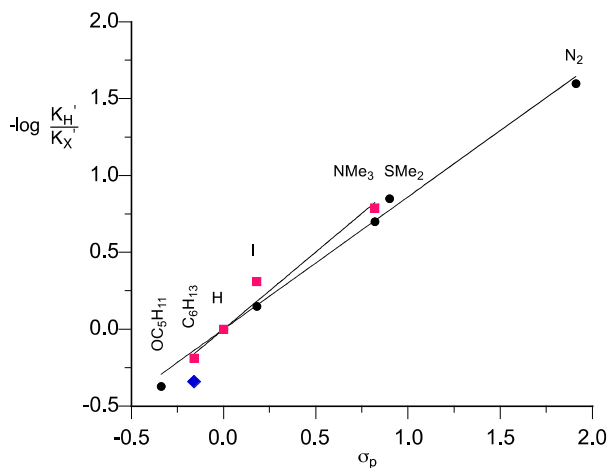
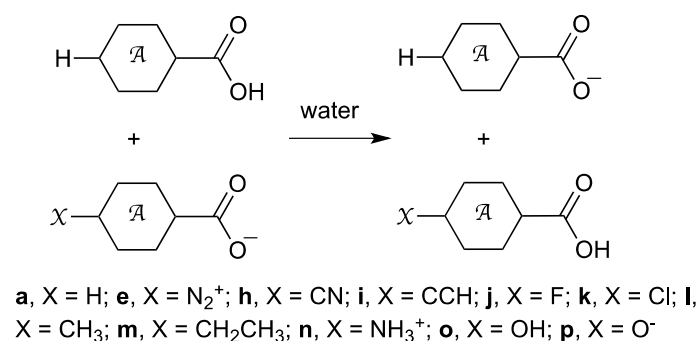


Figure 2. The Hammett plot of $\Delta pK_a'$ values for derivatives of [closo-1-CB₉H₈-1-COOH-10-X] **1** (black dots, $\rho = 0.87 \pm 0.04$, $r^2 = 0.99$) and [closo-1-CB₁₁H₁₀-1-COOH-12-X] **2** (red squares, $\rho = 1.00 \pm 0.09$, $r^2 = 0.97$) in 50% EtOH (v/v) at 24 °C. The blue diamond represents the datapoint for **1c**.

Analysis of the relatively short series of acids **2** demonstrated a better correlation with the field/inductive parameters $F(X)$ than that found for the 10-vertex derivatives **1**. Thus, correlation of $\Delta pK_a'$ values for four acids **2a–2d** with the $F(X)$ parameters gave a comparable ρ and smaller intercept ($\rho = 1.02 \pm 0.13$, $\beta = -0.10$, $r^2 = 0.97$) than the same set of 10-vertex analogues **1a–1d** ($\rho = 0.99 \pm 0.25$, $\beta = -0.19$, $r^2 = 0.89$). This might suggest that the field/inductive mechanism is more important for transmission of electronic effects in 12-vertex cluster **F**, whereas the resonance mechanism is more significant in the 10-vertex cluster as is the case for benzene. This conclusion is consistent with results of computational analysis for the 10- and 12-vertex clusters, which demonstrated greater electronic interaction of π substituents with the 10-vertex clusters compared to 12-vertex analogues.⁸

To confirm the experimental results, free energy change, ΔG_{298} , for the isodesmic reaction shown in Scheme 3 was calculated using the B3LYP/6-31G(d,p) method and the PCM solvation model for each series of acids. Substituents used in the isodesmic reaction were simple, typically second row elements, to avoid complications of conformational potential energy surface (Scheme 3).²⁹



Scheme 3.

Results for benzoic acid derivatives show that the calculated ΔG_{298} values generally follow the trend of the Hammett parameters $\sigma_p(X)$, and the correlation is satisfactory ($\rho = 6.05 \pm 0.24$, intercept = 0.42 ± 0.16 , $r^2 = 0.99$), after removing datapoints for **n** (X = NH₃) and **p** (X = O⁻). The isodesmic reaction for the former is excessively exothermic due to high basicity of the dianion, while the value for the latter reaction is higher than expected by about 2 kcal/mol. To avoid systematic errors, free energy change in isodesmic reactions for series **1** and **2** were compared directly to those of benzoic acid derivatives and results are shown in Figure 3.

Both series of monocarbaborate acids show good correlation with the analogous values for benzoic acid derivatives. In general, substituents in both series **1** and **2** have smaller effect on acidity of the parent acid than in benzoic acid series. This is reflected in the slopes of the best fit functions that are smaller than unity, $m = 0.63$ in series **1** and $m = 0.53$ for series **2**, and consistent with the experimentally observed approximately 60% efficiency of transmission of electronic effects in benzoic acid derivatives. Interestingly, the computational results predict higher exotherm for the isodesmic reaction involving the alkyl derivatives of monocarbaborates (**l** and **m**) than the corresponding OH derivatives **1n** and **2n**, while calculations for benzoic acid derivatives are consistent with the order of $\sigma_p(X)$ values ($\sigma_p(\text{Me}) = -0.17$, $\sigma_p(\text{OH}) = -0.37$). The computational results for the monocarbaborate acids are consistent with the experimental findings of lower than expected acidity of 10-hexyl acid **1c**, and suggest stereoelectronic origin of the effect rather than aggregation in solutions (see above).

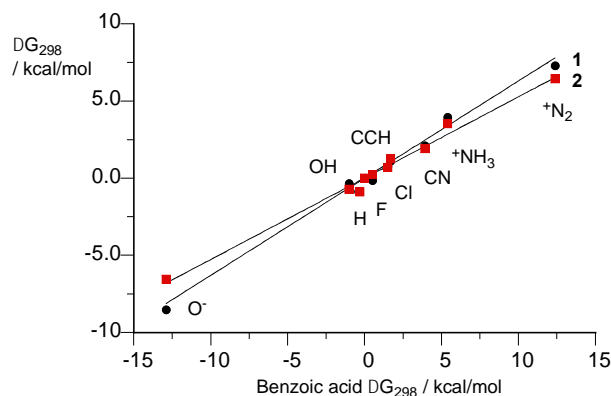


Figure 3. The plot of ΔG_{298} for isodesmic reaction in Scheme 3 for series **1** (black dots, $m = 0.63 \pm 0.02$, $r^2 = 0.99$) and **2** (red squares, $m = 0.53 \pm 0.02$, $r^2 = 0.99$) versus ΔG_{298} values for benzoic acid derivatives. Datapoints for **l** and **m** are excluded.

7.2.2.3 Conclusions

Analysis of experimental results demonstrated that apparent dissociation constants pK_a measured for series **1** and **2** correlate well with $\sigma_p(X)$ substituent parameters and poorly with inductive/field parameters $F(X)$. This suggests that both resonance and inductive mechanisms are important in transmitting electronic effects through the [*closo*-1-CB₉H₁₀]⁻ and [*closo*-1-CB₁₁H₁₂]⁻ clusters. The resulting reaction constants ρ indicate that the monocarbaborate cages **E** and **F** are good conduits for transmission of substituent effects, and their effectiveness is about 60% relative to that of benzene, or about 75% considering the normalized constant ρ' . Additional datapoints are necessary for a more accurate determination of the reaction constants ρ .

Computational analysis of relative acidity in each series of acids is consistent with experimental results and demonstrates similar effectiveness of transmission of electronic effects through the monocarbaborate cages **E** and **F**, 63% and 53% respectively, relative to that of benzene. The calculations also showed lower than expected acidity of alkyl monocarbaborate carboxylic acids, which is consistent with experimental observations in series **1**. Further light into the nature of the transmission mechanism might be shed by detailed computational analysis of the data in the context of the “antipodal” effect.

Iodo acid [*closo*-1-CB₉H₈-1-COOH-10-I]⁻ (**1b**) and dinitrogen acid **1e** proved to be convenient and versatile precursors to several derivatives of the parent acid **1a**. Preparation of a larger number of derivatives of carboxylic acid **2a** requires further developments in the chemistry of iodo acid [*closo*-1-CB₁₁H₁₀-1-COOH-12-I]⁻ (**2b**).

7.2.2.4 Computational details

Quantum-mechanical calculations were carried out with the B3LYP^{34,35} method and 6-31G(d,p) basis set using the Gaussian 09 package.³⁶ Geometry optimizations were undertaken using appropriate symmetry constraints and default convergence limits. Vibrational frequencies were used to characterize the nature of the stationary points and to obtain thermodynamic parameters at 25 °C. Zero-point energy (ZPE) corrections were scaled by 0.9806.³⁷ Geometry optimizations and vibrational frequency calculations were conducted using the PCM solvation model³⁸ in conjunction with the keyword SOLVENT=WATER.

7.2.2.5 Experimental section

Melting points are not corrected. NMR spectra were obtained at 128.4 MHz (¹¹B) and 400.1 MHz (¹H) in CD₃CN unless specified otherwise. ¹H NMR spectra were referenced to the solvent, and ¹¹B NMR chemical shifts were referenced to an external boric acid sample in CH₃OH that was set to 18.1 ppm.

Preparation of acids **1b**, **1c**, **1g**, **3**, and **5**, ester **7**, and isolation of acid **1a** was described before.^{23,27} Synthesis of iodo acid **2b**,^{21,31} hexyl acid **2c**,²¹ and amino acid **11**²⁴ is described elsewhere.

pK_a' Measurements

Apparent acidity constants (*pK_a'*) were determined by potentiometric titration at 24±0.1 °C. The *pK_a'* for each compound was calculated as an average of *pK_a'* values determined at individual points using the Henderson-Hasselbach equation in a range of ±0.25 pH units from the half neutralization point³⁹ for at least three titrations. Selected compounds were dissolved in EtOH/H₂O (4.00 mL, 1:1 vol/vol, ~0.01 M) and covered

with parafilm to minimize evaporation of the solvent. Neutralization was achieved under moderate stirring with 0.02 M NaOH in EtOH/H₂O (1:1, vol/vol), which was added in 50 μ L increments using a digital pipette. After addition of NaOH, the pH was recorded upon stabilization (~30 seconds). The pH electrode was calibrated in aqueous buffer (pH = 4.0, 7.0, and 10.0) followed by conditioning in EtOH/H₂O (1:1 vol/vol) for several hrs until the pH reading stabilized. The pH of a 3.1 mM solution of PhCOOH in EtOH/H₂O (1:1 vol/vol) half-neutralized with NaOH showed the value of 5.75 \pm 0.02 after several hours, in accordance with literature.^{33,40}

Corrections for free hydrogen or hydroxyl ions or ionic strength of the medium were not made.

All pK_a ' values in the region of ± 0.25 pH from the half neutralization point were analyzed statistically and results are shown in Table 1. Using this protocol, the pK_a ' value for benzoic acid (0.01 M solution) was obtained 5.66 \pm 0.01, while the standardized value in 50% EtOH at 25 °C is 5.72.²⁵

Preparation of [*closo*-1-CB₉H₈-1-COOH-10-NMe₃] (1d).

A suspension of amino acid^{23,27} [*closo*-1-CB₉H₈-1-COOH-10-NH₃] (**3**, 0.100 g, 0.56 mmol), [NMe₄]⁺OH⁻ • 5H₂O (0.506 g, 2.79 mmol), and CH₃I (0.35 mL, 5.6 mmol) in CH₃CN (10 mL) was stirred overnight at rt. The mixture was filtered, and solvent removed *in vacuo*. The crude mixture was passed through a short silica gel plug (CH₂Cl₂), and the resulting residue was washed with hot hexane giving 0.130 g of crude methyl ester **4**: mp 120-125 °C; ¹H NMR (CD₃CN) δ 1.16 (br q, J = 142 Hz, 4H), 1.75 (br q, J = 158 Hz, 4H), 3.46 (s, 9H), 3.93 (s, 3H); ¹¹B NMR (CD₃CN) δ -22.7 (d, J = 149 Hz, 4B), -17.0 (d, J = 153 Hz, 4B), 44.8 (s, 1B).

Methyl ester **4** was hydrolyzed for 3 hr at 50 °C in CH₃OH (4 mL) containing KOH (0.100 g, 1.78 mmol). Water was added (2 mL) and CH₃OH removed. 10 % HCl (10 mL) was added, and the mixture was extracted with Et₂O (3 x 5 mL). The organic layers were combined, dried (Na₂SO₄), and evaporated giving 0.110 g (89% yield) of acid [*closo*-1-CB₉H₈-1-COOH-10-NMe₃] (**1d**) as a light yellow solid. The product was dissolved in CH₂Cl₂, solution filtered through a cotton plug (to remove insoluble particulates), solvent removed, and the resulting acid **1d** was further purified by repeated recrystallization from aqueous CH₃OH: mp >260 °C; ¹H NMR (CD₃CN) δ 1.16 (br q, *J* = 143 Hz, 4H), 1.75 (br q, *J* = 157 Hz, 4H), 3.46 (s, 9H), 9.62 (br s, 1H); ¹¹B NMR (CD₃CN) δ -22.6 (d, *J* = 145 Hz, 4B), -16.9 (d, *J* = 161 Hz, 4B), 44.6 (s, 1B). Anal. Calcd for C₅H₁₈B₉NO₂: C, 27.11; H, 8.19; N, 6.32. Found: C, 27.38; H, 8.19; N, 6.25.

Preparation of [*closo*-1-CB₉H₈-1-COOH-10-SMe₂] (**1f**)

A suspension of protected mercaptan [*closo*-1-CB₉H₈-1-COOH-10-SCHNMe₂] (**5**, 0.100 g, 0.40 mmol),^{23,27} [NMe₄]⁺ OH⁻ · 5H₂O (0.290 g, 1.59 mmol), and CH₃I (0.25 mL, 4 mmol) in CH₃CN (10 mL) was stirred overnight at rt. The mixture was filtered, and the solvent removed *in vacuo*. The crude residue was passed through a short silica gel plug (CH₂Cl₂), solvent evaporated, and the residue washed with hot hexane giving 84 mg of crude methyl ester **6**: mp 115-118 °C; ¹H NMR (CD₃CN) δ 1.24 (br q, *J* = 145 Hz, 4H), 1.88 (br q, *J* = 159 Hz, 4H), 3.01 (s, 6H), 3.94 (s, 3H); ¹¹B {¹H} NMR (CD₃CN) δ -20.2 (4B), -14.8 (4B), 33.7 (1B).

Methyl ester **6** was hydrolyzed at 50 °C in CH₃OH (4 mL) containing KOH (0.100 g, 1.78 mmol) for 3 hr. Water was added (2 mL) and CH₃OH removed. 10 % HCl (10 mL) was added, and the mixture was extracted with Et₂O (3 x 5 mL). The organic

layers were combined, dried (Na_2SO_4), and evaporated giving 0.075 g (84% yield) of acid [*closo*-1- CB_9H_8 -1-COOH-10-SMe₂] (**1f**) as a light yellow solid. The product was dissolved in CH_2Cl_2 , solution filtered through a cotton plug (to remove insoluble particulates), solvent removed, and the resulting acid was recrystallized from aqueous CH_3OH and then toluene containing a few drops of acetonitrile: mp 217-220 °C; ^1H NMR (CD_3CN) δ 1.23 (br q, $J = 142$ Hz, 4H), 1.89 (br q, $J = 158$ Hz, 4H), 3.01 (s, 6H), 9.67 (s, 1H); ^{11}B NMR (CD_3CN) δ -20.2 (d, $J = 147$ Hz, 4B), -14.8 (d, $J = 160$ Hz, 4B), 33.6 (s, 1B). Anal. Calcd for $\text{C}_4\text{H}_{15}\text{B}_9\text{O}_2\text{S}$: C, 21.40; H, 6.73. Found: C, 21.67; H, 6.79.

Preparation of [*closo*-1- CB_9H_8 -1-COOH-10-OC₅H₁₁]⁺[NEt₄]⁻ (1g**[NEt₄]).**

Method A. A solution of dinitrogen acid [*closo*-1- CB_9H_8 -1-COOH-10-N₂] (**1e**, 0.080 g, 0.42 mmol)^{23,27} and freshly distilled 1-pentanol (3 mL) was heated at 120 °C for 1 hr. As the reaction progressed, bubbling of N₂ was observed. The reaction mixture was cooled to rt, and excess 1-pentanol was removed by short-path distillation (90 °C, 1 mmHg) leaving crude product as a brown solid. The crude material was heated at 50 °C in CH_3OH (5 mL) containing KOH (0.050 g, 1.25 mmol) for 3 hr to hydrolyze small amounts of ester that were formed during the thermolysis. Water was added (2 mL) and CH_3OH removed. 10 % HCl (10 mL) was added, and the mixture was extracted with Et₂O (3 x 5 mL). Half of the Et₂O was evaporated, and water (2 mL) was added. The remaining Et₂O was evaporated and the aqueous layer filtered to remove insoluble material. [NEt₄]⁺Br⁻ (0.088 g, 0.42 mmol) was added to the filtrate resulting in the formation of a precipitate which was isolated by extraction into CH_2Cl_2 (3 x 5 mL). The CH_2Cl_2 layers were combined, dried (MgSO_4), and evaporated giving 0.094 g (86% yield) of [*closo*-1- CB_9H_8 -1-COOH-10-OC₅H₁₁]⁺[NEt₄]⁻ (**1g**[NEt₄]) as a light brown solid

residue. The product was further purified by passage through a cotton plug (CH₂Cl₂) to remove insoluble particulates followed by recrystallization from toluene containing a few drops of CH₃CN: mp 177-179 °C; ¹H NMR (CD₃CN) δ 0.00-2.00 (br m, 8H), 0.94 (t, *J* = 7.2 Hz, 3H), 1.20 (tt, *J*₁ = 7.3 Hz, *J*₂ = 1.9 Hz, 12H), 1.35-1.52 (m, 4H), 1.80 (quint, *J* = 7.1 Hz, 2H), 3.15 (q, *J* = 7.3 Hz, 8H), 4.07 (t, *J* = 6.7 Hz, 2H), 9.18 (br s, 1H); ¹¹B NMR (CD₃CN) δ -28.7 (d, *J* = 138 Hz, 4B), -20.6 (d, *J* = 156 Hz, 4B), 52.3 (s, 1B). Anal. Calcd for C₁₅H₄₀B₉NO₃: C, 47.44; H, 10.62; N, 3.69. Found: C, 47.59; H, 10.73; N, 3.71.

Method B. A solution of methyl ester **7** (0.100 g, 0.489 mmol) and freshly distilled 1-pentanol (4 mL) was heated at 125 °C for 1 hr. Excess 1-pentanol was removed *in vacuo*, the resulting crude ester **8** was dissolved in CH₃OH (5 mL) containing KOH (0.014 g, 2.45 mmol), and the resulting mixture was heated at 50 °C for 5 hr. Water was added (3 mL) and CH₃OH removed. 10 % HCl (10 mL) was added, and the mixture was extracted with Et₂O (4 x 5 mL). About half of the Et₂O was evaporated, and water (3 mL) was added. The remaining Et₂O was evaporated and the aqueous layer filtered to remove insoluble material. [NEt₄]⁺Br⁻ (0.103 g, 0.489 mmol) was added to the filtrate resulting in the formation of a precipitate, which was isolated by extraction into CH₂Cl₂ (3 x 5 mL). The CH₂Cl₂ layers were combined, dried (MgSO₄), and evaporated giving 0.154 g (83% yield) of [*closo*-1-CB₉H₈-1-COOH-10-OC₅H₁₁][NEt₄]⁺ as a light yellow solid. The product was purified as described in method A.

Preparation of [*closo*-1-CB₁₁H₁₀-1-COOH-12-NMe₃] (2d)

The amino acid²⁴ [*closo*-1-CB₁₁H₁₁-1-COOH-12-NH₃] (**11**, 0.100 g, 0.493 mmol) was methylated as described for the amino acid **3** to give 0.101 g of methyl ester **12**: mp

232-233 °C; ^1H NMR (CD_3CN) δ 1.20-2.60 (br m, 10H), 2.76 (s, 9H), 3.57 (s, 3H); ^{11}B { ^1H } NMR (CD_3CN) δ -14.7 (d, J = 160 Hz, 10B), 8.3 (1B).

The methyl ester **12** was hydrolyzed as described for methyl ester **4**, and the acid **2d** was isolated in 79% yield as white crystalline solid: mp >260 °C; ^1H NMR (CD_3CN) δ 1.20-2.60 (br m, 10H), 2.76 (s, 9H), 9.2 (br s, 1H); ^{11}B NMR (CD_3CN) δ -14.2 (d, J = 121 Hz, 10B), 8.8 (s, 1B). Anal. Calcd for $\text{C}_5\text{H}_{20}\text{B}_{11}\text{NO}_2$: C, 24.50; H, 8.22; N, 5.71. Found: C, 24.85; H, 8.22; N, 5.67.

Attempted preparation of [*closo*-1- CB_9H_8 -1-COOH-10-CN] $^-\text{[NMe}_4\text{]}^+$ (**1h**[NMe_4])

Acid [*closo*-1- CB_9H_8 -1-COOH-10- N_2] (**1e**, 0.100 g, 0.526 mmol) was added to dry molten [NBu_4] $^+\text{CN}^-$ (2.61 g, 9.74 mmol) at 130 °C under a blanket of Ar in three portions. Gas evolution was observed. The brown homogenous reaction mixture was further stirred for 1 hr. The solution was cooled, and 10 % HCl (10 mL) was added resulting in precipitation. The precipitation was filtered giving 0.176 g of a light yellow/orange solid.

The filtrate was extracted with Et_2O (3 x 5 mL). Half of the Et_2O was evaporated and H_2O (1 mL) was added followed by complete removal of Et_2O . Attempts to precipitate the cyano acid with [NEt_4] $^+\text{Br}^-$ were unsuccessful. The aqueous layer was acidified with 10 % HCl (10 mL), and the product was extracted with Et_2O (3 x 5 mL). The organic layers were combined, dried (Na_2SO_4), and evaporated giving 0.015 g of a light red film: ^{11}B { ^1H } NMR (CD_3CN) δ -20.5 (4B), -15.1 (4B), 23.6 (1B).

The red film was dissolved in CH_3OH (2 mL), treated with [NMe_4] $^+\text{OH}^- \cdot 5\text{H}_2\text{O}$ (7 mg, 0.039 mmol) and solvents removed. The resulting residue was repeatedly washed with Et_2O . After drying 0.022 g of a brown crystalline residue identified as crude

1h[NMe₄] was obtained: mp 101-108 °C dec; ¹H NMR (CD₃CN) δ 0.5-2.50 (m, 8H), 3.07 (s, 12H); ¹¹B NMR (CD₃CN) δ -20.6 (d, *J* = 137 Hz, 4B), -15.2 (d, *J* = 161 Hz, 4B), 23.4 (s, 1B); IR ν_{CN} = 2210 cm⁻¹; ESI-HRMS(-): Calcd. for C₃H₉B₉NO₂ *m/z*: 189.1515; found; 189.1526.

The light yellow/orange solid contained up to four boron species possibly related to C-H insertion into the [NBu₄]⁺ cation: ¹¹B {¹H} NMR (CD₃CN) δ major signals -25.6, -20.5, -19.1, -15.2, 46.1.

Preparation of [*closo*-1-CB₉H₈-1-COOCH₃-10-N₂] (7) and [*closo*-1-CB₉H₈-1-COOCH₃-6-(1-NC₅H₅)] (10).

A 4:5 mixture of [*closo*-1-CB₉H₈-1-COOH-10-I]⁻NMe₄⁺ (**1b**) and [*closo*-1-CB₉H₈-1-COOH-6-I]⁻NMe₄⁺ (11.5 g, 32.54 mmol) was aminated with lithium hexamethyldisilazane (LiHMDS, 0.49 mol, 488 mL, 1.0 M in THF) in the presence of Pd₂dba₃ (0.595 g, 0.65 mmol) and 2-(dicyclohexylphosphino)biphenyl (0.912 g, 2.603 mmol) as similarly described for pure **1b**.^{1,2} The resulting 2:3 mixture of amino acids [*closo*-1-CB₉H₈-1-COOH-10-NH₃] (**3**) and [*closo*-1-CB₉H₈-1-COOH-6-NH₃] (**3**) (2.12 g, 11.8 mmol) was suspended in anhydrous CH₃CN (10 mL) containing anhydrous pyridine (4.8 mL) and diazotized with nitrosonium hexafluorophosphate (NO⁺[PF₆]⁻, 6.19 g, 35.37 mmol) added in 6 portions at 10 min intervals at -15 °C as similarly described before.^{1,2} The reaction mixture was stirred for 1.5 hr at -15 °C, volatiles removed, 10% HCl (20 mL) added, and the residue stirred vigorously until all solids had dissolved. The aqueous solution was extracted with Et₂O (3 x 15 mL), the Et₂O layers were combined, washed with H₂O, dried (Na₂SO₄), and evaporated to dryness giving 3.76 g of crude mixture of [*closo*-1-CB₉H₈-1-COOH-10-N₂] (**1e**) and [*closo*-1-CB₉H₈-1-COOH-6-(1-NC₅H₅)] (**9**).³

The mixture was passed through a short silica gel plug (CH₃OH/CH₂Cl₂, 1:19) giving 1.60 g (8.38 mmol) of a mixture of **1e** and **9** as a white solid.

The mixture (650 mg) was dissolved in ether (15 mL), cooled in ice bath, treated with a solution of diazomethane (generated from 4.32 g, 41.92 mmol of *N*-methyl-*N*-nitrosourea) and stirred for 1 hr. The reaction mixture was evaporated to dryness giving 681 mg of a white solid. The crude material was washed with hexane and passed through a short silica gel plug (hexane/ethyl acetate 4:1, v/v) giving 360 mg of pure [*closo*-1-CB₉H₈-1-COOCH₃-10-N₂] (**7**) as a white solid. The silica gel plug was then washed with EtOAc giving 351 mg of [*closo*-1-CB₉H₈-1-COOCH₃-6-(1-NC₅H₅)] (**10**) as a white solid, which was recrystallized from aqueous MeOH followed by toluene/*iso*-octane mixture: mp 119-120 °C; ¹H NMR (CD₃CN) δ 2.85 – 0.1 (br m, 7H), 3.95 (s, 3H), 5.55 (q, *J* = 158 Hz, 1H), 7.75 (dd, *J*₁ = 7.7 Hz, *J*₂ = 6.8 Hz, 2H), 8.28 (tt, *J*₁ = 7.8 Hz, *J*₂ = 1.4 Hz, 1H), 8.46 (d, *J* = 5.6 Hz, 2H); ¹¹B NMR (CD₃CN) δ -25.3 (d, *J* = 146 Hz, 1B), -20.1 (d, *J* = 142 Hz, 2B), -16.2 (d, *J* = 158 Hz, 2B), -11.2 (d, *J* = 158 Hz, 2B), -5.3 (s, 1B), 30.3 (d, *J* = 164 Hz, 1B). Anal. Calcd for C₈H₁₆B₉NO₂: C, 37.60; H, 6.31; N, 5.48. Found: C, 37.97; H, 6.49; N, 5.42.

NMR spectra for protonated and deprotonated acids **1** and **2**

1. The salt of acid **1a–1c**, **1g**, or **2a–2c** was suspended in 10% HCl and extracted into ether. The ether extract was dried (Na₂SO₄), solvent evaporated to dryness, and the residue was analyzed by NMR in CD₃CN.

2. The carboxylic acid **1** or **2** (~5 mg) was dissolved in CD₃CN and small excess [NMe₄]⁺OH⁻•5H₂O (~1.2 equiv) was added. After 5 min NMR was recorded. Results are shown in Table S1.

Table S1. ^{11}B NMR chemical shift for the B(10) atom in acids **1** and B(12) atom in acids **2** as acid extracts and upon deprotonation in CD_3CN .

Compound	substituent	Neutral	Acid extract	basic
1a	H	34.3	35.1	27.8
1b	I	20.1	20.6	14.8
1c	<i>n</i> - C_6H_{13}	47.3	47.8	40.3
1d	$^+\text{NMe}_3$	44.6	–	39.7
1e	$^+\text{N}_2$	20.3	–	16.6
1f	$^+\text{SMe}_2$	33.6	–	27.9
1g	<i>n</i> - $\text{C}_5\text{H}_{11}\text{O}$	52.3	47.1	47.5
2a	H	-6.7	-6.1	-8.8
2b	I	-16.2	-16.5	-17.8
2c	<i>n</i> - C_6H_{13}	4.6	4.6	-1.6
2d	$^+\text{NMe}_3$	8.8	–	6.6

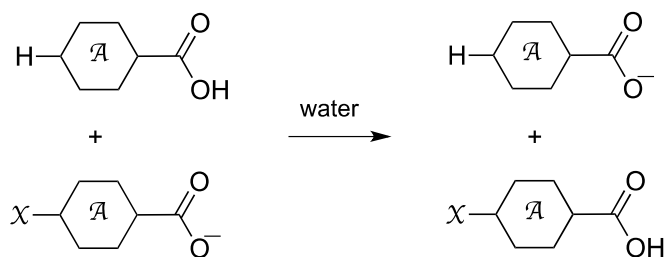
Quantum-mechanical Calculations

Quantum-mechanical calculations were carried out with the B3LYP^{4,5} method and 6-31G(d,p) basis set using the Gaussian 09 package.⁶ Geometry optimizations were undertaken using appropriate symmetry constraints and default convergence limits. Vibrational frequencies were used to characterize the nature of the stationary points and

to obtain thermodynamic parameters at 25 °C. Zero-point energy (ZPE) corrections were scaled by 0.9806.⁷ Geometry optimizations and vibrational frequency calculations were conducted using the PCM solvation model⁸ in conjunction with the keyword SOLVENT=WATER.

Carboxylic acids **1e–1k** and **1p** and their benzoic analogues were optimized in C_s point group symmetry, while their anions in C_{2v} point group symmetry, with the exception of 4-N₂⁺-C₆H₄-COO⁻ (C_2 symmetry). For derivatives containing the OH, CH₃, CH₂CH₃, and ⁺NH₃ substituents two conformers were optimized with appropriate symmetry constraints (typically C_s), and the lower energy conformer was used for computing ΔG_{298} of the isodesmic reaction. Carboxylic acids in series **2** were optimized without symmetry constraints. Results are shown in Table S2 and graphically presented in Figure 3 in the main text.

Table S2. Free energy change in isodesmic reaction involving the parent and substituted carboxylic acids



Substituent X		Benzene	{ <i>closo</i> -1-CB ₉ }	{ <i>closo</i> -1-CB ₁₁ }
		ΔG_{298} (kcal/mol)	1 ΔG_{298} (kcal/mol)	2 ΔG_{298} (kcal/mol)
e	⁺ N ₂	12.38	7.31	6.46
h	CN	3.93	2.10	1.93
i	C≡CH	1.51	0.76	0.70
j	F	0.52	-0.14	0.25
k	Cl	1.69	1.11	1.27
l	CH ₃	-0.39	-0.85	- ^a
m	CH ₂ CH ₃	-0.31	- ^a	-0.89
n	⁺ NH ₃	5.40	3.95	3.54
o	OH	-1.00	-0.33	-0.70
p	O ⁻	-12.89	-8.52	6.55

^a Normal mode analysis showed 1 small imaginary frequency after geometry optimization without symmetry constraints.

7.2.2.6 Acknowledgements

This project was supported by the NSF grant (DMR-0907542).

7.2.2.7 References

- (1) Schwab, P. F. H.; Levin, M. D.; Michl, J. *Chem. Rev.* **1999**, *99*, 1863.
- (2) "Molecular Wires and Electronics", *Top. Curr. Chem.* **2005**, *257*, and references therein.
- (3) Roberts, J. D.; Moreland, W. T., Jr. *J. Am. Chem. Soc.* **1953**, *75*, 2167.
- (4) Reynolds, W. F. *Prog. Phys. Org. Chem.* **1983**, *14*, 165.
- (5) Schleyer, P. v. R.; Najafian, K. *Inorg. Chem.* **1998**, *37*, 3454.
- (6) King, R. B. *Russ. Chem. Bull.* **1993**, *42*, 1283.
- (7) Pakhomov, S.; Kaszynski, P.; Young, V. G., Jr. *Inorg. Chem.* **2000**, *39*, 2243.
- (8) Kaszynski, P.; Pakhomov, S.; Young, V. G., Jr. *Collect. Czech. Chem. Commun.* **2002**, *67*, 1061.
- (9) Kaszynski, P. In *Anisotropic Organic Materials-Approaches to Polar Order*; Glaser, R., Kaszynski, P., Eds.; ACS Symposium Series: Washington, D.C., 2001; Vol. 798, p. 68.
- (10) Droz, L.; Fox, M. A.; Hnyk, D.; Low, P. J.; MacBride, H. J. A.; Vsetecka, V. *Collect. Czech. Chem. Comm.* **2009**, *74*, 131.
- (11) Heřmanek, S.; Hnyk, D.; Havlas, Z. *J. Chem. Soc., Chem. Commun.* **1989**, 1859.
- (12) Bühl, M.; Schleyer, P. v. R.; Havlas, Z.; Hnyk, D.; Heřmanek, S. *Inorg. Chem.* **1991**, *30*, 3107.
- (13) Fox, M. A.; MacBride, H. J. A.; Peace, R. J.; Wade, K. *J. Chem. Soc., Dalton Trans.* **1998**, 401.

- (14) Wedge, T. J.; Herzog, A.; Huertas, R.; Lee, M. W.; Knobler, C. B.; Hawthorne, M. F. *Organometallics* **2004**, *23*, 482.
- (15) Fox, M. A.; Roberts, R. L.; Baines, T. E.; Le Guennic, B.; Halet, J.-F.; Hartl, F.; Albesa-Jové, D.; Howard, J. A. K.; Low, P. J. *J. Am. Chem. Soc.* **2008**, *130*, 3566.
- (16) Le Guennic, B.; Costuas, K.; Halet, J.-F.; Nervi, C.; Paterson, M. A. J.; Fox, M. A.; Roberts, R. L.; Albesa-Jové, D.; Puschmann, H.; Howard, J. A. K.; Low, P. J. *C. R. Chimie* **2005**, *8*, 1883.
- (17) O. Exner *Correlation Analysis of Chemical Data*, Plenum Press, New York, 1988.
- (18) Hansch, C.; Leo, A.; Taft, R. W. *Chem. Rev.* **1991**, *91*, 165.
- (19) For other studies of dissociation constants for derivatives of C₂B₁₀H₁₂ see: Plešek, J.; Heřmanek, S. *Coll. Czechoslov. Chem. Commun.* **1979**, *44*, 24 and *ibid* **1981**, *46*, 687.
- (20) Ringstrand, B.; Balinski, A.; Franken, A.; Kaszynski, P. *Inorg. Chem.* **2005**, *44*, 9561.
- (21) Ringstrand, B.; Jankowiak, A.; Johnson, L. E.; Kaszynski, P.; Pocięcha, D.; Gorecka, E. *J. Mater. Chem.* **2012**, *22*, 4874.
- (22) Ringstrand, B.; Monobe, H.; Kaszynski, P. *J. Mater. Chem.* **2009**, *19*, 4805.
- (23) Ringstrand, B.; Kaszynski, P.; Young, V. G., Jr.; Janoušek, Z. *Inorg. Chem.* **2010**, *49*, 1166.
- (24) Pecyna, J.; Denicola, R. P.; Gray, H.; Ringstrand, B.; Kaszynski, P. *to be published*.
- (25) Shorter, J. *Pure Appl. Chem.* **1997**, *69*, 2497.
- (26) Zdanovich, V. I.; Parnes, Z. N.; Kursanov, D. N. *Doklady Akad. Nauk SSSR, Engl. Transl.* **1965**, *165*, 1112.

- (27) Pecyna, J.; Denicola, R. P.; Ringstrand, B.; Jankowiak, A.; Kaszynski, P. *Polyhedron* **2011**, *30*, 2505.
- (28) Jin, F.; Confalone, P. N. *Tetrahedron Lett.* **2000**, *41*, 3271.
- (29) For details see Supporting Information.
- (30) Ringstrand, B.; Kaszynski, P.; Young, V. G., Jr. *Inorg. Chem.* **2011**, *50*, 2654.
- (31) Valašek, M.; Štursa, J.; Pohl, R.; Michl, J. *Inorg. Chem.* **2010**, *49*, 10247.
- (32) Hammett, L. P. *J. Am. Chem. Soc.* **1937**, *59*, 96.
- (33) Roberts, J. D.; McElhill, E. A.; Armstrong, R. *J. Am. Chem. Soc.* **1949**, *71*, 2923.
- (34) Becke, A. D. *J. Chem. Phys.* **1993**, *98*, 5648.
- (35) Lee, C.; Yang, W.; Parr, R. G. *Phys. Rev. B*, **1988**, *37*, 785.
- (36) Gaussian 09, Revision A.02, M. J. Frisch, *et al.*
- (37) Scott, A. P.; Radom, L. *J. Phys. Chem.* **1996**, *100*, 16502.
- (38) Cossi, M.; Scalmani, G.; Rega, N.; Barone, V. *J. Chem. Phys.* **2002**, *117*, 43;
Cammi, R.; Nennucci, B.; Tomasi, J. *J. Phys. Chem.* **2000**, *104*, 5631, and references therein.
- (39) Albert, A.; Serjeant, E. P. *The Determination of Ionization Constants: A Laboratory Manual*, 2nd ed.; Chapman and Hall Ltd: London, 1971.
- (40) Wilcox, C. F., Jr.; McIntyre, J. S. *J. Org. Chem.* **1965**, *30*, 777.

Part V. Summary and outlook

The overall focus of my dissertation was on the development of the fundamental chemistry of the [*closo*-1-CB₁₁H₁₂]⁻ (**1**) and [*closo*-1-CB₉H₁₀]⁻ (**2**) anions as well as investigation of properties of new materials based on these clusters.

My work began with the preparation of the iodo acid [*closo*-1-CB₉H₈-1-COOH-10-I]⁻ (**3**), which can be obtained on a multigram scale from decaborane, B₁₀H₁₄. The improved protocol for the preparation of iodo acid **3** was used to prepare a series of sulfonium acids [*closo*-1-CB₉H₈-1-COOH-10-(4-C_nH_{2n+1}C₅H₄S)] (**4**). The sulfonium acids served as precursors to polar esters **5** (Figure 1).

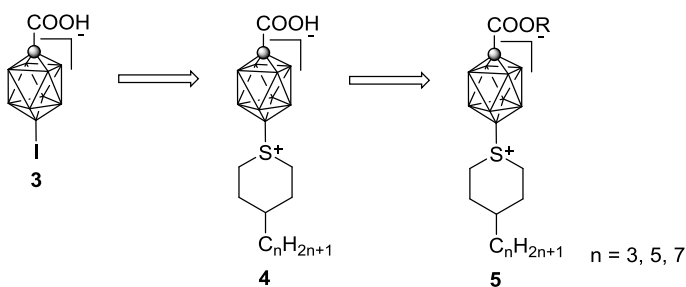


Figure 1. Polar materials based on sulfonium acids **4**.

The polar compounds were investigated in pure form as well as additives to nematic hosts in the context of materials for electrooptical applications. The materials were found to be compatible with the hosts, and some of them exhibited nematic behavior. Experiments demonstrated that the esters enhanced the dielectric response of the mixtures containing them and maintained compatibility with the nematic hosts. Esters **6** and **7** were found to be the most effective additives with reasonably high solubility and large extrapolated $\Delta\epsilon$ values of about 70 (Figure 2).

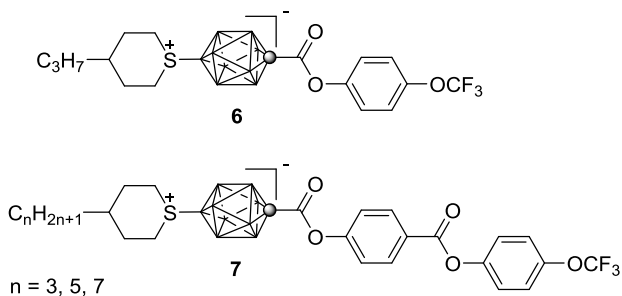


Figure 2. Selected polar esters based on sulfonium acids.

Well-developed synthetic methodology allowed for access to 1-pyridinium derivatives of the [*closo*-1-CB₁₁H₁₂]⁻ (type **1C**, see Table 1) and [*closo*-1-CB₉H₁₀]⁻ (type **2C**) anions. Such zwitterions are now accessible in acceptable yields, and in a more convenient manner. The properties of the new materials were examined by thermal, optical, and in some cases by UV-vis, powder X-ray and dielectric methods (Figure 3). The compounds were found to exhibit mesogenic behavior and to be effective low-concentration additives to nematic hosts.

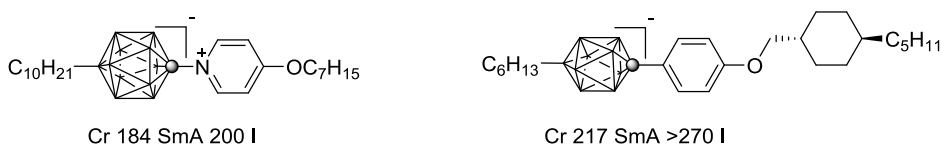


Figure 3. Selected mesogenic pyridinium zwitterions based on **1** (left) and **2** (right).

Polar materials of type **1F** (Figure 4) became more accessible through an improved synthetic route, which allowed for investigation of their properties and insight into the stability of 12-dinitrogen derivatives of **1**.

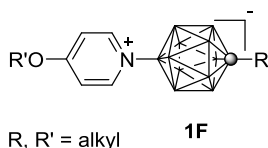


Figure 4. Pyridinium zwitterions of type **1F**.

Thus, in addition to applied science and technology, my research also contributed to the fundamental aspect of liquid crystal science. Investigation of polar and non-polar pairs of esters based on the [*closo*-1-CB₁₁H₁₂]⁻ and [*closo*-C₂B₁₀H₁₂] contributed to the fundamental knowledge about the influence of dipole moment on mesophase stability (Figure 5). It was found that uniform change in dipole moment does not correspond to a uniform change in clearing temperatures.

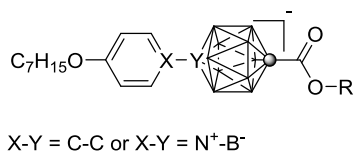


Figure 5. Polar / non-polar materials based on [*closo*-1-CB₁₁H₁₂]⁻ and [*closo*-1,2-C₂B₁₀H₁₂] clusters.

Properties of anion-driven ionic liquid crystals based on clusters or anions **1** and **2** were also investigated and helped to better understand the effect of the connecting group on mesogenic properties of ionic liquid crystalline materials.

Lastly, electronic properties of anions **1** and **2**, which are considered three-dimensional σ -aromatic analogues of benzene, their interactions with substituents and ability to serve as conduits of electronic effects were better understood by investigation of dissociation constants of substituted carboxylic acids derived from the clusters.

The combination of boron clusters and organic molecules not only allows to examine fundamental aspects of liquid crystals, but also offers access to a new class of hybrid liquid crystalline materials with unique properties. Boron clusters have proven to be effective structural elements of nonpolar, polar and ionic liquid crystals. Judicious choice of substituents allows for manipulation of polarity, phase structure, mesogenic and photophysical behavior and electronic properties of the materials. While the chemistry and properties of polar materials based on the $[closo-1-CB_{11}H_{12}]^-$ and $[closo-1-CB_9H_{10}]^-$ anions is well investigated, further development in the area of ionic liquid crystalline materials based on the $[closo-1-CB_{11}H_{12}]^-$, and to a lesser extent $[closo-1-CB_9H_{10}]^-$, anion is still needed. Recent advancements in functionalization methods of boron clusters not only extend the scope of substituents that can be introduced, which virtually permits for synthesis of all materials of type **1A-1F** and **2A-2F** (see Table 1, Chapter 1), but also allow for access to a new class of materials based on the $[closo-B_{12}H_{12}]^{2-}$, $[closo-B_{10}H_{10}]^{2-}$ dianions. This offers a great opportunity to study and understand structure-property relationship in liquid crystalline materials derived boron clusters.